Small Molecules for Controlling Stem Cell Differentiation

HENDERSON, ANDREW,PAUL

Department of Chemistry
&
Department of Biological and Biomedical Sciences

Small Molecules for Controlling Stem Cell Differentiation

Andrew Paul Henderson

A thesis submitted for the degree of Doctor of Philosophy

2011

Declaration

The work described herein was carried out in the Department of Chemistry, or the Department of Biological and Biomedical Sciences, University of Durham between October 2007 and September 2011. All of the work is my own, except where specifically stated otherwise. No part has previously been submitted for a degree at this or any other university.

Statement of Copyright

Abstract

Stem cell homeostasis and differentiation are controlled by the complex interplay of a wide range of signalling pathways and small molecules, including all-*trans*-retinoic acid (ATRA). The endogenous effects elicited by ATRA, have led to its use in numerous *in vitro* protocols as a tool for cell differentiation. However, ATRA isomerises and degrades under standard laboratory conditions and furthermore, is rapidly metabolised *in vivo*, which leads to pleotropic effects and a high efficacious dose response. Consequently, synthetic analogues that are structurally and/or functionally equivalent to ATRA have been developed, as alternative pharmacological tools to further the understanding of this molecular pathway and control cell differentiation.

In this study a small library of synthetic retinoids were prepared, which were designed to probe structural size, conformation and biological function, while being more resistant to cellular metabolism and isomerisation. Their stability towards fluorescent light was examined along with their activity in four different stem cell models. Two compounds, AH60 and AH61 were found to inhibit cellular proliferation and induce neural differentiation, through acting on the retinoic acid receptor pathway. Compared to ATRA, AH60 was approximately 10-fold more active, while AH61 was 100-fold more active in two of the cell models tested. These compounds are described comprehensively herein, and should be suitable and convenient alternatives to ATRA and 13cRA for use in *in vitro* studies carried out by cell and molecular biologists.

In addition, an unrelated small molecule, neuropathiazol, has been synthesised to further characterise both the chemistry involved in its production and its biological activity in controlling cell differentiation. This compound was highlighted in the literature as an alternative to ATRA, for inducing neural differentiation in neural progenitor cells. We have further investigated its potential to differentiate other neural stem cell types and pluripotent stem cells. In addition potential analogues of neuropathiazol are discussed, as compounds of this nature are potentially highly useful for selectively controlling neural differentiation.

Acknowledgements

I would like to thank the following people who have helped make this thesis possible:-

My supervisors Prof. Andy Whiting, Prof. Stefan Przyborski and Prof. Todd Marder, for their support, inspiration and guidance throughout the four years.

Dr. Alan Kenwright, Ian McKeag and Catherine Heffernan for acquisition of high field NMR. Dr. Mike Jones, Lara Turner and the National Mass Spectrometry Service Centre, Swansea, for mass spectrometry. Judith Magee for elemental analysis. Dr. Andrei Batsanov for X-ray crystal analysis.

All members, past and present, of the three research groups, for making the labs a fun and enjoyable place to work. I would particularly like to thank Dr. Jon Knowles for support in the synthesis of the polyene systems; Dr. Vikki Christie, for training in cell culture, flow cytometry and immunohistochemistry; Bridie Murray for RT-PCR guidance.

My family for their continued support throughout the last 26 years of my studies.

Finally, a very special thanks to Kirsten for all her love and support, and always being able to make me laugh.

Table of Contents

Chapter VII: Experimental…….

List of Abbreviations

9cRA	9-*cis*-Retinoic Acid
13cRA	13-*cis*-Retinoic Acid
AD	Activation Domain
ADH	Alcohol Dehydrogenase
AF-1	Ligand-Independent Activation Function
AF-2	Ligand-Dependant Activation Function
AHPC	Adult Hippocampal Progenitor Cell
APC	Adenomatous Polyposis Coli
APL	Acute Promyelocytic Leukemia
ARAT	Acyl-CoA Retinol Acyltransferase
AS cell	Adult Stem Cell
ATRA	All-*trans*-Retinoic Acid
BMP	Bone Morphogenetic Protein
brs	Broad Singlet
BSA	Bovine Serum Albumin
cAMP	Cyclic Adenosine Monophosphate
CDI	1'1-Carbonyldiimidazole
Ci	Cubitus Interruptus
CK1	Casein Kinase 1
CNS	Central Nervous System
Co-A	Co-Activator
Co-R	Co-Repressor
Cos	Costal 2
CRABP	Cellular Retinoic Acid Binding Protein
CRBP	Cellular Retinol Binding Protein
CS cell	Cancer Stem Cell
CSL family	CBF1/Su(H)/LAG1 Family
CYP	Cytochrome
d	Doublet
DAPT	*N*-[*N*-(3,5-difluorophenacetyl)-1-alanyl]-*S*-phenylglycine t-butyl ester

DBD	DNA-Binding Domain
DCM	Dichloromethane
dd	Doublet of Doublets
DG	Dentate Gyrus
DMEM	Dulbecco's Modified Eagle's Medium
DMF	Dimethylformamide
DMSO	Dimethyl Sulfoxide
DNA	Deoxyribonucleic Acid
DRIP	D-Receptor Interacting Protein
Dsh	Disheveled
EC cell	Embryonic Carcinoma Cell
EG	Embryonic Germ Cell
EGF	Epidermal Growth Factor
EI	Electron Impact
ES	Electrospray
ES cell	Embryonic Stem Cell
ESC	Epithelial Stem Cell
FCS	Fetal Calf Serum
FGF	Fibroblast Growth Factor
FITC	Fluorescein Isothiocyanate
GDF	Growth and Differentiation Factor
GFAP	Glial Fibrillary Acid Protein
GFP	Green Fluorescent Protein
Gli	Glioblastoma
GS cell	Germline Stem Cell
GSK-3	Glycogen Synthase Kinase 3
Fu	Fused
FSK	Forskolin
HAT	Histone Acetyl Transferase
HDAC	Histone Deacetylase
Hh	Hedgehog
hNSC	Human Neural Stem Cell

HhSC	Hedgehog Signaling Complex
HPC	Hematopoietic Progenitor Cell
HSC	Hematopoietic Stem Cell
IPA	Isopropyl Alcohol
iPS cell	Induced Pluripotent Stem Cell
IUPAC	International Union of Pure and Applied Chemistry
LBD	Ligand Binding Domain
LBP	Ligand Binding Pocket
LEF	Lymphoid Enhancer Factor
LIF	Leukemia Inhibitory Factor
LPL	Lipoprotein Lipase
LRAT	Lecithin:Retinol Acetyltransferase
LRP	Lipoprotein Receptor-Related Protein
LTD	Long-Term Depression
LTP	Long-Term Potentiation
M	Molar
maGS	Multipotent Adult Germline Stem Cell
MAPK	Mitogen-Activated Protein Kinase
Me	Methyl
mGS cell	Multipotent Germline Stem Cell
MN	Motor Neuron
m.p.	Melting Point
MSC	Mesenchymal Stem Cell
NADP(H)	Nicotinamide Adenine Dinucleotide Phosphate
NCoR	Nuclear Receptor Co-Repressor
NF	Neurofilament
NMR	Nuclear Magnetic Resonance
NPC	Neural Progenitor Cell
NPT	Neuropathiazol
NSC	Neural Stem Cell
NT	Nuclear Transfer
NTs	Neurotrophins

OB	Olfactory Bulb
PBS	Phosphate Buffered Saline
Pct1	Patched-1
PGC	Primordial Germ Cell
PI-3K	Phosphatidylinositol-3-kinase
PKA	Protein Kinase A
PLCγ	Phospholipase Cγ
PPAR	Peroxisome-Proliferation Activated Receptor
P-Ser	Phosphoserine
RA	Retinoic Acid
RALDH	Retinal Dehydrogenase
RAMBA	Retinoic Acid Metabolism Blocking Agent
RAR	Retinoic Acid Receptor
RARE	Retinoic Acid Response Element
RBP	Retinol Binding Protein
REH	Retinyl Ester Hydroxylase
ROLDH	Retinol Dehydrogenase
r.t.	Room Temperature
RT-PCR	Real Time Polymerase Chain Reaction
RXR	Retinoid X Receptor
RXRE	Retinoic X Response Element
s	Singlet
SAR	Structure-Activity-Relationship
SCID	Severe Combined Immunodeficient
SD	Standard Deviation
SDE	Standard Error
SDR	Short-Chain Dehydrogenase/Reductase
SGZ	Subgranular Zone
Smads	Selected Intracellular Mediators
SMCC	Srb and Mediator Protein-Containing Complex
Smo	Smoothened
SMRT	Silencing Mediator for the Retinoid and Thyroid Receptor

SPS	Solvent Purification System
SSC	Skin Stem Cell
SSEA-3	Stage Specific Embryonic Antigen-3
Sufu	Supressor of Fused
SVZ	Subventricular Zone
t	Triplet
TCF	T-Cell Factor
TGF-β	Transforming Growth Factor-β
THF	Tetrahydrofuran
TLC	Thin Layer Chromotography
TMS	Trimethylsilyl
TMTN	1,1,4,4-Tetramethyl-1,2,3,4-tetrahydronapthalene
TRAP	Thyroid Hormone Receptor Associated Protein
TTR	Transthyretin
UV	Ultra Violet
VAD	Vitamin A Deficiency
VDR	Vitamin D_3 Receptors
VM	Ventral Mesencephalon
VPA	Valproic Acid
$^{V}/_{V}$	Volume per Volume

Chapter I

Literature Review

1.1 Introduction

The study of how organisms grow and develop, encompassing cell growth, differentiation and morphogenesis, is termed developmental biology. Stem cells play a vital role in this field, in both embryogenesis and adult homeostasis. A detailed understanding of both the pathways involved, and ways in which they can be controlled is an integral part of advancing stem cell research.

Multiple molecular mechanisms control stem cell renewal, proliferation and differentiation, including signalling by Notch, Wnt, Hedgehog (Hh), FGF and retinoic acid (RA) (see section 1.3 for a detailed discussion and references within). The use of both natural and synthetic compounds specifically designed to act on these individual pathways has recently played a substantial role in advancing this area of research. Compounds are designed to act at a particular point in the pathway, at a precise concentration, to bring about a set response. Thus, small molecules can be administered to stem cell cultures to bring about controlled differentiation, self-renewal or proliferation. The overall aim of this area of research is therefore to achieve the precise control of stem cells to generate new cells and tissues for research. This would then allow for better drug screening assays, disease modelling profiles and potentially therapeutic applications using stem cells.

1.2 Stem Cells

The term 'stem cell' is given to a cell if it has the ability to both self-renew and produce differentiated cellular subtypes. They can be derived from both the embryo and distinct areas of the adult.[1] One method of classification, is based around their developmental potential or potency (Figure 1.1).

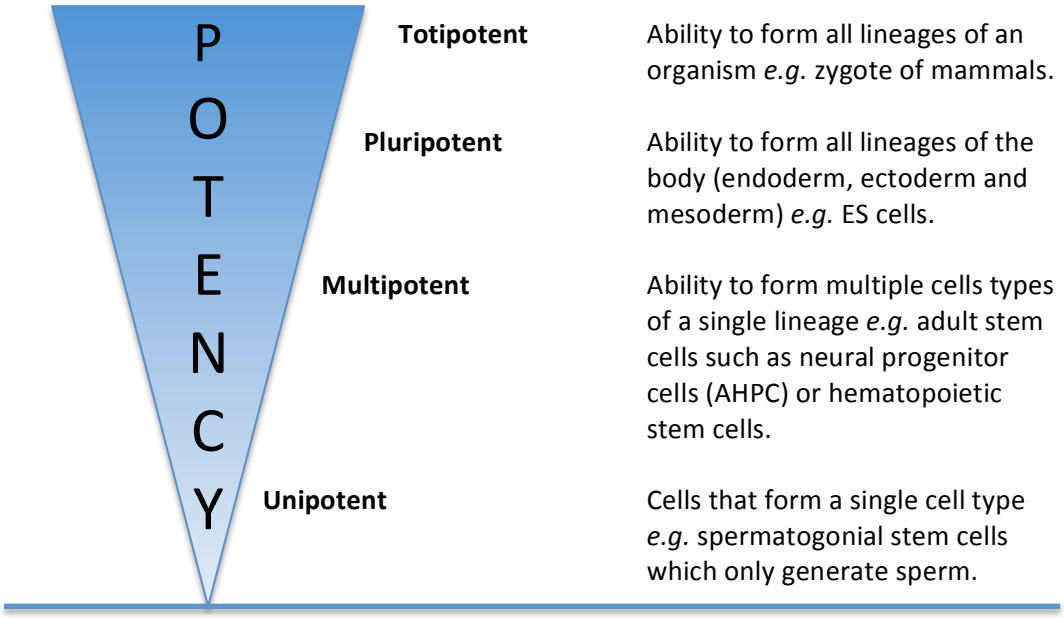

Figure 1.1 Potency definitions. Adapted from Jaenisch *et al.*[1]

In mammals, only the zygote and early blastomeres can generate the entire organism, including extraembryonic tissue and are therefore termed *totipotent*.[1] Most embryonic stem (ES) cells are an example of *pluripotent* cells, which both self-renew and have the ability to form any somatic fetal, or adult cell type. Initially described over three decades ago in mouse, ES cells possess the ability to differentiate into all three of the developing germ layers, the ectoderm, endoderm and mesoderm.[2, 3] They cannot however contribute to the extraembryonic lineages of the trophoblast or primitive endoderm, therefore, differentiating them from the *totipotent* cells of the zygote and early blastomere.[4] Stem cells derived from the

postnatal animal are termed adult stem (AS) cells. AS cells are generated during embryogenesis and thereafter regulated by precise stage-specific programs, controlling both their homeostasis and differentiation.[5] AS cells are more restricted than ES cells in that they can give rise to only a limited number of lineages, and thus are termed *multipotent*. They are normally involved in homeostatic self-renewal, but additionally, have the ability to repair tissues upon injury. This role makes them an exciting prospect for therapeutic uses and as drug targets. One example is hematopoietic stem cells (HSCs), which reside in the bone marrow of adult mammals and provide a life long source of blood precursors that subsequently differentiate to produce mature blood cells.[6] Stem cells which posses the ability to form only a single lineage are termed *unipotent*. Examples of theses include hepatocytes, found in the liver and spermatogonial stem cells, which can only produce sperm.[7]

1.2.1 Induced Pluripotent Stem Cells

In addition to the stem cells described above, there are two further categories of stem cell. The first, induced pluripotent stem (iPS) cells, are stem cells that have been created from somatic cells. These have the major advantage in that therapeutically one could generate pluripotent stem cells directly from the somatic cells of the patient. This would circumvent issues such as tissue rejection and ethical issues associated with human embryos. Three strategies have to date been employed in inducing pluripotency in mouse somatic cells, nuclear transfer (NT), fusion and forced expression of defined factors (Figure 1.2).[8]

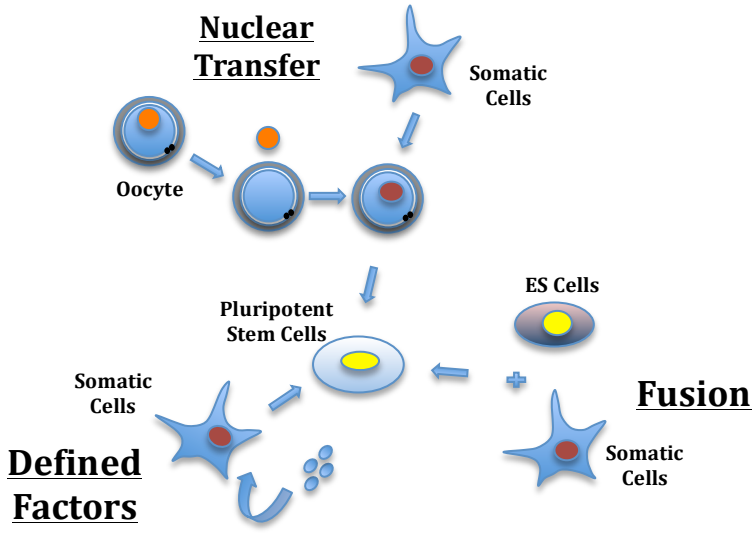

Figure 1.2 Methods of generating pluripotent stem cells from adult somatic cells. Adapted from S. Yamanaka.[8]

1.2.1.1 Nuclear Transfer

NT is defined as the introduction of a nucleus from a donor somatic cell into an enucleated oocyte to generate a clone species. NT was first reported in the early 1950's, although it was not until the late 1990's that a viable mammalian offspring, derived from fetal and adult mammalian cells was first described in sheep.[9, 10] This was quickly followed by subsequent somatic cloning in additional species including rabbit, cow, mouse, cat, pig and goat.[11] The generation of live animals confirmed that terminally differentiated somatic cells could be reprogrammed to an embryonic state, capable of directing the development of a healthy organism.

The process of nuclear cloning described above is inherently inefficient, resulting in the death of most clones attributed to faulty reprogramming.[12] Generating ES cells, rather than cloned animals, appreciatively, is significantly more efficient, as demonstrated with mouse blastocytes.[13] No biological or molecular differences are observed when comparing ES cells derived from either NT, or fertilised embryos, suggesting NT ES cells are as useful as ES cells from fertilised embryos.[14]

1.2.1.2 Fusion with ES Cells

Fusion is the process by which somatic nuclei are reprogrammed to an undifferentiated state by combination with embryonic cells to show pluripotency. The first example of this process was demonstrated in 1976 by fusion of thymocytes (hematopoietic progenitor cells) with embryonic carcinoma (EC) cells.[15] Electrofusion has subsequently been used with mouse ES cells, and more recently fusion with human ES cells has been reported.[16-18] Currently, little is known about the mechanisms of reprogramming by fusion, and the full extent to which the somatic genome is reprogrammed is unknown.

1.2.1.3 Reprogramming by Defined Factors

The successful reprogramming of differentiated cells by both nuclear transfer, or fusion suggests that ES cells contain the correct factors to induce the transformation. In 2006 Takahashi and Yamanaka successfully identified four of these factors from a wider screen of twenty four.[19] They demonstrated the successful reprogramming of mouse embryonic fibroblasts, and adult fibroblasts, back to ES-like cells by introducing, Oct-3/4, Sox2, c-Myc and Klf4 under ES cell culture conditions. The four transcription factors were introduced through viral-mediated transduction followed by selection for the expression of *Fbx15*.[19] Although these cells displayed highly analogous morphologies, proliferation patterns and teratoma formation characteristics to ES cells, upon transplantation into blastocysts the iPS cells could not generate adult or germline chimeras. Indicating that the reprogramming was somewhat inadequate.[19] More recently, three groups generated iPS cells in which the activation of endogenous Oct-4 or Nanog genes was used as a selection criterion. This resulted in cells that were fully reprogrammed to a pluripotent ES cell state.[20-22]

A number of more recent studies have extended this research into human systems, using both the four factors described above and others including Nanog and LIN28.[23-25] For the process to develop further the use of oncogenes needs to be resolved, as cancer is a common side effect.[21] In an attempt to overcome this, a number of

groups have demonstrated that the c-Myc gene is dispensable. Both mouse and human iPS cells have been attained without the c-Myc transduction, albeit with a lower efficiency and at a slower rate of reprogramming.[25-27] The formation of c-Myc tumours can therefore be eliminated yet tumours developing from the transduction of other retrovirus-transduced transcription factors such as Oct-4 may arise. One solution to this is to remove the use of retroviruses altogether and use gene transfer or deliver the protein factors in cell-permeant forms.[28] Another is to use small molecules that interact with specific pathways, which has successfully been demonstrated through the replacement of Sox2 with the molecule SB 431542 (discussed in the following section).[29]

If these concerns were overcome iPS cells do hold a significant potential in that they circumnavigate any ethical issues, as human embryos are not harmed. Furthermore, they also have the potential to generate patient-specific cells thus eliminating rejection by the immune system of cell transplants. Finally, the technique could be used to generate iPS cells from patients with specific diseases. These iPS cells could then be differentiated into discrete cellular populations on which treatment strategies and disease pathogenesis studies could be undertaken.[28]

1.2.1.4 Culture Induced Reprogramming

In addition to the three methods described above, Matsui *et al.* reported that pluripotent embryonic germ (EG) cells could be generated from the long-term culture of primordial germ cells (PGC).[30] Furthermore, additional work has been reported on the generation of chimera-competent pluripotent stem cells after long-term culture of bone marrow cells.[31] More recently, pluripotent stem cells have been generated from culturing both germline stem (GS) cells from neonate mouse testes and adult mouse testes.[32, 33] These were designated multipotent germline stem (mGS) cells and multipotent adult germline stem (maGS) cells respectively. mGS cells were shown to be similar to ES cells over a number of criteria, including proliferation, morphology and teratoma formation.[32]

Though clearly reported in the literature, there is still some apprehension to the significance of the data, with some questioning whether or not the process has been clearly proven. While some somatic cell lineages may transdifferentiate, the events are too rare to play any significant role in physiological repair, and until fully verified could potentially be as a result of other cellular events, such as fusion.[1]

1.2.2 Cancer Stem Cells

The final category of stem cells is the cancer stem (CS) cell. CS cells are dormant or slow cycling tumour cells, which retain the ability to reconstitute tumours.[34] As in normal tissue, tumours have a functional and morphologic heterogeneity hierarchy, organised and supported by CS cells. Albeit, CS cells do not always constitute the minor component of the tumour, with mouse studies indicating the amount of CS cells vary dramatically between individual tumours.[35]

CS cells, like all other stem cells, can both self-renew and differentiate to form any part of the tumor.[36] Due to their slower rate of proliferation, possessing either a dormant or large slow growing phase, most anti-cancer agents are inadequately effective, as they are designed to target proliferation and cellular division.[34] Hence, long gaps between relapses in certain cancers are attributed to CS cells.[37]

At present, there is a vast array of evidence supporting the existence of CS cells in many carcinomas, although there are still many issues to be resolved. Currently, CS cells samples are relatively impure and there is a lack of outright markers to use for identification.[35] Furthermore, still to be demonstrated is formation of solid tumours developed from a single transplanted CS cell, such as those used to generate teratocarcinoma cells.[38]

1.2.3 Adult Stem Cell Types

In addition to the types of stem cells described thus so far, more specialised subset categories of stem cells have been identified. As discussed, AS cells are generated

during embryogenesis and subsequently regulated by precise stage-specific programs, controlling both their homeostasis and differentiation.[5] Thus, a number of subsets of *multipotent* stem cells of particular tissues have been identified, which will be discussed in more detail below.

1.2.3.1 Mesenchymal Stem Cells (MSCs)

Mesenchymal stem cells are found in both the embryo and adult and are responsible for the formation and repair of bone cells (osteocytes), cartilage cells (chondrocytes) and fat cells (adipocytes), in addition to other connective tissues such as tendons (tenocytes) and myo-tubes. As the cells divide, they become more committed to a specific lineage, with the end-stage cells involved in the construction of a unique tissue type. Studying both embryonic and adult MSCs has helped develop new therapeutic strategies for the treatment of skeletal tissues, with self-cell repair of these conditions the ultimate aim.[39-41]

1.2.3.2 Hematopoietic Stem Cells (HSCs)

In addition to MSCs, the bone marrow contains one other discrete population of adult stem cell, termed hematopoietic stem cells. This distinct population, are better characterised and understood than MSCs and are solely responsible for the lifelong production of blood cells.[6, 41, 42] They have the ability to self-renew (generating at least one daughter cell with HSC potential), in addition to, differentiating into both lymphoid (T cell, B cell, natural killer cells and lymphoid dendritic cells) and myeloid (all other lineages) blood cells.[42] As well as HSC, *multipotent* hematopoietic progenitor cells (HPCs) have been identified. These have the same self-renewal ability and lineage potential but only for a limited time period, therefore HSCs are required for lifelong support.[42]

1.2.3.3 Epithelial Stem Cells (ESCs)

The epithelia is a continuous sheet of tightly linked cells that make-up surfaces (*e.g.* the epidermis) and linings (*e.g.* the respiratory and digestive tracts) of the body. They provide protection, as well as, regulating nutrient and water uptake and glandular secretions. As most epithelia are replaced constantly through out life (know as tissue homeostasis) a subset of self-renewing stem cells are required, and these have been identified as epithelial stem cells (ESCs). These cells can produce the entire cell phenotypes found in the epidermis, including goblet cells, paneth cells, absorptive cells and enteroendocrine cells. For a detailed review on ESCs see Blanpain *et al.*.[43]

1.2.3.4 Skin Stem Cells (SSCs)

More recently, a distinct subset of stem cells that maintain and repair the skin's epidermis have been identified. These skin stem cells have the ability to give rise to different epidermal cell lineages, including the surface barrier (keratinocytes), sweat glands, hair follicles and their associated sebaceous glands. To retain a homeostatic environment, a constant cellular turnover is required. This process in now thought to be controlled by several skin stem cells, located in specific epidermal regions, which maintain discrete compartments of the skin.[44-46]

1.2.3.5 Neural Stem Cells (NSCs)

The final subset of stem cells to be discussed is neural stem cells. Initially identified in the early 1990s, in fetal rat and mouse brain, they are capable of generating the three main phenotypes of the central nervous system (CNS), neurons, astrocytes and oligodendrocites.[47] Neural differentiation is an early event in mammalian embryogenesis, occurring soon after germ layer differentiation, with the formation of the neural plate. Further development leads to the formation of the neural tube, which initially consists of a morphologically similar set of cells, termed NSCs, which form the neuroepithelial lining. These NSCs, like all other stem cells, have the ability

to divide symmetrically (self-renew) or differentiate into a progeny of cells from which the mature cells of the CNS develop (for a detailed overview of CNS development see Kennea and Mahmet).[47, 48]

In addition to fetal NSCs, the subsequent confirmation that neurogenesis occurs in the adult brain, overturned a long term theory that we are born with all the nerve cells we require.[49] Currently, neurogenesis has been shown to occur throughout adulthood in two areas of the adult mammalian CNS: the olfactory bulb (OB) and the dentate gyrus (DG) of the hippocampus.[49] Neuronal cells develop in the adult OB are generated from neural progenitor cells (NPCs) found in the anterior part of the subventricular zone (SVZ).[50] Neurogenesis occurring in the DG of the hippocampus in adult humans is also controlled by NPCs generated in the subgranular zone (SGZ). These progenitor cells have the ability to differentiate into both neuronal and glial cells in the granular layer.[51, 52] Additionally, similar neurogenesis has been shown to occur in a number of other adult species, including rat and mouse (see Taupin and Gage for a full review).[49] It remains completely unclear whether NPCs are truly *multipotent*, although the demonstration that a population of self-renewing progenitor cells, cultured from NPCs from the adult brain regions discussed previously, suggests that these cultures contain NSCs.[49, 53] Furthermore NSCs have the potential to be derived from more primitive cells, such as pluripotent ES or EC cells, under the correct differentiation conditions.[53]

NSCs and NPCs are very exciting, both therapeutically, and as a research tool for developing our understanding of CNS development. In addition, the controlled differentiation of cells already committed to a neuronal lineage may hold the solution to a number of neurodegenerative diseases, such as Parkinson's, Alzheimer's and Huntington's diseases.[54-56] Both embryonic NSCs, such as the ReNcell VM line, and adult NPCs, such as the rat hippocampal HCN-nitGFP cell line, have been isolated and cultured successfully *in vitro*.[57, 58] Differentiation protocols have been published for these cell lines, including withdrawal of growth factors (epidermal growth factor (EGF) and fibroblast growth factor (FGF)) and addition of small molecules (all-*trans* retinoic acid (ATRA)) and neurotrophins (NTs).[57, 59, 60]

Currently these protocols are not highly efficient and reliable, meaning we are someway off successfully utilising NSCs/NPCs to their full potential.

1.3 Pathways Involved in Stem Cell Modulation

To be able to design and synthesise small molecules to control stem cells, an understanding of the molecular pathways involved in their maintenance and differentiation is required. Alongside advances in stem cell biology, the roles of a limited set of signaling cascades/pathways have been identified. This section will cover the six main pathways involved in regulating stem cells, the canonical Wnt cascade, hedgehog (Hh) signaling, the transforming growth factor-β superfamily (TGF-β), Notch, fibroblast growth factor (FGF) and retinoic acid (RA) pathways.

1.3.1 Canonical Wnt Cascade

The canonical Wnt cascade is crucial to the regulation of both stem cells and progenitors, having being linked to proliferation, self-renewal and differentiation.[61] Wnt signaling has been identified as having an integral role in cell maintenance and growth in the epidermal, intestinal and haematopoietic systems. In addition, dysregulation of the Wnt pathway has been associated with certain cancers, specifically where cancer stem cells are believe to be involved (see Reya and Clevers for a detailed review).[61]

The canonical Wnt cascade, as it is now known, first began to be understood after the discovery that the Drosophila polarity gene *Wingless* and the murine proto-oncogene *Int-1* had a common origin.[62] Briefly, when Wnt is not bound, β-catenin is targeted for proteasomal degradation by a group of proteins known as the destruction complex. This consists of two scaffolding proteins, axin and adenomatous polyposis coli (APC), and two kinases, casein kinase 1 (CK1) and glycogen synthase kinase 3 (GSK-3). Newly synthesised β-catenin, once bound, is sequentially phosphorylated on a set of conserved serine and threonine residues. The phosphorylation recruits ubiquitin ligase, which targets β-catenin for degradation and, in turn, inhibits the expression of the target genes. This has the effect of inhibiting stem cell differentiation and self-renewal. Upon Wnt binding, the destruction complexes can no longer bind β-catenin, as axin now interacts with

lipoprotein receptor-related protein (LRP) and/or disheveled (Dsh), although the exact mechanism is currently unspecified. This leads to an accumulation of β-catenin within the cell, which is then transported to the nucleus where it interacts with T-cell factor (TCF) and lymphoid enhancer factor (LEF) to bring about gene expression.[63] Both pathways are summarized in Figure 1.3.

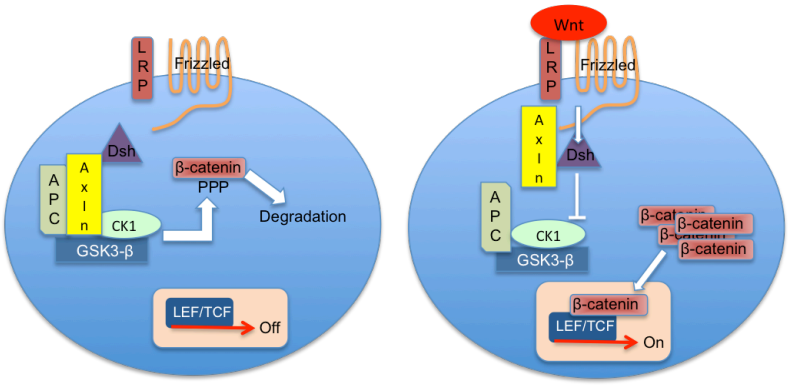

Figure 1.3 Canonical Wnt signaling pathway. Unbound (left cell) β-catenin is targeted for degradation by the destruction complex and genes remained switched off. Bound (right cell), the destruction complex is uncoupled, β-catenin builds up and relocates to the nucleus where it initiates gene transcription through interaction with LEF/TCF. Adapted from Reya and Clevers.[61]

1.3.1.1 Small Molecule Modulation of Wnt Pathway

As the pathway effects stem cell differentiation and proliferation small molecules, which can interact, have the potential to affect their outcome. One such class, are the GSK-3β inhibitors, which inhibit the phosphorylation/degradation of β-catenin, thus promoting target gene expression of the Wnt pathway. One example of such a compound is CHIR 99021, which has since been used in the generation of iPS cells in both mouse and humans.[64-66] In addition, the interaction of β-catenin with the transcription factors TCF/LEF has also been targeted by molecules such as PKF 115584, in an attempt to find alternative cancer treatments.[67] Approaching the pathway in the opposite direction, small molecule screens have identified molecules that inhibit the expression of Wnt genes, either through inhibiting Wnt production, or promoting β-catenin breakdown. Examples include IWP 2 and IWR 1.[68] In addition, the small molecule, XAV 939, has been identified as inhibiting the growth

of colorectal cancer cells, through stabilisation of the destruction complex, through a mode of action mechanistically similar to that of IWR 1.[69] The chemical structures of the Wnt modulators are shown in Figure 1.4.

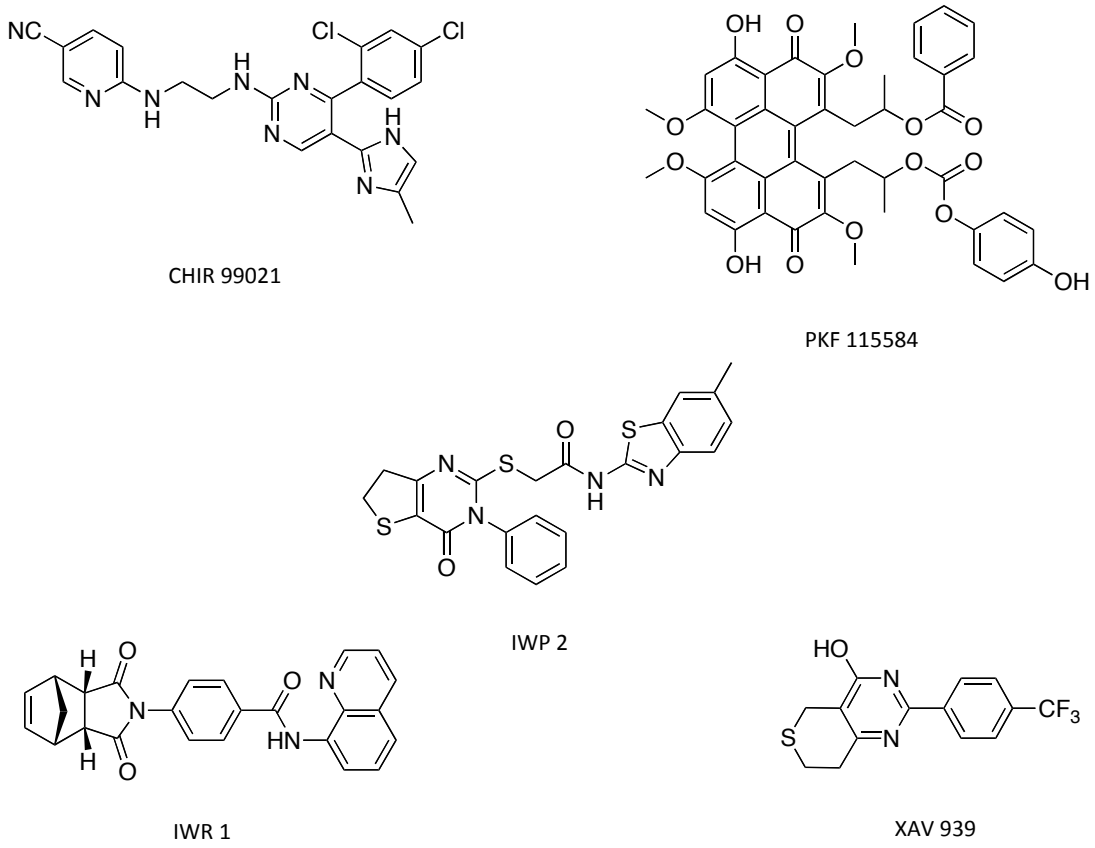

Figure 1.4 Small molecule modulators of the Wnt pathway.

1.3.2 Hedgehog Pathway

The hedgehog (Hh) signalling pathway has an intrinsic role in numerous processes in both embryogenesis and adult homeostasis, where it is involved in the maintenance of stem cell populations. The gene was first identified in the 1980s trying to understand body segmentation in *Drosophila*.[70] Subsequently, additional proteins have been identified as having roles within the pathway, which in turn has highlighted differences in the pathway between *Drosophila* and vertebrates (for a detailed review see Huangfu and Anderson).[71] In humans, irregularities in the pathway lead to a number of serious birth defects, including skeletal malformations

holoprosencephaly, craniofacial defects and polydactyly.[72] Furthermore, incorrect activation of the Hh pathway has been identified as being responsible for many basal cell carcinomas and other tumours.[73] In addition, vertebrates possess three Hh analogues Sonic, Indian and Desert Hh, however, current research suggests that these analogues all use the same signaling pathway. Signaling differences occur depending on the Hh molecule involved, for example Sonic Hh is involved in neural cell fate, while Indian Hh regulates digit formation.[74] For a more detailed review of the roles of the Hh family see Hooper and Scott.[75]

In brief, Hh proteins are secreted morphogens that initiate a response through binding of the Hh ligand to Patched-1 (Pct1), a 12 transmembrane protein receptor. When unbound, Pct1 inhibits Smoothened (Smo), but upon Hh binding Pct1 is inhibited, and Smo is activated. Downstream of Smo is a multi-protein complex known as the Hedgehog Signaling Complex (HhSC). This includes the Gli transcription factors (after glioblastoma) in mammals, or the Cubitus interruptus (Ci) in *Drosophilia*, bound to the Supressor of fused (Sufu) and serine/threonine kinase Fused (Fu). As Smo is no longer inhibited, it becomes phosphorylated by protein kinase A (PKA) and CK1. All three kinases, PKA, CK1 and GSK-3 are then released from the kinesin-like molecule Costal 2 (Cos), which prevents the cleavage of the transcription factors (Ci or Gli). Un-cleaved Ci or activated Gli (Gli^{Act}) is no longer inhibited by Sufu or Cos2 and enters the nucleus to induce the transcription of Hh target genes. In the absence of the Hh ligand, Smo remains repressed by Pct1 and the HSC remains bound together. Sequential phosphorylation leads to Ci being cleaved and/or processing or Gli3 into its repressor form (Gli^{Rep}). These cleaved/reprocessed transcription factors (Ci or Gli^{Rep}) enter the nucleus and acts as repressors, inhibiting Hh gene expression.[74, 76] The pathway is summarized in Figure 1.5.

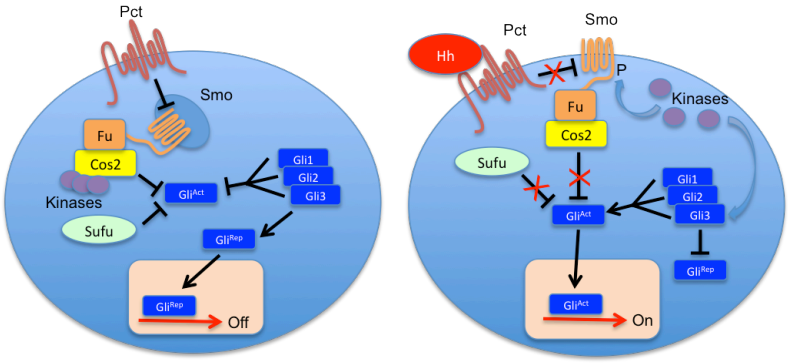

Figure 1.5 Hedgehog signaling pathway in mammals. Unbound (left cell) Pct inhibits Smo preventing its accumulation in the cilium. The activation of Gli proteins (Gli^{Act}), is inhibited by Sufu and Cos2. Gli3 is reprocessed into its repressor form (Gli^{Rep}), which inhibits gene expression. In the presence of Hh ligand (right cell), Pct inhibition is releaved. Smo is targeted to the cilium and activates Gli proteins, while inhibition by Sufu and Cos2 is repressed. Gli3 processing is inhibited and activated Gli initiated gene expression. Adapted from Huangfu and Anderson and Østerlund and Kogerman.[71, 74]

1.3.2.1 Small Molecule Modulation of Hedgehog Pathway

As discussed previously for the Wnt pathway, small molecules had been identified that act on the Hh pathway. At present, this pathways has one of the largest groups of small molecule activators, hence only a small number will be reviewed here. Most of these modulators have ben identified as acting on Smo, including the antagonists cyclopamine,[77, 78] and the SANT family 1-4,[79] and the agonists purmorphamine,[80, 81] and SAG.[79] Molecules acting on alternative sites include GANT 61,[82] which inhibits Gli mediated gene transactivation and JK 184, an antagonist of Hh activity which has no activity at Smo.[83] The chemical structures of the Hh modulators are shown in Figure 1.6.

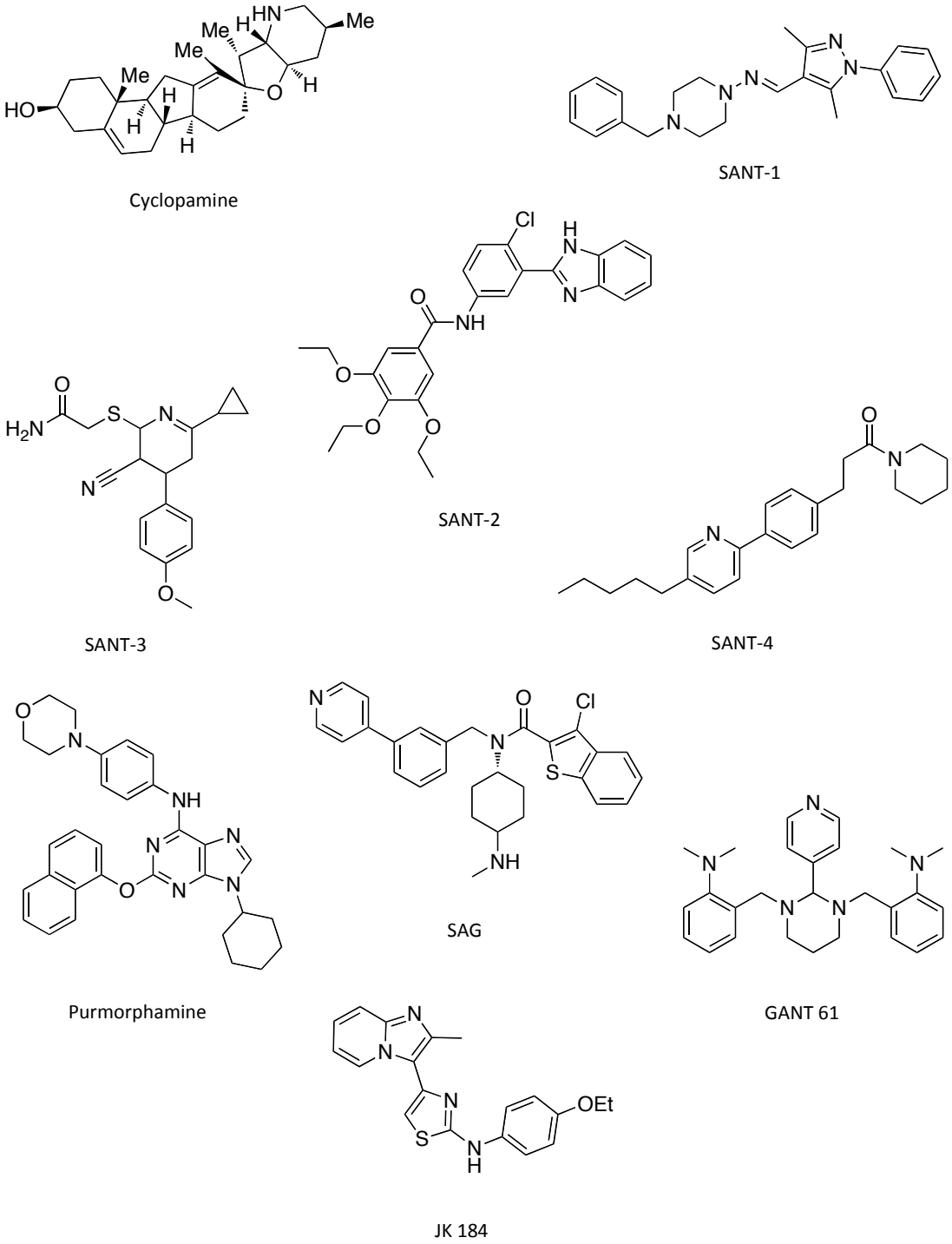

Figure 1.6 Small molecule modulators of the Hedgehog pathway

1.3.3 Transforming Growth Factor-β Superfamily

The transforming growth factor-β (TGF-β) superfamily is comprised of over 60 different structurally related growth factors, including bone morphogenetic proteins

(BMPs), Activins, Nodal, growth and differentiation factors (GDFs) and TGF-βs.[84] TGF-β, and other family members are expressed as disulfide-linked homodimers or heterodimers, and undergo proteolytic activation, a process which is highly regulated.[85] They are expressed widely in many cell types and have roles in tissue differentiation, affecting proliferation, migration and differentiation.[86]

The factors act on an inherently simple pathway, binding to a heteromeric receptor complex on the cell surface.[87-89] The receptor consists of two type I and two type II transmembrane serine/threonine kinases respectively, and upon growth factor binding transphosphorylation of the type I receptor by the type II receptor is induced. The activated type I receptors in turn phosphorylate selected intracellular mediators (Smads) at the C-terminus. The activated Smads then form a trimeric complex with a common Smad4. This complex relocates to the nucleus where it regulates the transcription of the target genes, through interactions with DNA binding transcription factors (X) and CBP or p300 coactivators.[90] The pathway is summarised in Figure 1.7.

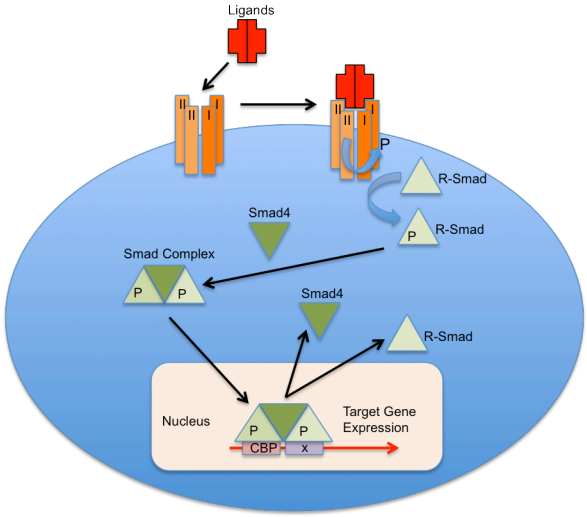

Figure 1.7 Transforming growth factor-β pathway. At the cell surface, the ligands bind a transmembrane receptor serine/threonine kinase complex (types I and II) which induces transphosphorylation of the type I receptor by the type II receptor kinases. The activated type I receptors phosphorylate selected Smads, and these receptor-activated Smads (R-Smads) then form a complex with a common Smad4. Smad complexes translocate into the nucleus, where they regulate transcription of target genes, through physical interaction and functional cooperation with DNA-binding transcription factors (X) and CBP. R-Smads and Smad4 shuttle between nucleus and cytoplasm. Adapted from Derynck and Zhang.[90]

The pathway is inherently simple, and although there are fewer receptors and even less Smads, the pathway is still substantially versatile.[90] This is brought about by interactions in the heteromeric receptor and Smad complexes, numerous proteins that interact with the receptors and Smads, and connections with sequence-specific transcription factors. For a detailed review of this versatility and specificity see Feng and Derynck.[86]

1.3.3.1 Small Molecule Modulation of TGF-β Superfamily

Perhaps due to the simplicity of the pathway, there have been relatively few reports of small molecules acting on the TGF-β pathway. Of those that have been reported, the first were inhibitors acting on the type I kinases of the hetertetrameric complex, such as SB 431542.[91] SB 431542 was initially characterised as stimulating proliferation, differentiation and sheet formation in endothelial cells derived from ES cells, although, more recently Ichida *et al.* demonstrated that it could replace Sox2 in reprogramming adult fibroblasts into iPS cells by inducing Nanog transcription.[29, 91] In

a separate chemical screen, Dorsomorphin, was identified as an inhibitor of BMP signaling, promoting cardiomyogenesis in ES cells.[92] Similar to SB 431542, Dorsomorphin also blocks activin receptor-like kinases. More recently, two small molecule agonists of the TGF-β pathway have been reported, namely IDE-1, and IDE-2. These compounds were identified from a large compound screen (>4000) and shown to direct endodermal differentiation in both mouse and human ES cells.[93] Chemical structures of TGF-β pathway modulators are shown in Figure 1.8.

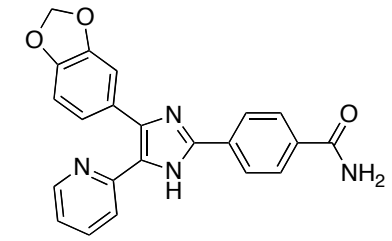

SB 431542

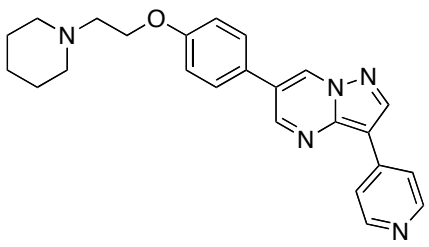

Dorsomorphin

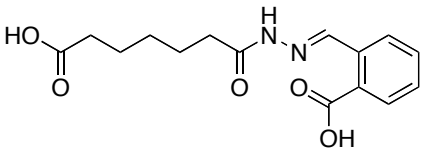

IDE 1

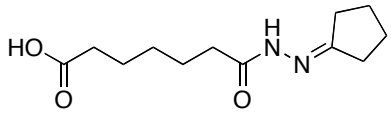

IDE 2

Figure 1.8 Small molecule modulators of the TGF-β pathway.

1.3.4 Notch Signaling

The Notch pathway acts differently to those pathways discussed previously, in that it signals only to adjacent cells. The signaling cascade determines both cell fate and pattern formation, a phenomenon key to reproducible development in multicellular life.[94,95] First identified almost 100 years ago in fruit flies which had 'notches' in their wings, it has since been identified as being responsible for mediating local cell-cell communication, fate and pattern formation, in all known metazoans.[96]

Notch is an unusual protein, as it functions at both the cell surface as a receptor but also in the nucleus, regulating gene expression. Classed as a single-pass

transmembrane protein, Notch contains an extracellular array of epidermal growth factor (EGF) repeats. Activation of Notch is triggered by a Delta-type ligand in a neighboring cell, which prompts two proteolytic cleavages of Notch, of which the second (S3) releases the Notch intracellular domain ($Notch^{intra}$). This translocates to the nucleus where its activates a transcription factor of the CBF1/Su(H)/LAG1 (CSL) family, by replacing the co-repressor (Co-R) complex with a co-activator (Co-A) complex, thus leading to gene activation (Figure 1.9).[94]

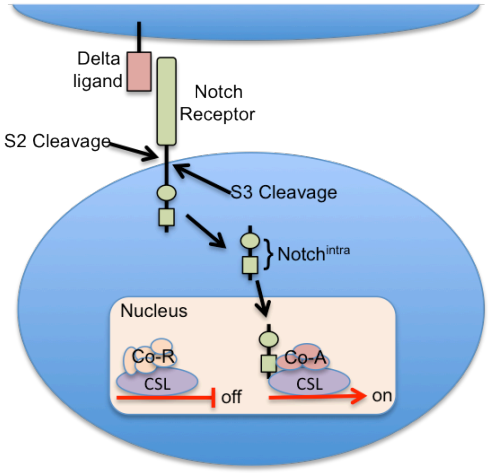

Figure 1.9 Fundamental actions of the Notch pathway. A Delta-type ligand from an adjacent cell activates the Notch receptor extracellular domain. This triggers two proteolytic cleavages (S2 and S3), which in turn releases the Notch intracellular domain ($Notch^{intra}$). $Notch^{intra}$ translocates to the nucleus where it initiates targeted gene expression through replacement of the co-repressor complex (Co-R) with the co-activator complex (Co-A) on the transcription factor CSL. Adapted from Lai.[94]

1.3.4.1 Small Molecule Modulation of the Notch Pathway

There are few reported small molecules that target the Notch pathway, albeit two antagonists *N*-[*N*-(3,5-difluorophenacetyl)-1-alanyl]-*S*-phenylglycine t-butyl ester (DAPT) and MRK 003 have been identified. DAPT was shown to reduce cell differentiation, while MRK 003 induced programmed cell death.[97, 98] The chemical structures of both compounds are shown in Figure 1.10.

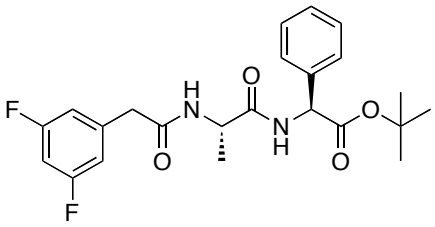

DAPT

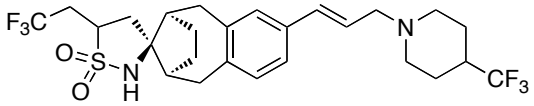

MRK-003

Figure 1.10 Small molecule modulators of the Notch pathway.

1.3.5 Fibroblast Growth Factor Signaling

The FGF signaling pathway incorporates 22 FGF members and 4 receptors. Consequently, this elaborate signaling network has many roles in development, including controlling proliferation, differentiation and migration, while in the adult it is involved in tissue repair.[99, 100] In addition to FGF involvement in many developmental processes, its dysregulation is accordingly associated with many cancers.[101]

Briefly, FGF signaling is activated by one of its ligands binding to a specific receptor, which causes the receptor to dimerise and the tyrosine kinase section to phosphorylate. The activated tyrosine kinase receptor then recruits specific proteins associated with the signaling cascade and activates them through phosphorylation.[102] There are a number of proteins/pathways associated with FGF signaling, including phospholipase Cγ (PLCγ),[103] Ras/mitogen-activated protein kinase (MAPK) pathway[104, 105] and phosphatidylinositol-3-kinase (PI-3K) (Figure 1.11).

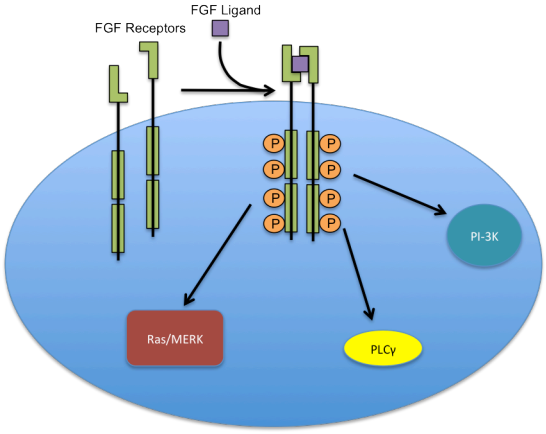

Figure 1.11 Simplified representation of the FGF pathway. An FGF ligand binds to the receptors causing dimperisation and subsequent phosphorylation. The activated receptor complex then phosphorylates downstream proteins, which elicit the FGF response. Adapted from Powers, McLeskey and Wellstein.[102]

1.3.5.1 Small Molecule Modulation of the FGF Pathway

As the pathway diverges considerably, incorporating a number of other signaling pathways, small molecules that specifically target FGF signaling generally act on the early stages of the pathway. One example is, PD 173074, which inhibits the FGF receptor, effectively antagonizing the effects of FGF on proliferation and differentiation.[106] Alternatively, small molecules have been identified/developed that target specific downstream pathways within FGF signaling. Two such examples are, PD 0325901 and CI-1040, both of which target the MAPK pathway.[107] CI-1040 has since undergone multicenter Phase II clinical trials for treatment of patients with advanced non-small-cell lung, breast, colon and pancreatic cancer.[108] The chemical structures of FGF modulators are shown in Figure 1.12.

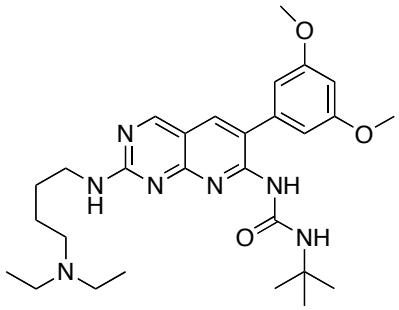

PD 173074

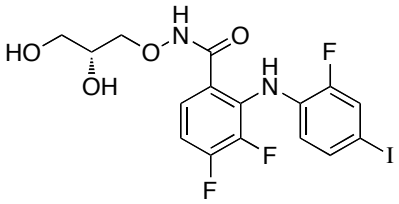

PD 0325901

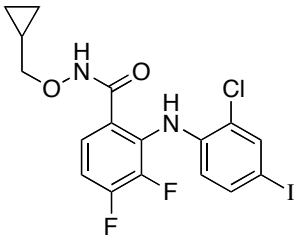

CI-1040

Figure 1.12 Small molecule modulators of the FGF pathway.

1.3.6 Retinoic Acid Signaling

The final pathway to be discussed is the retinoic acid pathway. This pathway is very complex and is involved in many developmental processes. Consequently, the retinoic acid pathway has been the focus of many developmental studies to identify small molecules with the ability to modulate specific responses. The following section will review what constitutes a retinoid, natural retinoid metabolism, storage and transportation and the mechanisms behind retinoid action, as these fundamentals are required to understand the roles retinoids play in cell differentiation and control. The functions of the endogenous ligands will be reviewed including their roles both in *in vivo* and *in vitro*. Finally, the limitations of the natural ligands will be discussed and how these have been addressed through the design of synthetic compounds.

1.3.6.1 Retinoids

Vitamin A (retinol) was first identified in 1913 as an essential fat-soluble nutrient present in butter fat and cod liver oil (Figure 1.13).[109] Over 60 years later, Sporn proposed the term 'retinoid' to broaden the base of thinking from just that of vitamin A. He wished to emphasize the greater potential of this class of molecules beyond that of nutrition and vision, and encourage understanding of the mechanistic relationships between metabolites of retinol and steroids.[110] The description of retinoids further evolved into the formal International Union of Pure and Applied Chemistry (IUPAC) structure based definition, which is: 'A class of compounds consisting of four isoprenoid units joined in a head-to-tail manner. Formally derived from a monocyclic parent compound containing five carbon-carbon double bonds and a functional group at the terminus of the acyclic portion'.[111] Subsequent use of the term more widely has extended it to describe a family of compounds that includes natural dietary vitamin A, its metabolites (ATRA, 9cRA and 13cRA (Figure 1.13)) and several thousand synthetic analogues. This is based around the common understanding that all molecules included, are either structurally related to retinol, and/or can elicit specific biological responses through binding to one or more of the retinoid receptors.[112, 113] Further classification from IUPAC was published in the late 1990's advising that retinoic acid analogues, which are unable to replace the full range of biological activities of retinol, are to be distinguished as 'retinoate analogues'.[114]

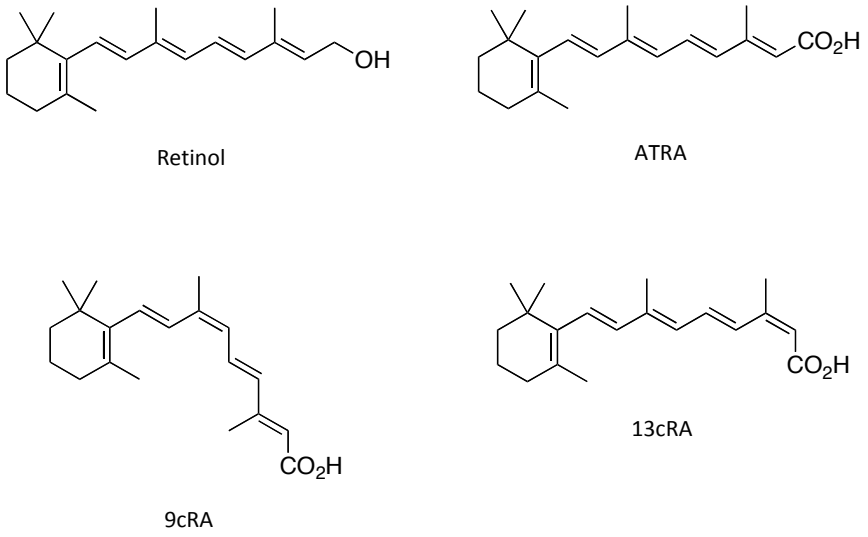

Figure 1.13 – Chemical structures of Retinol, ATRA, 9cRA and 13cRA.

1.3.6.2 Retinoid Metabolism, Transport and Storage

Humans along, with all other animal species, are incapable of *de novo* vitamin A synthesis, thus it is an essential dietary requirement. It can be attained as pre-formed vitamin A, in the form of retinyl esters from animal fats (such as fish, liver or dairy products), or as pro-vitamin A carotenoids (β-carotenoid). Once digested these carotenoids can then be converted into apo-carotenoids or retinal (Figure 1.14).[113]

The process, identified by Moore in the 1930s, occurs in the small intestine.[115] The enzyme that cleaves β-carotene (Figure 1.14) yielding two molecules of retinal, was later identified as β,β-carotene-15,15'-mono-oxygenase.[116, 117] An additional, asymmetric carotene cleavage, has since been discovered that yields two molecules of β-apocarotenals with different chain lengths.[118] The enzyme responsible for this cleavage, β,β-carotene-9',10'-di-oxygenase, cleaves a number of carotenoids, including β-carotene and lutein (Figure 1.14).[119] The larger fractionated section of the molecule can then be enzymatically shortened into retinoic acid or retinal. Retinal formed by these enzymes in the intestine is then reduced to retinol, although the retinal reductases remain unidentified.[113] Retinol is then absorbed by enterocytes, where it is bound to cellular retinol-binding protein type II (CRBP-II, also

known as RBP2). CRBP-II facilitates retinol esterification, catalysed by the enzyme lecithin:retinol acetyltransferase (LRAT). In addition, unbound cellular retinol is esterified by acyl-CoA retinol acyltransferase (ARAT), thus ensuring all retinol is processed accordingly.[120] The biological significance of CRBP-II, and subsequent esterification, is to solubilise the ligand, ensuring correct transportation and action while protecting it from degradation.[120, 121] Most retinyl esters are then packaged into chylomicrons,[122] which are large lipoprotein complexes that are subsequently secreted into the intestinal lymph in which they form chylomicron remnants.[123] It should be noted also, that some retinol is secreted into portal circulation unesterified.[124]

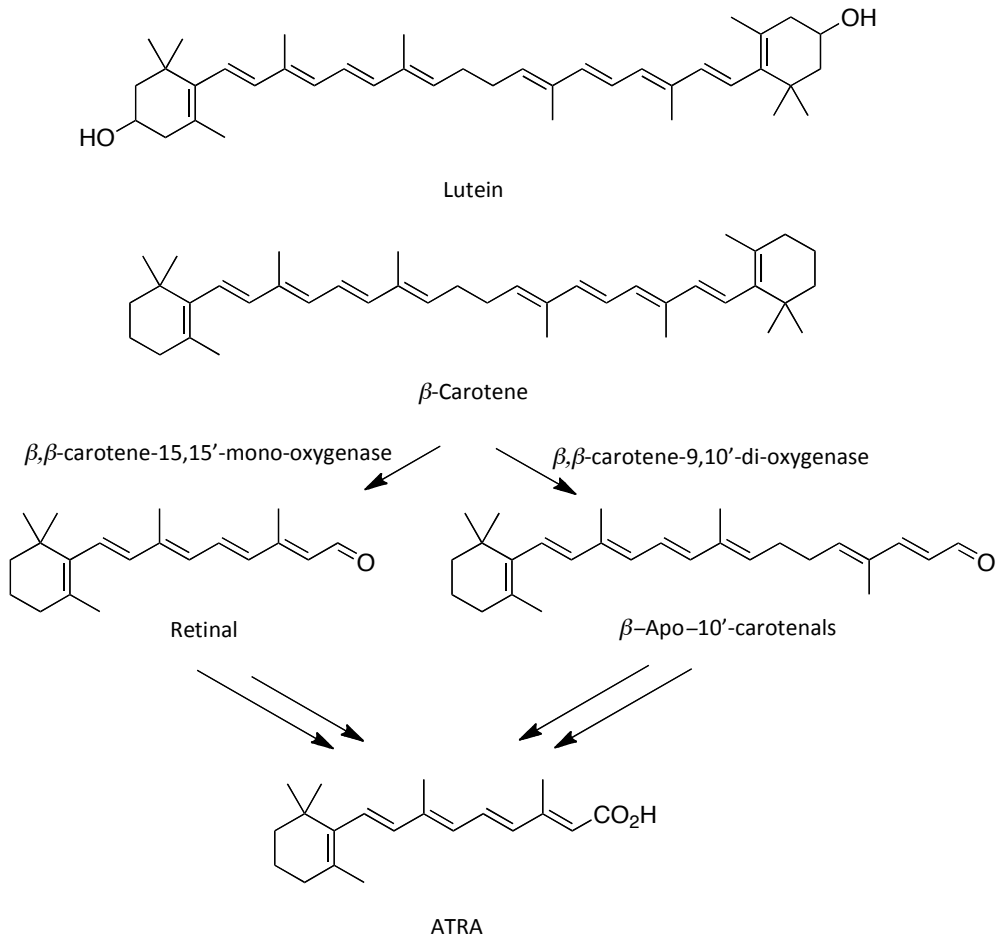

Figure 1.14 – Chemical structures of lutein, β-carotene, retinal and apo-10'-carotenals.

Most chylmicrons are then transported to the liver, where the retinyl esters are hydrolysed by retinyl ester hydrolase back to retinol.[125] Retinol is subsequently bound by a second cellular retinol-binding protein (CRBP-I, also known as RBP1) and processed for either secretion into the blood plasma or hepatic storage.[126] Retinol is stored as an esterified form in perisinusoidal stellate cells within the liver, in which both CRBP-I and LRAT are highly expressed and play pivotal roles.[113] The liver plays a key role in maintaining plasma retinol levels over a narrow range (constant blood concentration of 1-2 μM), storing 50-90% of the bodies total vitamin A content, and releasing it when required.[127]

Before secretion from the liver, retinol is bound to plasma retinol-binding protein (RBP4), and it remains associated with this protein as it is transported around the vascular system.[128, 129] The protein itself consists of a hydrophobic pocket that can bind and protect retinol during transport.[130] RBP4 can transport retinol alone, however most retinol is transported from the liver as an RBP4-transthyretin complex (RBP4-TTR), as this prevents glomerular filtration.[131] Retinol is then targeted to specific cells that contain the RBP4 cell membrane receptor, STRA6. STRA6 facilitates the transfer of retinol across the cell membrane to cytoplasmic cellular retinol-binding proteins (CRBPs).[132-135] In addition to binding to STRA6, passive diffusion is also believed to transport retinol across the cell membrane, as the general structure of all retinoids enables them to easily partition into the lipid phase of the membrane.[136-138] Furthermore, as RBP4 has been shown to have no binding affinity for 9cRA, 13cRA or any synthetic retinoids screened, their progression from the blood serum into cells/tissues is most likely to occur through indiscriminate diffusion.[138, 139]

Once inside the cell, retinol contributes to the synthesis of the major active retinoid metabolite, ATRA. Retinol is initially bound to CRBP, of which humans have four.[140] Retinol bound to CRBP is then oxidised reversibly to retinal by retinol dehydrogenase (ROLDH).[141] *In vitro*, many alcohol dehydrogenases (*e.g.* ADH1, ADH3 and ADH4) and members of the SDR (short-chain dehydrogenase/reductase) family (*e.g.* RDH1, RDH5 and RDH11) have been characterised as catalysing this process (for a more

detailed review refer to Blomhoff and Blomhoff).[113] The final oxidation of all-*trans*-retinal to ATRA is catalysed by retinal dehydroganase (RALDH). There are three different RALDH enzymes and their expression is varied through out different cell types, depending on their specific requirement for ATRA synthesis.[142] CRBPs have a high binding affinity for both retinol and retinal but not ATRA, thus ATRA is released upon production and is subsequently bound to cellular retinoic acid binding proteins I and II (CRABP-I and CRABP-II).[143, 144] CRABP-I has been shown to bind and store free ATRA, thus inhibiting its potential biological activity,[145] whereas CRABP-II is thought to aid in the local transport of ATRA to its receptors, increasing the cellular response to ATRA.[146] Thus, the CRABPs act to regulate the amount of intracellular ATRA available to the nuclear receptors, protecting the cell from ATRA-excess. Finally, the biological actions of the retinoids (ATRA or its isomers 9cRA or 13cRA) are elicited through binding to their cognitive nuclear receptors. These are classified into two types, the retinoic acid receptors (RARs) and the retinoid X receptors (RXRs), both of which will be reviewed in more detail later in this Chapter.[147-149] The overall process is summarised in Figure 1.15.

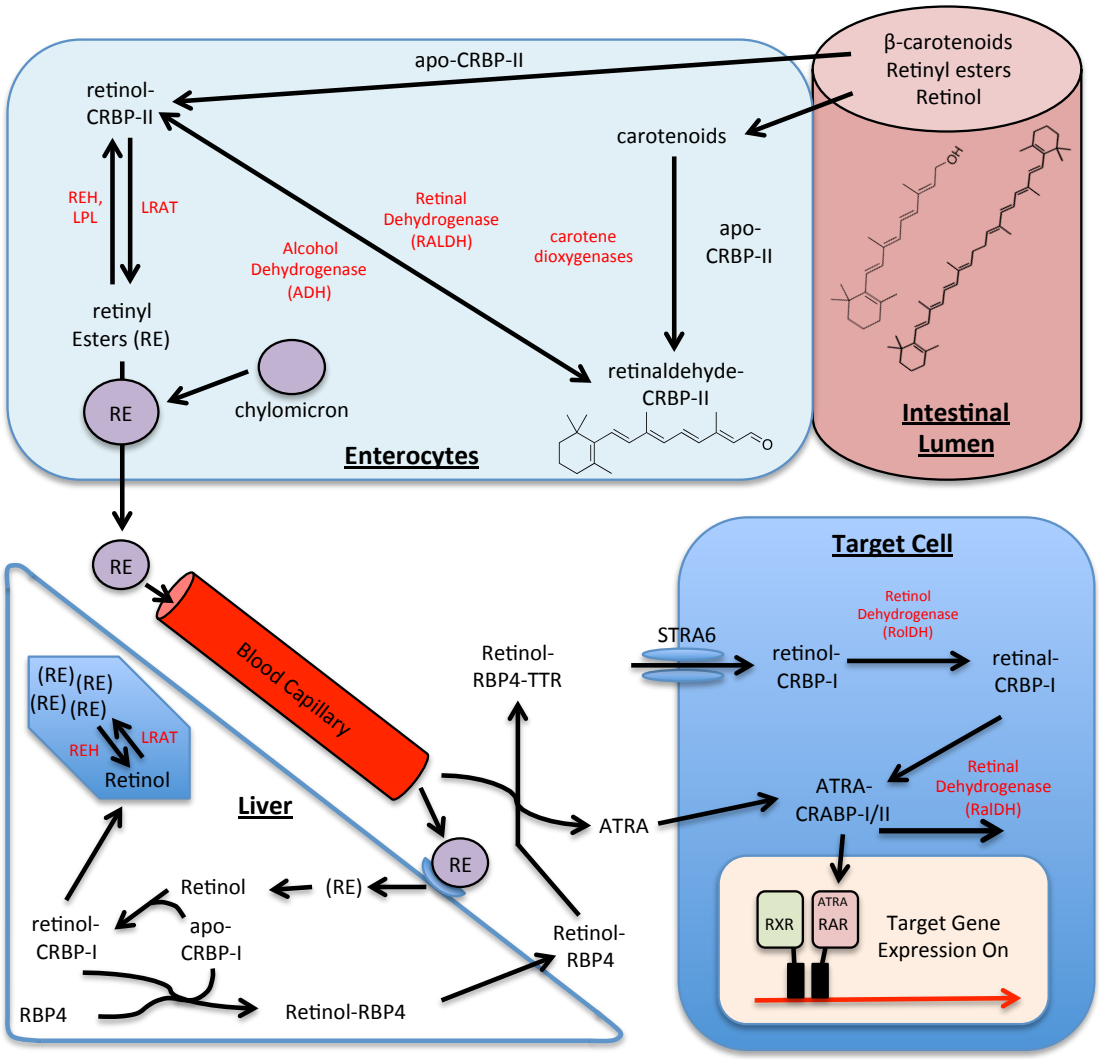

Figure 1.15 - The major pathways of retinoid transportation, storage and signal transduction in the body. Abbreviations: CRBP = cellular retinol binding protein, LPL = lipoprotein lipase, LRAT = lecithin-retinol acyltransferase, REH = retinyl ester hydroxylase, RBP = retinol binding protein and TTR = transthyretin. Adapted from Blomhoff and Blomhoff.[113]

1.3.6.3 Retinoid Receptors

As discussed above, there are two types of retinoid receptor, the RARs and the RXRs, both located in the nuclear envelope.[148, 149] Both receptor types belong to the steroid/thyroid superfamily of nuclear receptors, and act as ligand inducible transcriptional regulation factors.[150] They are classified based on variations in primary structure, the responses they have towards different ligands and their ability to modulate specific genes.[144] Composed of a modular structure, each retinoid

receptor contains five to six structural domains, termed A to F.[151] The two principal domains are the DNA-binding domain (DBD), and the ligand-binding domain (LBD). The DBD contains two highly conserved zinc-finger motifs (two antiparallel β-strands and a α-helix coordinated by a zinc atom), which enable the receptor to target DNA sequences known as hormone response elements. The LBD controls transcriptional regulation, and consists of the ligand-binding pocket (LBP), a dimerisation surface and a ligand-dependant transcriptional activation function (AF-2). The remaining domains are less well defined, with the *N*-terminal region (A/B domain) containing a ligand-independent activation function (AF-1) and an activation domain (AD). The D domain corresponds to a linker region, and hence has a pivotal role in the correct orientation of the LBD, and DBD within the bound dimer. Finally, there is the *C*-terminal (F domain) for which there is no assigned function, and does not exist in RXRs (Figure 1.16).[152]

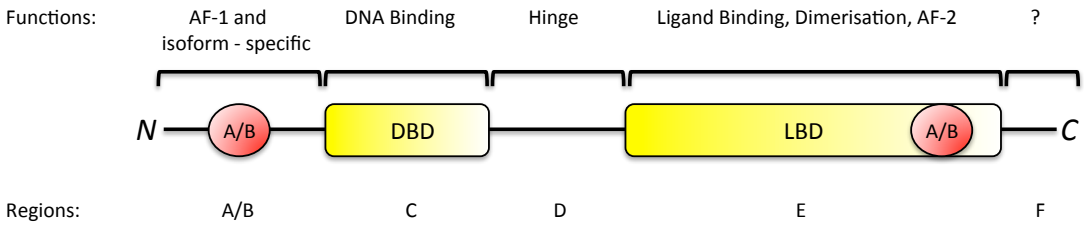

Figure 1.16 - Structural and Functional organisation of a retinoid receptor. Adapted from de Lera, Bourguet, Altucci and Gronemeyer.[152]

Signalling through the retinoid pathway is predominantly induced through receptor dimers, the most common being the RAR/RXR heterodimer, which is responsible for eliciting retinoid signals *in vivo*.[153, 154] In the absence of the retinoid agonist, the RAR/RXR heterodimer is bound to co-repressor proteins. These include nuclear receptor co-repressor (NCoR), silencing mediator for the retinoid and thyroid receptor (SMRT), and other associated factors, including histone deacetylases (HDACs) and DNA methyl transferases. The overall combination has the effect of repressing gene transcription, due to a condensed chromatin structure.[155-157]

The biological response is stimulated through the binding of an agonist (*e.g.* ATRA) to the RAR site of an RAR/RXR heterodimer, not through binding to the RXR.[158] When the agonist binds to the RAR, a conformational change occurs, in which the co-repressors are displaced, and co-activators recruited. The ligand-bound dimer complex can now bind onto a specific DNA sequence with high affinity. These sequences are in the promoter regions of specific genes, and termed retinoic acid response elements (RARE). The RAREs are direct repeats of the canonical motif 5'-PuG(G/T)TCA and are distinguished by their separation pattern of five, two, or one nucleotides (termed DR5, DR2 and DR1 respectively).[159] In DR5 and DR2 sequences the RAR/RXR dimer is associated with the RAR occupying the 3' element and the RXR the 5' (5'-RXR/RAR-3'), and this leads to a positive transcription of those target genes. The opposite is true for DR1 sequences, with the heterodimer being reversed (5'-RAR/RXR-3'). The consequence is that no transcription occurs, including when an agonist binds, as the co-repressors remain tightly bound.[160, 161] DR2 and DR5 elements have since been identified in many promoters of genes associated with the biological responses brought about by the retinoids.[148]

Binding of the ligand-bound dimer generally leads to a basal level of transcription. This encourages co-activators, including histone acetyl transferases (HATs) and histone arginine methyltransferases, to also bind to the complex. Once bound, the complete complex can fully open the chromatin structure, which ultimately leads to the transcription of the specific gene, and the required cellular response.[155-158, 162] The process is summarised in Figure 1.17.

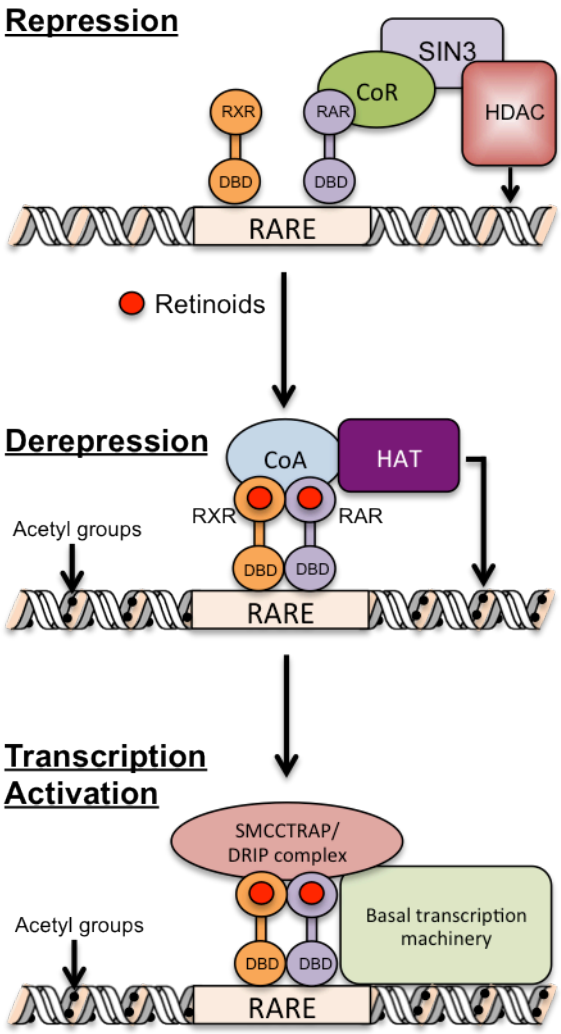

Figure 1.17 - Mechanisms of repression, depression and activated transcription. In the absence of agonists, co-repressor complexes (CoR) link the receptor complex to histone deacetylases (HDACs) through SIN3, resulting in chromatin condensation and gene silencing. Upon agonist binding to the receptors, a conformational change is induced, destabilising the CoR complex and allowing co-activators (CoA) to bind. CoAs recruit histone acetyltransferases (HAT) resulting in acetylation of histone amino-terminal tails, thus, inducing chromatin decondensation. Finally, a third multi-subunit complex, termed Srb and mediator protein-containing complex (SMCC), or thyroid-hormone-receptor-associated protein (TRAP), or D-receptor interacting protein (DRIP) establishes contact with the basal transcriptional machinery, leading to increased transcription. Adapted from Altucci and Gronemeyer.[162]

In addition, to further complicate the pathway, it should also be noted that there are multiple different types of RARs and RXRs (discussed in more detail in the following section). These form multiple different RAR/RXR heterodimers, and homodimers (RXRs only), and bind to different RAREs. Overall, these combined factors lead to the vast complexicity seen within the retinoid signalling pathway.[148, 149]

1.3.6.3.1 Retinoic Acid Receptors

The first receptor was discovered simultaneously by the groups of Chambon and Evans in 1987, and subsequently termed RAR-α1.[163, 164] RARs are presently classified into three subtypes, RAR-α, RAR-β and RAR-γ, all originating from three distinct genes.[163-168] A differential pattern of expression is observed for each of the subtypes, with RAR-α being ubiquitous in adults, whereas RAR-β and RAR-γ are more specific.[169] Each subtype also contains several isoforms that differ from each other in their *N*-terminal region. These arise from alternative splicing patterns and differential usage of two promoters. RAR-α and RAR-γ have two major isoforms (α1 and α2, and, γ1 and γ2 respectively), whereas RAR-β has four (β1-4). These four isoforms are due, in part, to the initiation of two different promoters (β1 and β3 being initiated from the P1 promoter, while β2 and β4 are initiated from the P2 promoter). The P2 promoter, is known as the downstream promoter, and is induced by retinoids, owing to the presence of a RARE.[148]

RARs must function as heterodimers, pairing with one of the three RXRs α, β or γ (elaborated further in the following section).[148] Additionally, they require the binding of a specific agonist to initiate transcription, although it has been suggested that RAR-β not bound to a ligand may act as a transcriptional regulator, as it has poor association to the co-repressors.[158] ATRA is an example of a *pan*-RAR agonist, binding with equal affinity to all three subtypes, although there are multiple examples of subtype specific compounds.[170] The RAR/RXR heterodimer ligand complex then binds to specific RAREs and initiates targeted gene expression (discussed previously).

1.3.6.3.2 Retinoic X Receptors

The second type of nuclear receptors, the RXRs, where initially discovered in 1990, and can also be divided into three subtypes, RXR-α, RXR-β and RXR-γ.[171] Each subtype also contains at least two isoforms (α1 and α2, β1 and β2 and γ1 and γ2 respectively).[172] Like the RARs they also have differential and spatial patterning, with RXR-α being limited to expression in the liver, skin, kidney and lung, in both the adult and embryo, with RXR-β having a more ubiquitous expression pattern.[148, 149] Unlike the RARs they are not modulated by ATRA, instead they are modulated by 9*c*RA, which has the ability to bind all RARs and RXRs.[170, 173]

RXRs are able to act as both homodimers, pairing up with themselves, or heterodimers, pairing with RARs, or other receptor compounds, such as peroxisome-proliferation-activated-receptors (PPARs), thyroid hormone and vitamin D_3 receptors (VDRs).[174] In contrast to RAR agonists, RXR selective agonists (also termed rexinoids) are unable to activate transcription upon binding to the RXR. This is because rexinoid binding does not induce the co-repressors to dissociate, so for transcription to occur a RAR ligand must also be present. This is referred to as RXR subordination, or silencing.[149, 158] Although, as a heterodimer with an RAR receptor, their role is better defined as synergistic, as they allosterically increase the potency of the RAR ligands for their receptors.[175, 176]

As RXRs also form RXR/RXR homodimers, it was hypothesised they must additionally act *via* another signalling pathway, possibly binding to retinoic X response elements (RXREs). This hypothesis has since been validated, and RXR/RXR homodimers are known to bind to specific DNA sequences through a DR1 element, although their exact role has yet to be defined.[177]

Overall, RXRs have the ability to affect multiple hormone signalling pathways. Additionally, with their varied tissue expression patterns this further helps to illustrate the complexity and varied role played by retinoids and their receptors in many biological systems.

1.3.6.4 Endogenous Retinoid Function

Natural retinoids are essential for the life of all chordates, and are involved in the modulation of a wide variety of biological processes, during both embryogenesis and adulthood. Some of these essential roles include vision,[178] immune competence,[179] reproduction,[180] maintenance of epithelial surfaces,[113] embryonic growth and development[181] and cellular regulation and differentiation.[182-184,] In humans, inadequate intake of vitamin A leads to vitamin A deficiency (VAD), which is characterised by several ocular features, including xerophthalmia (dry eyes) and night blindness, as well as poorer immune responses.[113] ATRA, the most potent naturally occurring biological metabolite, can both prevent and resolve the consequences of VAD.[185]

In developmental terms, the ability of the retinoids, particularly ATRA, to promote differentiation,[182-184] apoptosis[186] and spatial positioning of cells,[187] means retinoids play a key role in the growth of various tissues and organs. Specifically, in terms of neurogenesis, retinoids have numerous roles in both the developing central nervous system (CNS) within the embryo[188] and regeneration of the developed CNS in adults.[189] Alterations to the levels of ATRA in the developing brain and CNS lead to many abnormalities.[188, 190] While in the adult CNS, ATRA is involved in the synaptic plasticity seen in the hippocampus.[191] Certain areas in the adult CNS, including the hippocampus, basal ganglia, olfactory bulbs and auditory afferents have also been identified as possessing the capability to synthesise ATRA.[192] Furthermore, it has been demonstrated that ATRA is required in an early phase of adult neuronal differentiation, in the dentate gyrous.[193]

In addition, further studies have also shown a clear link between the retinoids and higher cognitive functions, including spatial learning and memory. This is believed to be caused through neuronal remodelling in the hippocampus, which has also been linked to long-term depression (LTD) and long-term potentiation (LTP).[191] In a supporting study, VAD in rats induced a significant deficit in both memory and spatial learning, which could be reversed by the re-introduction of vitamin A.[194]

Christie *et al.* provide a more detailed review of the role retinoids play in the adult nervous system and their potential therapeutic uses.[195]

1.3.6.5 Conclusions

The vast biological profile exhibited by ATRA and its natural metabolites has lead to much interest in using these molecules, and synthetic analogues, as both therapeutic treatments and tools for research, particularly in controlling the differentiation of stem cells. Consequently, more than 4000 compounds related to retinol and ATRA have been synthesised and published, and many of these have been screened for potential biological activity, an area that will be reviewed further in the following section of this Chapter.

1.4 Small Molecule Control of Cell Differentiation

In attempts to harvest the full potential of stem cells, many groups have looked to chemical control as a solution. There are many advantages to using small molecules over more traditional genetic approaches to understanding a biological phenomenon. These include the high degree of temporal control one can achieve when using a small molecule, as it can potentially disturb specific functions of single or multiple proteins. Furthermore, the effects can be finely regulated through simple changes in concentration.[196]

As technology in automation and analysis has developed, small molecule libraries of compounds have been designed as a simple and cost effective approach to identifying potential targets. These libraries span from large lead discovery collections of over 2 million compounds, associated with pharmaceutical companies, to smaller focused collections of approximately 10 thousand compounds, generally comprised of one or two specific classes.[197] This is in an attempt to identify new families of compounds, which would help unlock the full potential of these cells. As there are multiple different potential fates for stem cells, specific libraries are screened in an attempt to identify molecules with a particular desired biological activity. In addition, there are different types of stem cell, from *pluripotent* ES cells to *multipotent* stem cells of specific tissues, all of which are then species specific (see previous sections for more detail). Consequently, the number of possible targets and components is high and currently tens of molecules have been identified as being controllers of stem cell fate, some of which have been highlighted throughout this review, but for a more detailed review see Lyssiotis *et al.*.[197]

In addition to screening large novel libraries, other approaches include targeting specific pathways, or known natural products in an attempt to enhance or identify novel uses *in vitro*. Additionally, the screening of known drug compounds has been carried out in an attempt to identify new uses for these known compounds. All of these processes will now be reviewed in more detail.

1.4.1 Retinoic Acid Control of Cell Differentiation

Another approach is to utilise natural molecules and known pathways. One pathway where this has been exploited successfully is the retinoic acid pathway (discussed in detail in the previous section). The establishment of the role retinoids play in differentiation *in vivo*, and the induction of plasminogen activator synthesis in chicken embryo fibroblasts by ATRA, led to the first example of retinoic acid being used to induced differentiation *in vitro*.[184, 198, 199] Teratocarcinoma stem cells treated with ATRA were shown to display multiple phenotypic changes, consistent with differentiation into endoderm.[199] Since then multiple EC cell lines have been induced to differentiate using ATRA. These include the mouse EC cell lines, F9, which upon ATRA treatment differentiates to primitive, parietal and visceral endodermal cells, and P19, which differentiates to endodermal and neuronal cells.[200-202] Other EC cell lines include, GCT27 and NCCIT, which displayed the ability to form extraembryonic endoderm, and keratin, glial fibrillary acid protein (GFAP), and neurofilament-positive somatic cells**,** when exposed to ATRA respectively.[203, 204]

One of the more studied lineages is that derived from the EC stem cell line TERA2. In 1984 Andrews published data that EC TERA2 cell lines NTERA2/D1 and NTERA2/B9, could differentiate comprehensively when exposed to ATRA. This was characterised by the disappearance of stage-specific embryonic antigen-3 (SSEA-3), routinely expressed by human EC cells, in addition to morphological changes, including the appearance of neurons that stain positive for neurofilament proteins.[205-207] Additionally, a later investigation looking at transcriptional profiling in NTERA2/D1 cells, showed ATRA regulated the expression of Pax6 and Nkx6.1. These data indicated that neurons derived from these pluripotent cells were characteristic of neuroectodermal cells of the ventral phenotype.[208] Subsequently, further sublineages were developed, most notably TERA2.cl.SP12, which upon ATRA treatment lose their expression of cell-surface pluripotent markers (SSEA-3, SSEA-4 and TRA-1-60), while simultaneously acquiring antigens associated with neuroectodermal derivatives (VINIS-56 and A2B5).[209-211] Further evaluation of the TERA2.cl.SP12 lineage showed that prolonged exposure to ATRA led to the formation

of mature functioning neurons, containing functional receptors and ion channels indicative of native neurons.[212, 213] ATRA induced differentiation is not confined just to EC cells. There are a number of examples in which ES cells have been induced to differentiate also using ATRA.[200] These include the generation of epithelial cells from the AB1 murine ES cell line, and the formation of neural progenitor cells (visualised as neural rosettes) and motor neurons (analysis of HB9 expression), from the human ES cell line H9.[59, 214-216] Furthermore, the group of T. M. Jessell showed that mouse ES cells could be induced to generate motor neurons (MNs) and the pathway used *in vitro* recapitulates the steps of MN generation *in vivo*. Briefly, the protocol involved primary neutralisation, followed by the caudalisation of neural cells before ventralising the caudalised cells, using relevant signalling factors including ATRA. ES cell-derived MNs were then shown to populate embryonic spinal cord and target muscles through extending axons and generating synapses.[217]

Furthermore, the isolation of NCSs and NPCs from both rodent and human species has generated much interest, in particular in the development of new therapies for neurodegenerative diseases.[54-58, 60, 218-220] At the forefront of this area of research is the ability to manipulate these cell types *in vitro* to produce reliable and reproducible differentiation, which subsequently may transpire into therapeutic treatments. ATRA has a well-characterised role *in vivo* in both the development of the CNS during embryogenesis and synaptic plasticity seen in adults.[188, 190, 191] It is therefore not surprising that isolated adult rat hippocampus stem cell cultures differentiate to immature neurons upon exposure to ATRA, characterised by up-regulation of NeuroD, increased p21 expression and concurrent exit from the cell cycle.[60] Additionally, culturing of neurons without serum theoretically is more appealing as the process has greater controls, as serum contains multiple undefined factors. Defined supplements, such as B27, have become widely utilised because of this, and in addition to many other factors commonly include ATRA.[221] In addition, the differentiation of human neural progenitors has also shown to be enhanced through additional supplementation of retinoid analogues, including ATRA.[59]

1.4.1.1 Limitations of ATRA in Cell Differentiation

The wide biological effects elicited by ATRA make it an obvious drug target for many clinical applications and *in vitro* cell differentiation techniques. However, the usefulness of ATRA in both disease treatment (for a review of this area see Christie *et al.*)[195] and routine cell culture/differentiation, as described above, is severely hampered by ATRA's potent teratogenicity and rapid metabolism (see later discussion and Figure 1.19) in many cell types.[222-226] One hypothesised reason behind ATRA's toxicity and high dosage requirements, is its susceptibility to isomerise.[227] As ATRA (and indeed all natural retinoids) contain five conjugated double bonds, they are inherently unstable. Each bond is capable of isomerising, with each species likely to possess a different biological activity. Furthermore, it has since been determined that not only does ATRA isomerise under standard laboratory conditions, but also degrades into a number of other compounds.[228] A warning of this nature was conveyed by Muryama *et al.*,[229] who highlighted the potential detrimental effects of using ATRA as a tool for cell biology, as an investigator would not know exactly which compounds were being using.

1.4.2 Analogues of ATRA for Controlling Stem Cell Differentiation

Consequently, both academic and commercial organisations have turned to designing, synthesising and screening large numbers of molecules that are structurally and/or functionally analogous to ATRA. The ultimate aim being that these synthetic analogues display an improved biological response and in turn have reduced adverse side effects.

Roche carried out the first published work in this area, in the late 1960s. They prepared analogues of ATRA, through modification of the structure of retinol, where their aim was to identify compounds with a better therapeutic ratio than that of the parent compound.[230] Since then more than 4000 compounds related to retinol and ATRA have been synthesised and published, and many of these have been screened for potential biological activity.[231] Consequently, over the last forty years thousands

of retinoids have been synthesised and screened. The main focus of researching these molecules has been an attempt to demonstrate the clinical potential of the retinoid pathway and provide pharmacological tools to probe the endogenous functions of natural retinoids and their receptors.

1.4.2.1 Structural Requirements

In the late 1970s the relationship between structure and activity of different retinoids was first published.[232] Since then many analogues have been synthesised and screened, in an iterative approach, modifying key components in the basic structure of ATRA.[233-236] This research, alongside crystal structures of both the RAR and RXR ligand binding domains, in both the bound (*holo*) and unbound (*apo*) form (for a detailed review refer to Greschik and Moras[237]), has lead to the basic understanding of the ATRA pharmacophore that we have today. Currently, retinoids are considered to be comprised of three units (depicted in Figure 1.18 for ATRA), and discussed in more detail below.

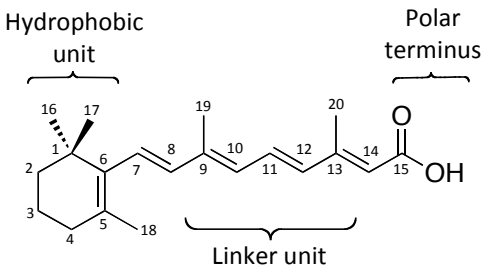

Figure 1.18 General perception of the structural units that comprise a retinoid.

The three key structural components are as follows:

1- A hydrophobic unit: relatively bulky in size, usually a planar lipophilic cyclohexene with alkyl substituents that can form van der Waals interactions with surrounding amino acid residues in the receptor binding pocket.
2- A conjugated linker unit: designed to confer the correct spacing and orientation between the two other regions to promote the highest degree of

binding interaction. This region can incorporate heteroatoms, which may confer isotype specificity and may be conformationally restricted, through the incorporation of aromatic rings.

3- A polar terminus: usually a carboxylic acid involved in the formation of hydrogen bonds and salt bridges.

This knowledge of the pharmacophore has aided in our advanced understanding of tolerable bioisosteric replacements for each of the fundamental structural components (summarised by Altucci *at al.*[233]). Initially, early synthetic derivatives were related closely to that of ATRA, while later generations display little if any resemblance to the parent compound.

Literature has shown that replacing the trimethylcyclohexenylvinyl unit (C_1-C_8) of ATRA, with a structurally similar 1,1,4,4-tetramethyl-1,2,3,4-tetrahydronaphthalene (TMTN) moiety, increases the biological potential.[238] This can be explained by the fact that the TMTN moiety helps to introduce greater stability, as it eliminates a section of the unstable polyene chain, removing one of the isomerisable bonds. In addition, and of greater importance, it no longer possesses any allylic protons or alkene double bonds susceptible to radical oxidation or epoxidation by cytochrome P450 (CYPs) or related enzymes (see Figure 1.19).[239-242] Therefore synthetic derivatives possessing this bioisostere are less susceptible to metabolism and are thus more likely to remain at a constant concentration within the cellular environment.

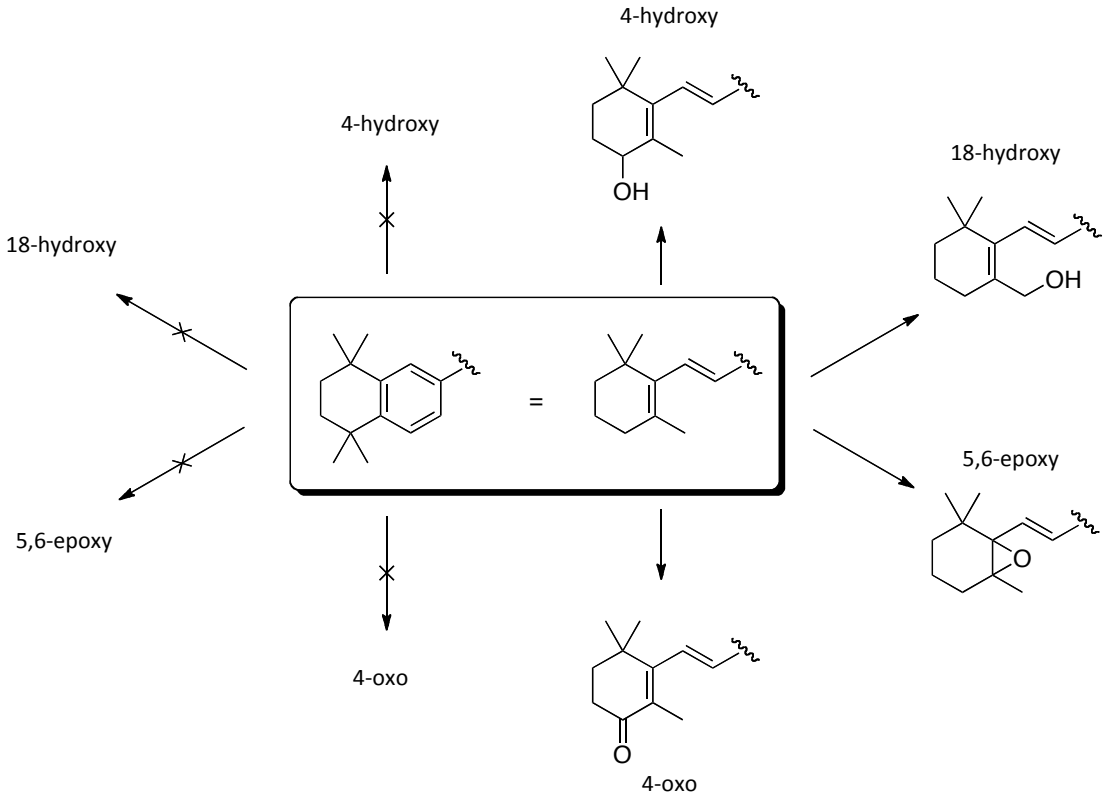

Figure 1.19 Oxidative products of ATRA metabolism, blocked by replacement with TMTN unit.

In addition to the TMTN core, our group has previously replaced the remainder of the polyene chain with a non-isomerisable acetylene linker and an aromatic ring functionalised at both the *para* (EC23) and *meta* (EC19) positions (Figure 1.20).[228] These modifications generate synthetic compounds know as arotinoids as they contain one or more aromatic rings. There are many other examples of arotinoids, including TTNPB and TTNN, refer to Barnard *et al.* for a more detailed review.[231] (Figure 1.20).

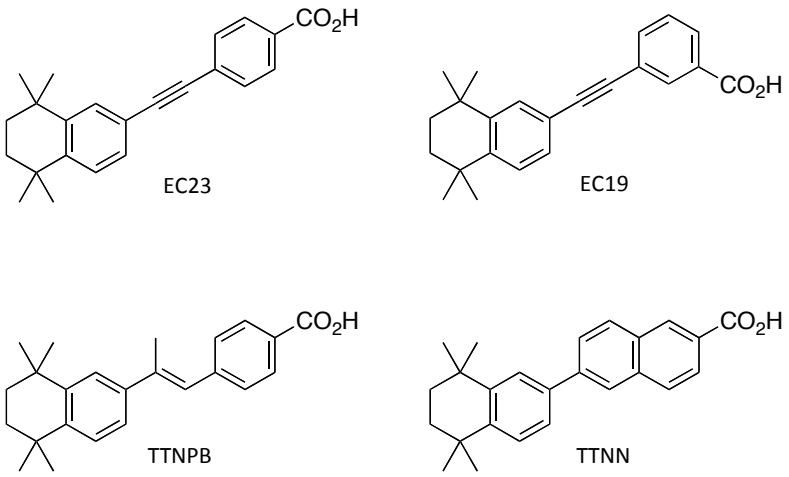

Figure 1.20 Chemical structures of EC23, EC19, TTNPB and TTNN.

1.4.2.2 Retinoic Acid Analogue Induced Neurogenesis

As discussed previously, ATRA induces differentiation in many cell lines, particularly down a neuronal lineage.[59, 60, 200, 202, 204-213, 216, 217] Although, inherent limitations in its structure, most notably its instability, and tendency to isomerise lead to pleiotropic effects.[222-229] Hence, many synthetic retinoids have been designed, and tested, in an attempt to produce analogues that induce differentiation more efficiently and reproducibly. This is especially important where reproduction of cell behaviour is required, for example, the consistent differentiation of stem cells into homogeneous populations of neuronal precursors and functioning neurons. These homogeneous cell populations could then be used as research tools, for drug development and screening.

One example of a more potent inducer of neurogenesis is EC23. It displays both a robust stability profile, as it cannot isomerise, as well as exhibiting a higher neurogenesis inducing activity.[59, 228] In a *pluripotent* stem cell model, exposure to EC23 formed populations of terminally differentiated neurons. Immunocytochemical analysis of neurofilament-200 (NF-200) in differentiated cultures showed EC23 to be a more potent inducer of neurogenesis than ATRA. In direct comparison to ATRA, EC23 induces larger numbers of neural cells with less variability.[228] In addition EC23

has been shown to induce neuronal differentiation in both ES cell systems, fetal NSCs and adult NPCs.[59, 243]

1.4.3 Alternative Small Molecule Inducers of Neurogenesis

Other approaches in identifying small molecule inducers of neurogenesis include, screening known natural products, for previously unknown effects. One early example was the discovery that the PKA agonist, forskolin (FSK), promotes neurogenesis of NSCs *in vitro* (structure shown in Figure 1.21). The mode of action of FSK, is to increase the intracellular cyclic adenosine monophosphate (cAMP) concentration, which blocks Hh signalling.[244] In addition, when FSK is used in combination with ATRA to differentiate NSCs, a greater number of neurons are observed.[245]

More recently, as the understanding of the CNS has developed, it was suggested that drugs that confer antidepressant behaviour do this through stimulating hippocampal neurogenesis *in vivo*.[197] Thus, screening chronic anti-depression drugs, identified fluoxetine, as being able to stimulate neurogenesis in the dentate gyrus of the rat hippocampus (structure shown in Figure 1.21).[246] This suggest that this molecule, and possibly others with similar anti-depression properties, are likely to promote the neurogenesis of NPCs and NSCs not only *in vivo* but also *in vitro*, although this has yet to be proved.

In addition to targeting specific pathways, natural products or known drug compounds, a greater understanding of the critical role chromatin modification plays in the regulation of cell-type-specific gene expression identified HDAC inhibitors as a likely target. Hsieh *et al*., demonstrated this through small molecule inhibition of HDACs, using valproic acid (VPA), promoted neuronal differentiation of adult rat NSCs (structure shown in Figure 1.21).[247] Furthermore, the NSCs differentiated specifically into neurons even under astrocyte and oligodendrocyte lineage-specific differentiation conditions *in vitro* and had anti-proliferative and neuronal inducing properties in the dentate gyrus of adult rats *in vivo*.[247]

In addition to the approaches described above, the screening of large compound libraries has identified novel compounds and structures, some of which specifically induce neurogenesis. One such screen, on a large heterocyclic library, carried out by Ding *et al.*, identified TWS119, a 4,6-disubstituted pyrrolopyrimidine, which induced neurogenesis in both mouse P19 EC cells and the ESC line D3. They further went on to identify the target of TWS119 as glycogen synthase kinase-3β (GSK-3β) providing the first evidence that GSK-3β is involved in neurogenesis of ESCs.[248]

A similar study carried out by Saxe *et al*., identified the orphan ligand phosphoserine (P-Ser) as an inhibitor or murine NSC proliferation and self-renewal, while enhancing neurogenic commitment and improving neuronal survival (structure shown in Figure 1.21). P-Ser was also shown to increase neurogenesis in human ES cell derived NPCs, suggesting that rodent and human pathways are in some part similar.[249]

Finally, in an additional study, using the same approach of screening a library of 50,000 compounds, Warashina *et al.* identified a class of compounds that selectively induced differentiation of hippocampal neural progenitors.[250] The class of compounds, 4-aminothiazols, were then subjected to a small structure-activity relationship (SAR) study, which identified neuropathiazol as being the most potent analogue (Figure 1.21). Treatment of the cells with neuropathiazol slowed cell proliferation and differentiated more than 90% into TuJ1 positive cells, with very few GFAP-positive cells visualised. In comparison, treatment with ATRA showed weaker antiproliferation activity, and large numbers of both TuJ1 and GFAP-positive cells were found. In addition, ATRA showed greater cytotoxicity compared to that of neuropathiazol. Cells incubated for greater time periods with neuropathiazol also demonstrated positive staining for mature neuronal markers neurofilament-H and MAP2ab, while real-time quantitative polymerase chain reaction (RT-PCR) analysis demonstrated Sox2 downregulation and NeuroD1 upregulation. Finally, they demonstrated that astroglial differentiation, induced by leukemia inhibitory factor (LIF) and BMP2, was inhibited by neuropathiazol but not by ATRA.[250]

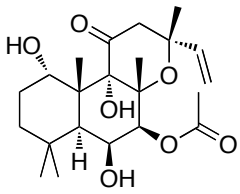

Forskolin

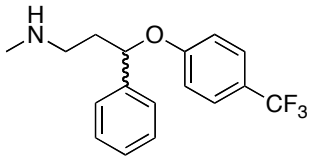

Fluoxetine

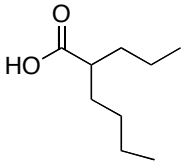

Valproic Acid

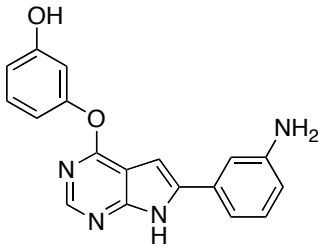

TWS119

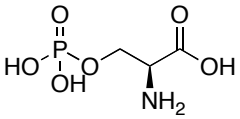

Phosphoserine (P-Ser)

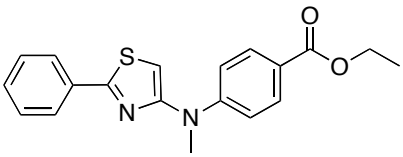

Neuropathiazol

Figure 1.21 Structures of small molecule inducers of neurogenesis.

1.5 Conclusions

A sizeable amount of research has been conducted to both understand stem cells, and the molecular pathways which ultimately control their fate. One area of this research has focussed on the discovery of new compounds, which can interact with specific pathways to generate a desired outcome. To date, small molecules have been identified and designed to act on each of the pathways involved in stem cell modulation.

There are two main ways in which the identification of novel modulators has been approached. The first, is the screening of large libraries of known compounds in an attempt to identify new molecular structures, which have the desired effect. The second, is to study the individual pathway, understand how to control the desired biological outcome, investigate the natural ligands, and design and screen new compounds which address any issues associated with the natural compound. Although both approaches have proven successful, with the identification of numerous new compounds, some of which are highlighted in this review, the first approach requires a significant amount of trial and error, specialised automated equipment and access to vast chemical libraries. It is therefore not surprising that the second approach is more widely used in academic situations, and one adopted by our research group in Durham, specifically targeting the retinoid pathway.

Currently, defined chemical control of stem cell fate is not completely reproducible and reliable, but with continued research this should be resolved in the near future. This will in turn hopefully lead to new therapeutic treatments and subsequently unlock the full potential of stem cells.

1.6 Project Aims

The main aim of this work is to develop synthetic retinoids to increase the reliability and reproducibility of stem cell differentiation, in particular, enhancing neural differentiation *in vitro*. The compounds must be novel in structure, be more stable than their natural equivalents, and more resistant to metabolism, as all these properties have been highlighted as problematic in previous screens. They will be designed around known limitations, and follow on from compounds previously developed in Durham, which demonstrate a strong potential.

The research detailed in this thesis builds on recent work into the synthesis and stabilisation of conjugated polyene chains, structure-activity-relationships of retinoids, and characterisation of their biological potential in both pluripotent cell models and those, which are already committed to a neuronal lineage.

In addition, molecules structurally unrelated to retinoids but with similar biological effects will be investigated further, in an attempt to elucidate their mechanism of action and identify compounds that induce reproducible and reliable cell differentiation.

Chapter II

Design, Synthesis and Stability Profiles of the Synthetic Retinoids

2.1 Introduction

The major active metabolite of retinol, ATRA, (also known as tretinoin) was the first to undergo total synthesis, in 1946, followed shortly after by that of retinol a year later.[251, 252] At around the same time, the biological potential of this family of molecules became apparent. Endogenous retinoids are distributed throughout the embryo and adult *in vivo*. They regulate a wide array of essential processes during both chordate embryogenesis and adult homeostasis including reproduction,[190] vision,[178] immune competence,[179] embryonic development[181, 253] and cellular differentiation, proliferation and apoptosis[182-184, 254] (See Chapter I for a more detailed discussion). These wide biological effects elicited by ATRA make it an obvious drug target for many clinical applications. Unfortunately, as discussed in Chapter I, there are a number of physical characteristics associated to ATRA that inhibit its use further in both *in vitro* cell culture protocols, or therapeutically. Our research group, and that of Muryama and colleagues, who highlighted the potential detrimental effects of using ATRA as a tool for cell biology, have emphasised these issues.[228, 229]

Consequently, both academic and commercial organisations have turned to designing, synthesising and screening analogous of ATRA. This is with the aim of identifying new retinoids with an improved biological response, overcoming the problems associated with the natural retinoids. Notably, one solution is to synthesise stable analogues, which have reduced isomerisation capabilities, thus, reducing the possibility of unwanted isomerisation products. This is in addition to blocking known metabolic sites to increase the half-life of the compound within the cell, thus, increasing its exposure to the receptors. This is possible through selecting known bioisosteres, such as the TMTN group discussed in Chapter I. Both are approaches adopted by our research group.

2.2 Aims and Objectives

Building on previous knowledge gained from work done on EC19 and EC23, a number of synthetic retinoid analogues were identified as potential targets. These were novel molecules designed to investigate what effects the size and conformation of the linker region would have on biological responses. As described above, there are many known bioisosteres for each of the key regions, yet to date the size of the linker region has not been fully investigated. We aimed to design and synthesise a series of analogues, with different polyene chain lengths and conformations to investigate both compound stability and biological efficacy. The initial targets are shown in Figure 2.1.

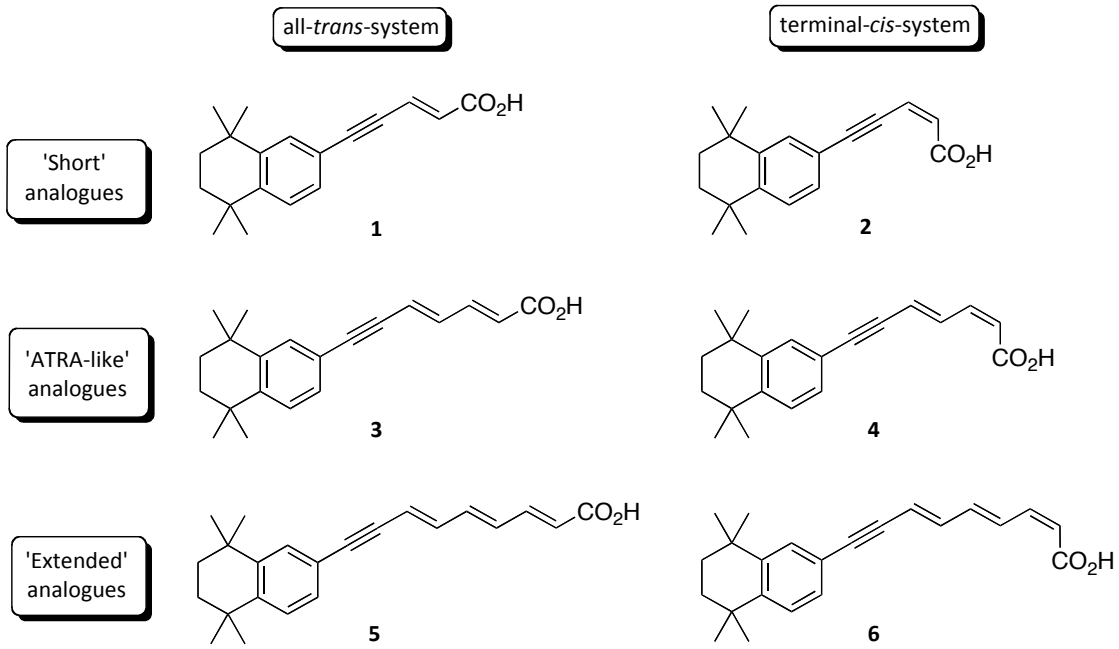

Figure 2.1 Proposed project targets.

The objectives of this work were initially to demonstrate the successful incorporation of a stable polyene chain into a retinoid analogue, mimicking that of their natural counter parts more closely. This would be supported through enhanced stabilisation, gained by using of other carefully selected bioisosteres. As previously discussed, the hydrophobic core of the target synthetic retinoids was to be a TMTN

group. This was chosen due to its increased stability and resistance to metabolic oxidation. It was envisaged that, coupled to an acetylene linker group, this would provide enough stabilisation to support one, two and possibly three conjugated double bonds. Thus, allowing us access to novel retinoids, which would be shorter, longer and of an identical length to their natural counter parts. Overall, providing us with a tool for probing the relationship in distance between the hydrophobic core and carboxylic acid group. The synthetic route used to synthesise these compounds would also enable us to create both isomers at any of the bonds, further probing the conformations of the binding pockets. Finally, the series would enlighten us in the stability of these compounds and highlight the number of conjugated bonds that can be tolerated in such as system. The overall objective was, therefore, to identify the relationship between polyene chain length, stability and biological potency.

2.3 Synthesis

2.3.1 Construction of the Core

The TMTN group has been synthesised, and the procedure optimised previously within our research group.[228] Briefly, the synthesis began with selective iodination of 1,1,4,4-tetramethyl-1,2,3,4-tetrahydronaphthalene **7**. This utilised an interesting adapted literature method using iodine, periodic acid, glacial acetic acid and concentrated sulphuric acid.[255] 6-Iodo-1,1,4,4-tetramethyl-1,2,3,4-tetrahydro-napthalene, **8**, was generated as a crystalline solid in an acceptable yield of 66%. Conversion of iodide, **8**, to the trimethylsilyl (TMS) protected acetylene, **9**, was subsequently undertaken through a palladium coupling reaction employing, bis-(triphenylphosphine)palladium(II) chloride, copper(I) iodide and trimethylsilyl (TMS) acetylene, under inert conditions. The product, 6-trimethylsilylethynyl-1,1,4,4-tetramethyl-1,2,3,4-tetrahydronapthalene, **9**, was isolated in a satisfactory yield of 67%. Finally, removal of the TMS protecting group afforded the desired hydrophobic core for the synthetic retinoids, 6-ethynyl-1,1,4,4-tetramethyl-1,2,3,4-tetrahydronapthalene, **10**, in a excellent yield of 97%. The synthesis is summarised in Scheme 2.1.

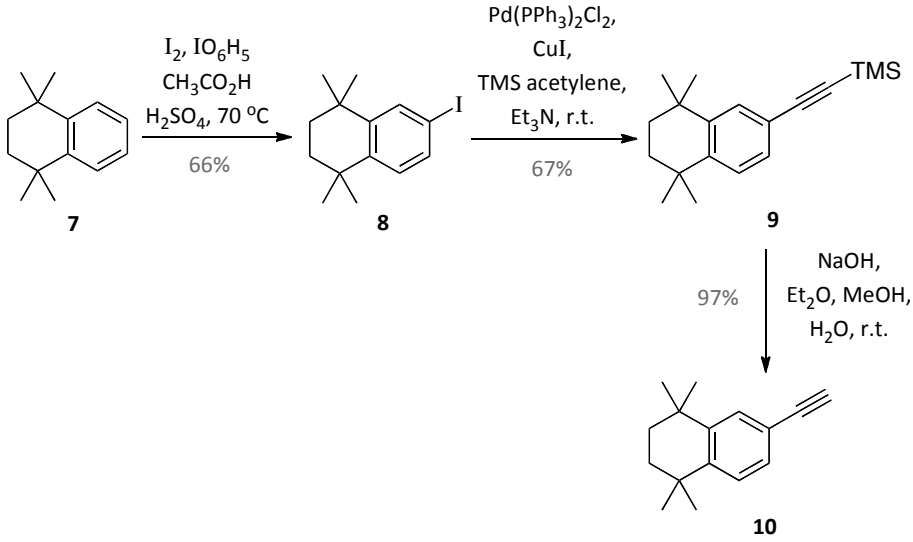

Scheme 2.1 Synthesis of the Hydrophobic Core.

2.3.2 Generation of the 'Short' Retinoids

With the hydrophobic core in hand, synthesis of the polyene chain section of the synthetic retinoids began. Initially, methyl propiolate, **11**, was treated with sodium iodide in acetic acid. The reaction is stereospecific and gave rise to the *cis*-isomer of the iodoacrylate, methyl 3-*Z*-iodoacrylate, **12**, in an acceptable yield. A portion of the *cis*-iodoacrylate, **12**, was subsequently removed and stored, while the remainder was converted to the *trans*-iodoacrylate, **13**. This was achieved by refluxing in hydroiodic acid and benzene, generating the desired compound, methyl 3-*E*-iodoacrylate, **13**, in a good 85% yield (Scheme 2.2).

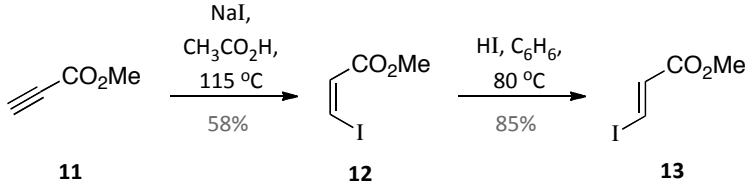

11 **12** **13**

Scheme 2.2 Generation of the *cis*- and *trans*-iodoacrylates.

With both isomers of the iodoacrylates available, each was subjected to two different reaction sequences. Firstly, a series of couplings and deprotections to extend the polyene chain by a further two carbons (this will be covered in the following section), and secondly, a coupling reaction to the core followed by deprotection to yield the 'short' retinoid analogues. Standard Sonogashira conditions were employed for the coupling reaction.[256, 257] Both the *cis*- and *trans*-isomers, **12** and **13**, underwent clean and efficient coupling to the core, **10**, with high yields obtained for both of 91% and 71% respectively (Scheme 2.3).

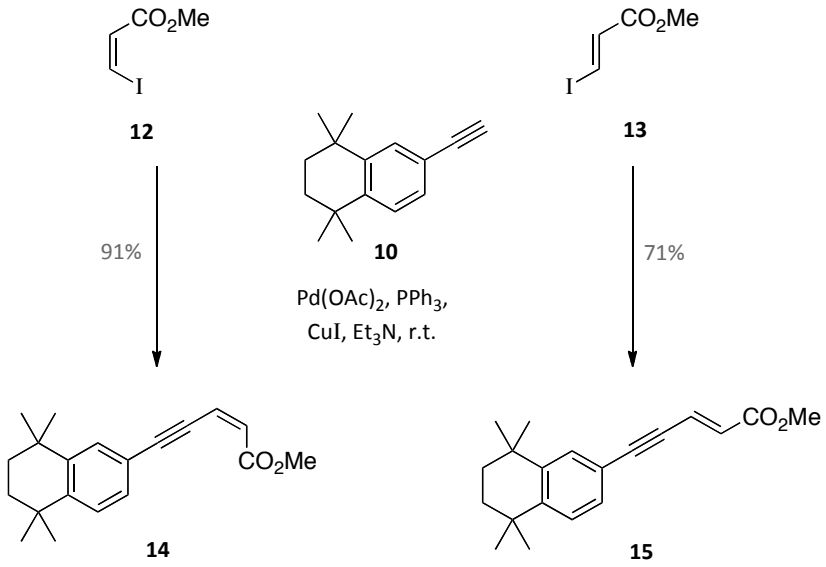

Scheme 2.3 Synthesis of the short esters.

Finally, a saponification reaction was employed to deprotect the methyl esters, **14** and **15,** yielding their corresponding acids. Initially, conditions using sodium hydroxide (20%) under reflux in tetrahydrofuran (THF) were investigated, as these were previously used to generate EC23 and EC19.[228] Unfortunately, these conditions proved to be too severe, with the *cis*-ester, **14**, degrading to a mixture of inseparable compounds, with the only identifiable product being 5,5,8,8-tetramethyl-5,6,7,8-tetrahydronapthalene-2-carbaldehyde, **16** (Scheme 2.4).

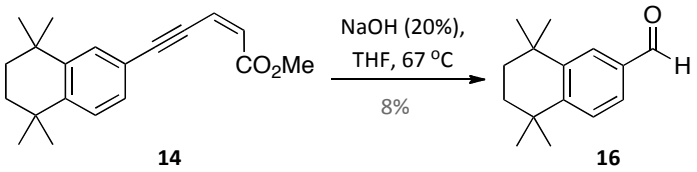

Scheme 2.4 Initial unsuccessful saponification conditions

Consequently, a milder set of conditions was required to keep the polyene section intact. The reagents subsequently employed, were lithium hydroxide (up to 5 equivalents) in a THF and water mixture in a 1:1 ratio at room temperature.[258, 259]

Both the *cis*- and *trans*-isomers, **14** and **15**, were successfully deprotected in high yields of 85% and 85% respectively, to generate the retinoids AH62 and AH36, **2** and **1** (Scheme 2.5).

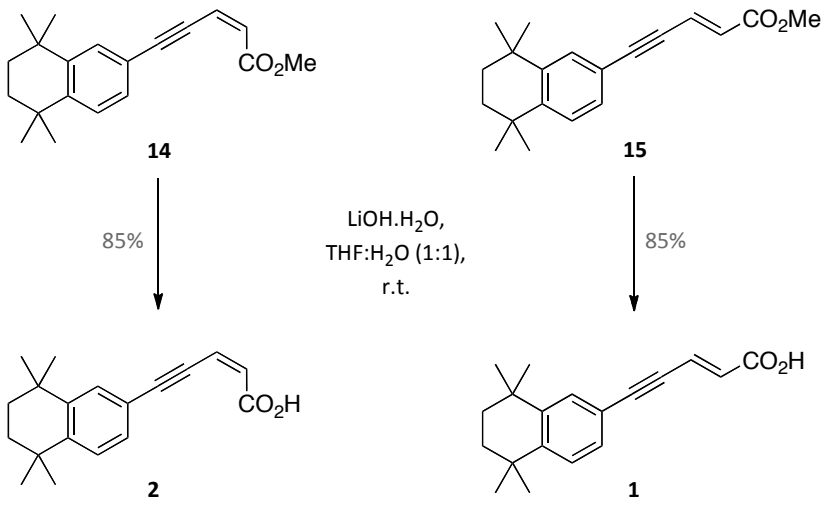

Scheme 2.5 Generation of the 'short' analogues

2.3.3 Polyene Chain Extention

With both isomers of the 'short' retinoid analogues successfully synthesised, the next target involved extending the polyene chain by two carbons to synthesise analogues of an identical size to that of the natural retinoids. As briefly mentioned, this initiated with coupling of the *cis*- and *trans*-iodoacrylates, **12** and **13**, previously synthesised, to 4,4,6-trimethyl-2-vinyl-1,3,2-dioxaborane, **17**, through a Heck-Mizoroki coupling.[260] Both reactions were successful, with isolated yields of 54% and 90% respectively (Scheme 2.6).[261]

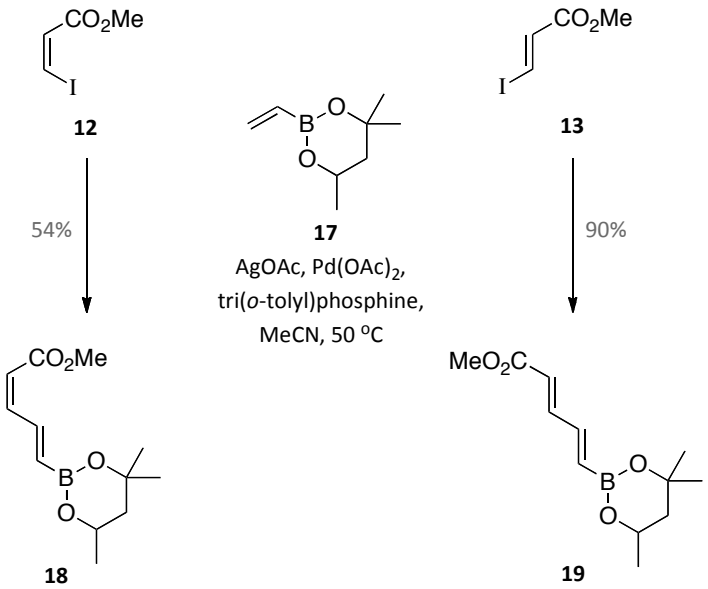

Scheme 2.6 Generation of the boronate analogues

Both the (2*Z*,4*E*)- and (2*E*,4*E*)-5-(4,4,6-trimethyl-[1,3,2-dioxaborinan-2-yl])-penta-2,4-dienoic acid methyl esters, **18** and **19**, were then subjected to iododeboronation reactions. The conditions utilised were developed within the Whiting group, to allow for the stereoselective replacement of the boron functionality with an iodine atom, thereby providing an accessible synthetic route to vinyl iodides.[262-265] The order in which the reagents are added is imperative, as this allows for the correct stereochemistry to be selected. The addition of iodine monochloride first, followed by that of sodium methoxide, leads to inversion at the boronate double bond. This comes about by the initial reaction of the olefin with iodine monochloride to generate an iodonium ion, **21**. This species then has two ways of collapsing, either to the saturated derivative, **22**, leading to *anti*-addition or, to the zwitterion, **24**. In the second instance this directs the chloride to the β-position of the molecule and ultimately leads to the formation of the vinyl chloride, **26**. Both pathways are in direct competition, but inclusion of pyridine and electron-rich R-groups has been shown to favour formation of the vinyl chloride, **26**. This can be rationalised in that the pyridine helps to displace chloride from the ion pair, promoting formation of the zwitterion, **24**. Conversely, when pyridine is omitted, and the R-group is of a strong electron withdrawing nature formation of the vinyl chloride, **26**, is disfavoured and

subsequently only the vinyl iodide, **23**, is detected. When the addition of the reagents is reversed, retention of the stereochemistry is observed. This comes about through addition of sodium methoxide to the boronate generating the 'ate'-complex, **27**. This complex then acts as a nucleophile attacking the strongly electrophilic iodine monochloride, and thus retaining the geometry of the double bond. The mechanism of both these reactions is summarised in Scheme 2.7.

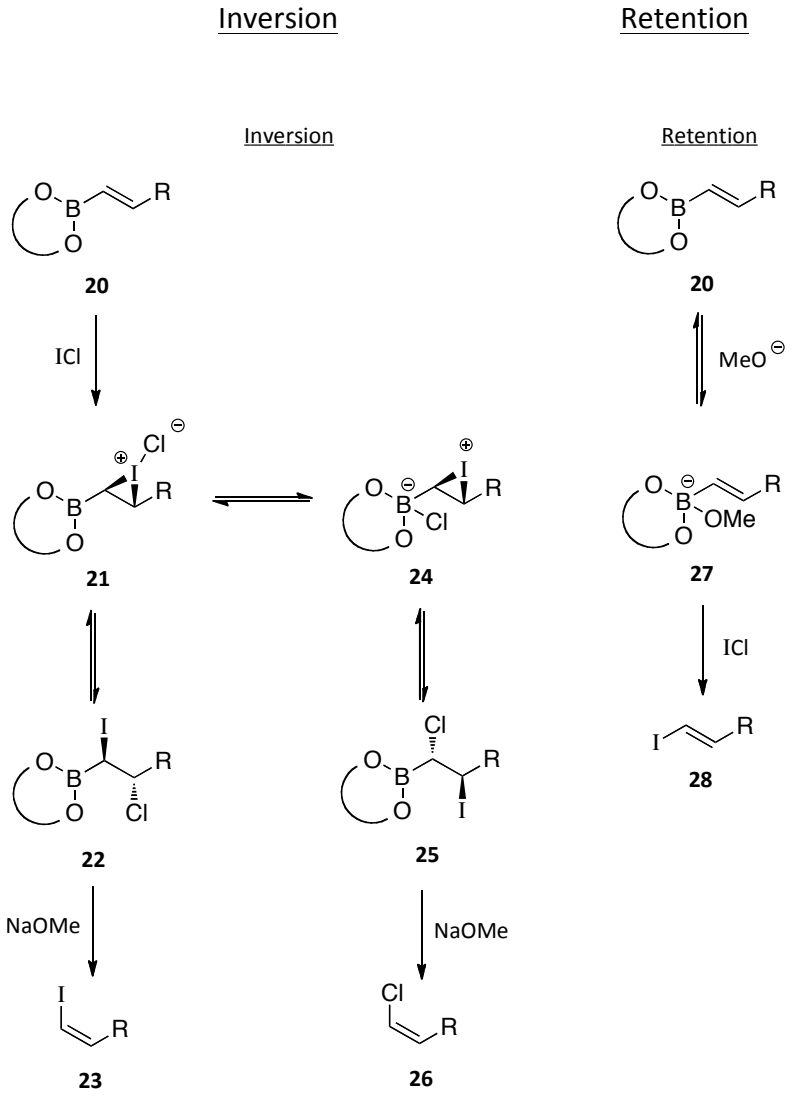

Scheme 2.7 Mechanistic rationalisation for the iododeboronation reactions.

An example of each reaction has been performed, firstly when (2*Z*,4*E*)-5-(4,4,6-trimethyl-[1,3,2-dioxaborinan-2-yl])-penta-2,4-dienoic acid methyl ester, **18**, was converted to (2*Z*,4*Z*)-5-iodopenta-2,4-dienoic acid methyl ester, **29**, in a 59% yield.[261]

And, secondly when (2*E*,4*E*)-5-(4,4,6-trimethyl-[1,3,2-dioxaborinan-2-yl])-penta-2,4-dienoic acid methyl ester, **19**, was treated with with sodium methoxide, followed by iodine monochloride to give (2*E*,4*E*)-5-Iodopenta-2,4-dienoic acid methyl ester, **30**, in a excellent 87% yield.[266] A summary of these reactions can be found in Scheme 2.8.

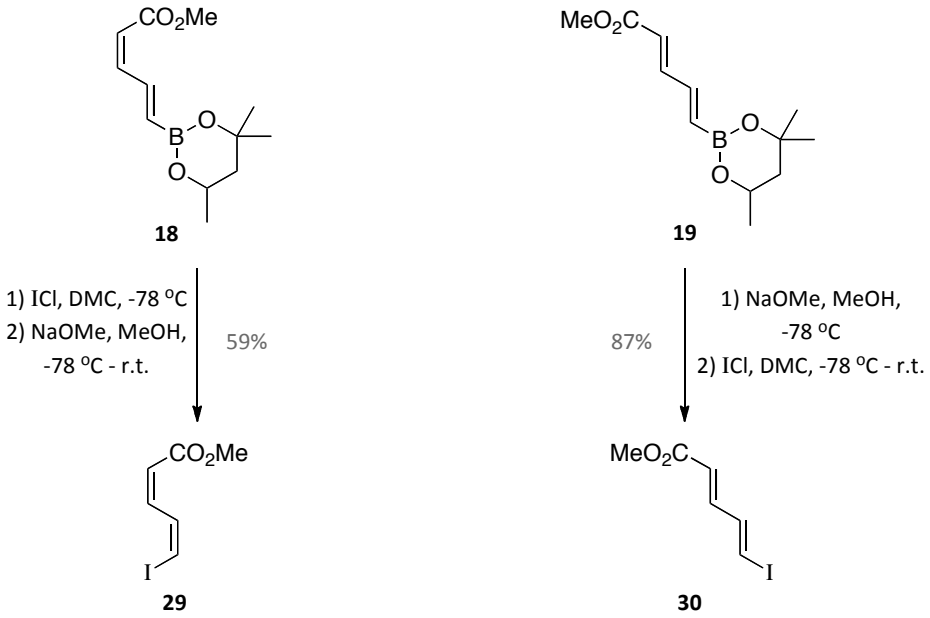

Scheme 2.8 Synthesis of the dienyl iodides

Previous work within our group,[261, 266] on both identical and similar dienyl iodide substrates, had revealed that these systems are highly sensitive to both light and air.[267] Both dienyl iodides, **29** and **30**, synthesised within this thesis showed high stereoselectivity for the desired isomer, similar to that reported previously of around 96:4. The source of the isomerisation generating small quantities of the alternate isomer is still uncertain. What is certain is that it is not down to poor selectivity in the iododeboronation reaction, as the isomerisation is seen at double bond adjacent to the carbonyl. Other explanations could include either reversible conjugate addition of the iodide anion, or acid-catalysed isomerisation.[267]

Presented with this knowledge, the dienyl iodides, **29** and **30**, were immediately coupled to the hydrophobic core, **10**, as it was perceived the polyene system was at

its least stable in the iodide form. Identical Sonogashira conditions were employed to those used in the synthesis the 'short' analogues, **1** and **2**. A coupling time of 18 hours was initially chosen as a compromise between yield and potential isomerisation that may occur, based on previous knowledge of their reactivity (Scheme 2.9). All reactions were carried out under reduced light conditions, including work-up and purification.

Characterisation of both esters revealed that the coupling was successful, but the high isomeric purity of the starting iodides, **29** and **30**, had been lost in the reaction and both products were a mixture of isomers. Separation of the isomers by SiO_2 silica gel column chromatography proved unsuccessful. Similarly, a reduction in the reaction time, to 5.5 hours, did provide an improvement in the ratio of isomers observed in the crude product, however, as the isomers, **31**, were inseparable this was ultimately futile.

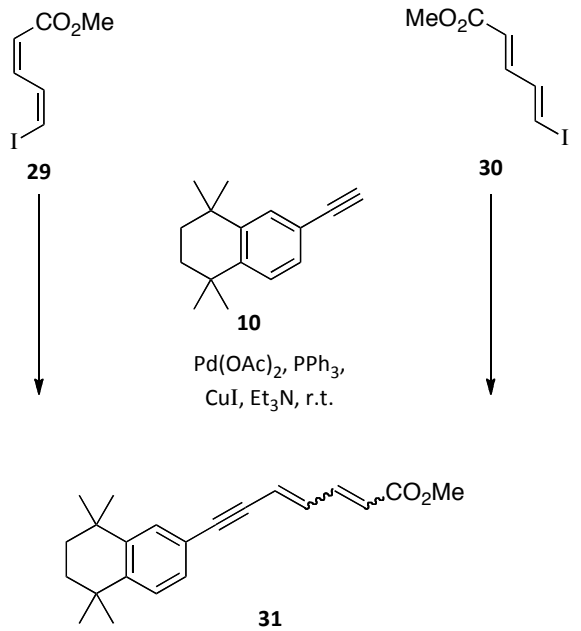

Scheme 2.9 Unsuccessful coupling of the dienyl iodides to the hydrophobic core.

Due to the inherent instability within the polyene system, an alternative approach was required. One possible solution was to lock the double bonds in their desired stereochemistry through cyclopropanation. If carried out early in the synthesis on

more stable analogues, such as the boronate esters, **18** and **19**, a stable reagent to couple to the hydrophobic core may have been achievable (Scheme 2.10). One problem with this proposed synthetic route was that it would destroy the conjugated system, associated with all retinoid analogues.

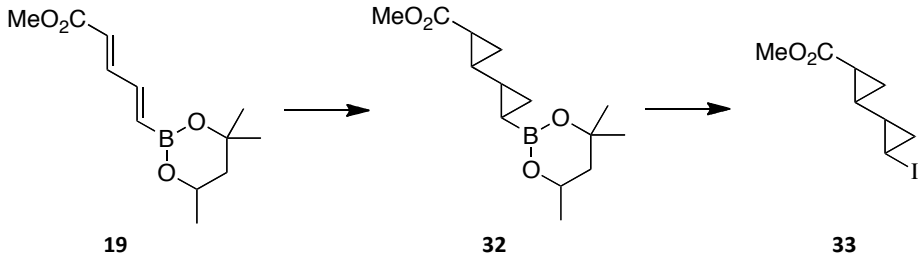

19 **32** **33**

Scheme 2.10 Proposed cyclopropanation of unstable intermediates.

Consequently, before we approached this route in any detail, we attempted a highly analogous synthesis to that of our initial idea, but with the addition of an extra methyl group. The idea stemmed from that displayed by nature, as all the natural retinoids, ATRA, 9cRA and 13cRA, are all based on a skip-methylated system. Even though these molecules display an inherent instability, as discussed earlier, we hypothesised the additional support gained through our chosen bioisosteres (TMTN and acetylene linker), coupled with the extra stability brought in by the methyl group would generate analogues with an overall improved stability profile.

2.3.4 Generation of 'Short' Methylated Analogues

The following synthesis is analogous to that of the one described previously. Briefly, methyl tetrolate, **33**, was treated with sodium iodide in acetic acid to yield (*Z*)-3-iodobut-2-enoic acid methyl ester, **34**, in an excellent yield of 95% as described in the literature.[268] As in the previous synthesis, a proportion of the compound was removed and stored for either: (1) coupling to the core, **10**, or (2) coupling to a vinyl boronate species to generate a dienyl iodide; while the remainder was converted to the *trans*-isomer, **35**. Isomerisation was carried out as described in the literature by Dudley *et al*.[268] with the exception of the use of high pressure. Consequently, longer

reaction times of 24-48 hours were employed, with the overall yield remaining relatively poor at 37% at best, with 40% of the starting material recovered. This resistance to isomerisation, compared to the un-methylated system, was somewhat encouraging, as we knew we desired a more rigid system. The reactions are summarised in Scheme 2.11.

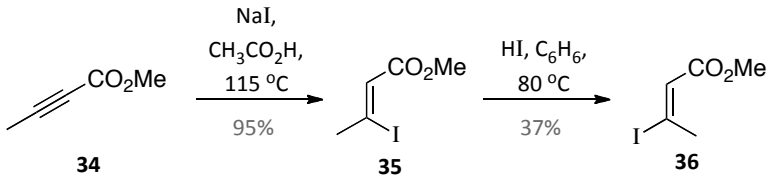

Scheme 2.11 Synthesis of the 3-iodobut-2-enoic acid methyl esters.

For a comparison with the un-methylated system on both stability and biological potential, the synthesis of the methylated 'short' retinoid analogues was attempted. Coupling of both the *cis*- and *trans*-isomers of the 3-iodobut-2-enoic acid methyl esters, **35** and **36**, to the TMTN core, **10**, was achieved using identical conditions as previously described. The (*Z*)- and (*E*)-3-methyl-5-(5,5,8,8-tetramethyl-5,6,7,8-tetrahydro-naphthalen-2-yl)-pent-2-en-4-ynoic acid methyl esters, **37** and **38**, were isolated in 63 and 99% yields, respectively, both after 24 hour reactions. The removal of the methyl esters was achieved *via* the procedure previously described in the un-methylated analogue synthesis. This was successful for the *trans*-methyl ester, **38**, generating (*E*)-3-methyl-5-(5,5,8,8-tetramethyl-5,6,7,8-tetrahydro-naphthalen-2-yl)-pent-2-en-4-ynoic acid, **40**, termed AH66, as an off-white solid in a poor yield. The low yield shown in this thesis is probably not an appropriate value and upon repetition this is most likely to increase inline with other values shown for related systems.

When (*Z*)-3-methyl-5-(5,5,8,8-tetramethyl-5,6,7,8-tetrahydro-naphthalen-2-yl)-pent-2-en-4-ynoic acid methyl ester, **37**, was exposed to the same conditions the desired product was not isolated. Instead, the reaction appeared to proceed *via* the addition of water across the acetylene, followed by cyclisation to form 6-hydroxy-4-methyl-6-

(5,5,8,8-tetramethyl-5,6,7,8-tetrahydro-naphthalen-2-yl)-5,6-dihydro-pyran-2-one, **39**, in an excellent 97% yield. All reactions are summarised in Scheme 2.12.

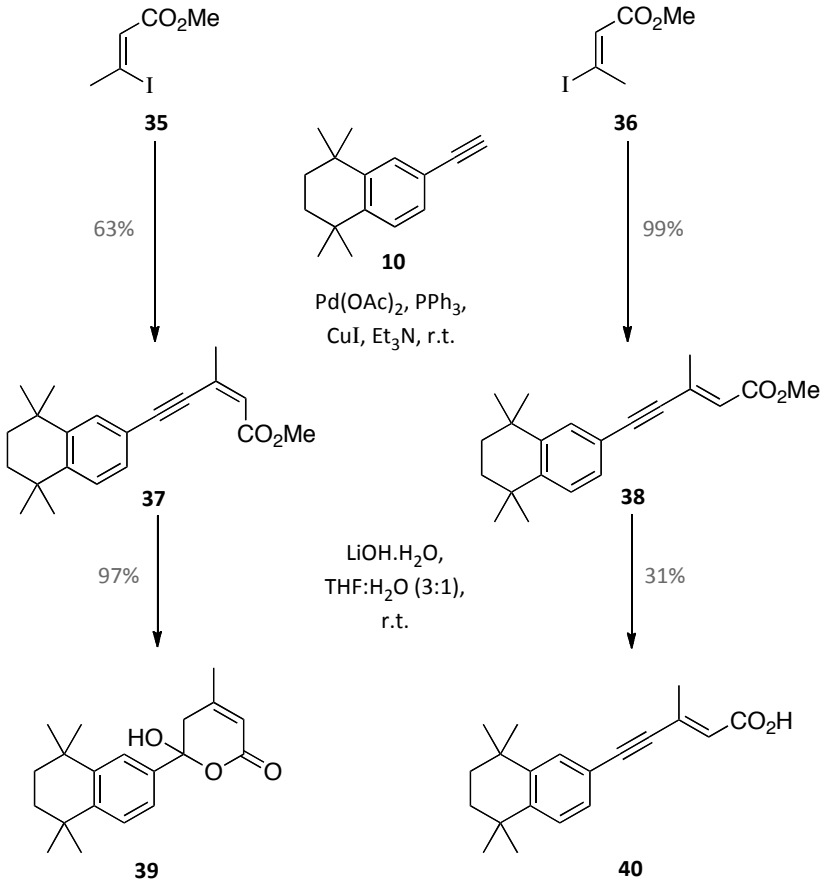

Scheme 2.12 Summary of the synthesis of the 'short methylated' analogues.

Two proposed mechanisms for the cyclisation are depicted in Figure 2.2. These are the most viable routes to the product as the alternative, a Michael-type addition, has the potential to isomerise. An explanation for why the cyclisation occurs in this system and not the un-methylated system is that the methyl group increases the pKa of the acid, thus allowing for its extraction more easily. For a direct comparison, both saponification reactions on the un-methylated and methylated esters were repeated under identical conditions using three equivalents of lithium hydroxide in a 3:1 THF:H_2O mixture, with the same products identified as previously stated. Consequently, only the *trans*-isomer, AH66, **40**, of the 'short' methylated system would be able to be screened.

Mechanism 1 - Basic Catalysed

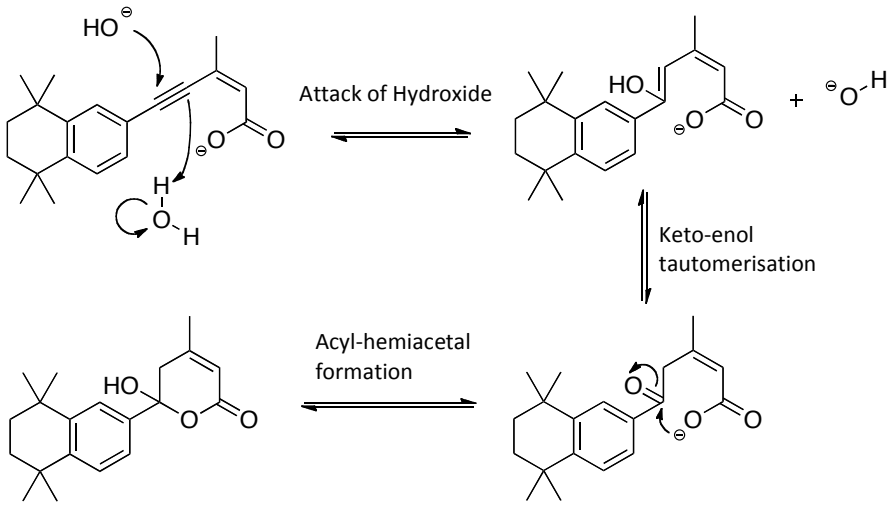

Mechanism 2 - Acid Catalysed

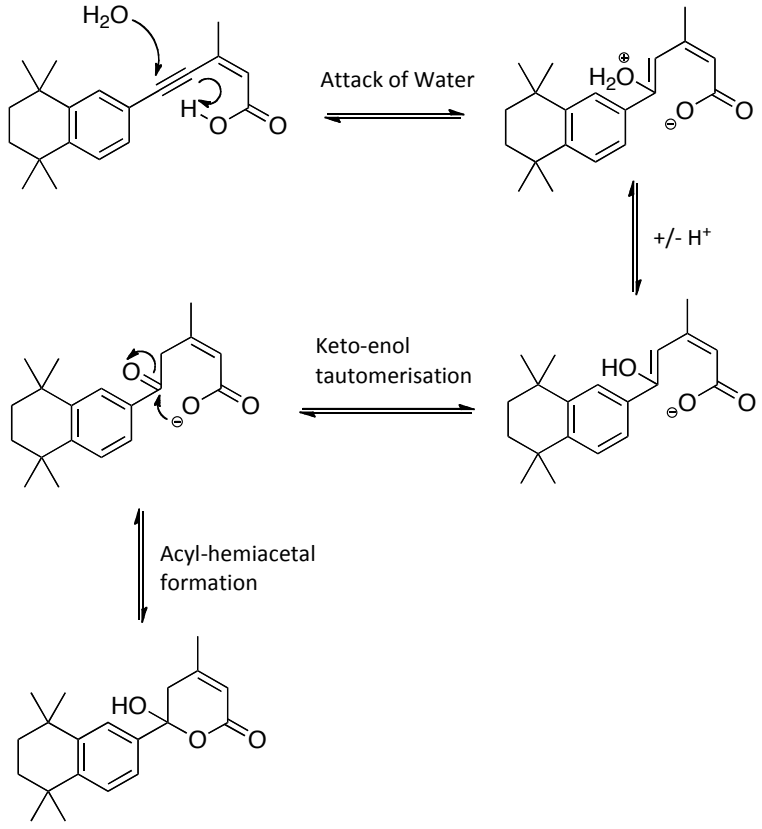

Figure 2.2 Proposed mechanisms for the formation of the acyl-hemiacetal.

2.3.5 Generation of 'ATRA-like' Analogues

As in the previous attempted synthesis we next desired compounds of an identical size to that of their natural counterparts. We envisaged that the extra methyl group would provide enough stability to enable Sonogashira coupling to the core. Initially, both the (*Z*)- and (*E*)-3-iodobut-2-enoic acid methyl esters, **35** and **36**, were coupled to 4,4,6-trimethyl-2-vinyl-1,3,2-dioxaborane, **17**, under identical Heck-Mizoroki conditions used in the previous synthesis. Both reactions were successful with the corresponding *cis*- and *trans*-compounds, **47** and **48**, isolated in 78% and 74% yields, respectively.[267] Identical, and simultaneous iododeboronation reactions were then employed to generate (2*Z*,4*E*)- and (2*E*,4*E*)-5-iodo-3-methyl-penta-2,4-dienoic acid methyl esters, **49** and **50**, in excellent yields of 98% and 86% respectively (Scheme 2.13).

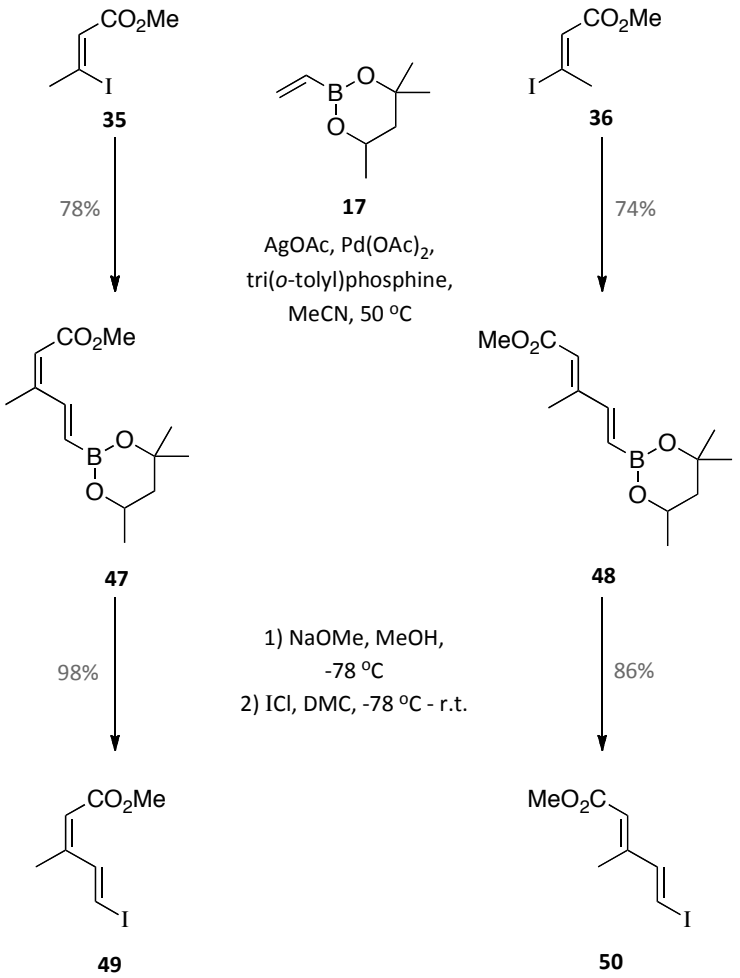

Scheme 2.13 Synthesis of the methylated stable dienyl iodides.

Interestingly, both dienyl iodides, **49** and **50**, were obtained as single isomers, and were far more stable when exposed to light and air compared to the un-methylated systems, based on ^{1}H nuclear magnetic resonance (NMR) spectroscopy. This enhanced stability was subsequently transferred through the coupling step to the core **10**, with both the (2*Z*,4*E*)- and (2*E*,4*E*)-2-methyl-7-(5,5,8,8-tetramethyl-5,6,7,8-tetrahydro-naphthalen-2-yl)-hepta-2,4-dien-6-ynoic acid methyl esters, **51** and **52**, isolated as single isomers in 88% and 76% yields respectively. There is still potential to improve these yields as both reactions were run in 5 hours so as to avoid any possible isomerisation. As these iodides now appear to be far more stable than any previously synthesised, increasing the reaction time may be possible, which one would hope in turn should improve the overall yield.

Finally, saponification using lithium hydroxide followed by re-crystallisation from acetonitrile yielded the two 'ATRA-like' analogues, (2*Z*,4*E*)- and (2*E*,4*E*)-2-methyl-7-(5,5,8,8-tetramethyl-5,6,7,8-tetrahydro-naphthalen-2-yl)-hepta-2,4-dien-6-ynoic acid, **53** and **54**, termed AH60 and AH61 respectively, in good yields of 77% and 82% respectively (reactions are summarised in Scheme 2.14).

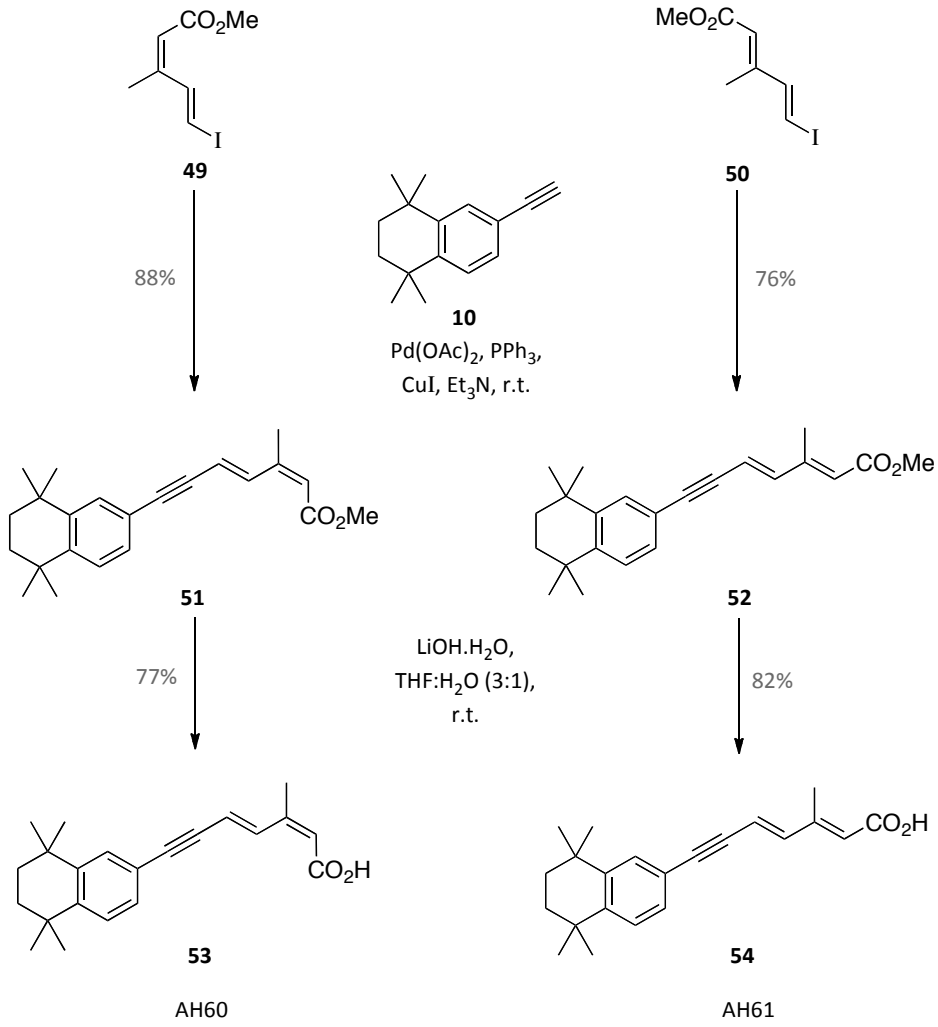

Scheme 2.14 Synthesis of the 'ATRA-like' analogues AH60 and AH61.

The desired stereochemistry was confirmed and can be clearly seen from the X-ray crystal structure obtained for AH61 (Figure 2.3).

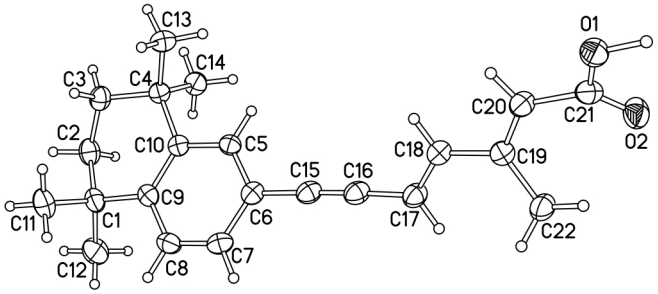

Figure 2.3 X-ray crystal structure of AH61.

2.3.6 Generation of Extended Analogues

Having now prepared three 'short' analogues, **1**, **2** and **40** (AH36, AH62 and AH66 respectively), and two 'ATRA-like' analogues, **53** and **54** (AH60 and AH61 respectively), an extended analogue was required to complete the outlined objectives. As previously discussed, the longer the conjugated system the greater the sensitivity of the compounds to light. It was, therefore, hypothesised that a trienyl iodide would be potentially difficult to handle. As a result, unlike all the previously discussed synthesise, only one isomer, the all-*trans* system, would be initially synthesised. This was chosen as it was perceived to be the most stable, and therefore, most likely to succeed.

Again, the synthesis is analogous to those already discussed. (2*E*,4*E*)-5-iodo-3-methyl-penta-2,4-dienoic acid methyl ester, **50** (synthesised previously), was coupled to 4,4,6-trimethyl-2-vinyl-1,3,2-dioxaborane, **26**, under the standard Heck-Mizoroki conditions. This reaction generated (2*E*,4*E*,6*E*)-3-methyl-7-(4,4,6-trimethyl-[1,2,3]-dioxaborinan-2-yl)-hepta-2,4,6-trienoic acid methyl ester, **55**, in an acceptable yield. Under appropriate iododeboronation conditions the corresponding trienyl iodide, (2*E*,4*E*,6*E*)-7-iodo-3-methyl-hpta-2,4,6-trienoic acid methyl ester, **56**, was isolated in 65% yield. Due to the assumed potential poor stability profile of this compound it was immediately coupled to the hydrophobic core, **10**. The reaction took place in 5 hours, yielding the product in a satisfactory 64% yield. Finally, the ester was deprotected to generate the 'extended' retinoid analogue (2*E*,4*E*,6*E*)-3-methyl-9-(5,5,8,8-tetramethyl-5,6,7,8-tetrahydro-naphthalen-2-yl)-nona-2,4,6-trien-

8-ynoic acid, **57**, termed AH98, in a good yield, however, unfortunately as two isomers in a ratio of 1:0.4. The reactions are summarised in Scheme 2.15.

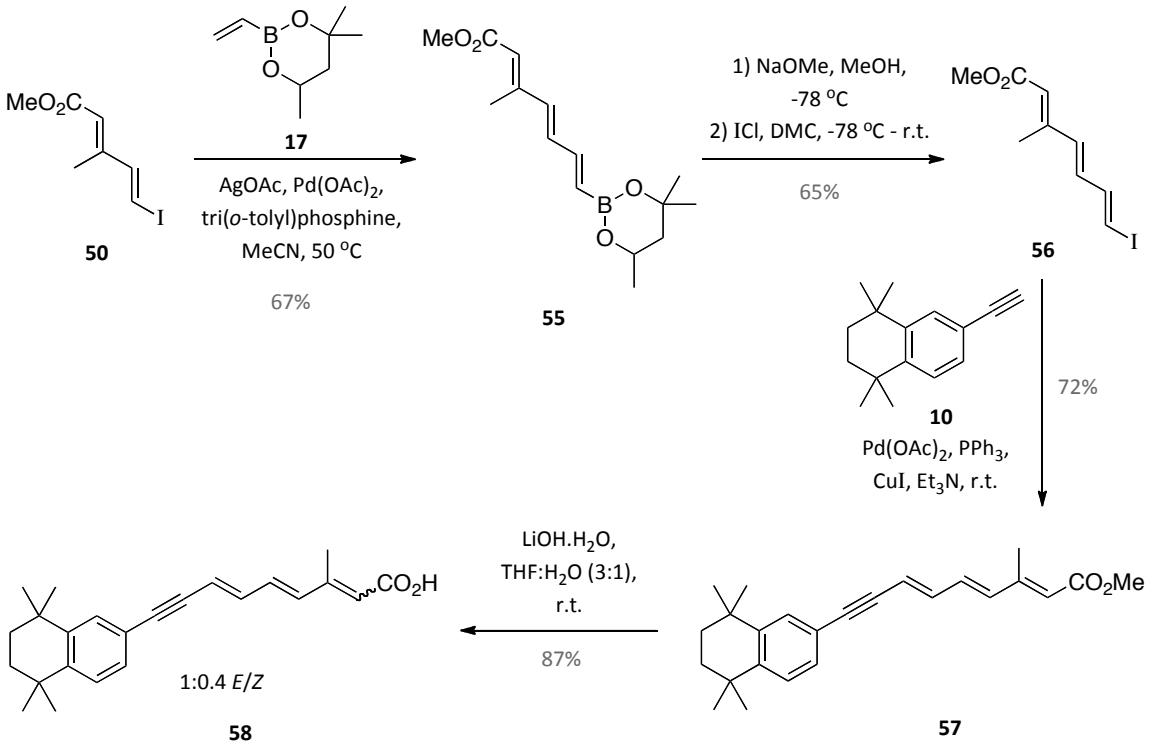

Scheme 2.15 Summary of the synthesis of the 'extended' analogue, AH98.

Due to the poor stability exhibited by the extended system, it was decided that only one analogue would initially be synthesised. Pending further testing, including both stability profiles and biological screening, further analogues would then been examined.

2.4 Stability Profiles

Subsequent to the synthesis of the compound series, the photostability of the synthetic retinoids was tested and compared to that of ATRA. The susceptibility of ATRA to undergo photoisomerisation and degradation when exposed to ordinary fluorescent light in the visible to near-ultra violet (UV) range has been previously demonstrated within our research group.[228] Briefly, ^{1}H NMR spectroscopy was used to investigate how much the compounds degraded over a set time period of continued exposure. Prolonged exposure to fluorescent light led to the advanced degradation of ATRA, whereby after three days only *ca*. 37% of the original compound remained. From the ^{1}H NMR spectra it is clear that not only is the molecule isomerising, but also degrading. On the other hand, ATRA was shown to be completely stable when stored in the absence of light for three days, as shown in Figure 2.4.[228] Subsequent work has indicated that ATRA can be safely stored for long periods of time in the absence of light, *ca.* six months or more (data not shown).

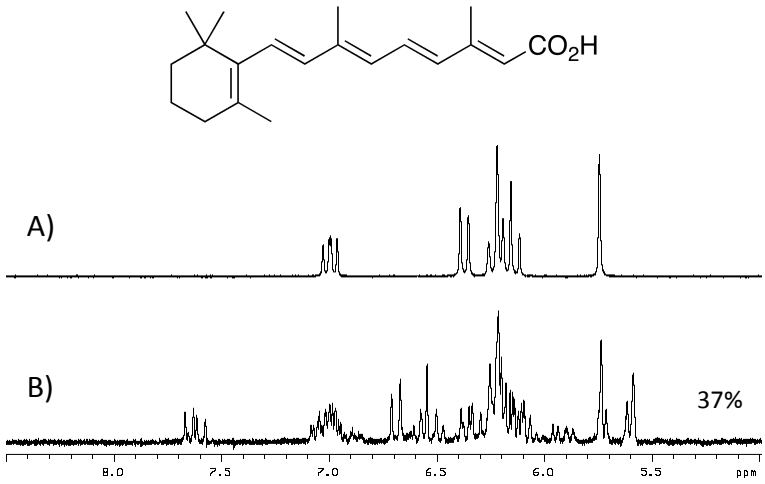

Figure 2.4 ^{1}H NMR spectra at 400 MHz of ATRA in dimethyl-sulfoxide-d_6 (DMSO-d_6) (5.0-8.5 ppm region) in the absence of light (A), and after 3 days exposure to white fluorescent light at a distance of 40 cm (B). The percentage value represents the amount of the original compound still present.

When the synthetic retinoids were exposed to the same wavelength of fluorescent light, also for three days, a clear relationship is seen between that of stability and

size. The 'short' analogues both un-methylated (AH36 and AH62) and methylated (AH66), **1**, **2** and **40**, show no signs of isomerisation or degradation after the three days. The 'ATRA-like' analogues (AH60 and AH61), **53** and **54**, display some slight signs of isomerisation but more notably there is no degradation. The 'extended' analogue, (AH98) **58**, displays the worst profile, as one would expect, but again only appears to shown signs of isomerisation rather than any degradation. The data is summarised in Figure 2.5, in which the percentage of remaining intact compound are displayed.

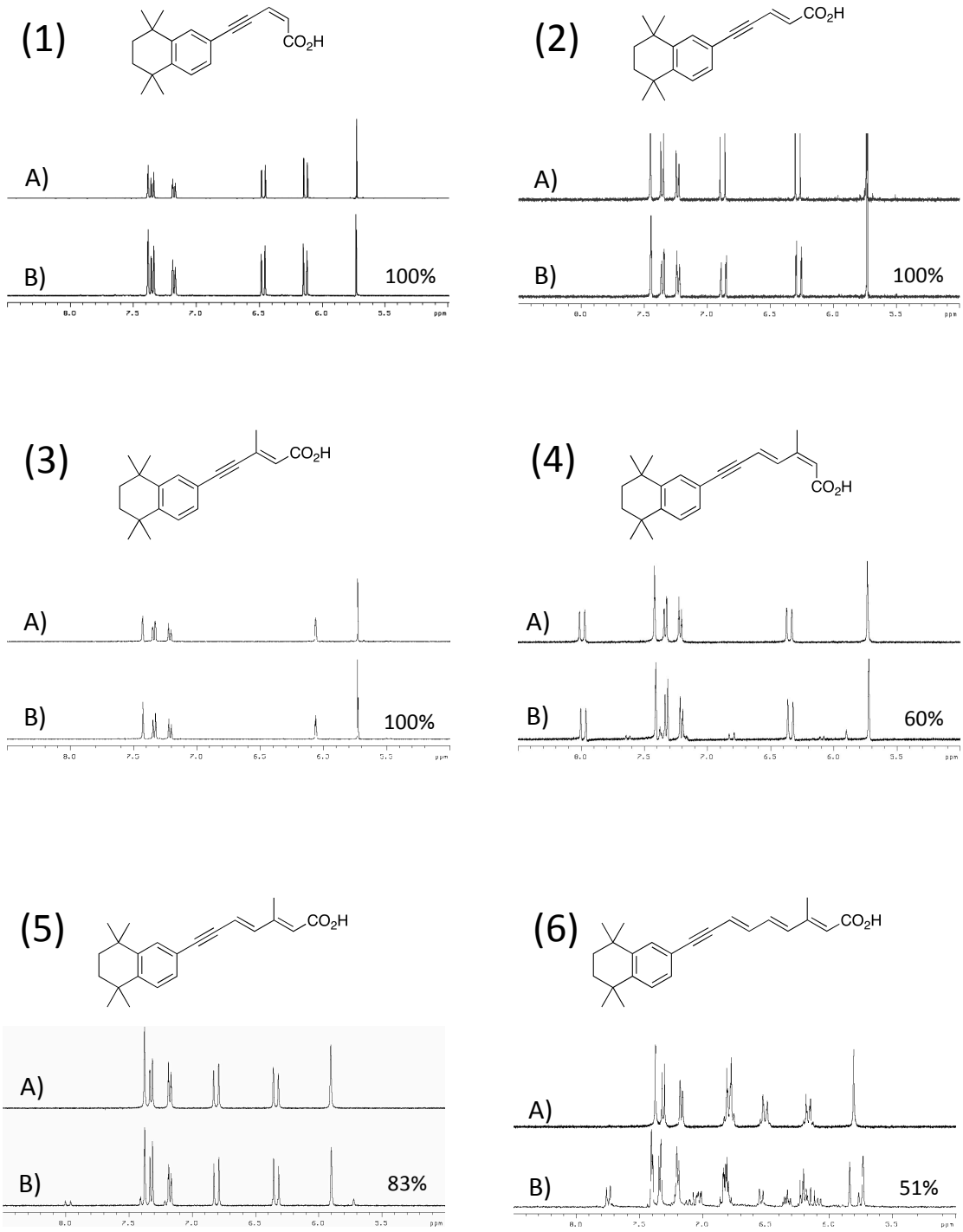

Figure 2.5 ^{1}H NMR spectra at 400 MHz of AH62 **2**, AH36 **1**, AH66 **40**, AH60 **53**, AH61 **54** and AH98 **58** (**1**)-(**6**) respectively, in DMSO-d_6 (5.0-8.5 ppm region) in the absence of light (A), and after 3 days exposure to white fluorescent light at a distance of 40 cm (B). The percentage value represents the amount of the original compound still present.

When analysed more closely, AH61, **54**, only isomerises to one other compound, AH60, **53**, with *ca*. 83% of the original molecule remaining intact. Conversely, AH60, **53**, isomerises to AH61, **54**, and one other isomer, the (2*Z*,4*Z*), displaying that the all *trans*-system is the most stable (Figure 2.6).

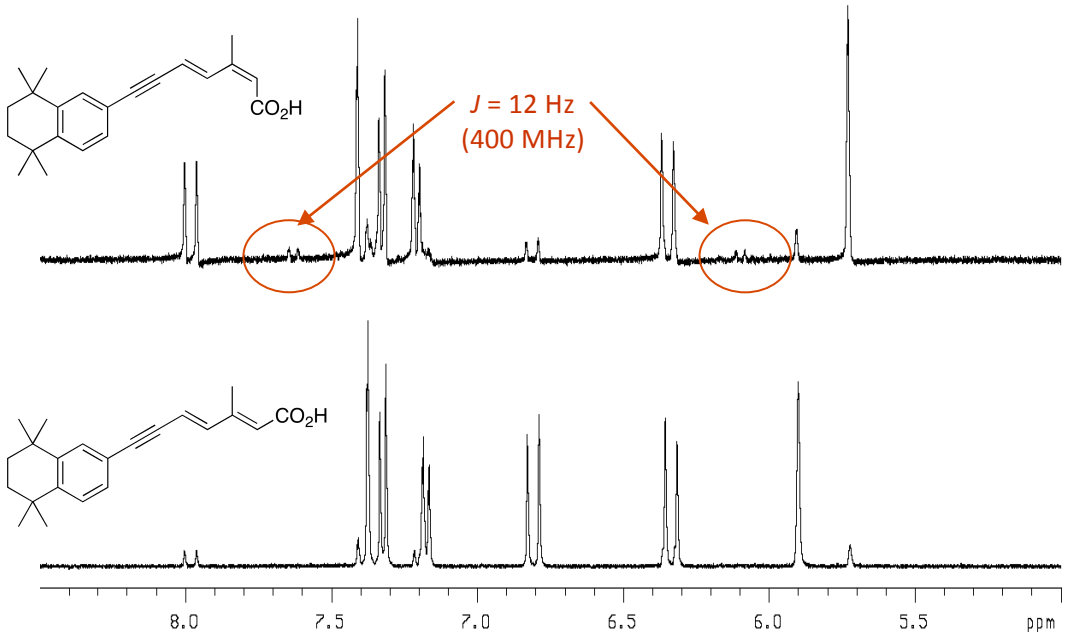

Figure 2.6 ^{1}H NMR spectra at 400 MHz of AH60 and AH61 in DMSO-d_6 (5.0-8.5 ppm region) after 3 days exposure to white fluorescent light at a distance of 40 cm. The overlayed spectra clearly demonstrate that AH61 only isomerises to AH60, whereas AH60 also isomerises to the other *cis*-isomer, highlighted by the *J* coupling of 12 Hz, as illustrated above.

To examine whether AH60, **53**, and AH61, **54**, would reach equilibrium in terms of isomerisation and at what ratio, NMR samples of both compound were continually exposed to the fluorescent light for up to two weeks. During this time AH60, **53**, became predominantly AH61, **54**, with one other isomer identified. AH61, **54**, similarly isomerised to AH60, **53**, and one other isomer, however, at a slower rate, with AH61, **54**, remaining the major isomer. The NMR plots and Table summarising the data are displayed in Figure 2.7.

AH60 **53** 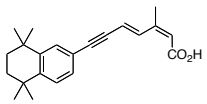

AH61 **54** 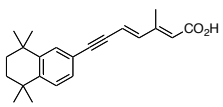

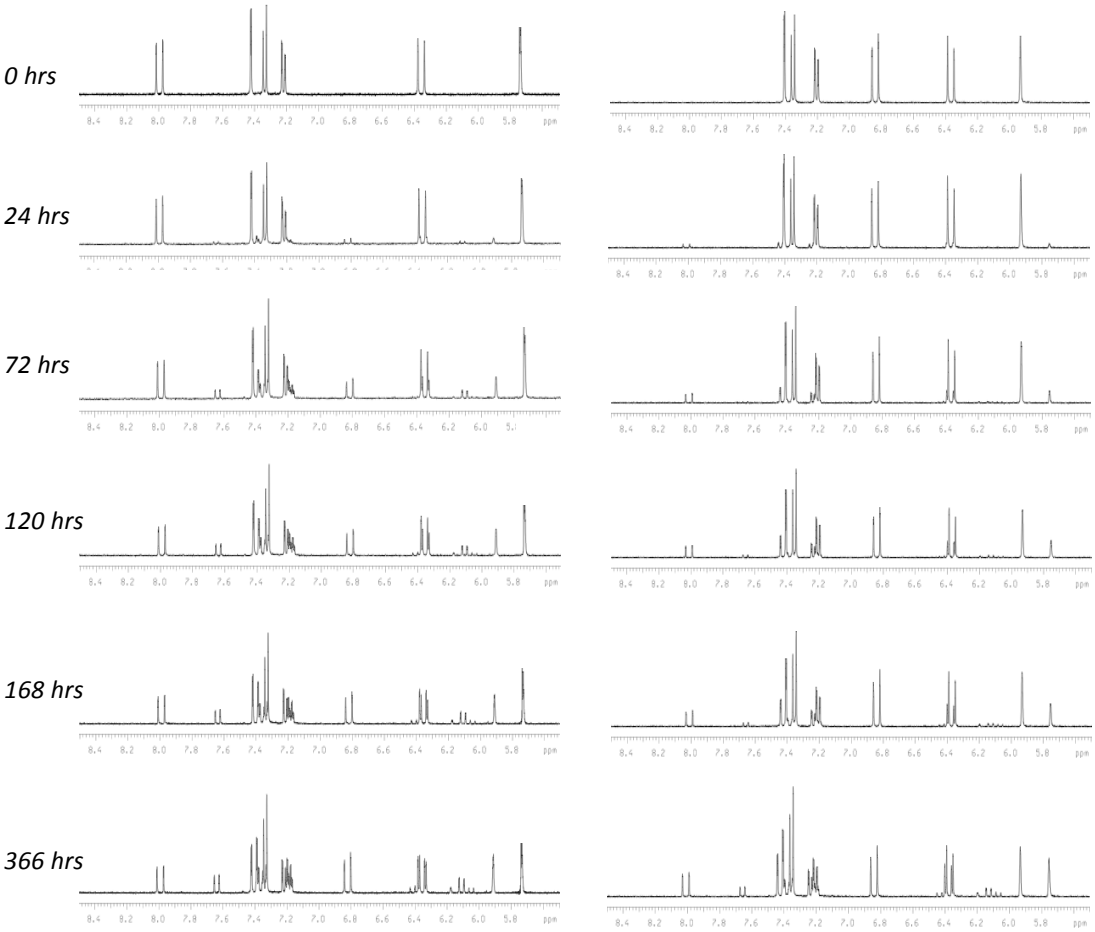

	***AH60* 53**	***AH61* 54**	***Other***
0 hrs	100 %	0 %	0 %
24 hrs	85 %	11 %	4 %
72 hrs	**60 %**	29 %	11 %
120 hrs	42 %	37 %	21 %
168 hrs	38 %	40 %	22 %
336 hrs	30 %	45 %	25 %

	***AH61* 54**	***AH60* 53**	***Other***
0 hrs	100 %	0 %	0 %
24 hrs	94 %	6 %	0 %
72 hrs	**83 %**	17 %	0 %
120 hrs	71 %	24 %	5 % (4 % *cis*)
168 hrs	65 %	29 %	6 % (5 % *cis*)
336 hrs	47 %	40 %	13 % (10 % *cis*)

Figure 2.7 ^{1}H NMR spectra at 400 MHz of AH60 **53** and AH61 **54** in DMSO-d_6 (5.0-8.5 ppm region) exposed to white fluorescent light at a distance of 40 cm for different time periods up to two weeks. The data is displayed graphically and summarised in the Tables below each set of spectra. Both compounds isomerise to each other and one other identifiable isomer. The increased stability of the all-*trans* system is highlighted as both in the parent mixture it remains the most predominant compound, while the corresponding isomer solution isomerises to a predominant solution of AH61 **54**. Equilibrium was never reached but these data suggests AH61 **54** would be the most predominant isomer at around 40-45%, followed by that of AH60 **53** and the remaining *cis*-isomer.

2.5 Conclusions

In summary, a series of novel related synthetic retinoids were successfully synthesised. The original design was modified by inclusion of an extra methyl group to allow for the synthesis of larger polyene chain containing molecules. Not all possible isomers and conformations were made, due to chemical restrictions such as self-cyclistations demonstrated in the short methyl containing *cis*-isomer. The 'extended' analogues were also suspended after synthesising only one analogue, as it was made up of a mixture of isomers. All further testing was then carried out on the compound as a mixture, and once analysed it would be possible to return in an attempt to optimise the system. One obvious target would be to add another methyl group to the system, mimicking that of the skip-methylated system displayed by nature, giving the target molecule displayed in Figure 2.8.

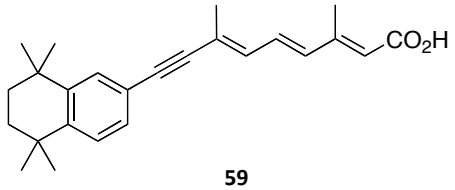

59

Figure 2.8

It is of note that all the synthetic compounds synthesised showed a significantly improved stability profile compared to that of ATRA.[228] The 'short' analogues (AH36, AH62 and AH66), **1**, **2** and **40**, display no signs of any isomerisation, whereas even though the 'ATRA-like' compounds (AH60 and AH61), **53** and **54**, isomerised, this is greatly reduced compared to that of ATRA, and more importantly they show no signs of degradation. What affect this had on any biological system was then examined and is discussed in the following Chapters.

2.6 Structure Reference Guide

The following compound names will be used when discussing the retinoids in the following Chapters.

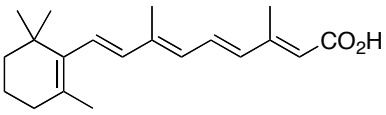

ATRA

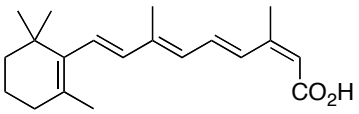

13cRA

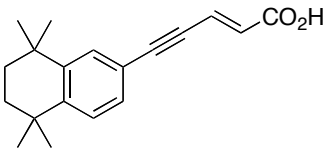

AH36 **2**

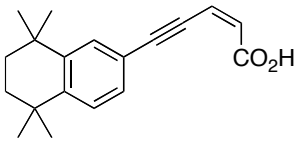

AH62 **1**

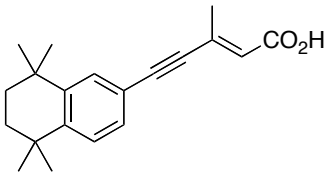

AH66 **40**

'Short' Analogues

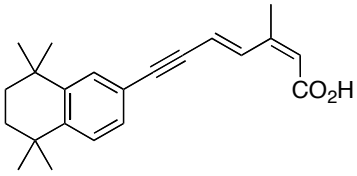

AH60 **53**

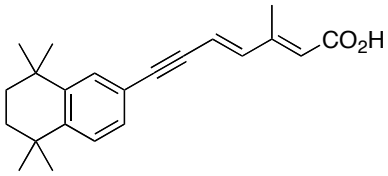

AH61 **54**

'ATRA-like' Analogues

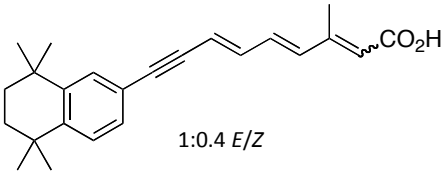

1:0.4 *E/Z*

AH98 **58**

'Extended' Analogue

Chapter III

Biological Evaluation of Synthetic Retinoids in Pluripotent Stem Cell Models

3.1 Introduction

3.1.1 Pluripotent Stem Cells and Model Systems

This Chapter aims to deal with the initial screening of the synthetic retinoids synthesised in Chapter II. As previously discussed, ATRA, the natural parent compound on which the synthesised compounds are based, possesses a wide range of biological activities. Therefore, to probe the roles of the synthetic analogues, a suitable model system linked to one of ATRA's endogenous effects was selected. ATRA is a well-known and well-published modulator of mammalian development and in particular cellular differentiation in both EC and ES cells (see Chapter I for a full discussion).[199, 200] ATRA acts through binding to nuclear receptors (RARs), and inducing the transcription of specific target genes. Ultimately, this leads to the cells differentiating into a number of different endodermal and neuronal cell derivatives.[200] Consequently, this makes these cell lines ideal model systems for evaluating neuronal induction properties of the different analogues synthesised.

The work covered in this Chapter has been carried out using mammalian EC cells, in which two different cell lines have been utilised, one murine and one human. At present, none of the compounds synthesised within this thesis have been evaluated in an ES system. Although both murine ES cells, and human ES cells, have long been isolated, there are still contentious ethical and source issues surrounding their use, which makes primary studies challenging.[2, 3, 269] ES cells are derived from *totipotent* cells of the mammalian embryo, and have subsequently been shown to be capable of both rapid proliferation and the potential to differentiate into a wide range of adult tissues, including germ cells.[270, 271] Human ES cells are of particular interest due to their possible valuable roles in improving *in vitro* toxicology, tissue engineering, drug discovery and cell therapy.[272-275] Additionally, it is widely believed that they may hold the potential to treat a wide range of degenerative diseases, including Alzheimer's and Parkinson's.[276-279] Interestingly, both mouse and human ES cells also exhibit many differences as well as similarities, and this can complicate matters further as one then needs to analyse species specific roles.[280]

Consequently, it is preferable to use a human model system to avoid any species variety. As discussed, human ES lines are not only contentious, but also time consuming and expensive to handle, due to their demanding cell culture protocols. Consequently, there has been considerable interest and research into model systems that can mimic ES cell behaviour. One such alternative, are EC cells. EC cells are pluripotent stem cells derived from teratocarcinomas, which are tumours of the germ cells.[38] They have been shown to be the malignant counterparts to ES cells and share many characteristics. Additionally, there are many advantages to their use over ES cells as they are more robust, not requiring feeder cells, and relatively easy to culture and passage.[281, 282] Furthermore, EC lines are the source of a large supply of both proteins and RNA's, and in general resist any spontaneous differentiation.[283, 284] It is, therefore, more appropriate that an EC cell line was chosen for this study.

3.1.2 Murine F9 EC Cells

The F9 cell line is one of the most widely used EC cell lines for studying *in vitro* differentiation. Isolated in 1973 from the teratocarcinoma OTT 6050, and depending on both reagents and culture conditions, these cells have the ability to differentiate into endodermal-like derivatives. It has, therefore, been widely used in many laboratories as a model to study the molecular mechanisms of differentiation.[285, 286] The cells grow rapidly, with an average doubling time of 8-10 hours in the exponential growth phase. Upon treatment with ATRA, the cells differentiate adopting a different phenotype. To identify compounds which activate retinoid signalling pathways, we have used an F9 cell line, chosen as these cells express endogenous α, β, and γ retinoic acid receptors.[167] The cell line chosen also contains a reporter assay that makes use of a retinoic acid response element (RARE) to drive a *lacZ* reporter gene.[287] This RARE is located within the *cis*-acting regulatory sequences of the human β-retinoic acid receptor gene.[288] It is comprised of 64 nucleotides, and responds to the α, β, and γ RAR subtypes.[289] The RARE had been transfected directly upstream of the *E. coli lacZ* gene, which confers retinoid responsivity to these genes.

Thus, the *lacZ* gene is used for histochemical detection of retinoid-responsive cells, measured by assaying β-galactosidase activity.

3.1.3 TERA2.cl.SP12 EC cells

One of the earliest, and frequently used human EC cell lines is the TERA2 cell line, initially isolated from a lung metastasis originating from a testicular germ cell tumour.[290] Problems with the purity of the original human TERA2 cell line meant producing accurate and reproducible studies challenging, as only 1-2% of cells were EC cells. Consequently, multiple cloned cell lines have been derived from the parent culture. These cloned cell lines contain an increased number of EC cells, but still have a varied ability to differentiate. Andrews *et al.* created the first such clone in 1984, by passage through a nude mouse, which displayed an adaption to growth *in vitro*, alongside retaining the capacity to differentiate into a diverse array of somatic tissues. This cell line was subsequently termed NTERA2.[291] A more recent sub-clone culture, termed TERA2.cl.SP12, was developed in 2001 by immunomagnetic sorting, followed by single cell selection for SSEA-3 positive cells and subsequent culture.[209] Characterisation of the TERA2.cl.SP12 cell line showed that in an undifferentiated state, the cells express SSEA-3, -4 and TRA-1-60, signifying they are in an EC cell state. Treatment with ATRA promotes the cells to differentiate, signified by the down-regulation of stem cell markers and up-regulation of neural markers A2B5 and VINIS-53. In addition, TERA2.cl.SP12 stem cells have similarly been shown to regulate neural genes, again in a well-defined manner. Further indication of their ability to differentiate was demonstrated upon grafting of the cells into severe combined immunodeficient (SCID) mice. Complex xenograft tumours, containing multiple cell types, including high proportions of both neural and epithelial derivatives were subsequently produced.[210, 211] Prolonged exposure to ATRA leads to the formation of a heterogeneous cell population, containing multiple mature functioning neurons.[212] Subsequent electrophysiological experiments show the neurons produced contain an array of functional receptors and ion channels with a pharmacological profile indicative of that defined for native neurons.[213] Consequently, this makes the

TERA2.cl.SP12 cell line an effective model system for the *in vitro* study of neurogenesis and for screening the novel retinoids synthesised.

3.2 Aims and Objectives

The aim of this Chapter was to evaluate the synthetic analogues synthesised in Chapter II on models of EC stem cells. From previous work, both within our research group and those of others, we know ATRA and some of its synthetic analogues induce neural differentiation in these stem cell model systems *in vitro*. More stable synthetic analogues (EC23 and EC19) have shown improved profiles to that of their natural counterpart, ATRA, and we aimed to test the new analogues synthesised in a similar manner.[228]

The main objectives, therefore, were to: (1) initially demonstrate that the synthetic compounds activated the inherent retinoic acid receptors, using the transfected F9 EC cell line; (2) analyse the compound's potential to induce differentiation in the TERA2.cl.SP12 EC cell line, looking at both the expression of cell surface antigens and gene profiles; (3) quantify the expressed markers; and (4) investigate concentration response profiles of active compounds.

3.3 Results

3.3.1 Effects of the Synthetic Retinoids on F9 Murine EC Cells

To compare the effects of the synthetic compounds *versus* known natural retinoid responses, cultures of F9 murine embryonal carcinoma cells containing a *lacZ* reporter line were incubated with 10 μM concentrations of each test compound. This was to determine whether the new analogues trigger the retinoid-signalling pathway, through binding of one or multiple RAR receptors (α, β, or γ). ATRA was also screened as the positive control, alongside control cultures, consisting of untreated F9 cells, and those treated only with the vehicle, DMSO. DMSO has been included in all investigations throughout this thesis as it is the solvent used to dissolve the compounds and thus allow for their administration.

The F9 cells exposed to no compounds, *i.e.* the untreated control, showed no positive results upon β-galactosidase staining as expected (Figure 3.1 (**A**)). Those exposed to the vehicle in general also displayed no positive cells, although in some cultures a small proportion of the population did stain positive. This is in contrast to F9 cells treated with ATRA, which stained strongly in response to β-galactosidase with a high percentage of blue cells visible (Figure 3.1 (**C**)). The 'short' retinoid analogues, AH36, AH62 and AH66, all displayed a very low percentage of cells staining positive, suggesting they do not bind to the RAR receptors (Figure 3 (**D**) (**E**) and (**F**)). Both the 'ATRA-like' analogues, AH60 and AH61, produced a positive number of cells similar to that of ATRA, (Figure 3 (**G**) and (**H**)). The 'extended' retinoid analogue, AH98, again showed a very low percentage of positive staining cells, giving an early indication that it binds poorly, if at all, to the RAR receptors (Figure 3 (**I**)).

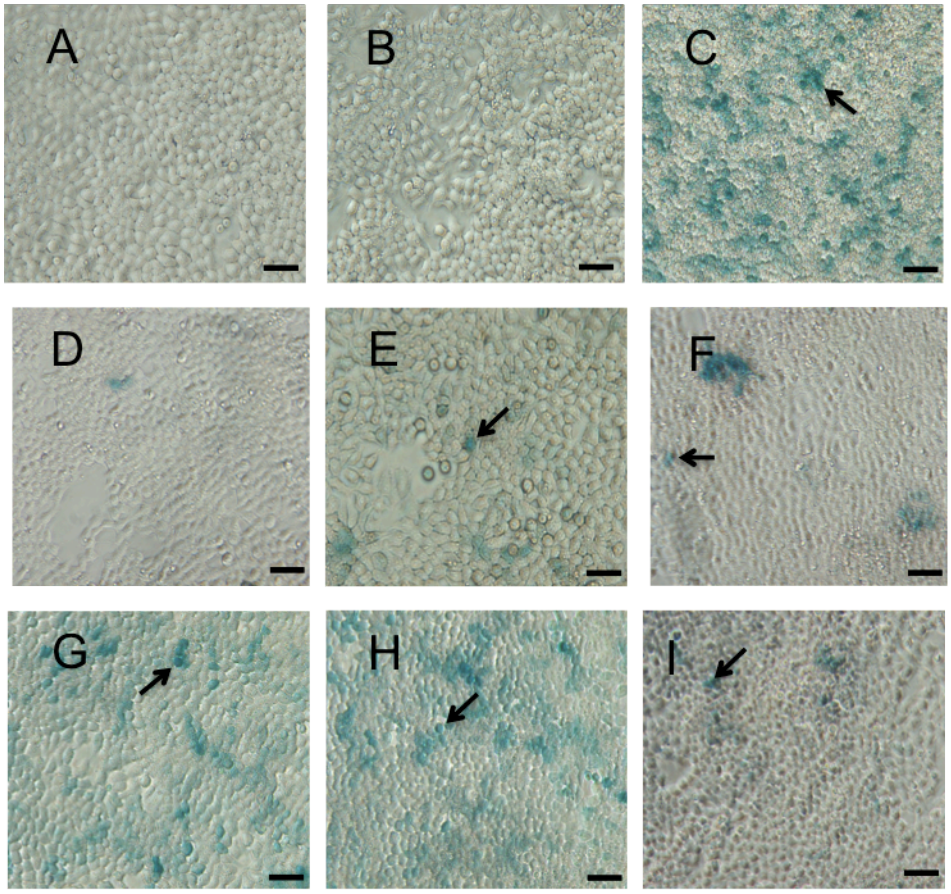

Figure 3.1 Phase micrographs showing *lacZ* gene expression visualised by X-gal staining for *β*-galactosidase in F9 murine EC cell cultures exposed to no compounds (un-treated control), vehicle (DMSO), 10 μM ATRA, AH36, AH62, AH66, AH60, AH61 and AH98 for 18 hours (**A**, **B**, **C**, **D**, **E**, **F**, **G**, **H** and **I** respectively). Arrows show examples of labelled positive cells. Scale Bars: 100 μm.

To quantify the amount of positively stained cells within each sample group, random triplicate images were recorded and analysed in ImageJ software. The number of positive (blue) cells in each field of view was recorded. The data are displayed graphically in Figure 3.2. Both AH60 and AH61 display significantly more positive cells than that of the vehicle, DMSO, therefore suggesting that they are inducing the response, not the solvent. There is no significant difference seen in the number of positive cells displayed for ATRA, AH60 or AH61 suggesting they all bind at a similar affinity to the receptors in this system. The level of positive cells for the 'short-*cis*-analogue' is nearly identical for that seen for DMSO suggesting that any positive cells in these cultures are likely to be as a result of the solvent, not the synthetic retinoid.

Similarly, there is no significant difference in the data for either of the 'short-trans-analogues', again suggesting that these too are incapable of binding to the receptors. The 'extended' analogue does display a significant up-regulation of the number of positive cells compared to DMSO, but this is significantly lower than that seen for ATRA and both the synthetic analogues AH60 and AH61.

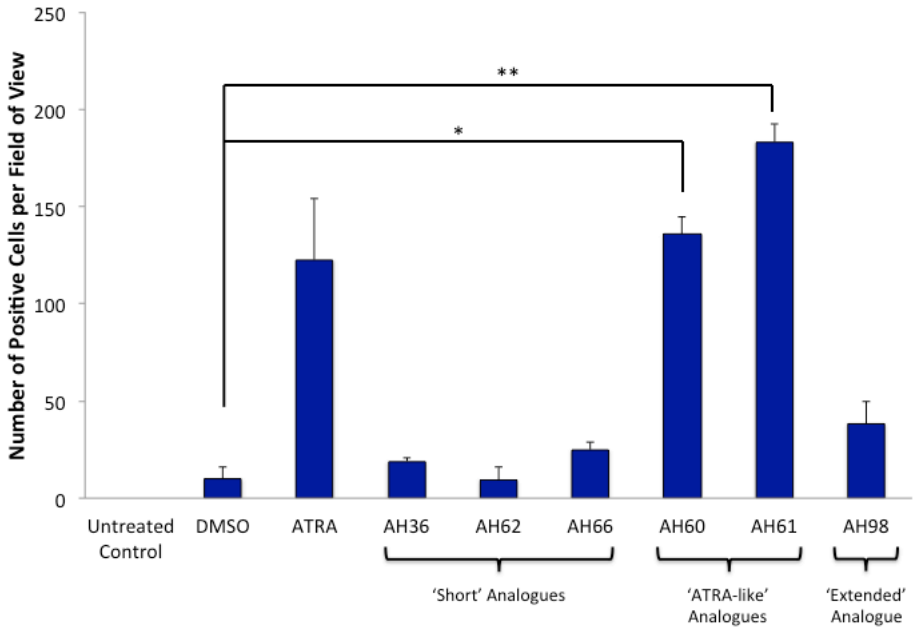

Figure 3.2 Quantification of the number of positive cells per field of view for each retinoid treatment. Results are presented with ± standard error (SEM), n=3. ** p≤0.005, * p≤0.05, Student's t-test corrected for multiple testing between compared sample populations using the Bonferroni correction.

The above figures give an early indication that both the 'short' and 'extended' analogues do not display a biological response analogous to that of ATRA, as they appear not to activate transcription associated with binding to the RAR receptors. An early hypothesis, and explanation for this lack of activity displayed by the 'short' analogues would be that they are not large enough to enter the receptors completely, and therefore, do not bind correctly. Further clarification of this data will be obtained through analysis in a second model, using the TERA2.cl.SP12 cell line.

3.3.2 Viability, Toxicity, and Morphological Analysis of Synthetic Retinoids on TERA2.cl.SP12 Cells

To analyse further the effects of the synthetic compounds *versus* both natural retinoid responses and other synthetic retinoids, cultures of TERA2.cl.SP12 EC cells were incubated with 10 μM concentrations of each compound. Concurrently, as in the previous model, control cultures were evaluated consisting of untreated, and therefore undifferentiated, cells, along with cultures exposed to the vehicle, DMSO.

3.3.2.1 Number of Viable Cells

Retinoid treated cultures were maintained for up to seven days, with the media changed every three days. The number of viable cells was analysed at three and seven days using a tetrazolium-based proliferation assay (MTS assay). Proliferating cells produce reducing equivalents such as NADPH and NADH, which reduce 3-(4,5-dimethylthiazol-2-yl)-5-(3-carboxymethoxyphenyl)-2-(4-sulfophenyl)-2H-tetrazolium, from a yellow salt to a soluble blue formazan product. The amount of the formazan product is then measured by reading the UV absorbance of the solution at 490 nm. This absorbance value is proportional to the number of viable cells in the culture (Figure 3.3).

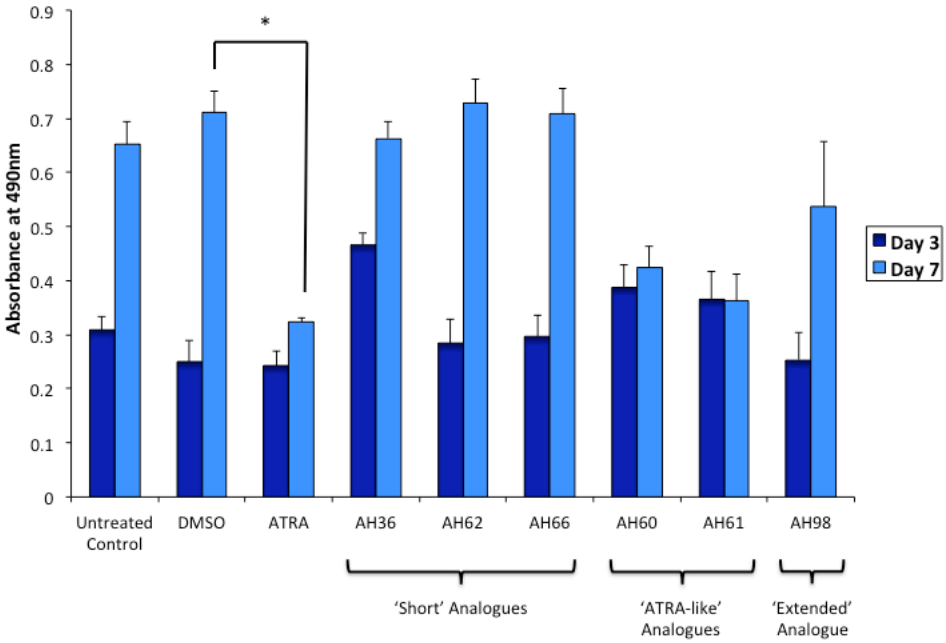

Figure 3.3 Analysis of the number of viable cells using an MTS assay kit. Cultures were exposed to 10 μM ATRA, AH36, AH62, AH66, AH60, AH61 and AH98, alongside untreated control and vehicle cultures. Analysis was done at 3 and 7 days. Cell number, expressed as an absorbance value, was attenuated in ATRA, AH60 and AH61 cultures, compared to the controls. However, those treated with the 'short ' analogues and the 'extended' analogue did not show a reduction in cell number compared to the controls. Results are presented with ± standard error (SEM), n=3. * p≤0.05, Student's t-test corrected for multiple testing between compared sample populations using the Bonferroni correction.

Untreated cultures, and those treated with DMSO, continued to proliferate rapidly and after seven days the cultures were highly confluent. Those treated with ATRA displayed a significantly reduced cell number compared to the vehicle, DMSO. This reduction in cell number is associated with a differentiating cell culture as the cells no longer proliferate but exit the cell cycle and commit to a specific lineage. Consistent with the data presented for the F9 cell line, there was no reduction in cell number for any of the 'short' synthetic analogues or the 'extended' analogue. This further supports that they are incapable of activating the retinoid pathway, and, in-turn, unable to arrest cellular proliferation and induce differentiation. A decrease in cell number was observed in cultures treated with AH60 and AH61,comparable to that of ATRA. This is consistent with both compounds initiating a response, as displayed in the previous data set.

3.3.2.2 Toxicity

Simultaneously, the toxicity of the compounds was assessed *via* measuring the number of apoptopic and viable cells (Figure 3.4 (**A**) and (**B**) respectively). Retinoid treated cultures were again maintained for seven days, with the media changed every three. Analysis was performed using Guava ViaCount reagent, on a Guave EasyCyte™ Plus System flow cytometer. All compounds assessed showed none significantly different levels of apoptopic cells and viable cells, indicating that at a concentration of 10 μM the compounds appear to not be toxic. Therefore, further analysis can be carried out using concentrations equal or below 10 μM, to assess the potential of the compounds to induce differentiation.

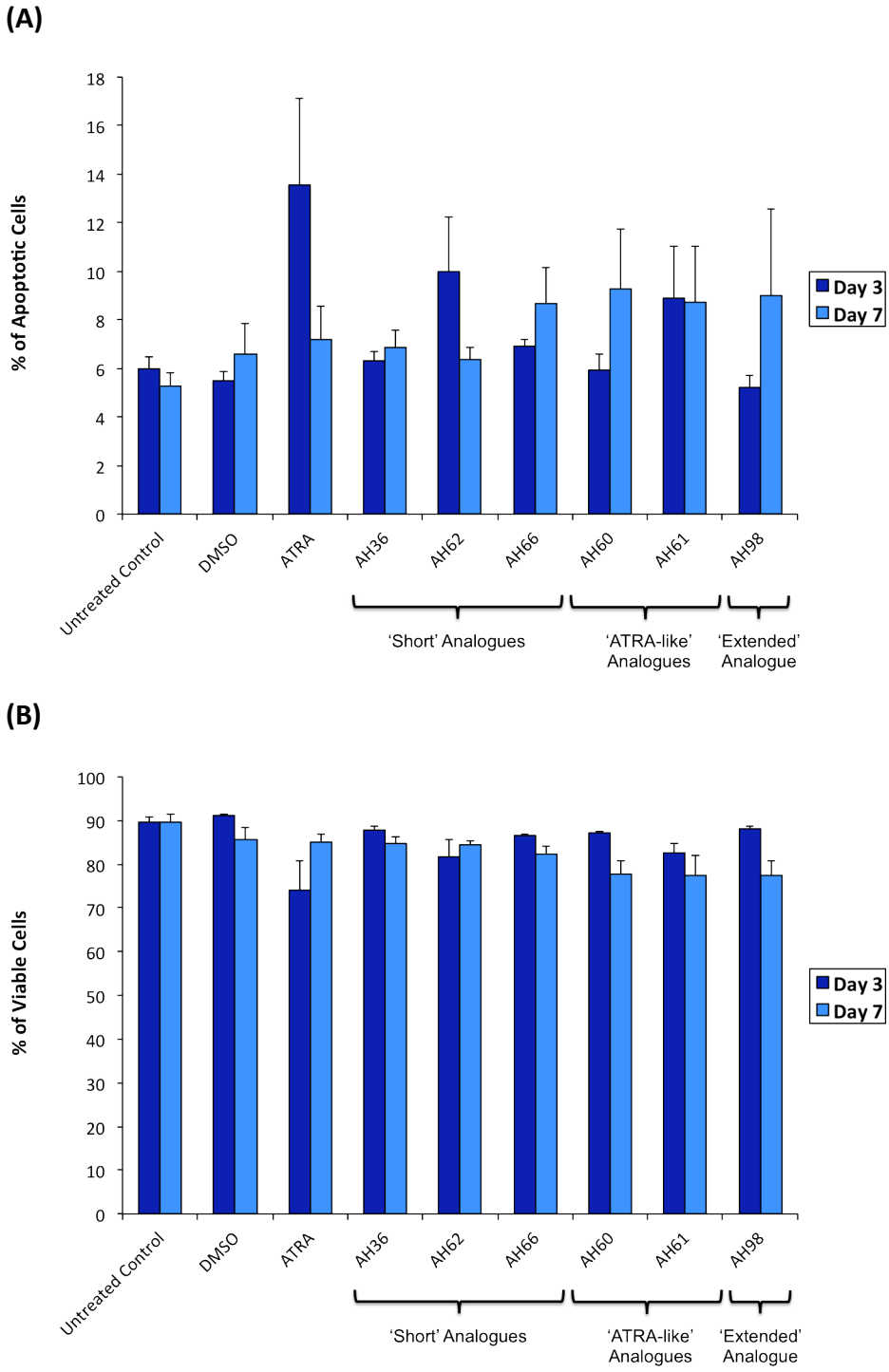

Figure 3.4 (**A**) Analysis of the number of apoptopic cells displayed as a percentage of the total population; (**B**) Analysis of the number of viable cells as a percentage of the total population. All cultures were exposed to 10 μM ATRA, AH36, AH62, AH66, AH60, AH61 and AH98, alongside untreated control and vehicle cultures. Analysis was done at 3 and 7 days. Results are presented with ± standard error (SEM), n=3. Per statistical analysis using the Student's t-test corrected for multiple testing between compared sample populations using the Bonferroni correction, there were no significant differences between any of the treatments.

3.3.2.3 Morphologies of Induced Cell Types

Analysis of the morphologies produced by each of the synthetic retinoids at 10 μM showed dramatic differences after seven days of incubation. Undifferentiated TERA2.cl.SP12 cultures are characterised by a homogeneous 'cobblestone' appearance displayed throughout the culture (Figure 3.5).

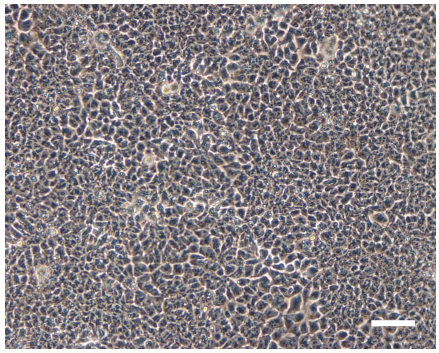

Figure 3.5 Confluent undifferentiated TERA2.cl.SP12 cells displaying a typical 'cobblestone' appearance. Scale Bar: 100 μm.

If cultured past optimal density, the cells start to become over confluent, layering upon one another, but still retaining a homogeneous phenotype. This is visible in cultures that were undifferentiated after seven days (Figure 3.6 (**A**)). A similar phenotype was seen for cultures treated with DMSO, and that of the 'short' retinoid analogues AH36, AH62 and AH66 (Figure 3.6 (**B**), (**D**), (**E**) and (**F**) respectively). Cultures exposed to ATRA displayed a far greater degree of heterogeneity, consistent with a differentiating culture (Figure 3.6 (**C**)). Although the culture appeared to be differentiating, seven days is too short a time to visualise any neural phenotypes, such as neural rosettes or individual neurons. This phenotype was also visible in cultures treated with AH60 and AH61, reinforcing their similarity to that of ATRA (Figure 3.6 (**G**) and (**H**)). In line with previous data, the 'extended' analogue AH98 displayed no phenotypic similarities to that of ATRA, and like the 'short' analogues the cells retained their undifferentiated phenotype (Figure 3.6 (**I**)).

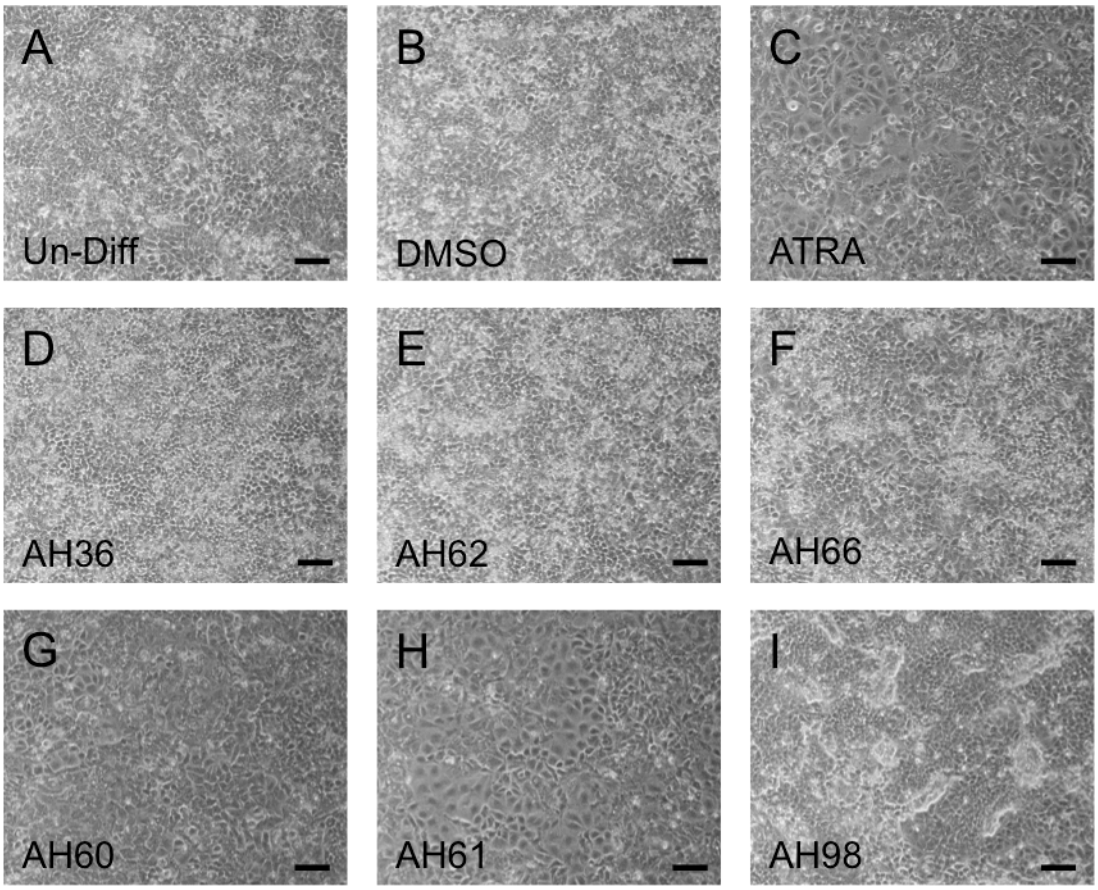

Figure 3.6 Morphologies of TERA2.cl.SP12 cells after 7 days treatment with retinoids. Undifferentiated cultures (**A**) retained a homogeneous appearance but with some cells layering as they become over confluent and sub-optimal. Treatment with DMSO (**B**), the 'short' retinoids AH36, AH62 and AH66 ((**D**), (**E**) and (**F**) respectively) and the 'extended analogue AH98 (**I**) all display an identical profile, indicating the cells remain in an undifferentiated state. Cultures exposed to ATRA (**C**) exhibit an extremely heterogeneous morphology, with significantly less cells per field of view, typical of a differentiating cell culture. Similarly, cultures exposed to AH60 (**G**) and AH61 (**H**) also displayed this morphology. Scale Bars: 100 μm.

Cultures exposed to ATRA, AH60 and AH61 were cultured for up to twenty one days. Those untreated and exposed to DMSO, and the 'short' and 'extended' analogues became over confluent and sub-optimal and were therefore not cultured past seven days. Both AH60 and AH61 appeared to mimic the profile exhibited by ATRA. They displayed a characteristic neural phenotype, with neural rosette-like areas and neurons visible under phase microscopy (Figure 3.7).

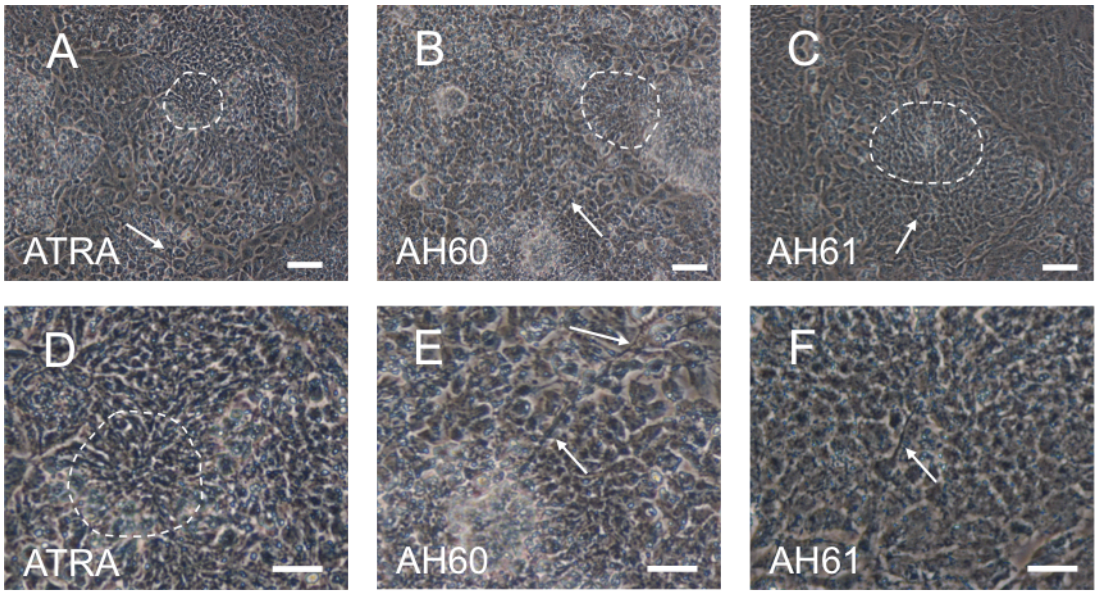

Figure 3.7 Phase images, both low and high magnification, of differentiated TERA2.cl.SP12 cultures after twenty one days of culture with ATRA (**A**/**D**), AH60 (**B**/**E**), and AH61 (**C**/**F**). Cultures exposed to all three retinoids exhibit a highly heterogeneous morphology, displaying many neural-like phenotypes, including neural rosettes (bordered area) and neuronal processes (arrows). Scale Bars: 100 μm low magnification, 50 μm high magnification.

Upon immunocytochemical staining with cytokeratin-8, a general marker of the cytoskeleton, this apparent similarity between all three compounds was reinforced. Unlike some synthetic compounds, such as EC19, both synthetic analogues AH60 and AH61 do not appear to induce the formation of a large flat cell type, which subsequently form large 'plaque' like areas.[228] Instead, they appeared to mimic the natural biological profile of ATRA generating a highly heterogeneous cell population (Figure 3.8).

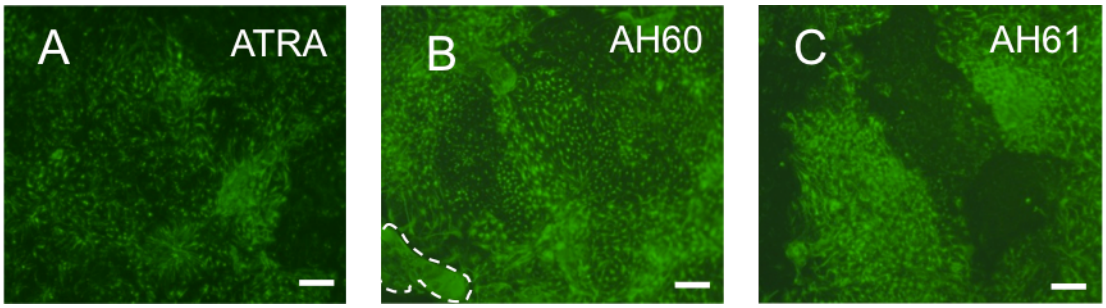

Figure 3.8 Cytokeratin-8 expression in cultures of TERA2.cl.SP12 cells cultured for twenty one days with either ATRA (**A**), AH60 (**B**) or AH61 (**C**). All cultures display a highly heterogeneous cell population, with little formation of 'plaques' consisting of large flat cells (bordered area). Scale bars: 50 μm.

3.3.3 Differential Regulation of Cell Surface Markers

The ability of the synthetic compounds to induce cellular differentiation in the TERA2.cl.SP12 cell line was further evaluated by analysing the expression profiles of known markers for both stem cell and differentiated phenotypes. Flow cytometry was performed on samples of cells treated with 10 μM of each retinoid, alongside untreated controls and those treated with DMSO. Cell profiles were analysed after 3 and 7 days. Day 0 data represents confluent untreated, and therefore, undifferentiated TERA2.cl.SP12 cell cultures. The expression levels of two stem cell antigens, SSEA-3 and TRA-1-60 (keratin-sulfate-associated glycoprotein stem surface marker) were investigated to assess loss of pluripotency (Figure 3.9 (**A**) and (**B**) respectively).[292, 293]

In undifferentiated cell cultures, both SSEA-3 and TRA-1-60 remain high as the cells retain their stem cell phenotype. A decrease in the expression level of both indicates that the cells are committing to differentiation. Consistent with known literature and as discussed earlier, both markers decreased in response to treatment with ATRA. In line with previous data discussed within this Chapter, similar expression profiles were visualised for AH60 and AH61, as was seen for ATRA. The only notable difference was the significantly greater drop-off in the expression of TRA-1-60 upon treatment with AH61. In cell cultures treated with the 'short' analogues AH36, AH62 and AH66 and 'extended' analogue AH98, expression levels of SSEA-3 and TRA-1-60

remained relatively high. These profiles match those seen for both the untreated controls and DMSO, supporting the phenotypes visualised under phase microscopy and the MTS assay previously carried out in the EC cell system.

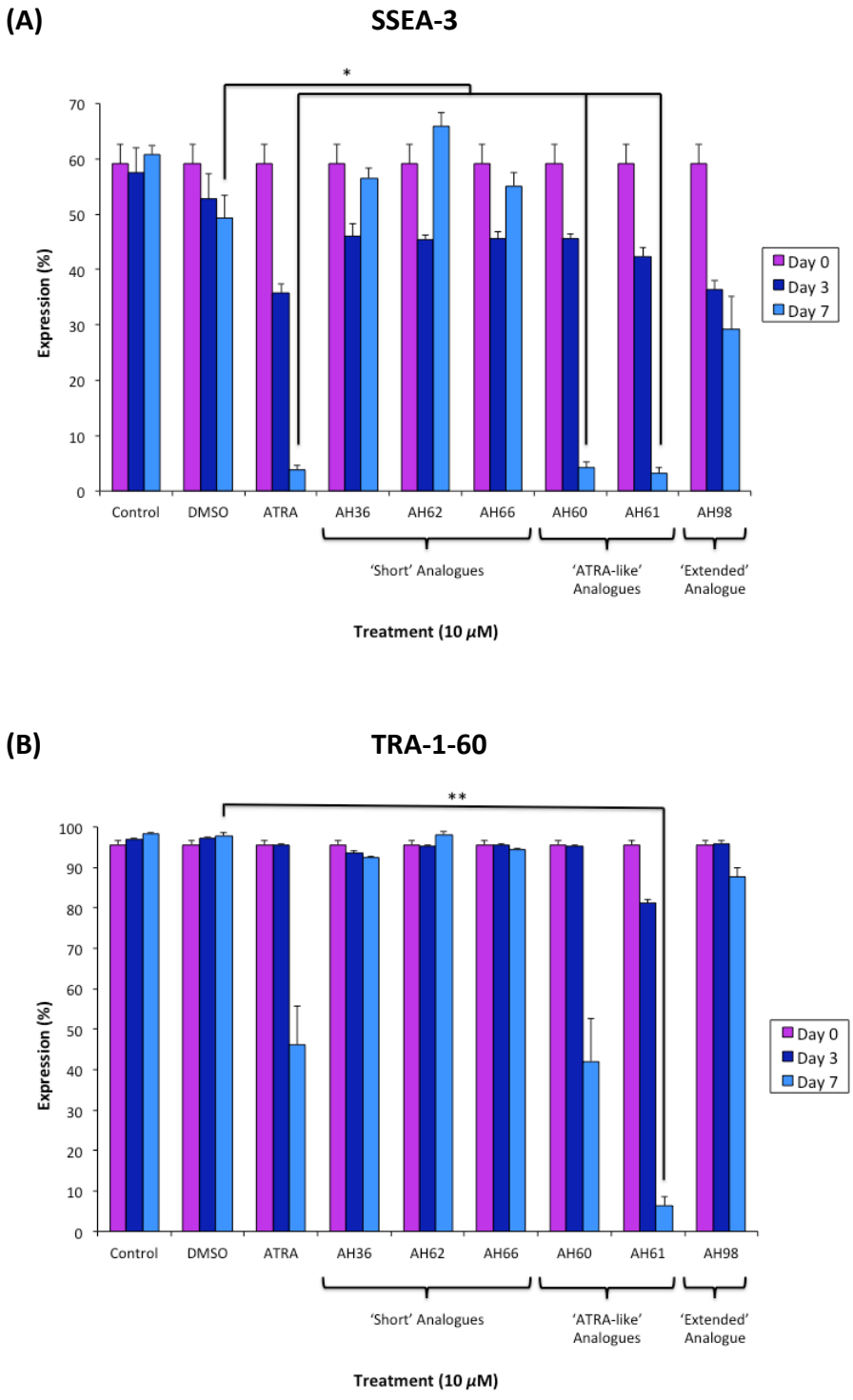

Figure 3.9 Flow cytometric analysis of markers of stem cells, SSEA-3 (**A**) and TRA-1-60 (**B**). TERA2.cl.SP12 cells were incubated with 10 μM concentrations of each retinoid for 7 days. Analysis was carried out at day 3 and day 7. Undifferentiated controls retained an unchanged profile over the 7 days. There was little variation seen for cultures exposed to DMSO, the 'short' analogues AH36, AH62 and AH66 and the 'extended' analogue, AH98. Those treated with ATRA, AH60 and AH61 all showed a significant drops in the expression of markers, particularly AH61. Results are presented with ± standard error (SEM), n=3. ** $p \leq 0.005$, * $p \leq 0.05$, Student's t-test corrected for multiple testing between compared sample populations using the Bonferroni correction.

As TERA2.cl.SP12 cells are well known for their ability to form neurons in response to treatment with retinoids, most notably, in response to ATRA, flow cytometry was accordingly used to assess the expression of A2B5 (ganglioseries antigen marking early-stage neural cells), as a measure of differentiation towards a neural lineage.[206] Consistent with previous data discussed, ATRA, AH60 and AH61 induced the expression of A2B5 in a comparatively similar manner. All the 'short' synthetic retinoids tested, AH36, AH62 and AH66, showed no increase in expression levels, consistent with them having an inability to induce neurogenesis. There was a slight increase in A2B5 expression seen for those cultures exposed to the 'extended' analogue, AH98, although this was not comparable to that seen for ATRA, and indeed AH60 or AH61. As expected both the untreated control and those treated with the vehicle showed no increase in A2B5 expression (Figure 3.10).

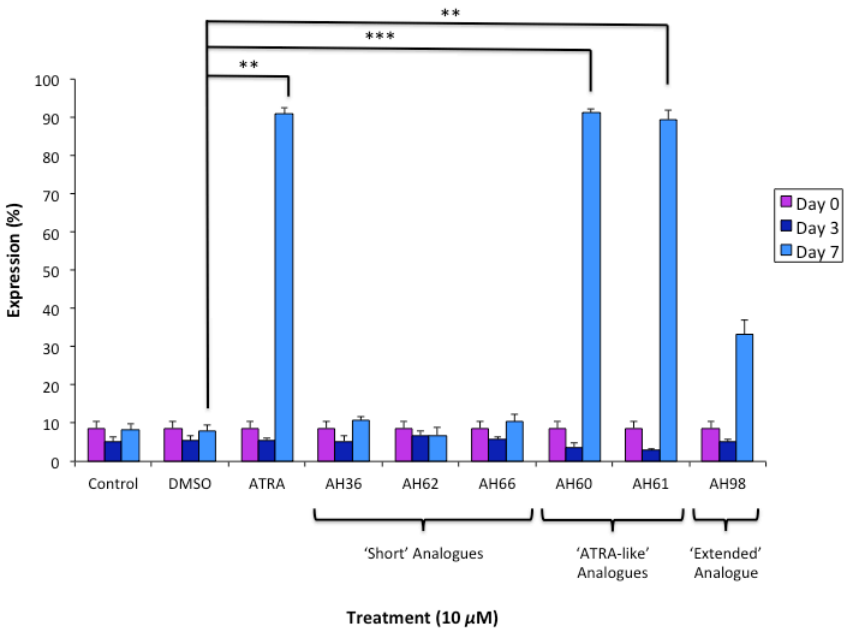

Figure 3.10 Flow cytometric analysis of a marker for early stage neural cells, A2B5. TERA2.cl.SP12 cells were incubated with 10 μM concentrations of each retinoid for 7 days. Analysis was carried out at day 3 and day 7. Undifferentiated controls and DMSO exposed cultures retained an unchanged profile over the 7 days as do those exposed to the 'short' analogues AH36, AH62 and AH66. The 'extended' analogue, AH98, did display an increase in expression, although this is approximately 50% of that seen for the positive control, ATRA. Those treated with AH60 and AH61 all showed a significant increase in expression of the marker, mimicking the profile seem for ATRA. Results are presented with ± standard error (SEM), n=3. *** $p \leq 0.0005$, ** $p \leq 0.005$, Student's t-test corrected for multiple testing between compared sample populations using the Bonferroni correction.

To summarise, both AH60 and AH61 appeared to mimic the biological profile of that seen for ATRA. The 'short' analogues AH36, AH62 and AH66 all demonstrated a complete lack of ability to induce any form of biological response. The 'extended' analogue, AH98, did show some potential, but this was significantly less than that exhibited by ATRA and both AH60 and AH61. The 'extended' analogue, AH98, has also been tested as a mixture of two isomers, and has been demonstrated to be unstable under standard laboratory conditions. Consequently, there was to be no further examination into the biological potential of these molecules, and all further work was focused around characterising the biological profile of both AH60 and AH61.

Expanding on the previous flow cytometry study, ATRA, AH60 and AH61 cultures were maintained for up to 14 days. All three markers screened previously were analysed (Figure 3.11).

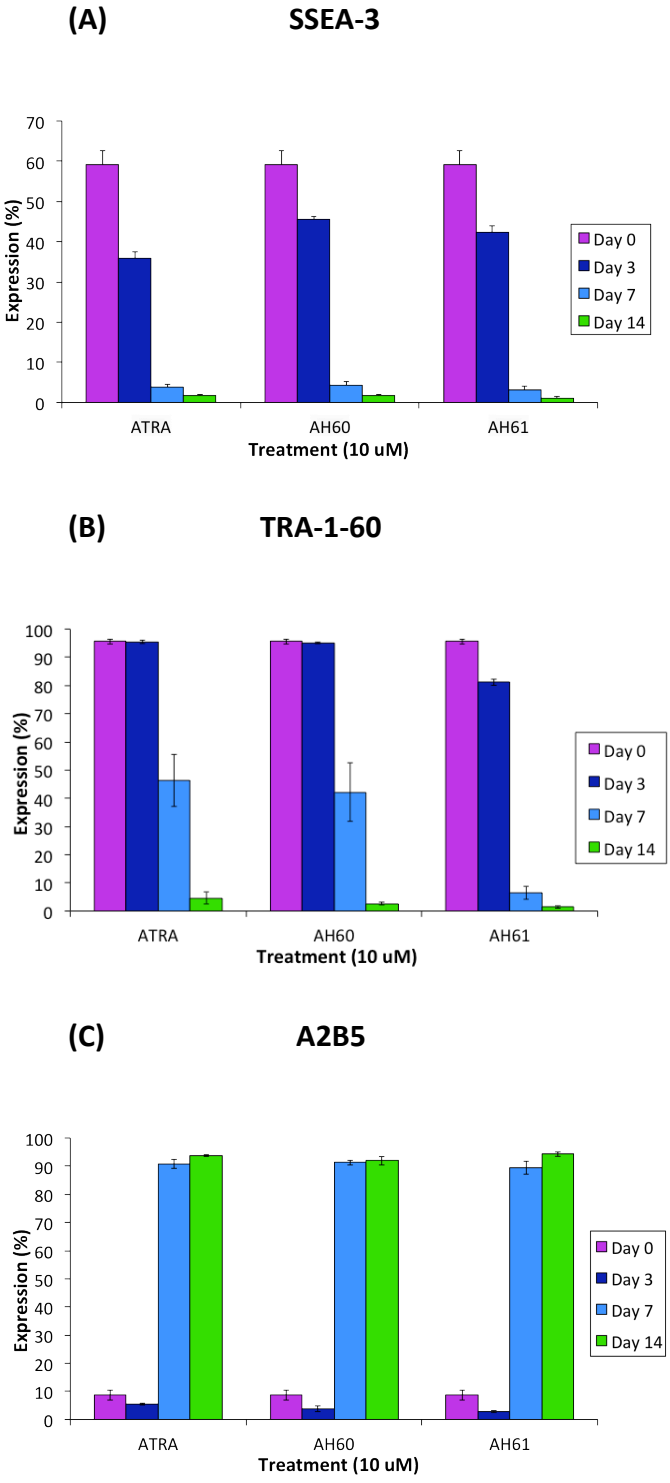

Figure 3.11 Flow cytometric analysis of markers of stem cells SSEA-3 (**A**) and TRA-1-60 (**B**), and a marker of early stage neural cells, A2B5 (**C**). TERA2.cl.SP12 cells were incubated with 10 μM concentrations of each retinoid for 14 days, with analysis carried out at days 3, 7 and 14. All retinoid treatments led to a decrease in both stem cell markers, and concurrently an increase in A2B5 expression. Results are presented with ± standard error (SEM), n=3. Per statistical analysis using the Student's t-test corrected for multiple testing between compared sample populations using the Bonferroni correction, there were no significant differences between any of the treatments.

The longer exposure time for all three retinoid treatments demonstrated that all three compounds completely eliminated the expression of both stem cell markers, while promoting the expression of A2B5 to greater than 95%. Overall, there was no significant difference in the expression profiles of SSEA-3, TRA-1-60 or A2B5, when exposed to all three compounds.

3.3.4 Analysis of Associated Gene Profiles

Further assessment of cellular differentiation in response to treatment with the synthetic retinoids was evaluated through the expression profiles of known genes. To allow for a direct comparison, samples of the cells analysed for flow cytometry at 3, 7 and 14 days were simultaneously analysed through real-time polymerase chain reaction (RT-PCR). Therefore, the analysis was undertaken on TERA2.cl.SP12 cells treated with retinoids at a concentration of 10 μM. Three known genes of interest were chosen to be examined, Nanog, Oct-4 and Pax6. The first two are essential regulators of early development and connected to the self-renewal of undifferentiated stem cells, in addition to being rapidly silenced during cellular differentiation.[294-297] The third, the paired-domain, homeodomain-containing transcription factor Pax6, was chosen to assess the neurogenesis properties of the retinoids, as it is essential for the development of much of the central nervous system.[298-301] The expression profiles of each gene over the 14 days are shown in Figure 3.12.

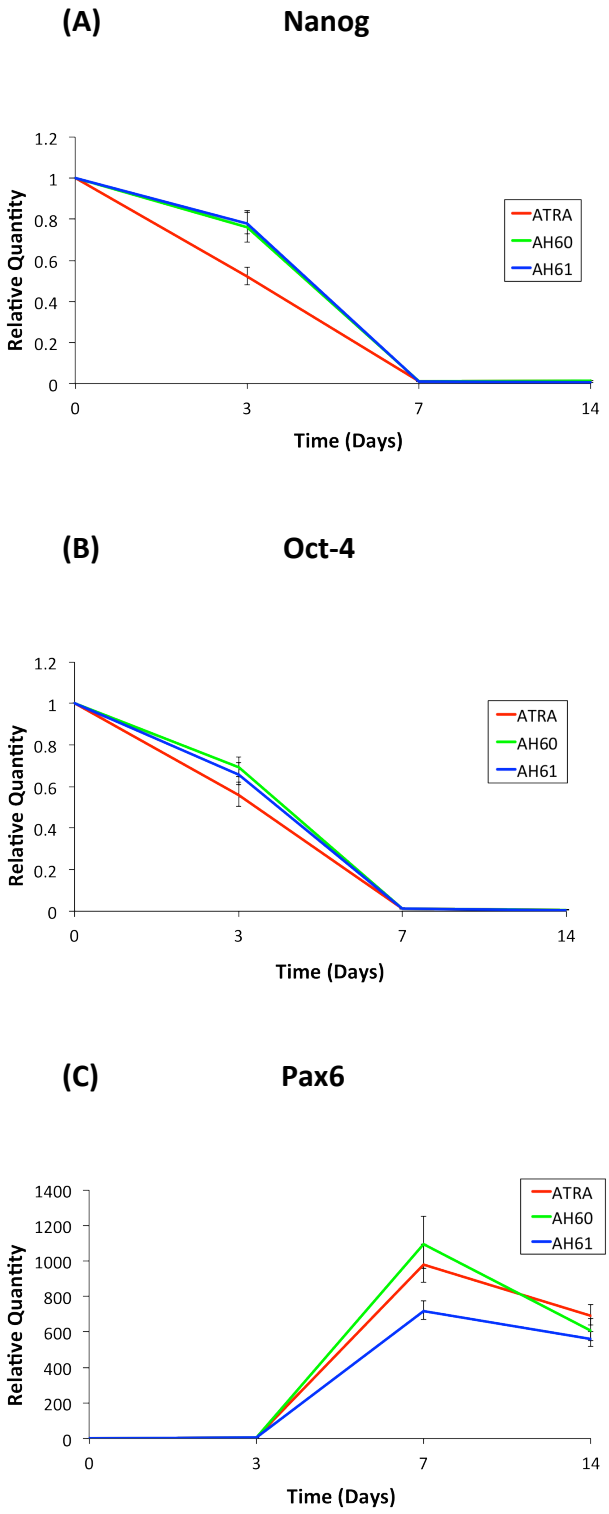

Figure 3.12 RT-PCR analysis of two genes associated with pluripotency, Nanog (**A**) and Oct-4 (**B**), and one associated with motor and ventral phenotypes, Pax6 (**C**). ATRA, AH60 and AH61 all supressed Nanog and Oct-4 to a similar extent, whereby after day 7 there was no longer any expression. In addition, both AH60 and AH61 led to an expression profile of Pax6 similar to that of ATRA. All gene levels are expressed as a relative quantity, which is the difference in gene expression between, undifferentiated TERA2.cl.SP12 cells and those exposed to a retinoid treatment. Results are presented with ± standard deviation (SD), n=3.

The expression of Nanog and Oct-4 was suppressed in cultures treated with both ATRA and synthetic analogues, AH60 and AH61, all in a similar manner. Consistently, Pax6 expression increased up to just after day 7, after which it decreased slightly to day 14. Again, all three retinoids, both natural and synthetic, showed a similar profile, thus further indicating that both AH60 and AH61 play a key role in inducing differentiation of TERA2.cl.SP12 cells.

Previous work carried out within the Przyborski research group (un-published work by Daniel Tams) on synthetic retinoid EC23 had shown that it displayed a different gene expression profile to that of ATRA. Analysis of early changes in gene expression (days 0-7), demonstrated that EC23 attenuated a change at a slower rate than that of ATRA. More significantly, it had become apparent that EC23 displayed a significantly different Pax 6 expression profile to that of ATRA, highlighting a difference in the molecules mode of action yet to be discussed in the literature. Therefore, the profiles of ATRA, AH60, AH61 and EC23 were examined simultaneously at days 1, 3, 5 and 7 (Figure 3.13). It was hypothesised that the increased molecular similarity of the AH series of compounds would lead to profiles closer to that of the natural molecule, ATRA.

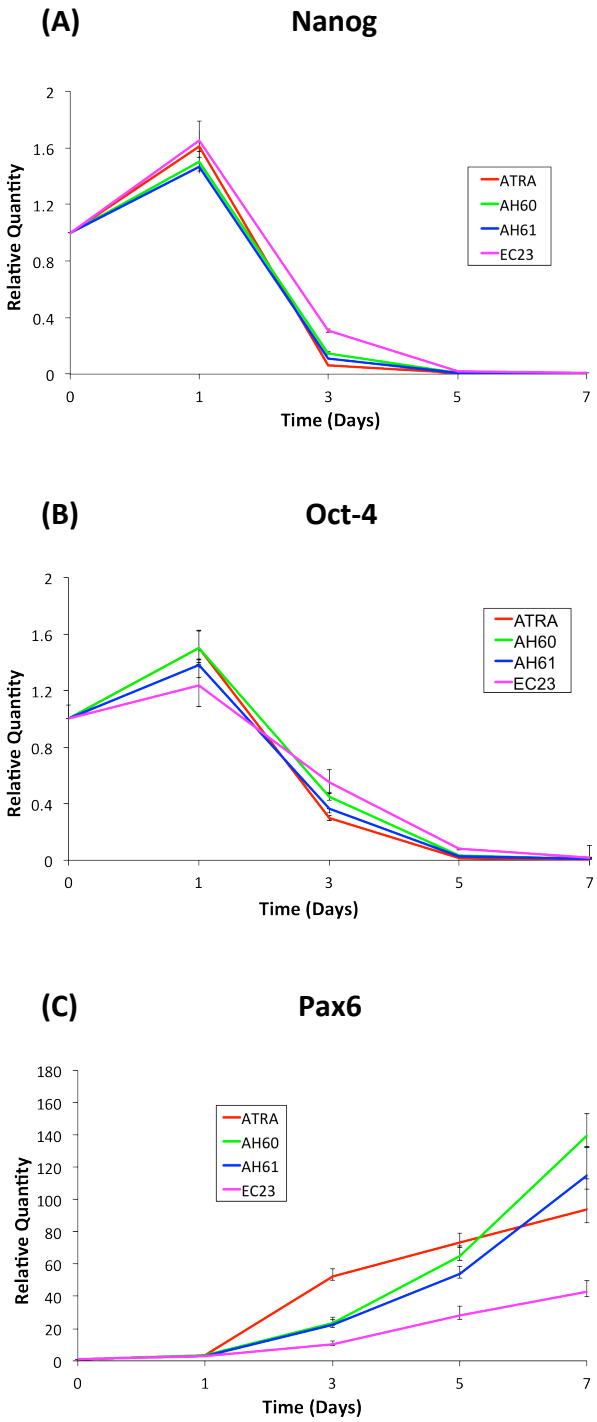

Figure 3.13 RT-PCR analysis of two genes associated with pluripotency, Nanog (**A**) and Oct-4 (**B**), and one associated with motor and ventral phenotypes, Pax6 (**C**). ATRA appears to suppress both Nanog and Oct-4 at a slightly faster than the synthetic compounds. Both AH60 and AH61 show little differences and mimic the profile exhibited by ATRA closely. EC23 also has a highly analogous profile, yet attenuates a response the slowest. Similarly, ATRA, AH60 and AH61 all lead to insignificant differences in levels of Pax 6 expression after 7 days, whereas EC23 is significantly lower. All gene levels are expressed as a relative quantity, which is the difference in gene expression between, undifferentiated TERA2.cl.SP12 cells and those exposed to a retinoid treatment. Results are presented with ± standard deviation (SD), n=3.

From the expression profiles, it is clear that the suppression of Nanog and Oct-4 due to retinoid treatment appears to occur more rapidly when using ATRA. Although it must be noted both AH60 and AH61 have profiles that are not significantly different. As demonstrated previously within the research group, EC23 is the slowest to have an effect, but after 5 days has suppressed both genes to the same extent as the other synthetic compounds. The most significant difference is in the expression of Pax6. EC23 does attenuate a relative increase in the expression of Pax6 compared to that of the control cultures, yet it is approximately 50% less than those seen for the other treatments. This is in contrast to both synthetic analogues, AH60 and AH61, which both display profiles not significantly different to that of ATRA after 7 days treatment.

As hypothesised, both AH60 and AH61 display profiles somewhere in between that of ATRA and EC23. This is perhaps not entirely unexpected due to their similar molecular structures, and could give an early indication into the affinity of each compound for the retinoid receptors. It should be emphasised though, that this is speculation and that to support this hypothesis, molecular binding studies would need to be carried out.

3.3.5 Induction of Neurogenesis: Visualisation of Neural Proteins

Confirmation that TERA2.cl.SP12 cells differentiate into a neuronal population in response to AH60 and AH61 was demonstrated by immunocytochemical staining. The expression of neuronal specific proteins was investigated using antibodies raised against the neuronal specific β-III-tubulin marker, TuJ1. In undifferentiated TERA2.cl.SP12 cells, low levels of expression are visualised, but upon treatment with ATRA there is a significant up-regulation. In conjunction with TuJ1 staining, the expression of the 200 kDa neurofilament protein (NF-200) was simultaneously examined. NF-200 is a cytoskeletal marker for mature neurons and often used for evaluating neurogenesis. Undifferentiated TERA2.cl.SP12 cells do not express NF-200, but NF-200 positive neurons have been identified in cultures treated with ATRA.

Cultures of TERA2.cl.SP12 cells were treated with both AH60 and AH61 at 10 μM for 21 days, alongside positive control cultures exposed to ATRA at 10 μM. Both synthetic analogues, AH60 and AH61, display a significant up-regulation of both markers consistent with that of ATRA (Figure 3.14). To quantify the data, the number of positive cell bodies (perykarya) per field of view for each culture treatment was counted, with the aid of ImageJ software. The data is displayed as the mean from three randomly selected immunostained images, for both TuJ1 and NF-200 (Figure 3.15). There is no significant difference seen in the expression of TuJ1 over the three retinoid treatments, with all three expressing the marker highly. Upon analysing NF-200 expression, cultures treated with AH61 have a significantly higher number of positive perykarya, compared to both ATRA and AH60. There appears to be no difference in the expression of NF-200 between both ATRA and AH60, inferring they are equally as active. Thus, at equal concentrations under the conditions tested AH61 appears to be a more potent inducer of neuronal differentiation than ATRA and AH60, as inferred by the increased number of mature (NF-200) neurons.

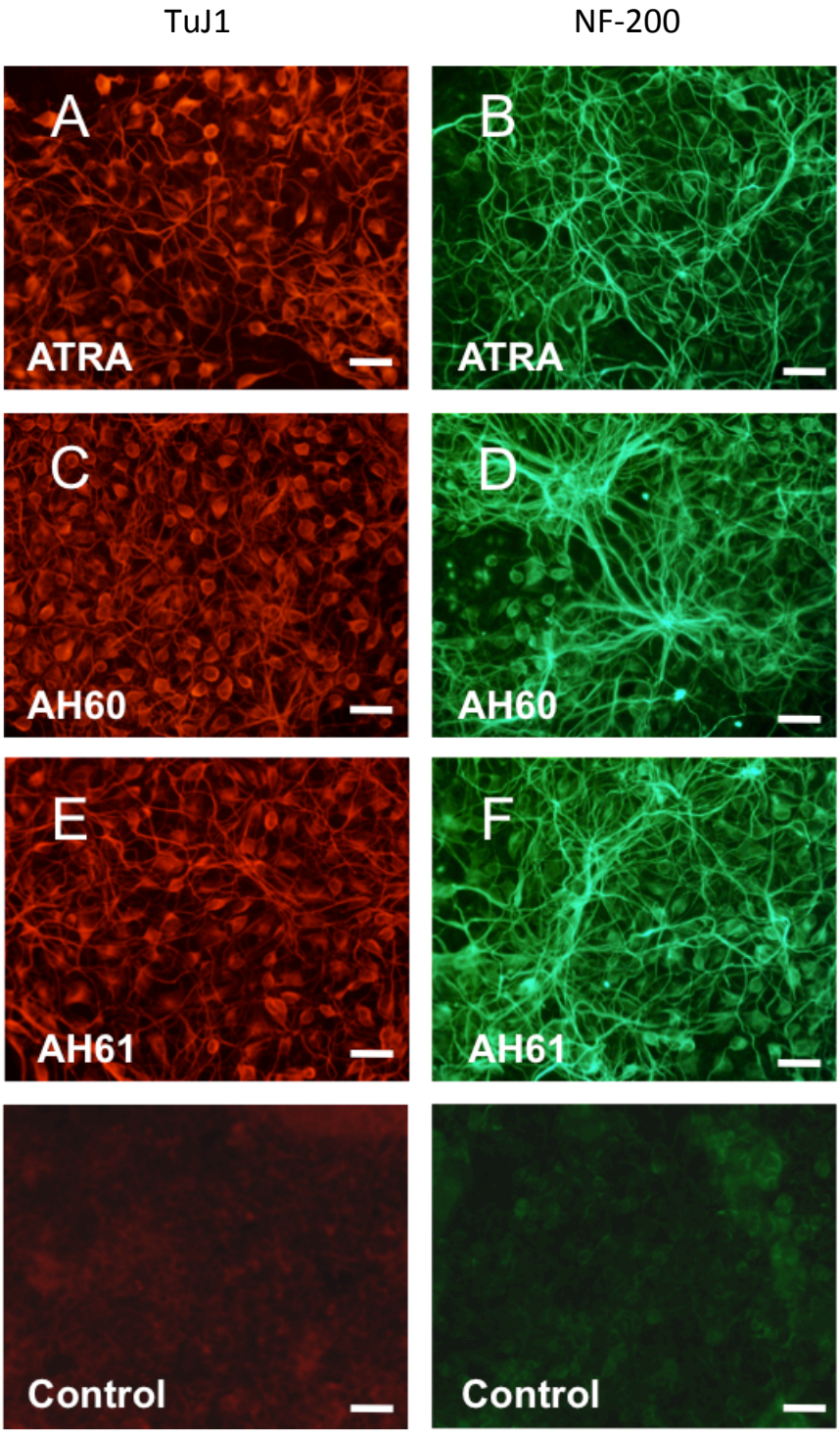

Figure 3.14 Conformation of neural differentiation in TERA2.cl.SP12 cell cultures incubated with 10 μM ATRA (**A** and **B**), AH60 (**C** and **D**) or AH61 (**E** and **F**). All retinoid treatments resulted in high expression of both TuJ1 and NF-200 markers. Control cultures (vehicle controls treated only with DMSO and no retinoid) displayed no expression of either marker. Scale bars: 50 μm.

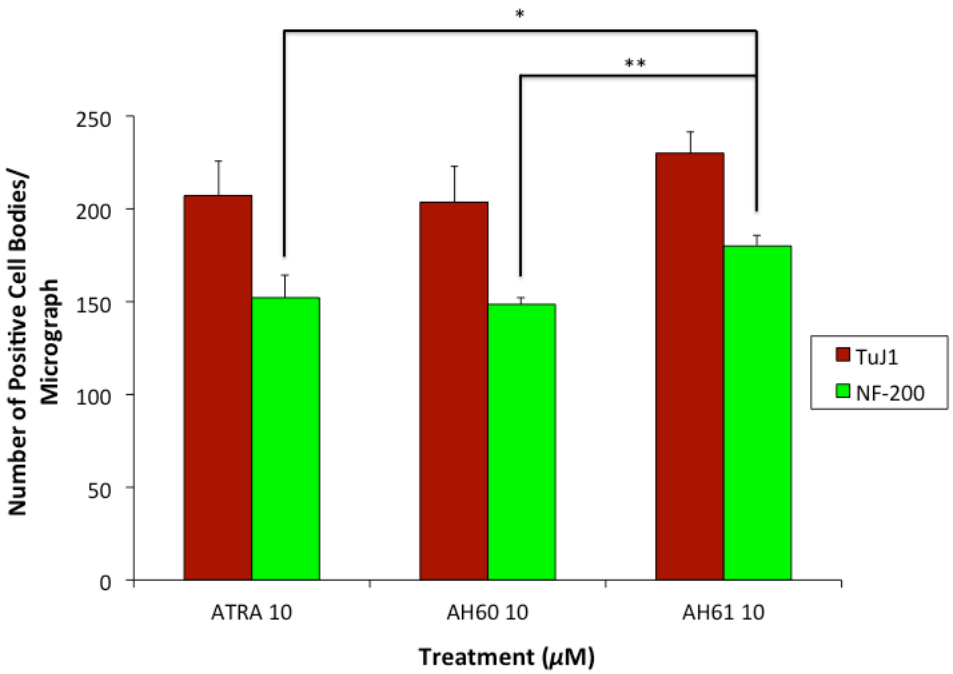

Figure 3.15 Plot displaying the quantification of the immunological data, as performed by counting labelled positive cell bodies. Cultures of TERA2.cl.SP12 EC stem cells incubated with 10 μM ATRA, AH60 or AH61 for 21 days, subsequently fixed and immunocytochemically stained for TuJ1 and NF-200. Using ImageJ software the number of positive cell bodies were counted on 3 random fields per treatment condition. AH61 induced a significant increase in expression of NF-200 over both ATRA and AH60 treatments. Values shown represent mean + standard error (SEM), n=3. **p≤0.005, *p≤0.05, Student's t-test corrected for multiple testing between compared sample populations using the Bonferroni correction.

This data collectively demonstrated that both ATRA and the synthetic retinoids behave in a similar manner, and induced the differentiation of pluripotent stem cells to form mature neural derivatives. In addition, the AH series appeared to induce a biological response closer to that seen for the natural ligand, ATRA, compared to that induced by EC23. In conjunction with their improved chemical stability, the current data indicated that the synthetic compounds are a credible alternative to ATRA as a biological tool for inducing neurogenesis in a pluripotent stem cell model system. Furthermore, some of the early data, including the reduced expression of the pluripotent cell surface marker TRA-1-60, and increased expression of the late neuronal marker, NF-200, point to an increased activity for the synthetic retinoid AH61.

3.3.6 Dose Response of the Synthetic Retinoids

To further probe the effectiveness of the synthetic compounds, a concentration study was undertaken to investigate their dose response. It was hypothesised that due to the modifications of the core, which block known metabolic oxidation sites, discussed in Chapter II, the compounds would be more effective at lower concentrations than that of ATRA. Previous research had demonstrated that ATRA is as effective at 1 μM as it is at 10 μM. Therefore, to investigate the dose response, a concentration range from 1 μM decreasing by a factor of 10 to 0.001 μM was chosen.

3.3.6.1 Flow Cytometry Analysis

As an initial screen, TERA2.cl.SP12 cells were cultured for 7 days with ATRA, AH60, AH61 and EC23 at 1 μM, 0.1 μM, 0.01 μM and 0.001 μM concentrations. Analysis of the cell population was undertaken at days 3 and 7, where day 0 represents untreated, and therefore, undifferentiated, TERA2.cl.SP12 EC cells. As in all previous studies, the same three markers were investigated, SSEA-3, TRA-1-60 and A2B5. The data for ATRA, AH60 and AH61 is presented in Figure 3.16.

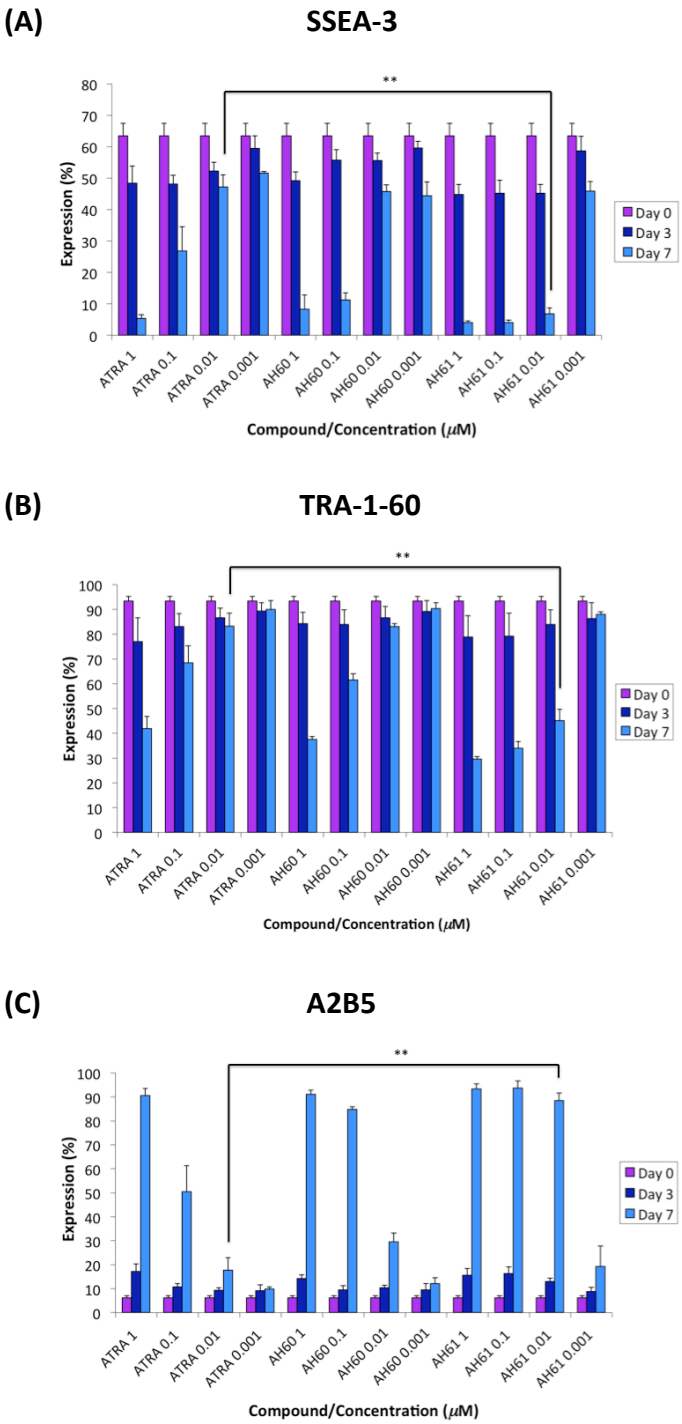

Figure 3.16 Flow cytometric analysis of markers of stem cells SSEA-3 (**A**) and TRA-1-60 (**B**), and a marker of early stage neural cells, A2B5 (**C**). TERA2.cl.SP12 cells were incubated with each retinoid for 7 days at either 1 μM, 0.1 μM, 0.01 μM or 0.001 μM, with analysis carried out at days 3 and 7. All retinoid treatments at 1 μM lead to a decrease in both stem cell markers, and concurrently an increase in A2B5 expression. Upon reducing the concentration to 0.1 μM the potency of ATRA is markedly reduced, while retained for both AH60 and AH61. At 0.01 μM only AH61 retains its ability to induce differentiation, while at 0.001 μM all the compounds are inactive. Results are presented with ± standard error (SEM), n=3. ** $p \leq 0.005$, Student's t-test corrected for multiple testing between compared sample populations using the Bonferroni correction.

A clear dose response curve was visualised for ATRA as the concentration was reduced by a factor of ten from 1 μM to 0.001 μM. At 1 μM, the expression levels of all three markers were at similar levels to those seen when using 10 μM (data presented previously), indicating the TERA2.cl.SP12 cells are differentiating. Reducing the concentration to 0.1 μM significantly increases/reduces expression levels of all three markers accordingly, indicating that only a small percentage of the cellular population were differentiating. Upon reducing the concentration to 0.01 μM and 0.001 μM, expression levels of all three markers was identical to the undifferentiated control cultures (representative of day 0). Therefore, for ATRA to be an effective tool for cellular differentiation, a concentration of 1 μM or higher is required. As clearly demonstrated, any further reduction leads to a severe decline in activity.

The profile seen for AH60 is similar in its overall trend, with the exception that the TERA2.cl.SP12 cells appeared to differentiate when exposed to 0.1 μM AH60. Suggesting that this analogue is approximately 10 fold more potent. More interesting, however, is the expression profile exhibited by AH61. This synthetic analogue retained its biological potency in this system even when the concentration was reduced to 0.01 μM, overall making it approximately 100 fold more active than natural ATRA.

When comparing the activity of AH61 to EC23, which was screened previously for a dose response, a clear similarity was observed. Both compounds displayed a nearly identical profile for all three markers, with no significant differences visualised. This data is consistent with both being 100 fold more active than their natural counterpart, ATRA (Figure 3.17)

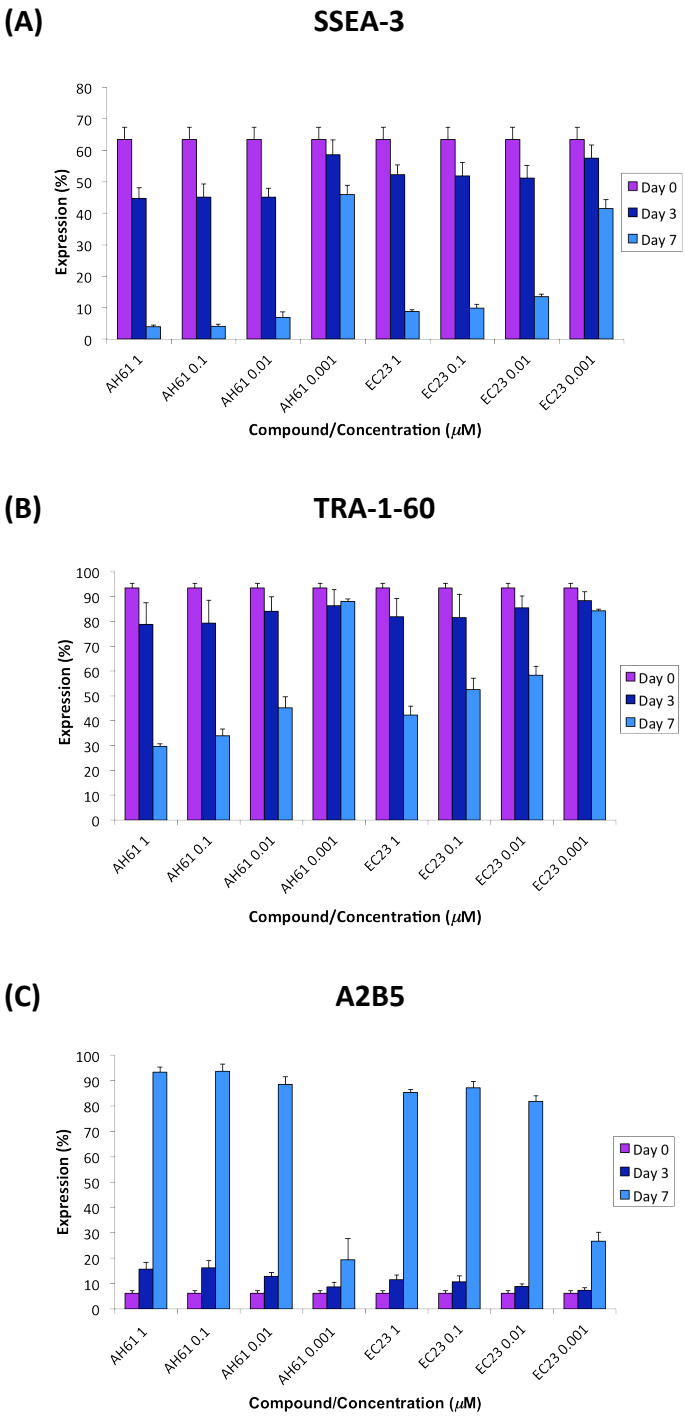

Figure 3.17 Flow cytometric analysis of markers of stem cells SSEA-3 (**A**) and TRA-1-60 (**B**), and a marker of early stage neural cells, A2B5 (**C**). TERA2.cl.SP12 cells were incubated with either AH61 or EC23 for 7 days at either 1 μM, 0.1 μM, 0.01 μM or 0.001 μM, with analysis carried out at days 3 and 7. Both, AH61 and EC23, supress SSEA-3 and TRA-1-60 expression to a similar extent over the concentration range. Similarly, they promote the expression of A2B5 in an identical manner. Overall, both compounds display activity down to 0.01 μM. Results are presented with ± standard error (SEM), n=3. Per statistical analysis using the Student's t-test corrected for multiple testing between compared sample populations using the Bonferroni correction, there were no significant differences between any of the treatments.

3.3.6.2 RT-PCR Analysis

As in the previous studies, a sample of the cell population for each treatment was removed and lysed before the remaining sample was analysed *via* flow cytometry (see section 3.3.4). RT-PCR was then employed to analyse the expression profiles of three genes of interest. Therefore, cell populations after treatment for 7 days over the concentration ranges 1 – 0.001 μM for ATRA, AH60, AH61 and EC23 were analysed. Again, the three genes of interest were, Nanog, Oct-4 and Pax6, as collectively these exhibit changes in the genotype associate with neural differentiation.

The first gene of interest to be analysed was Nanog. As the concentration of ATRA was reduced, the expression levels of Nanog increased, indicating a more pluripotent state. The expression profile was similar to that generated from the flow cytometry data, displaying a consistency across the two techniques (Figure 3.18 (**A**)). When exposed to AH60, both 1 μM and 0.1 μM concentrations completely suppressed Nanog expression, demonstrating that this molecule maybe more potent than previously thought. However, at 0.01 μM, Nanog expression was significantly reduced (Figure 3.18 (**B**)). Both AH61 and EC23 displayed highly analogous profiles. Both, completely suppressed any expression of Nanog after 7 days at a concentration of 0.01 μM or higher. As discussed previously within this Chapter, AH61 appeared to be able to bring about a change a gene expression faster than EC23, as seen by the expression levels at day 3. The reason for this is still unknown, although one hypothesis could be AH61's closer molecular resemblance to ATRA, compared to that of EC23 (Figure 3.18 (**C**) and (**D**) respectively).

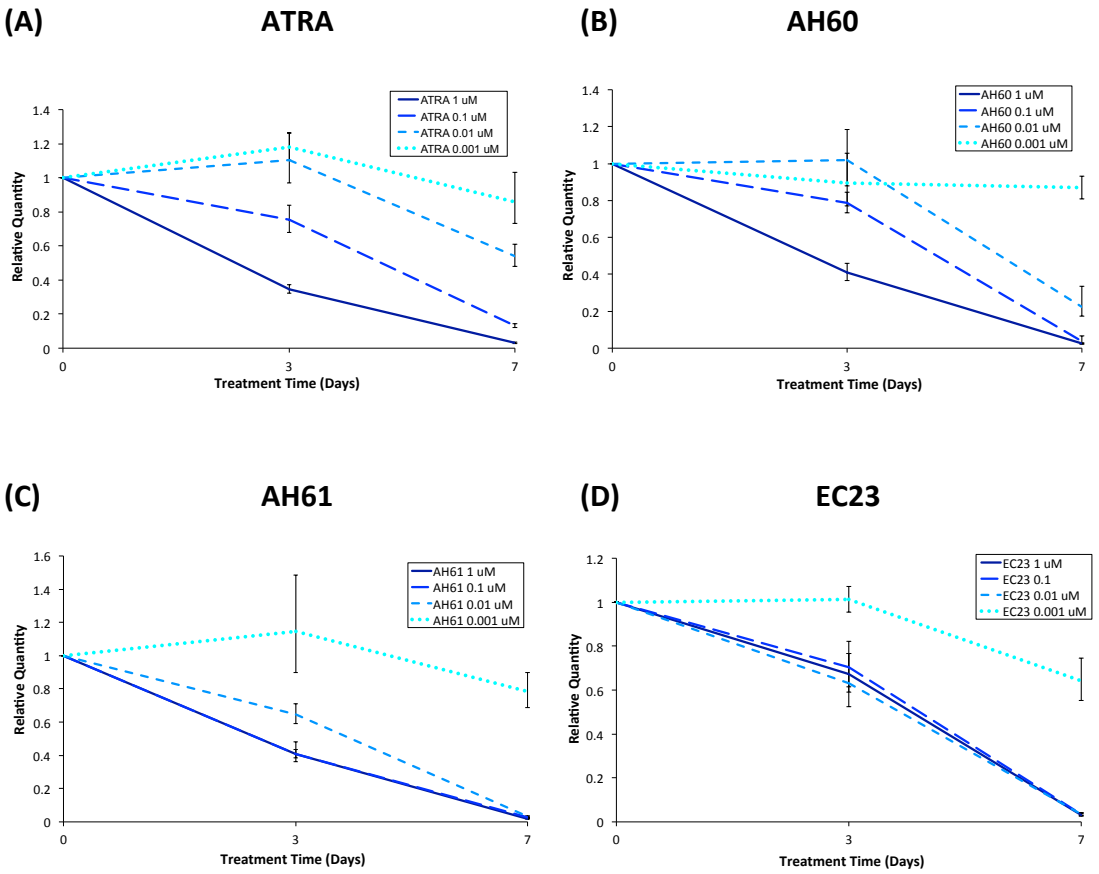

Figure 3.18 RT-PCR analysis of a gene associated with pluripotency, Nanog. Analysis was undertaken at days 3 and 7, after treatment with ATRA (**A**), AH60 (**B**), AH61 (**C**) and EC23 (**D**) at 1 μM, 0.1 μM, 0.01 μM or 0.001 μM. As the concentration of ATRA is reduced, expression of Nanog increased accordingly. A similar profile was seen with AH60, except for a greater decrease in expression seen at 0.01 μM. Both AH61 and EC23 displayed near identical profiles with complete suppression seen at 0.01 μM or higher concentrations, with the only difference being a slightly faster response when using AH61. All gene levels are expressed as a relative quantity, which is the difference in gene expression between, undifferentiated TERA2.cl.SP12 cells and those exposed to a retinoid treatment. Results are presented with ± standard deviation (SD), n=3.

The second gene of interest was Oct-4. Being a gene associated with pluripotency in stem cells, the expression profiles were hypothesised to be similar to those seen for Nanog. Again, all the compounds reduced the expression of the Oct-4 gene at 1 μM, with ATRA displaying a gradual increase in expression as the concentration was dropped. The synthetic compounds all displayed profiles and characteristics nearly identical to those displayed for Nanog expression (Figure 3.19).

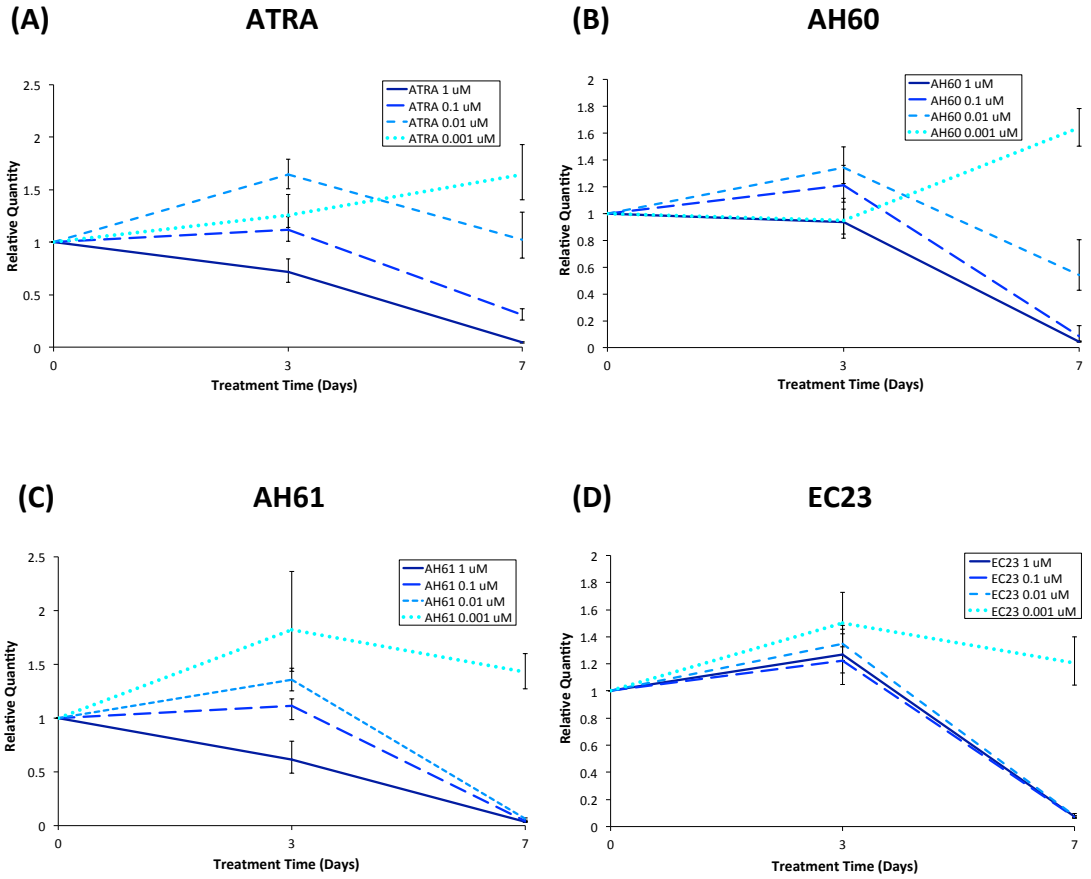

Figure 3.19 RT-PCR analysis of a gene associated with pluripotency, Oct-4. Analysis was undertaken at days 3 and 7, after treatment with ATRA (**A**), AH60 (**B**), AH61 (**C**) and EC23 (**D**) at 1 μM, 0.1 μM, 0.01 μM or 0.001 μM. As the concentration of ATRA was reduced, expression of Oct-4 increased accordingly. A similar profile was seen with AH60, except for a greater decrease in expression seen at 0.01 μM. Both AH61 and EC23 displayed near identical profiles with complete suppression seen at 0.01 μM or higher concentrations. The only difference is that AH61 attenuates a response slightly faster, as seen when analysing day 3 expression levels. All gene levels are expressed as a relative quantity, which is the difference in gene expression between, undifferentiated TERA2.cl.SP12 cells and those exposed to a retinoid treatment. Results are presented with ± standard deviation (SD), n=3.

One point to note was the sudden drop-off in activity seen for both AH61 and EC23. ATRA, and to some extent AH60, showed gradually increasing levels of expression as their active concentration was reduced. Conversely, cultures exposed to AH61 and EC23 either showed complete suppression of both Nanog and Oct-4, when treated at concentrations higher than 0.01 μM, or relatively no suppression, when the concentration was reduced to 0.001 μM. This would suggest the active concentration is somewhere between 0.01 μM and 0.001 μM.

Finally, the induction of Pax6 expression was investigated (Figure 3.20). This initially highlighted the inability of the parent compound ATRA to induce neural differentiation as only at 1 μM was there any induction of Pax6 expression. The profile displayed by AH60 correlated with that seen in the expression of the cell surface marker A2B5, with increased expression seen at both 1 μM and 0.1 μM. There was no induction of Pax6 expression when AH60 was administered at 0.01 μM, displaying that reduction of Nanog and Oct-4 is not entirely associated with neural differentiation. Previously, Pax6 expression had highlighted the only difference between the biological activity of AH61 and EC23. Whilst AH61 and ATRA both displayed a gradual and sequential drop off in Pax6 expression as the concentration was lowered, levels of expression at 0.01 μM AH61 were equivalent to levels seen at 1 μM ATRA. This strongly suggests a greater potential for AH61 to induce Pax6 expression over ATRA. EC23 displayed a more convoluted profile, in which the expression levels of Pax6 peaked, when EC23 was administered at 0.1 μM. As the concentration was increased to 1 μM, levels Pax6 expression reduced. It has subsequently been demonstrated within the group (un-published data produced by Daniel Tams) that 10 μM levels of EC23 further reduce the expression levels of Pax6, consistent with levels seen in the preliminary RT-PCR analysis discussed earlier in this chapter. At 0.01 μM, EC23 has a similar effect as that of 0.01 μM AH61 and upon reduction to 0.001 μM, no increase in expression of Pax6 is displayed.

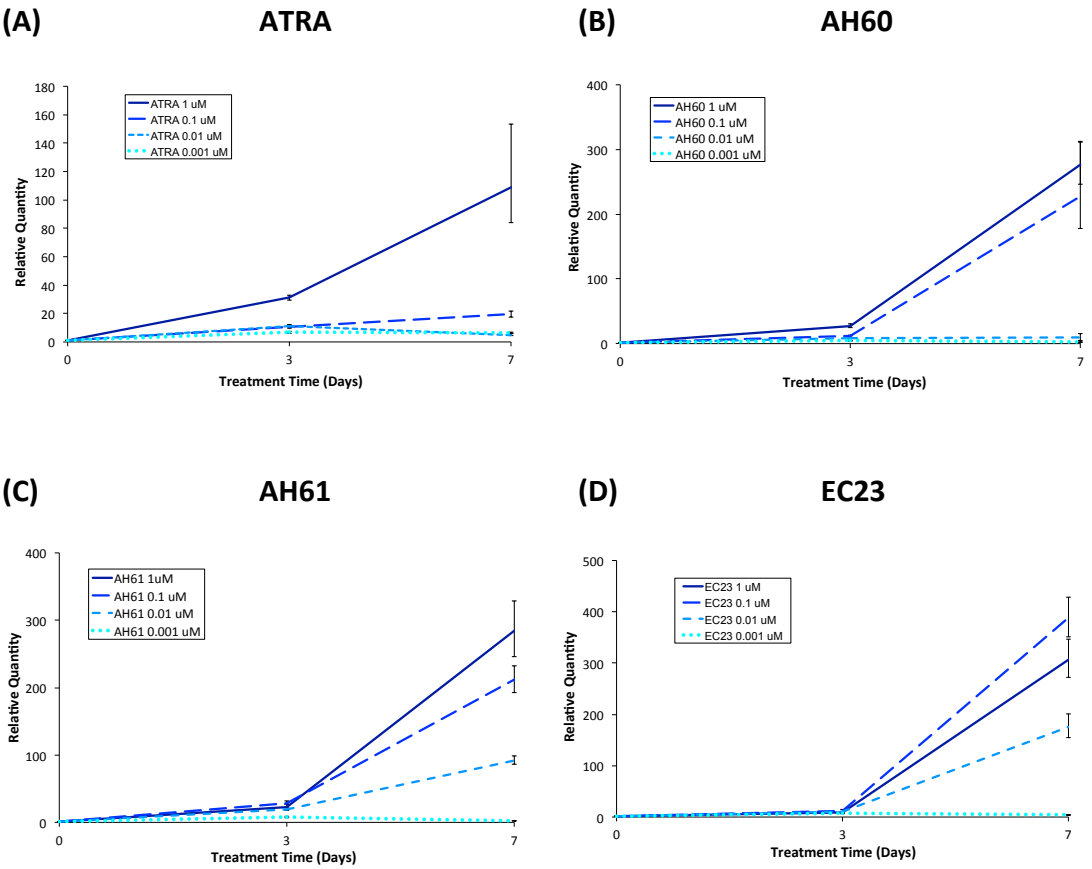

Figure 3.20 RT-PCR analysis of a gene associated with motor and ventral phenotypes, Pax6. Analysis was undertaken at days 3 and 7, after treatment with ATRA (**A**), AH60 (**B**), AH61 (**C**) and EC23 (**D**) at 1 μM, 0.1 μM, 0.01 μM or 0.001 μM. Treatment with ATRA only induced expression of Pax6 at 1 μM. AH60 led to increased expression at both 1 μM and 0.1 μM, while AH61 also showed a slight increase when incubate at 0.01 μM. EC23 overall displayed a very different profile, with the highest levels of Pax6 expression realised when incubated at 0.1 μM, followed by 1 μM then 0.01 μM. No compounds showed any increase in Pax6 expression at 0.001 μM. All gene levels are expressed as a relative quantity, which is the difference in gene expression between, undifferentiated TERA2.cl.SP12 cells and those exposed to a retinoid treatment. Results are presented with ± standard deviation (SD), n=3.

The similarities in the expression profiles of both Nanog and Oct-4 in TERA2.cl.SP12 cells when treated with AH61 and EC23 are highlighted when plotted on a single graph looking at expression only on day 7 (Figure 3.21 (**A**) and (**B**) respectively). Concurrently, examining the data in this format also highlights the stark differences in their Pax6 expression profiles. The greatest of which is the sharp peak seen at 0.1 μM for EC23. This data highlights the potential use for EC23 at that specific concentration for inducing Pax6 and any subsequent associated pathways.

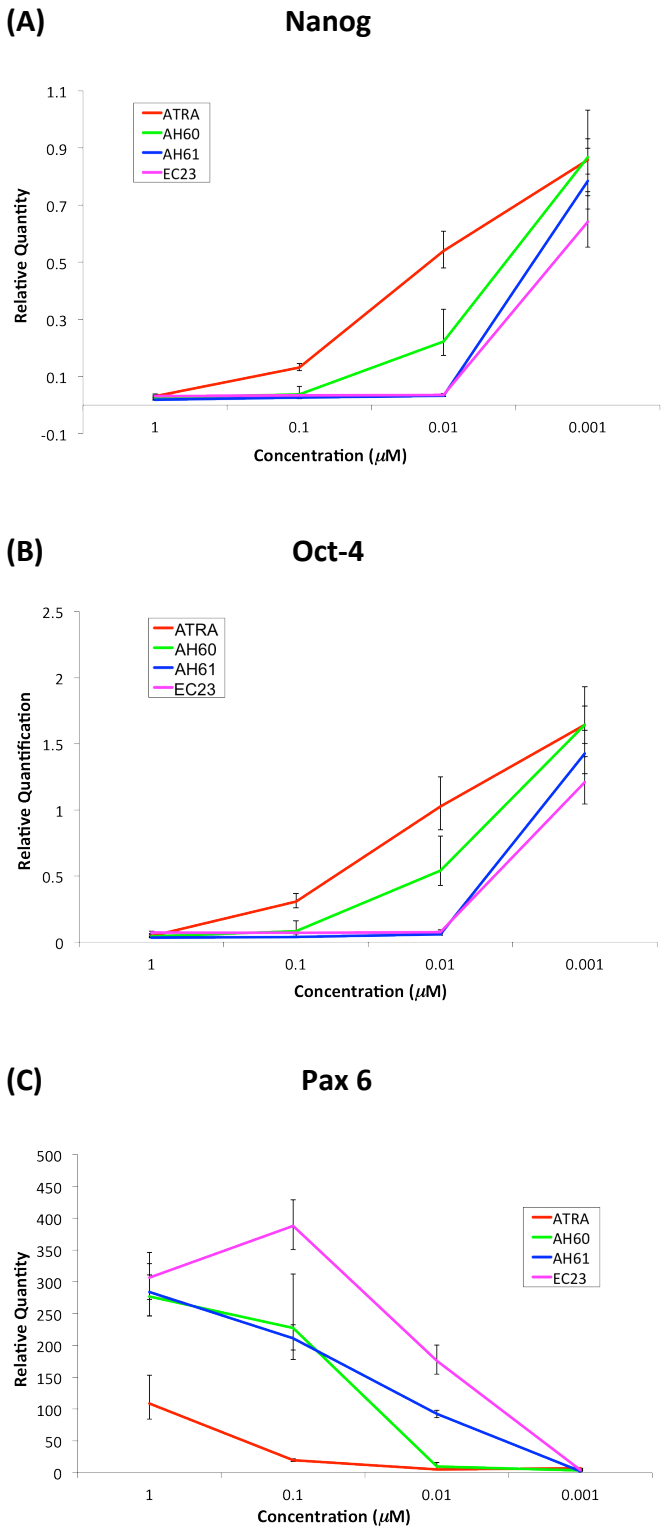

Figure 3.21 RT-PCR analysis of two genes associated with pluripotency, Nanog (**A**) and Oct-4 (**B**), and one associated with motor and ventral phenotypes, Pax 6 (**C**). Both AH61 and EC23 displayed identical profiles for Nanog and Oct-4 expression. EC23 was significantly better at inducing Pax 6 expression at 0.1 μM than any other retinoid tested. All gene levels are expressed as a relative quantity, which is the difference in gene expression between, undifferentiated TERA2.cl.SP12 cells and those exposed to a retinoid treatment. Results are presented with ± standard deviation (SD), n=3.

3.3.6.3 Analysis of Cellular Morphologies

The differences in the potency of AH60 and AH61 *versus* that of ATRA can be visualised by phase microscopy after just 7 days. Cultures exposed to 1 μM for all three treatments, show a heterogeneous cell population, indicative of cells differentiating (Figure 3.22 (**A**), (**D**) and (**G**) respectively). This is consistent with all the data presented for flow cytometry and RT-PCR. Treatment at a concentration of 0.1 μM and 0.01 μM for ATRA leads to an over confluent cell population (Figure 3.22 (**B**) and (**C**) respectively). Thus suggesting the compound is less effective at inducing differentiation as the general cell population continues to proliferate, supporting the data discussed above. When AH60 was applied to the cells at 0.1 μM, there appeared to be areas of heterogeneous cells but also areas that were highly confluent (Figure 3.22 (**E**). This suggests that, at this concentration the molecule is partly effective having lost a degree of its activity. Once reduced to 0.01 μM, the entire cell population appeared to continue to proliferate, with large areas of cell growing layered on top of one another (Figure 3.22 (**F**)). Consistent with both the data presented for the flow cytometry and RT-PCR, AH61 displayed a phenotype consistent with differentiating cells across all the whole concentration range of 1 μM, 0.1 μM and 0.01 μM (Figure 3.22 (**G**), (**H**) and (**I**) respectively). All three images display a heterogeneous cell population, with fewer cells per field of view. No data is shown for any compounds applied at a concentration of 0.001 μM as this lead to an over confluent cell population, with cell death, consistent with all the data presented previously.

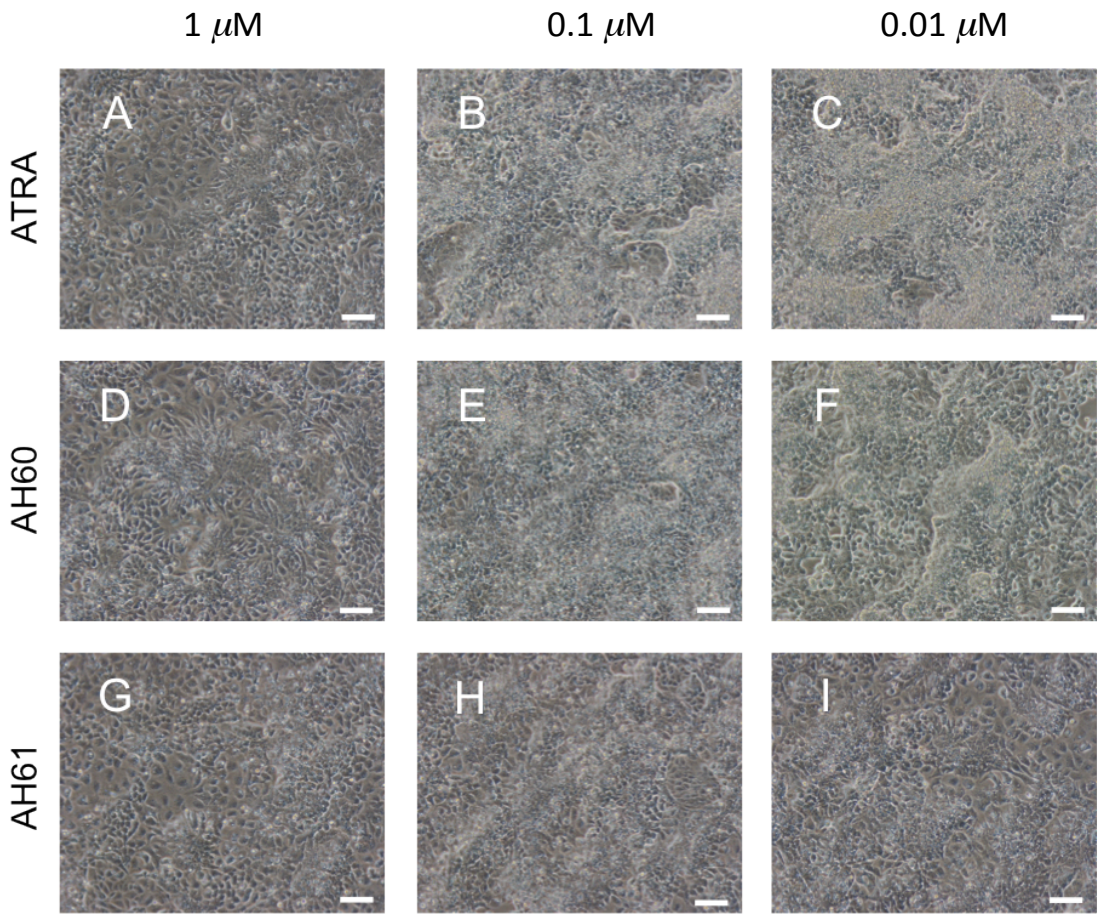

Figure 3.22 Phase images of TERA2.cl.SP12 cells after 7 days of culture with ATRA ((**A**), (**B**) and (**C**)), AH60 ((**D**), (**E**) and (**F**)) and AH61 ((**G**), (**H**) and (**I**)) at 1 μM, 0.1 μM and 0.01 μM. Cultures exposed to all three retinoids at 1 μM exhibited a highly heterogeneous morphology. This morphology is also seen in cultures incubated with AH61 at 0.1 μM and 0.01 μM, displaying that this retinoid retained its potency at these concentrations. AH60 displayed very low levels of differentiation seen at 0.1 μM, and in general both ATRA and AH60 at 0.1 μM and 0.01 μM are significantly over grown, indicative of a proliferative cell population. Scale Bars: 100 μm.

3.3.6.4 Immunocytochemical Analysis

Finally, the potential of each compound to induce the expression of neuronal specific proteins over a range of concentrations was examined by immunocytochemical staining. The expression was again investigated using antibodies raised against the neuronal specific β-III-tubulin marker, TuJ1, and the 200 kDa neurofilament protein, NF-200.

Cultures of TERA2.cl.SP12 cells were treated with ATRA, AH60 and AH61 at 1 μM, 0.1 μM and 0.01 μM for 21 days. Media was refreshed every 3 days, but cultures treated with ATRA and AH60 at 0.01 μM became over confluent and sub-optimal after 14 days and were, consequently, abandoned. Both markers were strongly expressed in cells incubated with 1 μM ATRA, AH60 and AH61, with many neuronal processes visible in all three cultures. A similar number of positive neuronal processes were visible in both 0.1 μM and 0.01 μM AH61 cultures. However, at 0.1 μM ATRA and AH60 fewer neuronal processes were apparent (Figure 3.23 and Figure 3.24). As carried out previously to quantify the data, the number of positive cell bodies (perykarya) per field of view for each culture treatment was counted, with the aid of ImageJ software. The data is displayed as the mean from three randomly selected immunostained images, for both TuJ1 and NF-200 (Figure 3.25 (**A**) and (**B**) respectively). There is no significant difference seen in the expression of TuJ1 at 1 μM over the three retinoid treatments, with all three expressing the marker highly as seen for 10 μM. Dropping the concentration to 0.1 μM sees levels of positive TuJ1 neurons drop in both ATRA and AH60 cultures, but remain high in AH61. Consequently the number of positive perykarya in 0.1 μM AH61 treated cultures is significantly higher then those treated with 0.1 μM ATRA or AH60. Furthermore, the number of positive perykarya remains significantly higher in 0.01 μM AH61 treated cultures compared to 0.1 μM ATRA and AH60. Upon analysing NF-200 expression, a similar pattern emerges, with AH61 cultures displaying significantly more positive perykarya over the same treatments as described for TuJ1. In addition, 1 μM AH61 treatment displays significantly more positive NF-200 perykarya than 1 μM ATRA or AH60 cultures. This is consistent with the data present previously at the 10 μM concentration range. Thus, at low (0.1 and 0.01 μM) concentrations, under the conditions tested, AH61 appears to be a more potent inducer of neuronal differentiation than ATRA and AH60, as inferred by the significantly increased number of neurons, both positive for TuJ1 and NF-200. AH61 remains nearly as active at a 100-fold drop in concentration. Furthermore, AH61 induces a significant increase in the expression of mature (NF-200) neurons across the entire concentration range investigated in this Chapter (10 μM-0.01 μM).

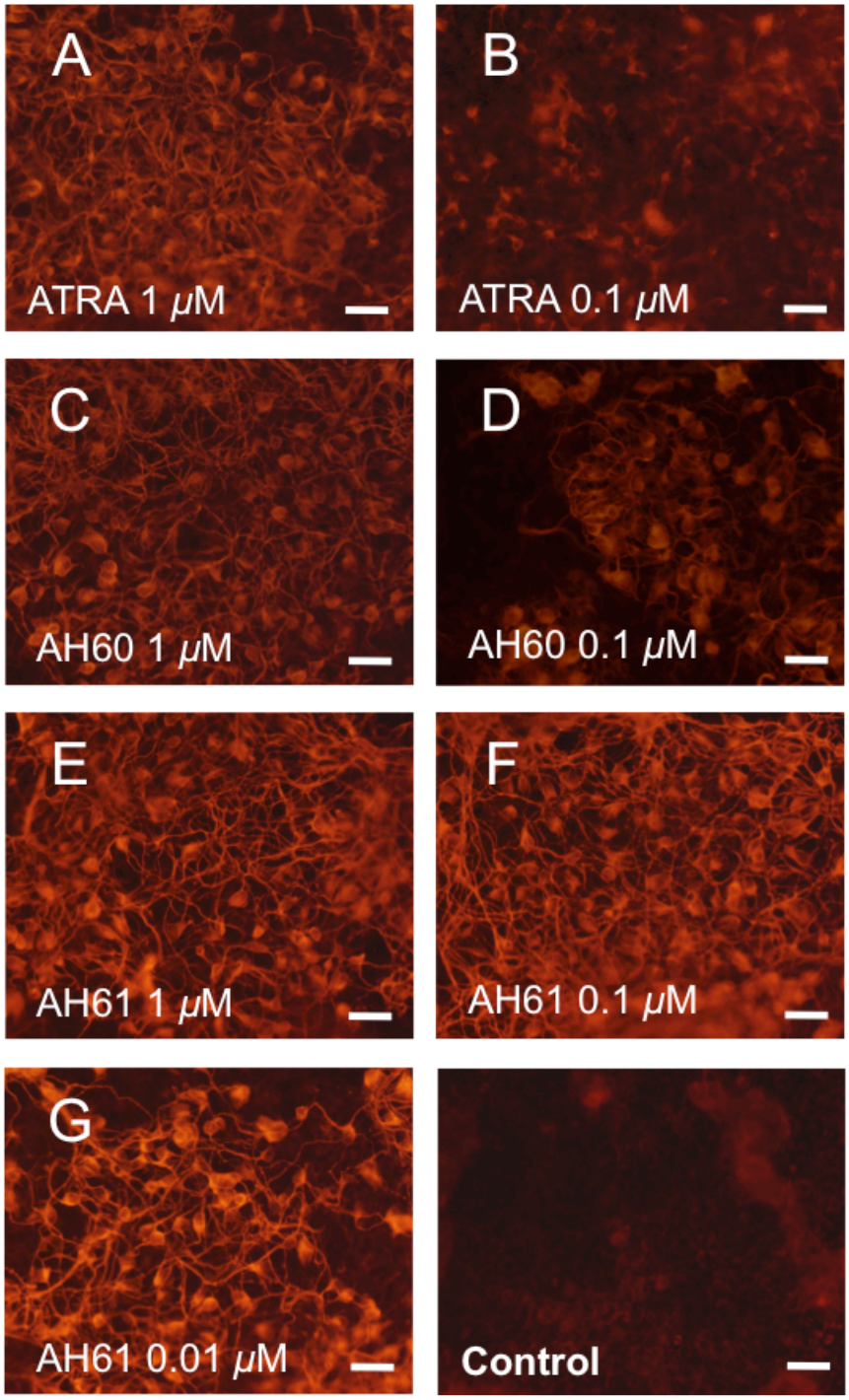

Figure 3.23 Induction of neural differentiation in TERA2.cl.SP12 cells. Cultures were incubated with either ATRA at 1 μM and 0.1 μM (**A** and **B**), AH60 at 1 μM and 0.1 μM (**C** and **D**) and AH61 at 1 μM, 0.1 μM and 0.01 μM (**E**, **F** and **G**) for 21 days. All cultures were stained for the neuronal marker β-III-tubulin. All cultures incubated with 1 μM concentrations of retinoid highly expressed β-III-tubulin, with long neuronal processes visible**.** In 21 day 0.1 μM ATRA and 0.1 μM AH60 cultures very few β-III-tubulin neurons were observed. However, 0.1 μM and 0.01 μM AH61 incubated cultures both exhibited expression profiles of β-III-tubulin similar to that seen in 1 μM ATRA. Control cultures (vehicle only) stain negative for β-III-tubulin. Scale bars: 50 μm.

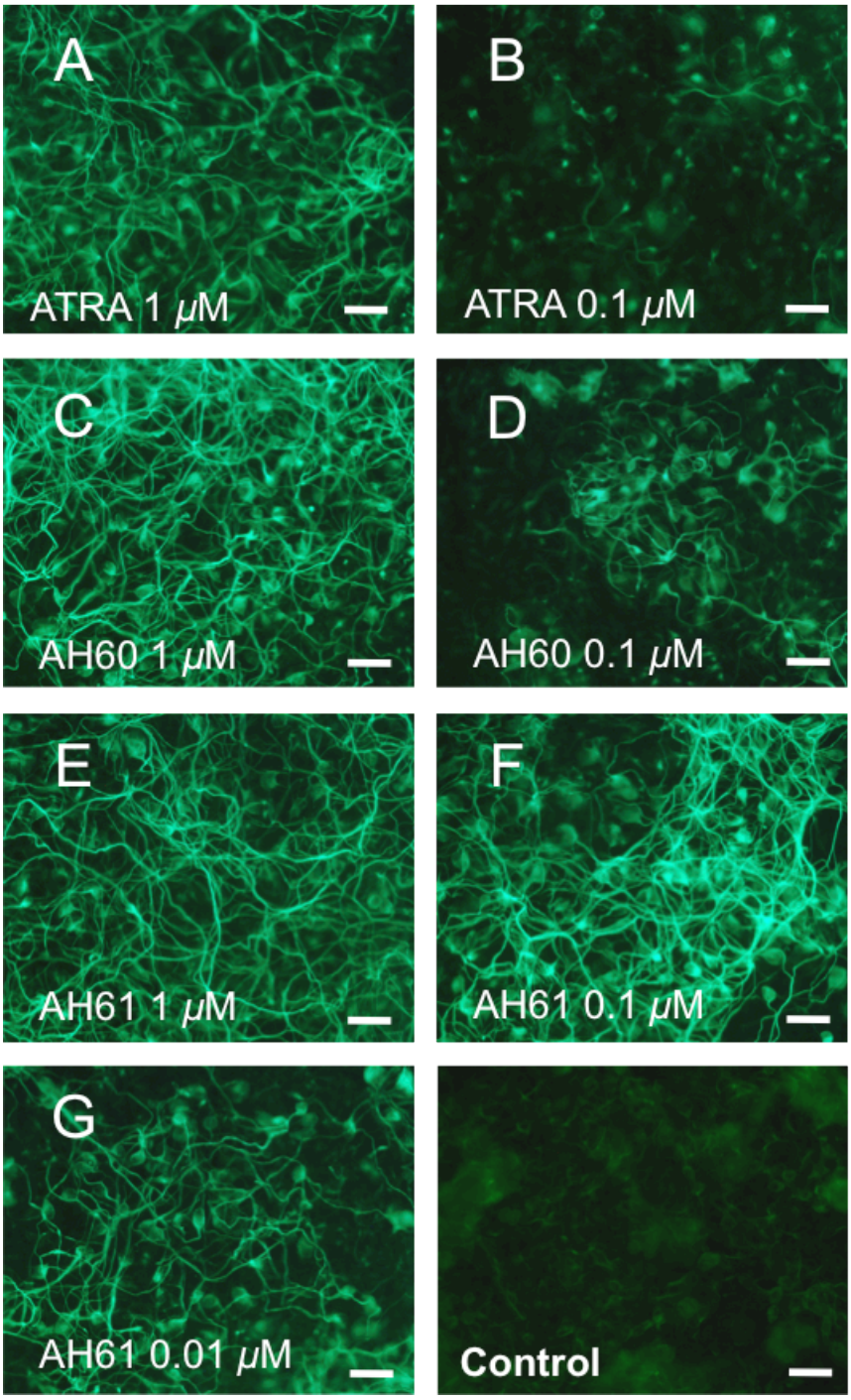

Figure 3.24 Induction of neural differentiation in TERA2.cl.SP12 cells. Cultures were incubated with either ATRA at 1 μM and 0.1 μM (**A** and **B**), AH60 at 1 μM and 0.1 μM (**C** and **D**) and AH61 at 1 μM, 0.1 μM and 0.01 μM (**E**, **F** and **G**) for 21 days. All cultures were stained for the late neuronal marker NF-200. All cultures incubated with 1 μM concentrations of retinoid highly expressed NF-200, with long neuronal processes visible**.** In 21 day 0.1 μM ATRA and 0.1 μM AH60 cultures very few NF-200 neurons were observed. However, 0.1 μM AH61 exhibited an expression profile of NF-200 similar to that seen in 1 μM ATRA. Furthermore at 0.01 μM AH61 NF-200 positive neurons were still highly expressed. Control cultures (vehicle only) stain negative for NF-200. Scale bars: 50 μm.

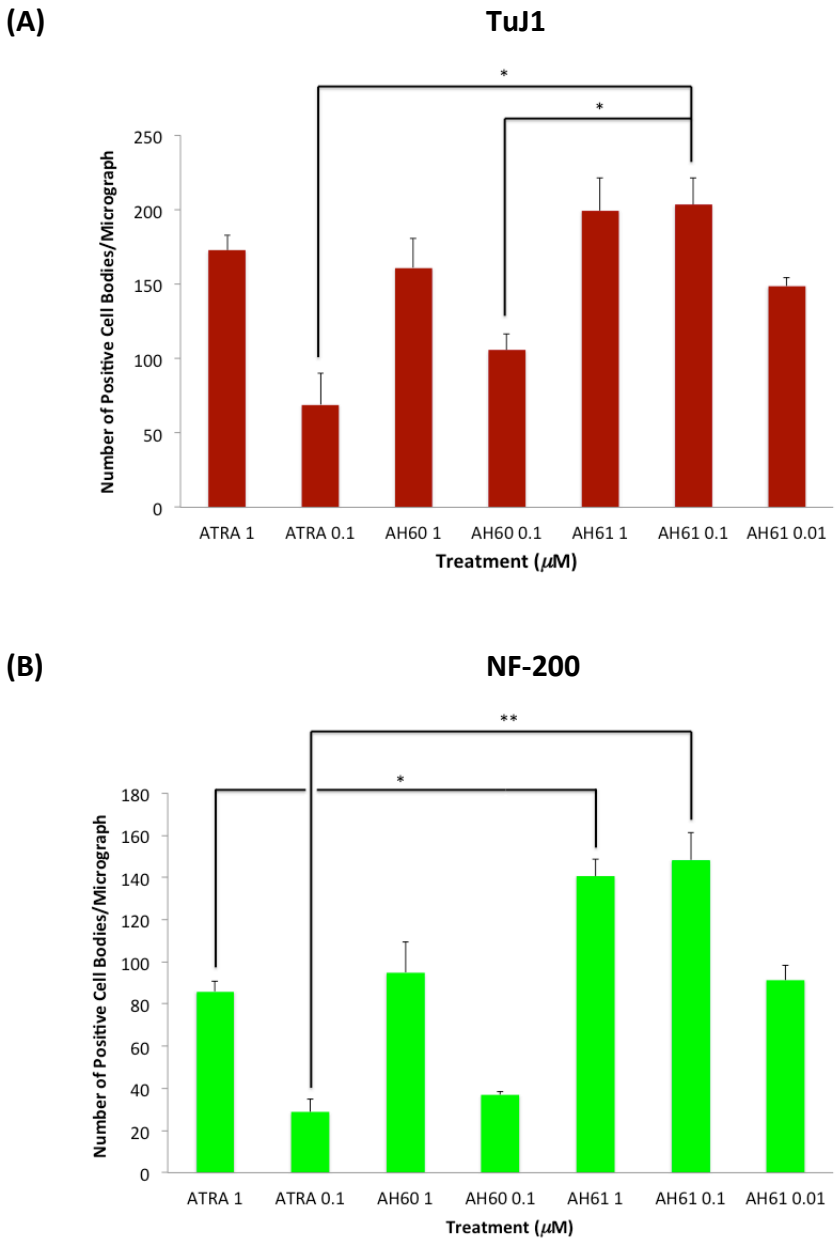

Figure 3.25 Plots displaying the quantification of the immunological data for (**A**) TuJ1 and (**B**) NF-200, as performed by counting labelled positive cell bodies. Cultures of TERA2.cl.SP12 EC stem cells incubated with 1 μM or 0.1 μM ATRA, AH60 and AH61, plus 0.01 μM AH61, for 21 days, subsequently fixed and immunocytochemically stained for TuJ1 and NF-200. Using ImageJ software the number of positive cell bodies were counted on 3 random fields per treatment condition. AH61 induced a significant increase in expression of both TuJ1 and NF-200 over both ATRA and AH60 treatments at 0.1 μM. The number of positive NF-200 perykarya in 1 μM AH61 treated cultures was also significantly higher than in 1 μM ATRA or AH60 treatments. Values shown represent mean + standard error (SEM), n=9. **p≤0.005, *p≤0.05, Student's t-test corrected for multiple testing between compared sample populations using the Bonferroni correction.

3.3.7 Metabolic Studies

All data presented thus far demonstrates that both synthetic compounds are more active than their natural analogue, ATRA. One hypothesis for their increase in potency is that they have a greater resistance to metabolism. This hypothesis is based on their adapted molecular structure, which has been designed to block natural metabolic sites, as discussed previously in Chapter II. To investigate this hypothesis, a flow cytometric study using liarozole hydrochloride (Figure 3.26) was undertaken.

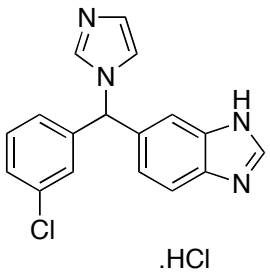

Figure 3.26 Chemical structure of Liarozole Hydrochloride.

Liarozole is a retinoic acid metabolism blocking agent (RAMBA), which is a compound designed to inhibit cytochrome P450 enzymes, effectively reducing ATRA metabolic oxidation. There are many known RAMBAs but the most studied is liarozole, and therefore, it was chosen for this study.[302-304] Liarozole has been used to treat patients with solid tumours undergoing ATRA therapy, in which it was demonstrated to increase the plasma concentrations of ATRA two-fold.[305] Clinically, this is important, as continual dosing of ATRA in patients with acute promyelocytic leukemia (APL) shows a progressive decline in the plasma concentration, suggesting ATRA induces its own catabolism *in vivo*.[306, 307] One solution to retaining a high plasma concentration throughout the treatment is to inactivate these enzymes with compounds such as liarozole.

Therefore, the study hoped to demonstrate, using the TERA2.cl.SP12 model, that the previous inactive concentrations of ATRA could be made active upon addition of

liarozole. Our hypothesis for increased potency at lower concentrations was that ATRA would be metabolised upon introduction to the cell culture, and only at high concentrations would enough remain to produce a response. With liarozole present, this effective concentration would be maintained, thus validating that liarozole was effective at inhibiting the metabolism of ATRA in this cellular model. Successively, the potency of the synthetic compounds would be assessed, again at previous concentrations shown to be inactive.

Hence, the study was carried out using ATRA at 0.1 μM and 0.01 μM, AH60 at 0.01 μM and 0.001 μM and both AH61 and EC23 at 0.001 μM. All the compounds at the concentrations stated above had no effect on TERA2.cl.SP12 cells, therefore, any changes seen are as a result of the addition of liarozole. The results are presented in Figure 3.27.

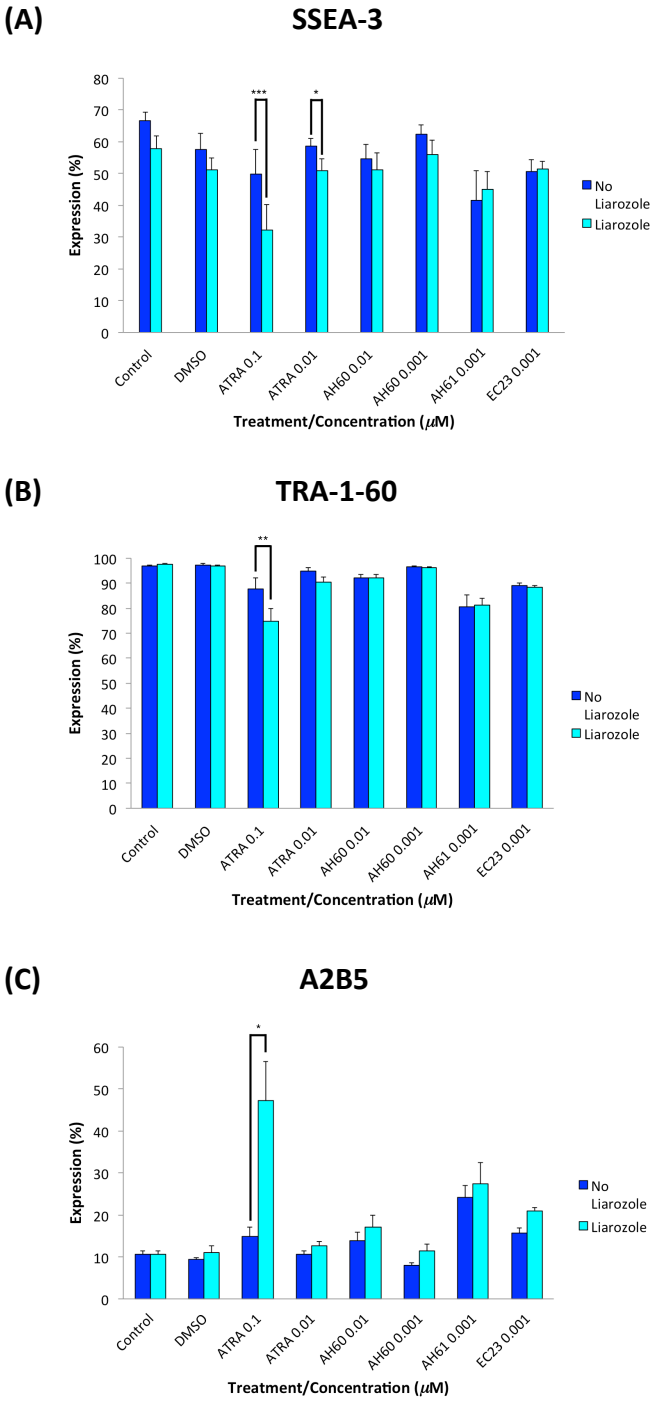

Figure 3.27 Flow cytometric analysis of markers of stem cells SSEA-3 (**A**) and TRA-1-60 (**B**), and a marker of early stage neural cells, A2B5 (**C**). TERA2.cl.SP12 cells were incubated with ATRA, AH60, AH61 or EC23 for 7 days at either 0.1 μM, 0.01 μM or 0.001 μM. Simultaneously, identical cultures were incubated with the addition of liarozole at 10 μM in addition to the above retinoid treatments. Addition of liarozole significantly increased the potency of ATRA at 0.1 μM over all three markers. A smaller effect was seen at 0.01 μM but still significant for some of the markers tested. There were no significant differences in any of the results for the synthetic compounds when treated with or without liarozole present. Analysis carried out at day 7. Results are presented with ± standard error (SDE), n=3. *** p≤0.0005, ** p≤0.005, * p≤0.05, Student's t-test compared to no liarozole.

From the data presented Figure 3.27, the only significant changes upon addition of liarozole into the culture medium, occurred in those incubated with ATRA at 0.1 μM. Both stem cell markers SSEA-3 and TRA-1-60 were down regulated, while in parallel A2B5 was up-regulated. At 0.01 μM, ATRA there were slight changes seen, which for some of the markers represented a significant change, but overall liarozole appeared to have little effect at this concentration of ATRA. For all the synthetic compounds, both treated and un-treated, liarozole conditions displayed no significant changes, thereby suggesting liarozole cannot improve their biological potential. These data suggests that the synthetic compounds may be more stable and resistant to cellular metabolism by cytochrome P450 enzymes, which in part could explain their improved biological potency at lower concentrations. It should be stressed that this was only a preliminary study into the metabolism of these compounds and further studies in additional model systems would need to be carried out before we could be sure that they are not metabolised *in vivo*.

3.3.8 Biological Potency of AH60

Throughout this Chapter, the biological profile exhibited by AH60 has been approximately 10 fold less potent than that of AH61, but additionally, 10 fold greater than ATRA. Upon administration, AH60 is a single pure isomer as identified by ^{1}H NMR spectroscopy, but from the stability studies carried out in Chapter II, we know the double bond, closest to the carbonyl, isomerises relatively readily to give AH61 under equilibrium. It is, therefore, not impossible that the effects elicited by AH60, as seen throughout this Chapter, are actually as a result of a small amount of the molecule isomerising to AH61 within the cell or culture media over the time course of an investigation.

To examine this, a flow cytometry study comparing ATRA, AH60 and 13cRA was undertaken. The purpose being: (1) to see if 13cRA was effective at inducing differentiation within the TERA2.cl.SP12 cell model system; (2) how this compared to that elicited by ATRA; and (3) how they both compared to AH60. The hypothesis being, if 13cRA has no effect, or a significantly reduced affect compared to ATRA,

then it would be likely that the effects seen for AH60 are actually due to AH61. If 13cRA does elicit a biological response, then that seen for AH60 is potentially as a result of itself, not that of AH61, and any increase in potency over 13cRA would theoretically be as a result of the molecule being less susceptible to metabolism.

Therefore, the ability of ATRA, 13cRA and AH60 to induce cellular differentiation in the TERA2.cl.SP12 cell line was evaluated by analysing the expression profile of SSEA-3, TRA-1-60 and A2B5. Flow cytometry was performed on samples of cells treated with 10 μM, 1 μM, 0.1 μM and 0.01 μM of each retinoid, alongside untreated controls and those treated with DMSO. Cell profiles were analysed after 7 days and the data is presented in Figure 3.28.

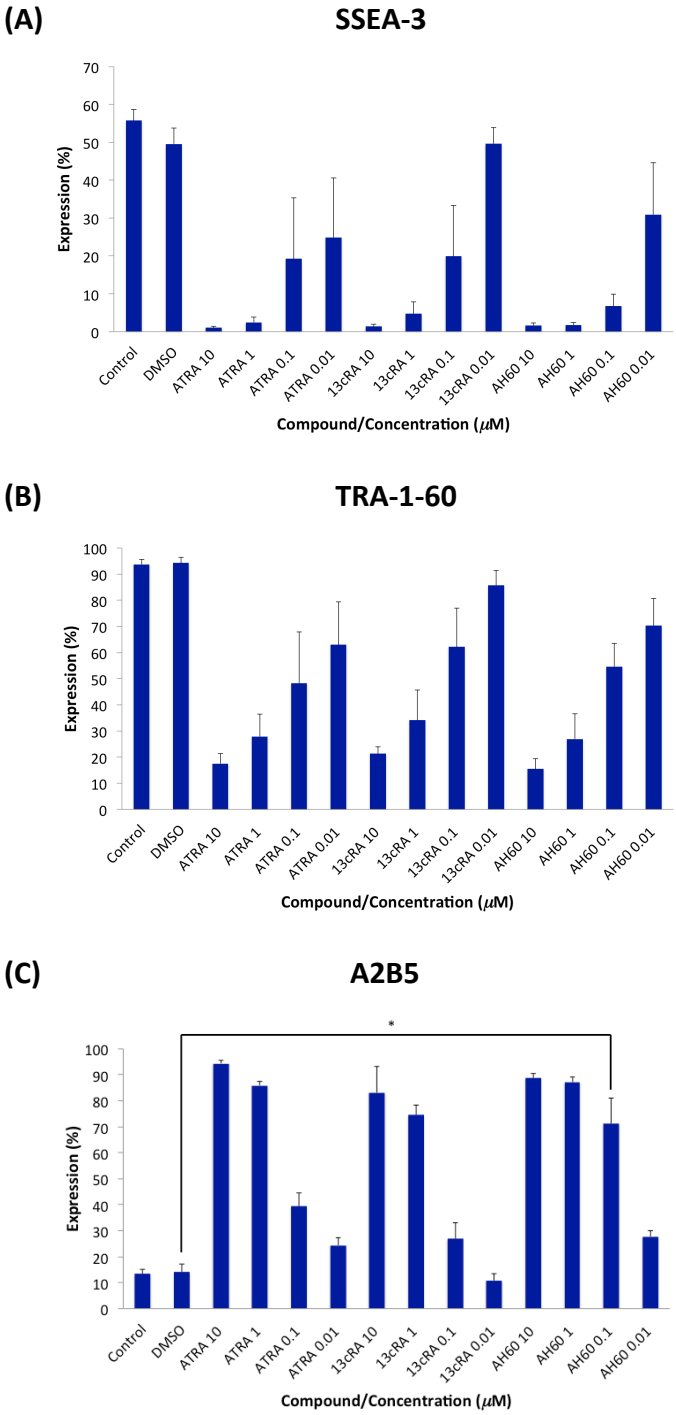

Figure 3.28 Flow cytometric analysis of markers of stem cells SSEA-3 (**A**) and TRA-1-60 (**B**), and a marker of early stage neural cells, A2B5 (**C**). TERA2.cl.SP12 cells were incubated with either ATRA, 13cRA or AH60 for 7 days at either 10 μM, 1 μM 0.1 μM or 0.01 μM, with analysis carried out at day 7. For controls, both untreated and DMSO treated cells were cultured simultaneously. The expression profiles of both ATRA and 13cRA are nearly identical across all three markers, with no significant differences. AH60 appears to be approximately 10 fold more potent, consistent with previous data presented. AH60 displayed a significantly larger number of A2B5 positive cells at 0.1 μM compared to DMSO, whereas ATRA and 13cRA display no significant differences to DMSO at this concentration. Results are presented with ± standard error (SDE), n=3. * $p \leq 0.05$, Student's t-test corrected for multiple testing between compared sample populations using the Bonferroni correction.

From the above graphs it is clear that 13cRA had a dose response similar to that of ATRA. As in previous studies, AH60 had a similar dose response albeit being approximately 10-fold more potent. Therefore, from this study we can infer that the terminal bond can have *cis*-stereochemistry and still induce differentiation in the TERA2.cl.SP12 model system. Additionally, the enhanced biological profile exhibited by AH60 over 13cRA, can be explained as a result of this molecule being more resistant to metabolism, due to its structural modifications. Unfortunately, this does not explain the lower potency compared to that of AH61, upon which, further studies would be required, such as looking at individual binding affinities. It does, however, indicate that potentially, this molecule does induce a response of its own, and that within the culture media, isomerisation may not be occurring. Again, further examination is needed before this can be established beyond doubt.

3.4 Discussion

The aim of this Chapter was to test the biological activities of the AH synthetic retinoid series on model human pluripotent stem cells. ATRA has been used to modulate EC stem cell fate for over thirty years, inducing many well-defined immunological and morphological changes.[199] The EC cell line chosen to carry out most of the investigations within this Chapter, TERA2.cl.SP12, retains the capacity to differentiate *in vitro*.[209] In addition, the ability of ATRA to induce neural differentiation in the TERA2.cl.SP12 cell line has been well documented.[211, 212] Upon exposure to ATRA, TERA2.cl.SP12 cells differentiate with approximately 10-15% of cells committing to become neurons.[308] Furthermore, it has been demonstrated that synthetic retinoid analogues, such as EC23, have enhanced biological profiles when compared to ATRA in this cell line.[228] This background knowledge therefore formed the basis for carrying out investigations into the differentiation capabilities of the synthetic retinoid AH series.

In all the investigations presented in this Chapter, initial retinoid treatment was carried out at a concentration of 10 μM, followed by subsequent dilutions when investigating their dose response. This concentration was chosen as it has previously been successfully used to differentiate TERA2.cl.SP12 cells.[211, 228] Furthermore, this concentration is at the higher end of those used for *in vitro* experiments that have currently been published, with higher concentrations leading to cell death.[309]

Initially, as the AH synthetic retinoids were designed to act on the retinoic acid pathway, an investigation was carried out to see if they bound RAR receptors. This utilised a different EC stem cell model, F9 EC cells, which expressed endogenous RAR receptors, but additionally contained a reporter assay, which used the RARE to drive a *lacZ* reporter gene. This model did not assess whether the synthetic retinoids would bind to RXRs, although, this was not detrimental to the investigation as RARs must function as heterodimers, pairing with one of the three RXRs α, β or γ.[148] In addition, the biological effects being assessed are those known to be elicited by

ATRA, and RXRs are not modulated by ATRA, but instead by 9*c*RA.[170, 173] As all the compounds in the AH series were linear in structure (*i.e.* similar to ATRA/13cRA) and the shape of the RXR ligand binding domain is an 'L' shape, binding to these receptors was thought of as highly unlikely.[237] Activation of the retinoid pathway was monitored and quantified by counting the number of positive cells per field of view. This clearly distinguished the 'ATRA-like' analogues, AH60 and AH61, from both the 'short' and 'extended' analogues, AH36, AH62, AH66 and AH98, as only the 'ATRA-like' compounds displayed a positive result. As there was no significant difference in the number of positive cells seen for treatment with ATRA, AH60 and AH61 there are no further conclusions that can be drawn. As ATRA is a *pan*-agonist, binding all the receptors with equal affinity, and both AH60 and AH61 are highly structurally similar, we would also hypothesise them to be *pan*-agonists.[170] Although, for this to be scientifically proven, binding studies for each of the individual receptors would be required.

The compounds were next tested in the TERA2.cl.SP12 EC cell model. Initially a tetrazolium colourimetic assay (MTS) was employed, to investigate the effects of the compounds on cell toxicity and proliferation.[310-314] The tetrazolium compound is reduced by viable cells to a soluble coloured product measured by UV absorbance. Compounds that induce differentiation should show a decreased proliferative capacity, and therefore this is a good early indicator in assessing the potential of any novel compound series.[243] The literature also suggests that differentiating cells still retain the capabilities to reduce the tetrazolium compound and, therefore, only compounds toxic to the cells would lead to no reduction, as there are no 'living' cells.[315] Those treated with DMSO, the 'short' analogues, AH36, AH62 and AH66, and the 'extended' analogue, AH98, all displayed an sharp increase in absorbance from day 3 to day 7, identical to that of the un-treated control. This shows these treatments have no effect on the growth of the TERA2.cl.SP12 cells, indicating that they do not induce any effects. The result that DMSO had no effect was also promising, as in some cell lines it has been reported that DMSO has both anti-proliferative and differentiating effects.[316-318] The cells treated with ATRA, AH60 and AH61 all displayed a similar absorbance for both day 3 and day 7, indicating that the

cells were not proliferating, and potentially differentiating. This is consistent with previous MTS assay data generated for other natural and synthetic retinoids, such as 9cRA, 13cRA, EC23 and EC19.[243, 319] Furthermore, the MTS data indicated that none of the treatments were toxic. This was also backed-up by a toxicity assay measuring the number of apoptopic and viable cells using Guava ViaCount reagent, on a Guave EasyCyte™ Plus System flow cytometer. This supports previously published literature, whereby, a concentration of 10 μM for retinoid treatment is tolerated in this system.[211, 228, 243, 309]

The morphology of any induced cell type was next investigated. Supporting all previous data, both the 'short' and 'extended' analogues, AH36, AH62, AH66 and AH98, displayed morphologies similar to both the un-treated control and DMSO, suggesting they have no effect on cellular proliferation or differentiation. Consistent with previously reported literature, treatment with DMSO (0.1% $^{v}/_{v}$) proved to be both non-toxic and not induce any signs of differentiation.[316, 318] This is important as any effects seen are therefore now as a result of the compound treatment, not the vehicle, DMSO. It is also important that for any future studies, a higher DMSO concentration is avoided as 1% $^{v}/_{v}$ DMSO has been reported to induce differentiation in TERA2 cells.[320] Consistent with the data obtained in the F9 cell line and the MTS assay, ATRA, AH60 and AH61 all induced phenotypic changes consistent with differentiation. Long-term culture (21 days) led to the formation of columnar cells, described as neural rosettes. These have been reported before, in both this cell type, and human and mouse ES cells, and are described as the developmental signature of neural progenitors.[321, 322] Therefore, AH60 and AH61 appear to mimic both natural and previously screened synthetic retinoids in their ability to induce neurogenesis in this cell line.[228, 243, 319] Furthermore, they appear to mimic the normal neuro-ectodermal development as seen in the human embryo.[323]

In addition to phase images, immunocytochemical staining was employed to investigate the formation of a larger flat cell type, known to form 'plaque' like areas. Previous studies had shown that the synthetic retinoid, EC19, in which the carboxyl group slightly shorter and pointing down, in relation to ATRA, favoured this cell type

over neural differentiation.[228, 243] As AH60 has a *cis*-terminal bond, this makes it somewhat structurally similar to EC19, although it is slightly larger in size by one atom. It was therefore investigated whether AH60 would induce these 'plaque' like areas. Consistent with all the data discussed previously, AH60 did not produce any more 'plaque' like areas than ATRA or AH61, suggesting that it acts in a similar manner to both of these retinoids and others which induce neurogenesis, such as EC23, and that EC19 has a separate biological profile, not seen in the AH series.[228, 243]

Finally, to confirm that both the 'short', AH36, AH62 and AH66, and 'extended', AH98, analogues did not induce differentiation in this pluripotent EC stem cell system, the expression of characteristic cell surface markers was investigated. Two stem cell markers, SSEA-3 and TRA-1-60, and a neural marker, A2B5, were chosen as they are well established in studying EC cell differentiation.[206, 292, 293] In addition, these markers have been used successfully to assess the differentiation capabilities of a number of retinoids in the TERA2.cl.SP12 cell line, including EC19, EC23, TTNN, 9cRA, 13cRA and ATRA.[228, 243, 319]

Flow cytometric analysis of the three antigens, supported all the data gathered previously, clearly distinguishing those compounds which induced differentiation from those that did not. Treatment with the 'short' and 'extended' analogues, AH36, AH62, AH66 and AH98, showed no changes in expression of the three markers, with both stem cell antigens retaining high levels of expression, while expression of the neuronal antigen remained low. This is identical to the expression seen for the un-treated control. Appreciatively, there was also no change in expression seen for those treated with DMSO, again reinforcing the literature that at this concentration it does not induce differentiation.[316, 318] In line with the morphological data, those treated with ATRA, AH60 and AH61 all induced up-regulation of the neural marker, with consistent down regulation of the stem cell markers. As all data obtained, indicated that both the 'short' and 'extended' analogues, AH36, AH62, AH66 and AH98, had no beneficial differentiation properties, no further analysis on these compounds was undertaken.

Analysis of the three antigens by flow cytometry over a 14 day period for ATRA, AH60 and AH61 showed that all three treatments completely suppressed the expression of both stem cell antigens, while promoting the expression of the neural antigen to greater than 95%. This is consistent with data published for both ATRA and EC23.[228] The level of expression of TRA-1-60 was lost significantly faster upon treatment with AH61, compared to that of ATRA or AH60. There was no direct comparison done with EC23, although comparing data presented in this Chapter to that of the published literature, AH61 appears to supresses TRA-1-60 levels quicker than any other synthetic retinoid tested in the system.[228] The exact reason for this is unknown, although it does suggest that AH61 might be slightly more active.

To further assess cellular differentiation in response to treatment with the synthetic retinoids expression profiles of known genes were analysed. Three genes of interest were examined. Nanog and Oct-4 are essential regulators of early development and connected to the self-renewal of undifferentiated stem cells. Furthermore they have been shown to be rapidly silenced during cellular differentiation.[294-297] The third, Pax6, was chosen to assess the neurogenesis properties of the retinoids, as it is essential for the development of much of the central nervous system.[298-301] Treatment with ATRA, AH60 and AH61 all lead to a rapid suppression of both Nanog and Oct-4, with no significant differences seen in any of the treatments. Previous, un-published work within the Przyborski research group (carried out by D. Tams) had highlighted the sluggish effect of EC23, seen when analysing these genes. This data was supported, although after 5 days of treatment all four retinoids showed identical gene profiles. The gene expression profile of Pax6 displayed the largest variation. This supports un-published data, that EC23 attenuated a relative increase in expression of Pax6 approximately 50% less than ATRA. As for both AH60 and AH61 their expression profiles are not significantly different to that of ATRA. This data highlights the similarity of the biological profile exhibited by the AH compound series to that of the natural ligand ATRA, in addition to showing variations in that of EC23 not seen before.

Finally, the induction of neurogenesis was confirmed through the visualisation of neural proteins. The expression of neuronal specific proteins was investigated using antibodies raised against the neuronal specific β-III-tubulin marker, TuJ1 and the 200 kDa neurofilament protein, NF-200. Both of which have been used to assess the neurogenesis properties of retinoids in TERA2.cl.SP12 line previously.[228] All retinoid treatments led to high levels of expression in both markers. In addition, AH61 treated cultures expressed levels of NF-200 significantly higher than those seen for AH60 or ATRA, again suggesting this analogue is more active. Comparing the level of NF-200 expression of AH61 to that of EC23, which has been published, suggests they would not be significantly different.[228] Although a direct comparison would be required to confirm this observation. Both treatments have also been quantified by cell counts, whereas a more accurate quantification method would be to examine the total protein content, through a Western Blot. This then has the potential to highlight any differences between AH61 and EC23.

The dose response of AH60 and AH61 was subsequently investigated, using identical techniques to those describe previously. Analysing cell surface markers, gene expression profiles, cellular morphologies and expression of neural proteins showed that AH60 was approximately 10-fold more active, while AH61 was approximately 100-fold more active, than ATRA. Reasons behind this are, ATRA is rapidly metabolised in many cell types, in addition to being highly susceptible to isomerisation.[222-227] Furthermore, it has since been published that not only does ATRA isomerise under standard laboratory conditions, but also degrades into a number of other compounds.[228] Therefore, it can be hypothesised that at lower concentrations of ATRA, its initial activity is lost quickly, as the compound is either rapidly metabolised or isomerised/degraded. The data presented in Chapter II, indicates that even though AH60 and AH61 do isomerise, this isomerisation is significantly slower than that seen for ATRA. Therefore higher levels of the active compound will remain in culture for longer, even under exposure to light. In addition, their structural modifications, specifically replacing the trimethylcyclohexenylvinyl unit (C_1-C_8) of ATRA, with a structurally similar TMTN moiety, has been demonstrated to increase biological potential.[238] This modification

helps in two ways: (1) It helps to introduce greater stability, as it eliminates a section of the unstable polyene chain, removing one of the isomerisable bonds; and (2) It no longer possess any allylic protons or alkene double bonds susceptible to radical oxidation or expoxidation by cytochrome P450 (CYPs) or related enzymes.[239-242] Preliminary experiments have displayed that both AH60 and AH61 appear not to be metabolised in TERA2.cl.SP12 cells, although further studies are required to confirm this. Therefore, the greater activities of both AH60 and AH61 over ATRA may be a result of either their increased stability under standard laboratory conditions (UV light) (as displayed in Chapter II), or their increased resistance to cellular metabolism. Either scenario would contribute to higher active levels of these retinoids being present in media/cells over a longer time period, and could therefore explain, in part, the enhanced levels of differentiation observed in the lower micromolar range.

An explanation for the improved potency of AH61 over AH60 is that its molecular structure confers greater affinity with and/or activation of the cognate cellular receptors. This is also consistent with the activity displayed by EC23, which structurally, is equivalent to an all-*trans*-system and subsequently displays near identical biological profile to that of AH61.[228, 243] Their only difference is their ability to induce the expression of Pax6. AH61 has a linear dose response, so that as the concentration is lowered, the levels of Pax6 expression also reduce. EC23 has a very distinct profile in that Pax6 expression peaks at 0.1 μM, although the reason for this is currently unknown.

In addition, if future experiments did confirm the initial theory that the AH series of compounds are resistant to metabolism, then synthetic analogues like AH61 may be an alternative solution for the treatment of APL. For successful APL treatment, a continuous effective concentration of plasma ATRA is desirable as it reduces the chances of patient relapse. Although the use of liarozole has shown promising results, as discussed earlier in this Chapter, constant plasma levels of ATRA are never maintained over the full course of treatment.[305] One alternative may be to use synthetic analogues of ATRA that are resistant to metabolism, such as AH61. They

would maintain their effective dose for longer as the body would be unable to remove them. Understandably, for this to be viable, they would also need to potentiate the same biological response exhibited by ATRA, which is to induce complete remission of the cancer.[324-326] Early data indicates the possible use of such synthetic analogues in cancer treatment looks potentially interesting.

Finally, it is likely that the biological effects elicited by AH60 are indeed as a result of the molecule, and not any isomerisation occurring in the cell or culture media to small quantities of AH61. Although it must be noted this is based on preliminary data, and the assumption that AH60 will behave and bind in a similar manner to 13cRA, as structurally they have been designed to be equivalent. Further analysis would be required if this was to be proved beyond reasonable doubt, although early data is consistent with that seen for 13cRA previously in this model system.[319]

3.5 Conclusions

The first conclusion that can be drawn is that the length of the retinoids is of paramount importance. All the 'short' analogues displayed no biological activity in any of the model systems that were screened. Therefore, the most obvious conclusion is that they are incapable of binding to the receptors, which bring about the biological response. The 'extended' analogue also displayed a very similar profile, with little, if any, activity seen in all the model systems. This could also be down to a lack of binding affinity for the receptors, and in this case possibly brought about by the increased instability in the polyene chain. Any isomerisation may lead to isomers which have a reduced affinity, and therefore, the low levels of activity that were seen in some of the biological screens may be as a result of any remaining active isomer. As we were unable to control the isomerisation to retain a single isomer, proving this would be very difficult. Overall this highlights an important structural feature, which up until now not been investigated.

The observed biological induced similarity of AH60 and AH61 to ATRA and EC23 highlights them as highly useful and exciting molecules for controlling *in vitro* stem cell differentiation. In particular, the increased activity of AH61 over that of ATRA, and its ability to mimic the biological profile of ATRA closer than that of EC23 may prove significantly useful. EC23 is known to be highly toxic, therefore limiting its use *in vivo*. Whether AH61 is as toxic is unknown and further research is required to investigate this, although, the inbuilt instability of the polyene chain may prove beneficial. Further investigations, in alternative cell systems, are now required to further verify the potential of these compounds.

Chapter IV

Evaluation of the Effect of Synthetic Retinoids on Neural Stem/Progenitor Cells

4.1 Introduction

Currently, all analysis of the biological potential of this series of synthetic retinoids has concentrated around their ability to induce differentiation in a pluripotent stem cell system. This Chapter follows on from previous work carried out within our research group, in which the ability of retinoids to direct differentiation of cells that are already committed to a neuronal lineage is evaluated.

NPCs and NSCs are highly valuable as they provide a renewable supply of differentiating neural cells. In recent years, there has been increased focus on utilising these cells as both a powerful research tool, and in the development of therapies for neurodegenerative diseases, such as Parkinson's, Alzheimer's and Huntington's diseases.[54-56] As discussed in Chapter I, ATRA has a well-characterised role *in vivo* in the developing CNS and subsequent synaptic plasticity seen in the adult.[188, 190, 191] Consequently, ATRA has been used as a tool for inducing or enhancing the differentiation of NPC/NSC lines *in vitro*.[59, 60] In addition, synthetic retinoids, including EC23, have demonstrated an enhanced activity, over ATRA in these cell lines.[59]

Two model systems have been assessed, one a human embryonic cell line, termed ReNcell VM, and the other an adult cell line from rat hippocampus, termed adult hippocampal progenitor cells (AHPC).

4.1.1 Human Embryonic Neural Stem Cells.

Most early work carried out on NSCs was on those derived from rodent sources, from which the potential of these cells was realised. Subsequently, there have been a handful of studies which have used human neural stem cells (hNSCs), identified by their ability to self-renew and multipotency. During the beginning of the last decade, Piper *at al.* demonstrated the production of neurons, possessing ligand and voltage-gated channels, derived from fetal NSCs.[219] Further studies demonstrated similar results, with the most successful being that developed by Wu *et al.*, in which fetal

hNSCs were differentiated into cholinergic neurons with action potentials, followed by successful grafts into adult rats.[220] The major limitation in these studies was the high mortality rate of the cells when grown in culture, with many cell lines unable to be passaged more than five times.[327]

More recently, Donato *et al.* described the production of two stable multipotent NSC lines, which can be continuously cultured and expanded as a monolayer, with no loss in viability.[57] The studies described previously were all limited to low passage numbers, whereas Donato *et al.* successfully demonstrated long-term culture, up to passage 46. The approach adopted was to immortalise the cells through insertion of a myc transcription factor, as this had been previously demonstrated to increase the normal life span of hNSCs *in vitro*.[328, 329] One cell line developed, the ReNcell VM line, was derived from the ventral mesencephalon of ten-week gestation fetal midbrains. The cell line was immortalised with v-myc, as this is thought to be the 'stemness' gene, thus deriving both proliferation and multipotency in the stem cells.[19] Under standard growth conditions, the cells appear as small polygonal cells with limited processes, indicative of an immature neural morphology, and stain positive for the neural stem cell marker, nestin. When differentiated, through withdrawal of the growth factors, FGF and EGF, positive immunohistological staining was visualised for neurons, astrocytes and oligodendrocytes. Adaption of this protocol, led to the development of electrophysiologically functional neurons signified with an increase in dopaminergic neurons.[57]

In a follow up study performed in our research laboratory, the incorporation of retinoids into the differentiation protocol was investigated.[59] It has been previously published that cells derived from this area of the brain are responsive to retinoic acid.[330] Consequently, the incorporation of both ATRA and the synthetic retinoid EC23 was investigated by administration at the point of growth-factor withdrawal. Both retinoids were shown to visually enhance neuronal differentiation, inducing increased maturation and stabilisation of the axonal cytoskeleton.

4.1.2 Adult Neural Progenitor Cells

In adults, neurogenesis declines until it ceases in the young adult mammalian brain, except in two areas, the olfactory bulb and the hippocampus, both of which produce new neurons throughout adult life.[245] The discovery of this phenomenon has led to a number of cells lines being established in an attempt to exploit this novel area. One of the earliest was a population of FGF-2 responsive neural progenitor cells isolated and cultured from adult rat hippocampus. The cell line was initially transfected with green fluorescent protein (GFP) and termed HCN-nitGFP, although it has subsequently been termed AHPC. When cultured *in vitro*, the cells expressed precursor, glial and neuronal cell markers and subsequent implantation into adult rat hippocampus demonstrated that not only could the cells survive, but they could also differentiate into terminal mature glia and neurons.[58] Further studies demonstrated analogous populations of neural progenitor cells could be isolated from both germinal zones and parenchyma of adult rat brain, and that FGF-2 played a vital role in both recruiting and maintaining the progenitor population *in vitro*.[218] Subsequent genetic marking of individual cells demonstrated that some of these progenitors isolated were self-renewing *multipotent* stem cells, supporting evidence that the adult brain does consist of some highly plastic central nervous system stem cells.[245] Withdrawal of FGF-2 was shown to stimulate some neuronal differentiation,[245] but additional treatment with ATRA or neurotrophins (NTs) further potentiated the process, with the end result of treatment with ATRA being a three fold increase in the number of neurons produced compared to FGF-2 withdrawal alone.[60] This is not surprising considering the retinoic acid pathway has since been identified as having a major role in the active re-modelling of the adult hippocampus.[191]

The cell line described above gives a good idea of the potential adult neural stem cells hold, but it must also be noted that differences, compared to those found in humans, may also transpire. This may be assumed as differences in rat and mouse progenitor cell lines have been described.[331] Therefore, it is also desirable to have a human model system to work with. One solution is that of the cell line described previously in 4.1.1, although using embryonic tissues often encounters societal and

ethical issues. Consequently, there has been much interest in isolating human adult hippocampal progenitor cells. For obvious reasons, obtaining living healthy adult brain tissue is not easily achieved. To date, two potential methods have been described in the literature. The first used surgically resected hippocampus from a range of male patients undergoing temporal lobe resections for medication-refractory epilepsy, aneurysm repair and traumatic edema. Neural progenitors cells were successfully identified and sorted in good numbers and purity, remained mitotically competent and matured into functional neurons.[332] The second, involved the isolation and successful propagation of neural progenitor cells from the human brain after death. Again, multiple tissue samples were taken from a range of patients of differing ages, with the post-mortem interval not exceeding 20 hours. The successful isolation of neural progenitor cells was demonstrated with the greatest numbers isolated from the hippocampus. Differentiation into neurons was subsequently induced with withdrawal of growth factors followed by addition of forskolin and retinoic acid.[333] Both methods hold the potential of providing a reliable source of adult human progenitor cells, which could then be used to assess adult neurogenesis in humans.

However, it can be assumed that evidence obtained from animal models will relate to some extent to humans, although the potential for differences should always be considered. Currently, especially for the preliminary screening of new potential modulators such as described within this thesis, animal models such as the AHPC line described above remain the most accessible and appropriate source of adult neural progenitors cells. Previous work within the group has used this cell line to assess the potential of both EC19 and EC23. AHPCs were shown to differentiate upon addition of ATRA and synthetic derivatives, with the expression of the neuronal marker TuJ1 and the glial marker GFAP being up-regulated.[243]

4.2 Aims and Objectives

The aim of the research presented in this Chapter was to investigate the effects of both AH60 and AH61, on both embryonic and adult neural progenitor cells, and compare them to the known responses of both ATRA and EC23. The rationale, behind repeating this investigation with both AH60 and AH61, was that they have a closer structural resemblance to ATRA, may potentially be less toxic than EC23, and therefore could be a better alternative for *in vitro* investigations in these cell systems.

The main objectives were to: (A) demonstrate that both AH60 and AH61 induce differentiation in both neural progenitor systems and compare this to that induced by both ATRA and EC23; (B) to investigate the dose response of the synthetic compounds and compare this to that previously seen in the EC model system; (C) compare the activity of AH60 to AH61 and see if trends seen within the EC stem cells are also visualised in the neural progenitors; and (D) investigate the toxicity of the compounds, to determine whether they appear less toxic than EC23 and mimic the profile of ATRA, or because they appear to be metabolically stable, have a profile consistent to that of EC23.

4.3 Results

4.3.1 Analysis of the Potential of AH60 and AH61 to Induce Neural Differentiation of ReNcell VM Cell Cultures.

This section deals with the effects of incorporating AH60 or AH61 into a commercial neural cell differentiation protocol. As discussed earlier, methods have been published regarding the differentiation of these cells into neural sub-types including a method involving retinoid incorporation undertaken in our laboratory. These known protocols make this cell line an ideal model to screen the novel retinoids. The standard differentiation protocol involves the removal of the two growth factors, FGF and EGF, from the proliferation media. Subsequent, addition of ATRA at the same time as removing the growth factors has been shown to significantly increase the number of differentiated cells, assessed through analysing neuronal markers. ATRA not only accelerates neurogenesis, but also the maturity of neuronal derivatives is enhanced after seven days in retinoid-supplemented media.[59]

As in the previous study, retinoids were added at the point of growth factor withdrawal, which signifies the initiation of differentiation in the commercial protocol. ReNcell VM cells were cultured under standard conditions in laminin coated flasks, as previously described by Donato *et al.* and Christie *et al*..[57, 59] Undifferentiated cultures, and control-differentiated cultures, were prepared alongside those treated with ATRA and the synthetic retinoids, AH60 and AH61. The control differentiation method used followed the standard differentiation protocol, involving the withdrawal of growth factors from the culture media. For cultures where retinoids are incorporated as part of the differential protocol, 1 μM ATRA, 1 μM AH60 or 1 μM AH61 were administered at the same time as the growth factors were withdrawn. All cultures were maintained in their respective media formulations for seven days, with the media replaced at the halfway point of the experiment. Phase micrographs were analysed after 7 days, Figure 4.1.

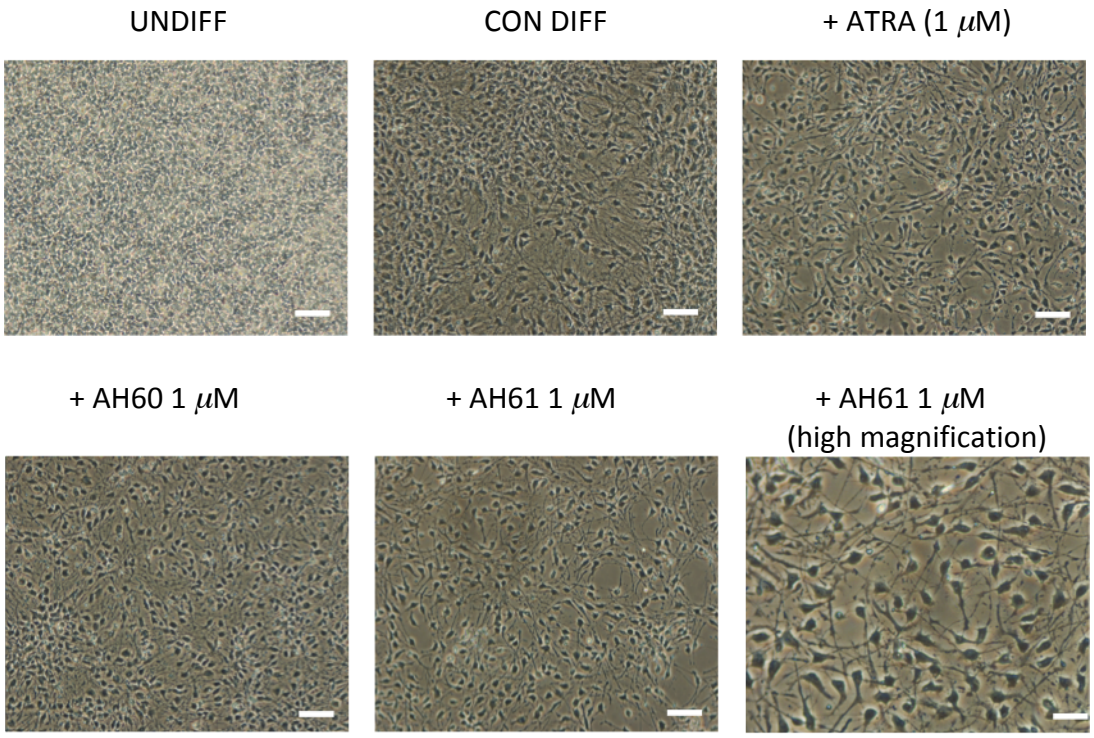

Figure 4.1 Morphologies of ReNcell VM cells after 7 days treatment. Undifferentiated cultures (UNDIFF) retained a homogeneous appearance with cells layering as they become over confluent and sub-optimal. Control differentiated cultures (CON DIFF), in which the growth factors, EGF and FGF were removed, showed areas of proliferative cells surrounded by more sparsely populated areas with numerous neural processes visible. Those treated with the retinoids, ATRA, AH60 and AH61 at 1 μM also showed high numbers of neuronal processes (see high magnification image) but retained a homogeneous differentiated cell population with no areas of proliferative cells visualised. Scale Bars: 100 μm (50 μm high magnification).

As described previously in the literature,[57, 59] removal of the growth factors (control differentiation) resulted in a shift from a homogeneous population of proliferative cells with a uniform morphology, to a heterogeneous cell population. This was characterised by areas of cells that appeared similar to those in the undifferentiated cultures *i.e.* proliferative cells, surrounded by areas of neuron-like cells, which were more thinly populated. Overall, on average, there is a 68% drop in cell number from the undifferentiated culture, confirming the cells are exiting the cell cycle and differentiating. Addition of the retinoids (either ATRA, AH60 or AH61) overall led to greater homogeneity in the cell population. In addition the total number of cells visible was also lower, with an average drop in cell number of 75%, compared to the undifferentiated control. This suggests the retinoids further enhance differentiation through promoting the cells to exit the cell cycle. Furthermore, the morphology of

the cells also changed, with the majority predominantly having neuron-like features (see Figure 4.1 high magnification image). Unlike the control-differentiated cultures, which still contained areas of cells that appeared to be proliferating, those treated with the retinoids appeared to have inhibited this cell type. This is consistent with data previously published for ATRA and EC23, indicating early on that both AH60 and AH61 appear to mimic the activity of these retinoids.

To further assess the potential of AH60 and AH61, immunocytochemical staining was performed to analyse the expression of the neuronal marker β-III tubulin, mature neuronal protein marker NF-200 and MAP2ab, a microtubule protein associated with neurogenesis. Fluorescence micrographs for β-III tubulin, NF-200 and MAP2ab expression, alongside inlayed images of the corresponding nuclear stains (Hoechst 33342), from cells grown under undifferentiated, control-differentiated and retinoid-supplemented conditions are displayed in Figure 4.2.

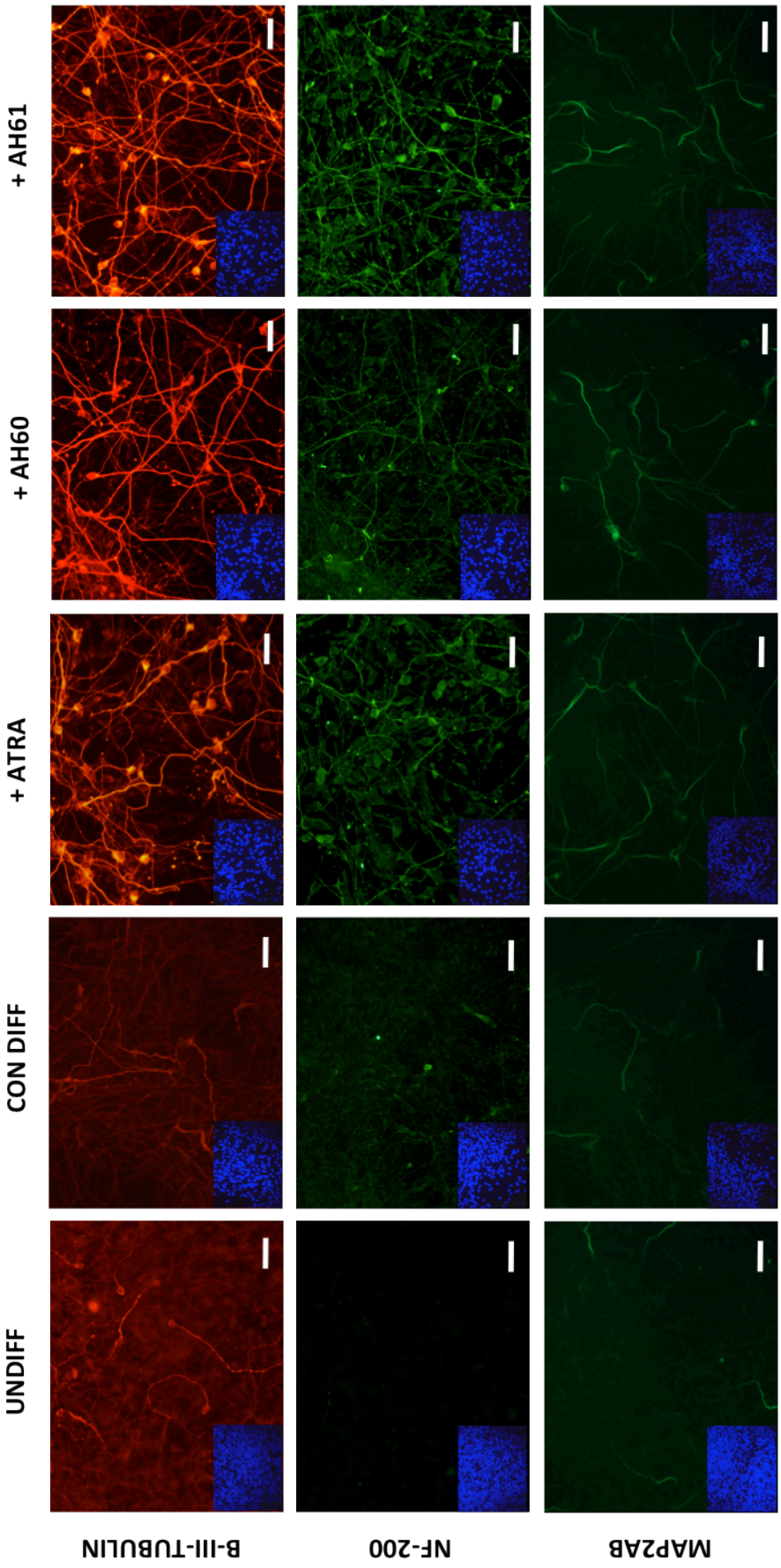

Figure 4.2 Conformation of enhanced neural differentiation in ReNcell VM cell cultures incubated with 1 μM ATRA, AH60 or AH61. Undifferentiated and control differentiated cultures display very few cells staining positive for any of the markers. Those treated with the retinoids, all display a significant up-regulation of expression for all the markers investigated. Scale bars: 50 μm.

From the images in Figure 4.2, it is clear to see that retinoid incorporation significantly up-regulates the expression of all three markers. Christie *et al.* published that the standard differentiation protocol resulted in approximately a 2.75-fold increase in the number of cells that stain positive for β-III-tubulin, and a 4.5-fold increase in the number of cells staining positive for MAP2ab, compared to undifferentiated samples. Notably, they did not see any increase in the expression for NF-200. Incorporation of ATRA at 100 nM (and similarly EC23) resulted in a dramatic and highly significant increase in all three markers, with β-III-tubulin expression increasing 9-fold, NF-200 40-fold and MAP2ab 15-fold.[59]

After immunocytochemical staining of AH60 and AH61 cultures, all images were quantified through cell counts and the number of positive cells expressed as a percentage of the total population visible per field of view. As in all previous work, three biological triplicates were obtained along with three independent images of each repeat. The data agreed with that previously published with regards to the control differentiation protocol, with similar levels of increase seen for β-III-tubulin and MAP2ab. As hypothesised for the synthetic compounds, and in line with previous screening, the incorporation of the synthetic retinoids led to a significant increase in the expression of all three markers. The concentration chosen to screen the synthetic retinoids initially was 10× higher than that previously published, so a direct comparison cannot yet be deduced. The reason for screening these molecules at an initially higher concentration was that previous work within our group (unpublished) had demonstrated that the cell line could tolerate some retinoids, such as ATRA, at this higher concentration. However, some synthetic retinoids, including EC23, were found to be toxic at this higher concentration and so were only analysed at 100 nM and lower. As both AH60 and AH61 are closer in molecular structure to ATRA, with some inbuilt instability, we hypothesised that they could possibly be tolerated at higher concentrations than the more stable synthetic analogue, EC23. This also allowed us to assess their toxicity, and build a comparison to that of EC23. From the images displayed in Figures 4.1 and 4.2, it is evident that both synthetic retinoids AH60 and AH61 are not toxic at 1 μM, supporting our theory that they act more like ATRA than the other previously screened synthetic

analogues. The increase in expression of each of the markers was quantified through cell counts and expressed graphically as a percentage of the total cell population, displayed in Figure 4.3.

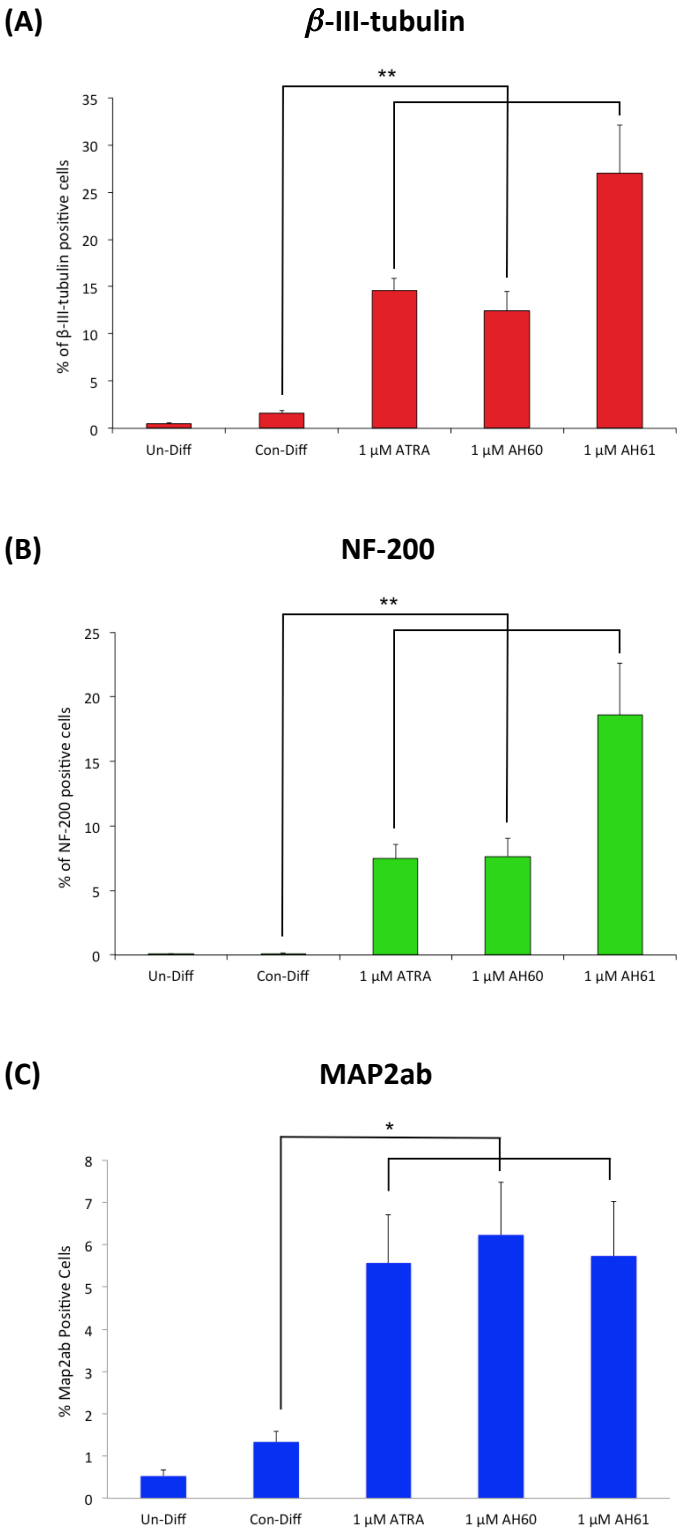

Figure 4.3 Plots displaying quantification of the immunological data as performed by counting positively labelled cells. The increased number of β-III-tubulin (**A**), NF-200 (**B**) and MAP2ab (**C**) positive cells in retinoid supplemented cultures was highly significant compared to control differentiated cultures (Con-Diff). Triplicate analysis was performed for reproducibility. Values shown represent mean + standard error (SDE), n=9. ** $p \leq 0.005$, * $p \leq 0.05$ Student's t-test corrected for multiple testing of sample populations using the Bonferroni correction.

Upon quantification, the increase in expression of all three markers was significant upon inclusion of all three retinoids. The profiles exhibited for ATRA and AH60 were identical with similar increases across all three markers visualised. More notably, AH61 induced further significant increases compared to that of ATRA and AH60 in both β-III-tubulin and NF-200 expression. This supports data previously obtained in the EC model suggesting that this synthetic analogue is appreciably more potent than its natural counterpart and its isomer AH60. Overall, these results show that retinoid supplementation using AH60 and AH61 increases the number of neuronal cells derived from ReNcell VM cultures and significantly increases neuronal maturity, as evidenced by NF-200 expression, comparable to that of ATRA for AH60 and significantly better when treated with AH61.

To investigate the dose response of incorporating retinoids into differentiating ReNcell VM cultures, retinoids were added at 0.1 μM, 0.01 μM and 0.001 μM. These concentrations were chosen as they represent those used in previous studies investigating the dose response of EC23.[59] As in the previous set of experiments at the higher concentration, the numbers of cells expressing β-III-tubulin, NF-200 and MAP2ab were measured. Both immunofluorescent micrographs and quantified cell counts display a clear dose response of all the retinoids, displayed in Figures 4.4 - 4.7.

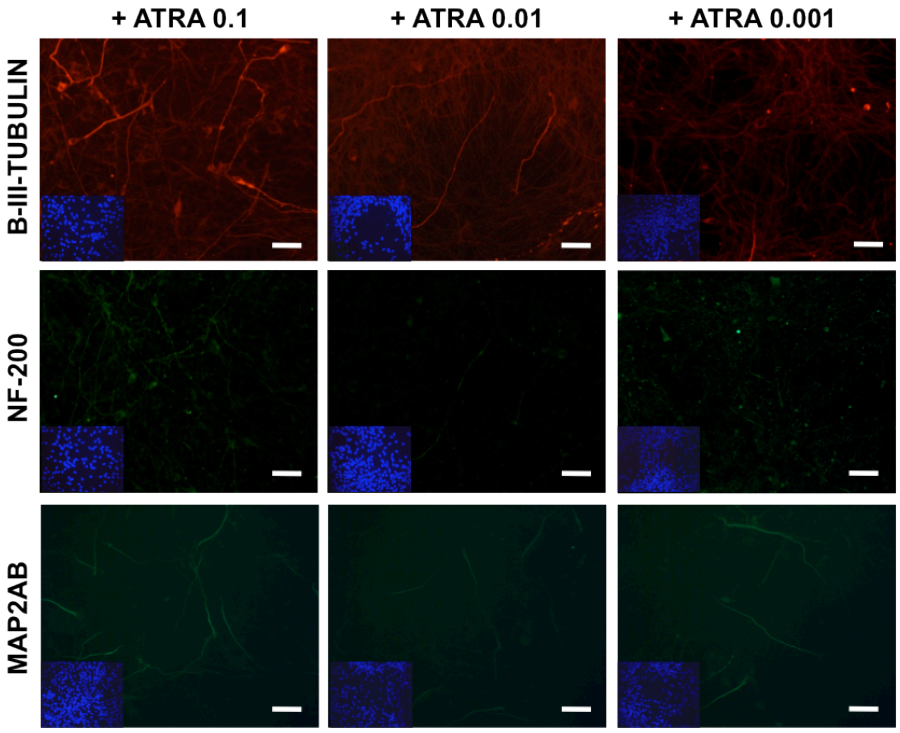

Figure 4.4 Cultures of ReNcell VM cells were induced to differentiate for 7 days under the standard differentiation protocol with the addition of ATRA at 0.1 μM, 0.01 μM or 0.001 μM. Scale bar: 50 μm.

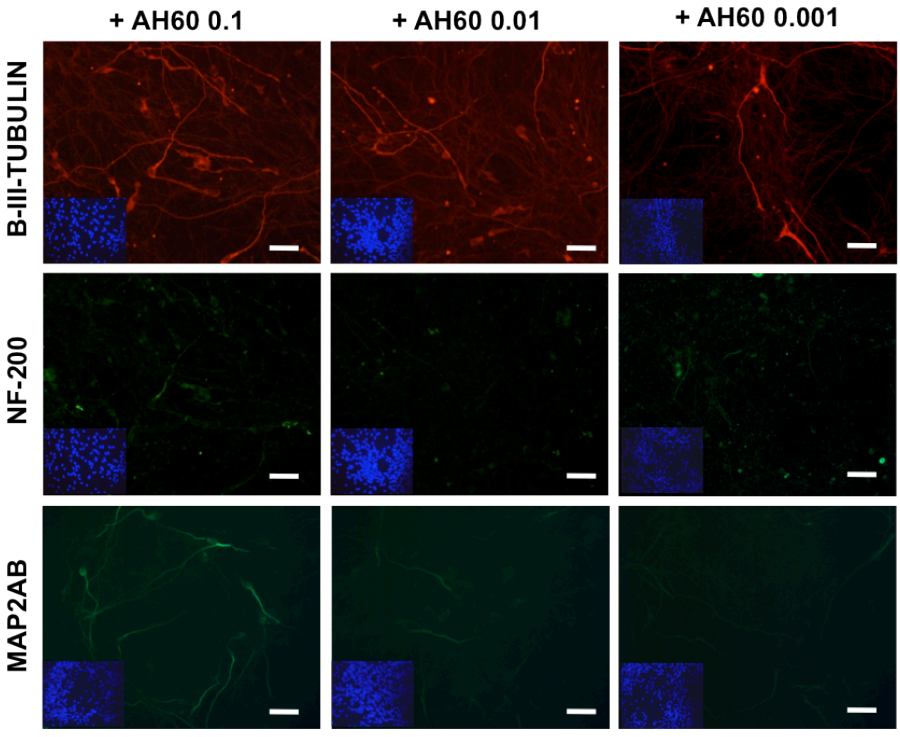

Figure 4.5 Cultures of ReNcell VM cells were induced to differentiate for 7 days under the standard differentiation protocol with the addition of AH60 at 0.1 μM, 0.01 μM or 0.001 μM. Scale bar: 50 μm.

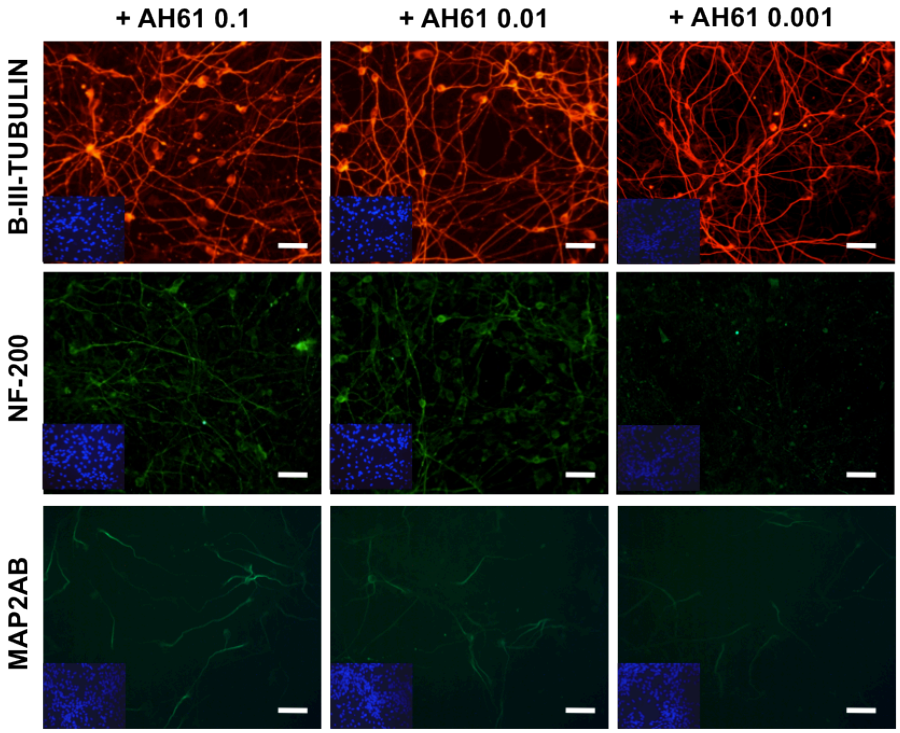

Figure 4.6 Cultures of ReNcell VM cells were induced to differentiate for 7 days under the standard differentiation protocol with the addition of AH61 at 0.1 μM, 0.01 μM or 0.001 μM. Immunological evaluation of β-III-tubulin, NF-200 and MAP2ab showed enhanced expression in AH61 treated cultures Scale bar: 50 μm.

From the immunofluorescent micrographs there is a clear and notable drop in the expression levels of all three markers for ATRA and AH60, compared to that seen at the higher concentration. This suggests both molecules are significantly less active once their concentration is reduced. Upon examination of cultures treated with AH61, this effect appears to be significantly reduced, with all three concentrations displaying strong immunofluorescent images, especially those stained for β-III-tubulin. This supports the data displayed in the previous EC model system, and therefore, again suggests that AH61 is more active at lower concentrations.

Upon quantification (as was done for the higher concentration), a clear dose response for all three compounds can be seen (Figure 4.7). AH61 produces significantly more positive staining for all three markers at both 0.1 μM and 0.01 μM. There is a sudden drop off at 0.001 μM but levels remain not significantly different to ATRA at 0.1 μM. This further supports our previous conclusion that AH61 is

approximately 100-fold more active than ATRA. There is no difference in the expression of β-III-tubulin or NF-200 for both ATRA and AH60, while AH60 only shows a slight, but significant, increase in MAP2ab expression at 0.1 μM. This suggests that AH60 is potentially less active in this system compared to the EC model used in Chapter 3. Currently, there is no data for 13cRA; this would be an interesting comparison to undertake in the future as 13cRA is more structurally comparable with AH60. Data collected from the EC model suggests that 13cRA is as equally potent to ATRA, and since AH60 and ATRA showed nearly identical profiles in this cell line, the hypothesis would be for 13cRA to do the same.

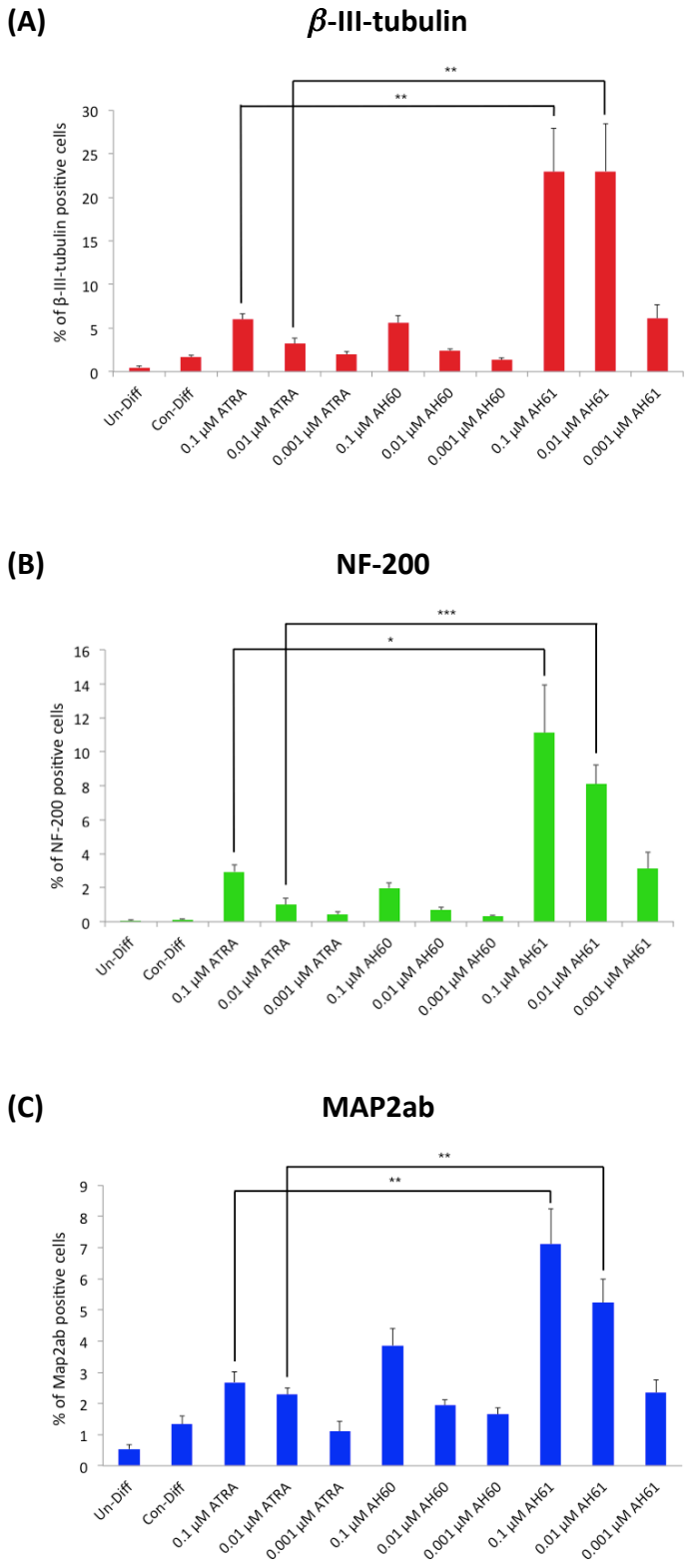

Figure 4.7 Plots displaying quantification of the immunological data as performed by counting positively labelled cells. The increased number of β-III-tubulin (**A**), NF-200 (**B**) and MAP2ab (**C**) positive cells in AH61 supplemented cultures was highly significant compared to ATRA supplemented cultures. Triplicate analysis was performed for reproducibility. Values shown represent mean + standard error (SDE), n=9. *** p≤0.0005, ** p≤0.005, * p≤0.05 Student's t-test corrected for multiple testing of sample populations using the Bonferroni correction.

Finally, a direct comparison of the potency of AH61 compared to that of EC23 was desired. Analysing the current data, and comparing this to work previously published on EC23 suggests that AH61 is a more potent inducer of neuronal differentiation in the ReNcell VM cell system.[59] To confirm this observation, cultures of ReNcell VM cells were incubated with ATRA, AH61 and EC23 at 0.1 μM and 0.01 μM, alongside both undifferentiated and standard control differentiated cells. The two concentrations chosen were those that exhibited the greatest differences when comparing data presented in this thesis to that previously published by Christie *et al*.[59] As in the previous experiment, ReNcell VM cells were cultured for seven days before being stained for the three neuronal markers, β-III-tubulin, NF-200 and MAP2ab. The images are presented in Figure 4.8.

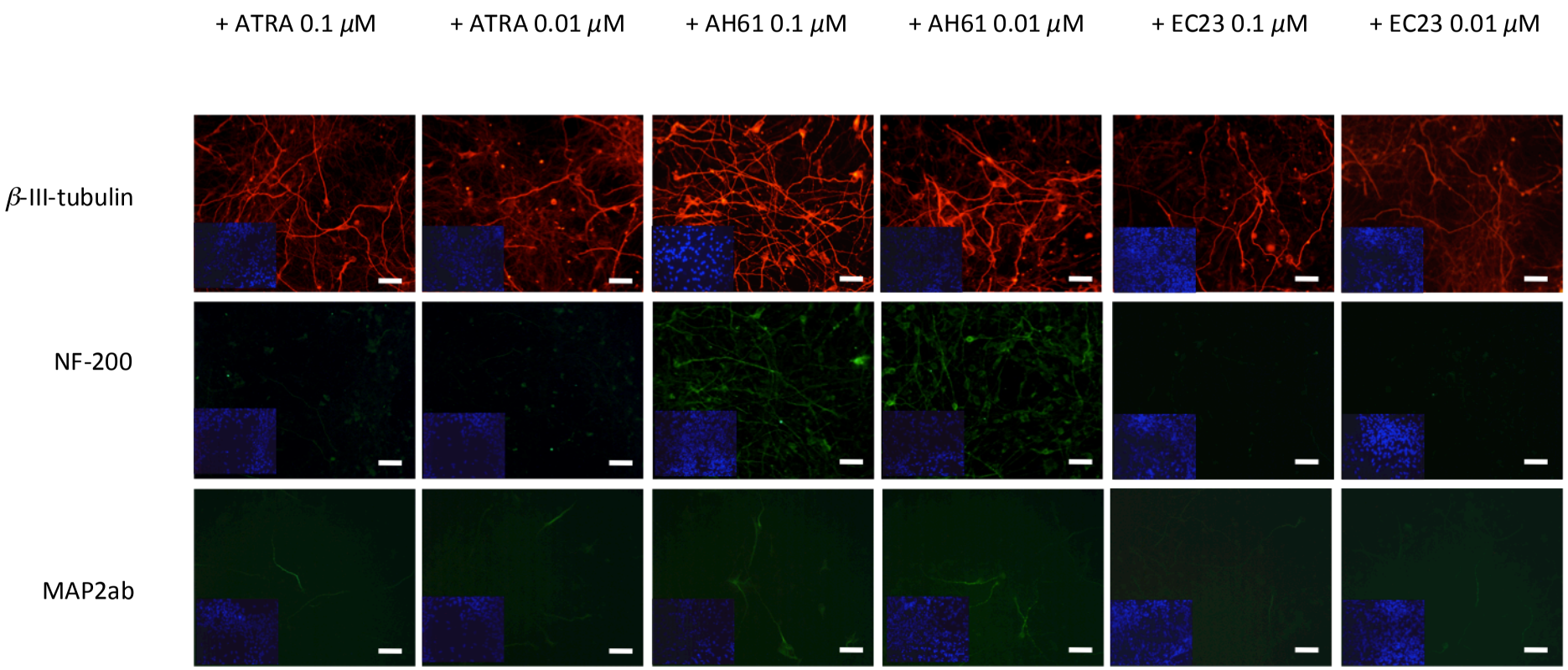

Figure 4.8 Cultures of ReNcell VM cells were induced to differentiate for 7 days under the standard differentiation protocol with the addition of ATRA, AH61 or EC23 at 0.1 μM and 0.01 μM. Immunological evaluation of β-III-tubulin, NF-200 and MAP2ab showed enhanced expression in AH61 treated cultures, but limited expression in both ATRA and EC23 treated cultures. Scale bar: 50 μm.

From the immunofluorescent micrographs, an increase in β-III-tubulin expression in cultures treated with AH61 is most notable. In addition, both NF-200 and MAP2ab expression appear to be up regulated in AH61 treated cultures, compared to both ATRA and EC23. Upon quantification (Figure 4.9), achieved through cell counts, the enhanced potency of AH61 over EC23 in inducing neural differentiation is clearly visible, with significant up-regulation of all three markers.

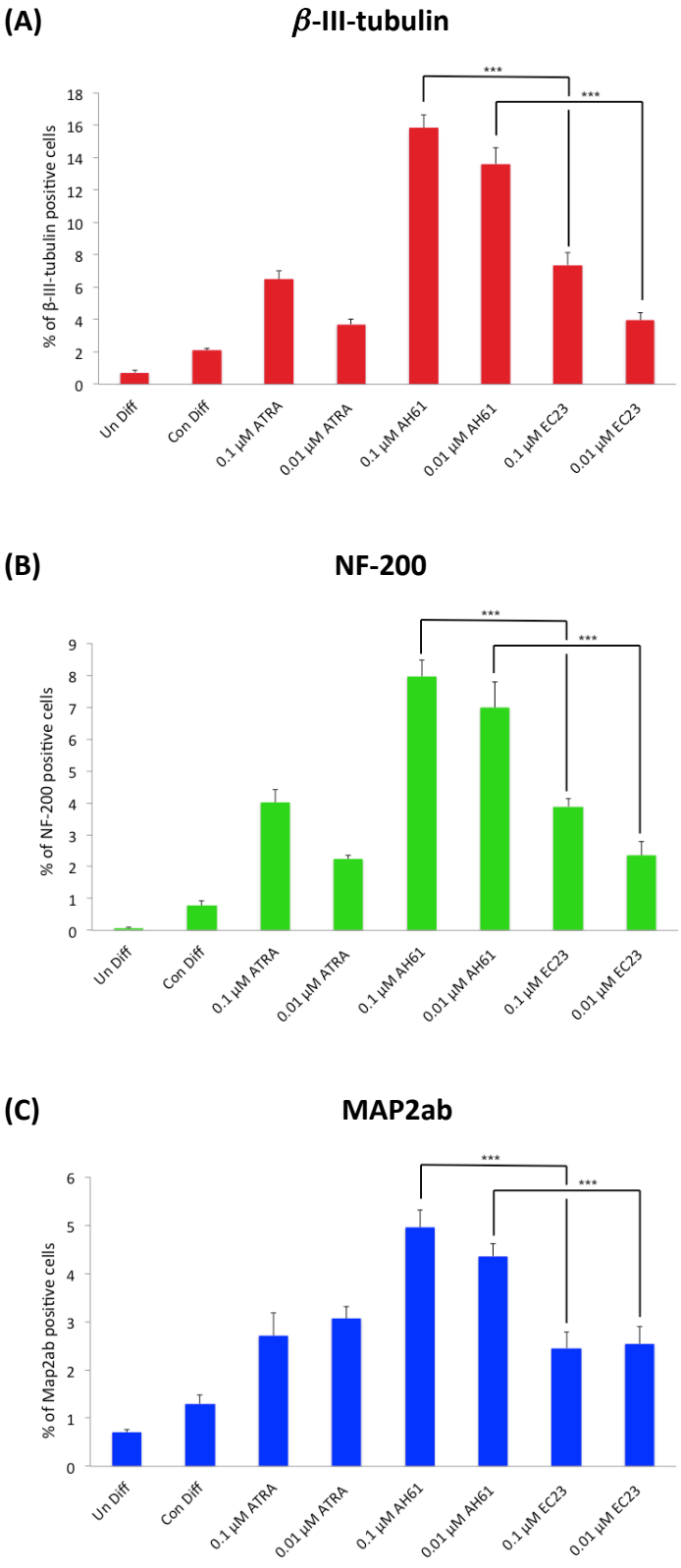

Figure 4.9 Plots displaying quantification of the immunological data as performed by counting positively labelled cells. The increased number of β-III-tubulin (**A**), NF-200 (**B**) and MAP2ab (**C**) positive cells in AH61 supplemented cultures was highly significant compared to EC23 supplemented cultures. Triplicate analysis was performed for reproducibility. Values shown represent mean + standard error (SDE), n=9. *** $p \leq 0.0005$, Student's t-test corrected for multiple testing of sample populations using the Bonferroni correction.

Having displayed that synthetic analogue AH61 significantly enhances neuronal differentiation in human fetal neuroprogenitor cells, we next wished to investigate its effects on an adult neuroprogenitor system.

4.3.2 Analysis of the Potential of AH60 and AH61 to Induce Neural Differentiation in Adult Hippocampal Neural Progenitor Cells.

The final section of this Chapter deals with the effects of incorporating AH60 and AH61 into differentiation protocols derived for the AHPC cell line. As discussed, treatment of this cell line with ATRA led to a three-fold increase in the number of neurons produced compared to FGF-2 withdrawal alone.[60] Therefore, we hypothesised that treatment with the synthetic AH analogues would increase this further, and potentially provide a homogeneous population of mature neurons.

For the cells to proliferate, FGF must be present, therefore, the standard differentiation protocol involves significantly reducing the concentration of FGF (20 ng/mL to 1 ng/mL), alongside the addition of retinoids. Undifferentiated, proliferative cells retain a homogeneous morphology, with each cell being distinctly rounded. The cell number is very high since they have continued to proliferate, with the final cell population sub-optimal as they are over confluent and begin to layer upon one another. Cultures in which only the concentration of FGF has been lowered exhibit an identical morphology, with no noticeable differences to those cultured in a high FGF concentration. Addition of the vehicle, DMSO, similarly shows no change in the cell morphology under phase microscopy (Figure 4.10).

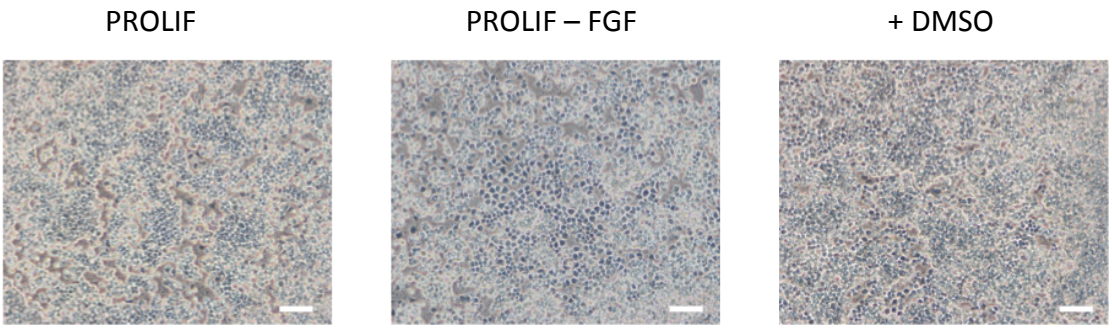

Figure 4.10 Morphologies of AHPC cells after 7 days culture, plated at 20,000 cells per well in a 4-well plate. Proliferative (undifferentiated) cultures (PROLIF) retained a homogeneous appearance of a rounded cell type where there are few cellular processes. Cultures in which the FGF concentration had been lowered to 1 ng/mL (PROLIF-FGF) displayed an identical morphology. Those treated with additional DMSO (same concentration as retinoid treatments) again displayed no morphological changes. Scale Bars: 100 μm.

To investigate the dose response of incorporating retinoids into differentiating AHPC cultures, retinoids were incorporated at 10 μM, 1 μM, 0.1 μM and 0.01 μM. These concentrations were chosen as they represent a broad spectrum in which we hypothesised the compounds would be active. Previous studies also undertaken on this cell line had demonstrated that it was highly sensitive to certain retinoids, notably EC23.[243] We have subsequently investigated whether the AH series would be tolerated more favourably. AHPC cells were cultured for seven days, with the media changed at the halfway time point. Phase images were then recorded and are presented in Figure 4.11.

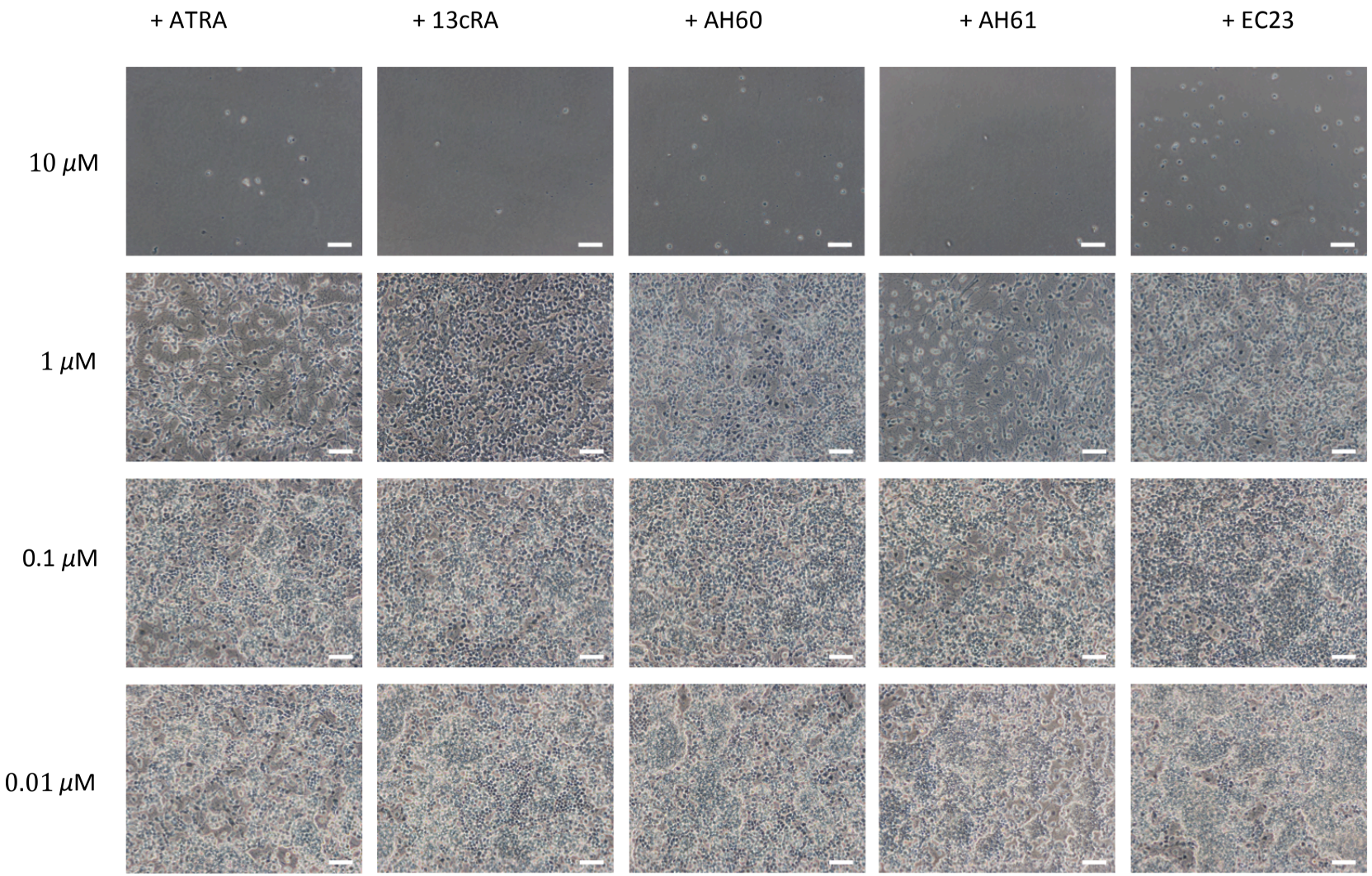

Figure 4.11 Morphologies of AHPC cells after 7 days culture with additional retinoids, plated at 20,000 cells per well in a 4-well plate. Those treated with any of the retinoids at 10 μM induced cell death with no live cells visible after 7 days of treatment. At 1 μM all retinoids used within this screen appeared to be tolerated. There were a greater number of neuronal processes visible, while cell numbers also appeared lower compared to the untreated controls. Both ATRA and AH61 appear slightly more active compared to the other treatments where there was greater proliferation. At both 0.1 μM and 0.01 μM, in all retinoid treatments, the cells appear to have proliferated, although there are large numbers of neuronal processes still visible around the cells. Scale Bars: 100 μm.

Incubation of all the retinoids at 10 μM led to complete cell death, indicating that they are toxic at this concentration. Consequently, no further evaluation was carried out at such high levels. At 1 μM, cell death was not observed and the general cell population appeared heterogeneous. A considerable number of cells expressing neuronal processes were visible throughout all the cultures (Figure 4.12). The number of cells present in these cultures appeared lower than those only exposed to the vehicle, DMSO, suggesting they also had an anti-proliferative activity. This was quantified through counting the number of nuclei per field of view for each culture treatment, with the aid of ImageJ software and DAPI immunocytochemical staining. The data are displayed as the mean from three randomly selected immunostained images (Figure 4.13). As the concentration was lowered, these effects became less visible, with all treatments displaying larger areas of cells with morphologies, similar to that of the cultures not subjected to retinoid treatments. The number of cells also increased indicative of the cells proliferating, rather than differentiating (Figure 4.13). However, for further clarification purposes a proliferation assay, such as a BrdU assay, would need to be completed to confirm this observation. Unlike any of the previous cellular screens, AH61 did not appear to have any advantageous effects at any concentration, compared to that of any of the other treatments, with all retinoid treatments at 0.1 μM and 0.01 μM displayed near identical morphologies.

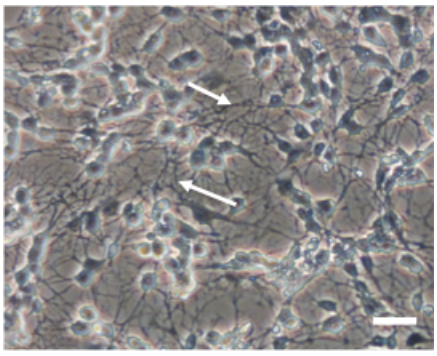

Figure 4.12 High magnification image of the cellular morphology of differentiated AHPC cell cultures after 7 days treatment with ATRA at 1 μM. Arrows indicate neuronal processes. Scale bar: 50 μm.

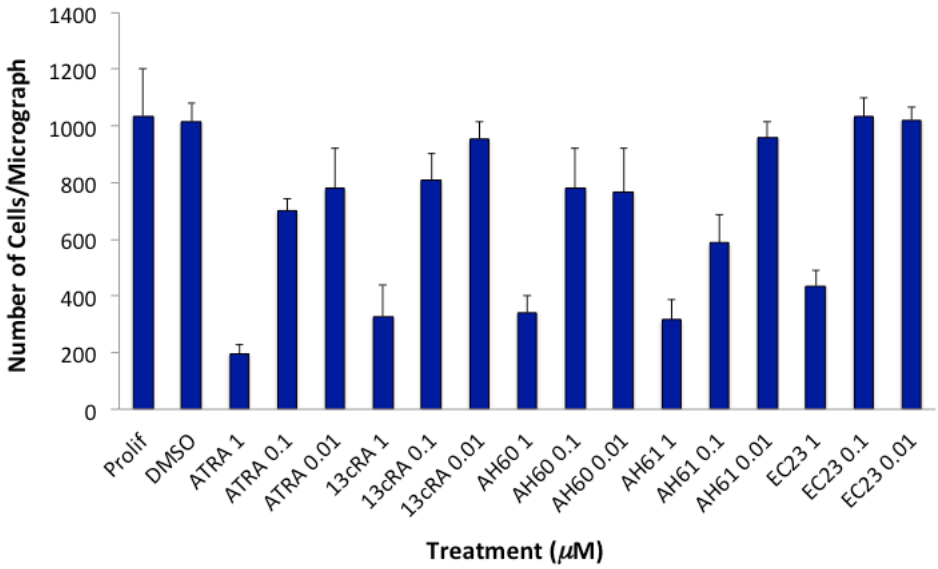

Figure 4.13 Plot displaying the quantification of cell number, as performed by counting DAPI labelled nuclei. Cultures of AHPCs incubated with, either 1 μM, 0.1 μM or 0.01 μM ATRA, 13cRA, AH60, AH61 or EC23 for 7 days, subsequently fixed and immunocytochemically stained for DAPI. Using ImageJ software the number of positive cell bodies were counted on 3 random fields per treatment condition. 1 μM treatment of each retinoid appeared to induce a decrease in the number of cells, suggesting at this concentration they were inducing differentiation. Values shown represent mean + standard error (SDE), n=3. Per statistical analysis using the Student's t-test corrected for multiple testing of sample populations using the Bonferroni correction, there were no significant differences.

To further evaluate the effects of the retinoid treatments, immunocytochemical staining was carried out looking at the expression of both neuronal and glial markers. These two markers were chosen because previously, the AHPC cell line had been characterised as being able to differentiate into both lineages. Thus, cultures were co-stained for β-III-tubulin and GFAP (Figure 4.14).

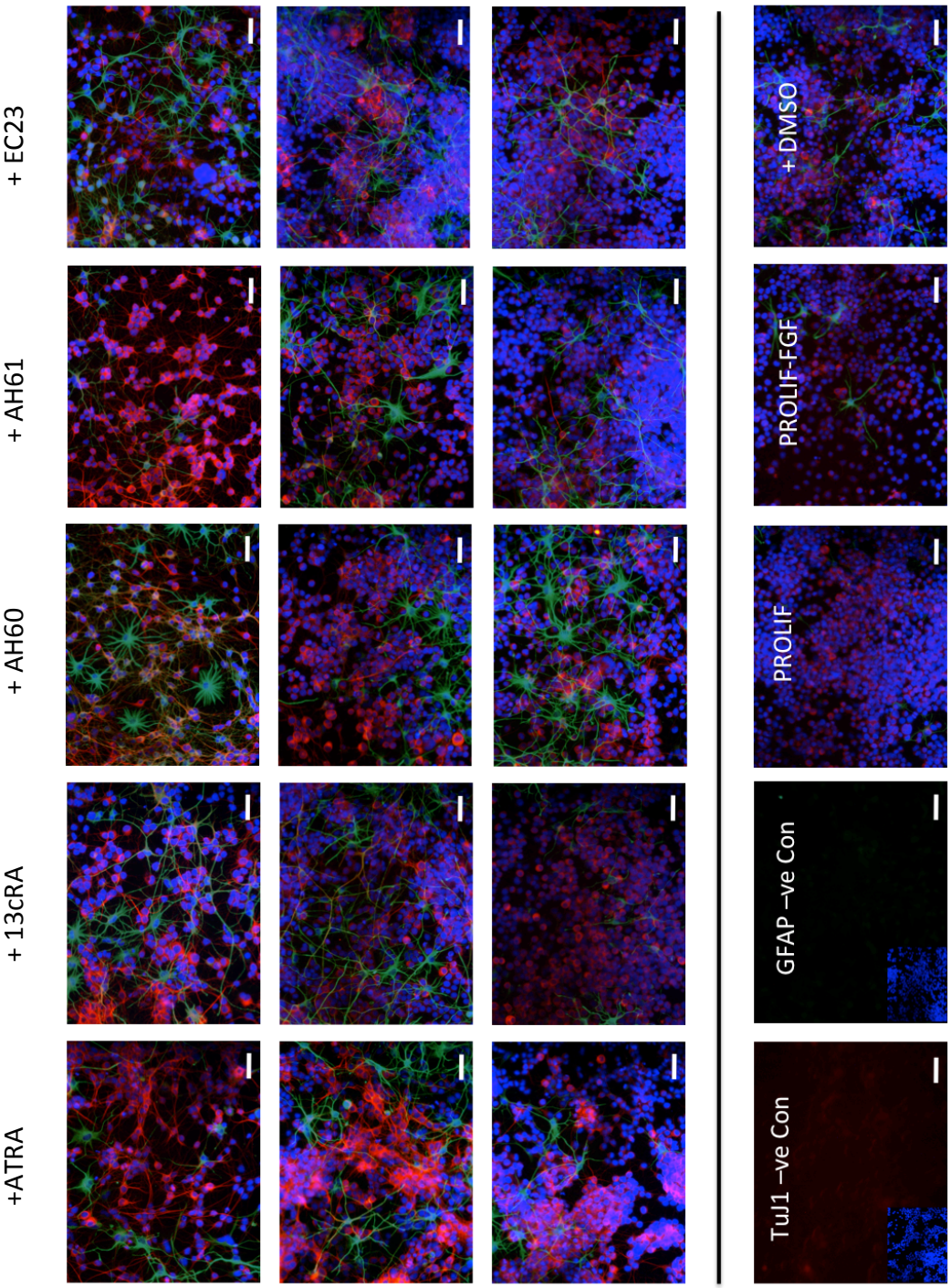

Figure 4.14 Immunofluorescent micrographs of AHPC cells incubated for 7 days with ATRA, 13cRA, AH60, AH61 or EC23 at 1 μM, 0.1 μM or 0.01 μM and stained for markers of neurons (TuJ1, red), astrocytes (GFAP, green) and with DAPI (blue) for nuclei. Those kept in proliferative media (PROLIF), proliferative media with reduced FGF concentration (PROLIF-FGF) stained in general negative for TuJ1 and GFAP. Those treated with DMSO similarly stained negative for TuJ1, but did display more cells positive for GFAP. All retinoid treated cultures stained positive for both markers at 1 μM, while at both 0.1 μM and 0.01 μM there was very few positive neuronal cells and a reduced number of positive astrocytes. In general the cultures at 0.01 μM were highly similar to those treated only with DMSO. Scale bar: 50 μm.

Those that were not treated with any of the retinoids (PROLIF and PROLIF-FGF) in general did not stain positive for either β-III-tubulin or GFAP. Upon addition of DMSO

there was no apparent increase in β-III-tubulin expression, although a slight increase in GFAP expression was noted. All cultures treated with 1 μM of retinoid stained highly for both markers. As the concentration was reduced, the cell population became denser and the number of positive β-III-tubulin cells decreased. GFAP expression also decreased to levels consistent with that seen for DMSO treatment alone. Quantification, through counting positively labelled cell bodies, was carried out on the active concentration of 1 μM (Figure 4.15). This preliminary quantification data suggest that there are no significant differences between any of the retinoid treatments, with each of them leading to a significant increase in the number of positive neuronal processes.

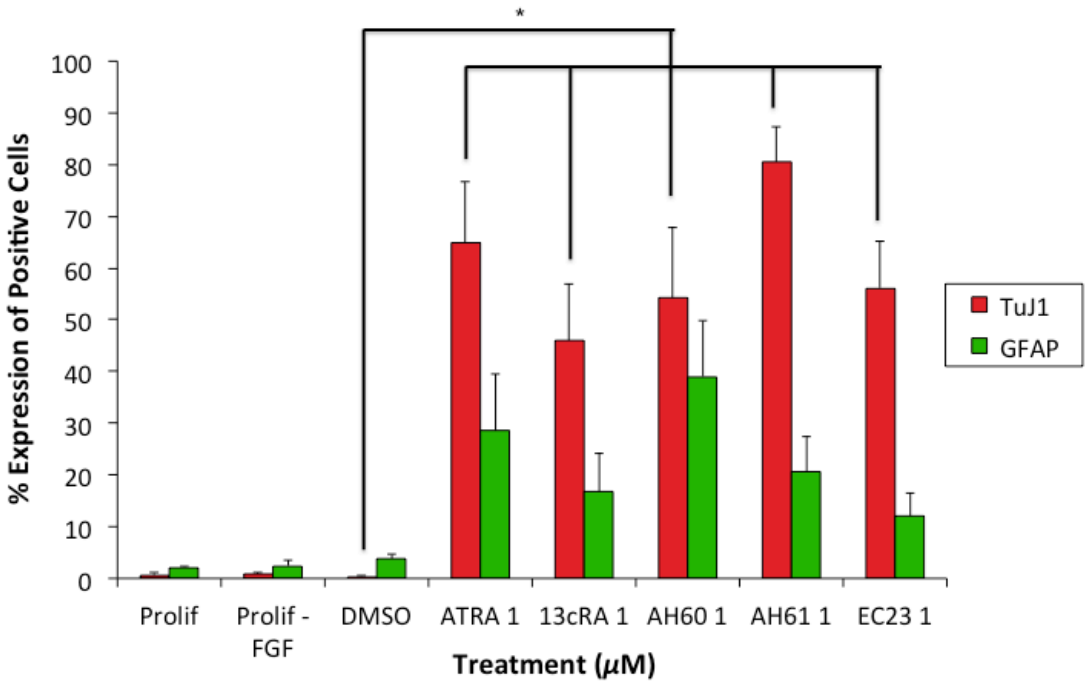

Figure 4.14 Plot displaying the quantification of the percentage expression of TuJ1 and GFAP, as performed by counting labelled cell bodies. Cultures of AHPCs incubated with 1 μM ATRA, 13cRA, AH60, AH61 or EC23 for 7 days, subsequently fixed and immunocytochemically stained. Using ImageJ software the number of positive cell bodies were counted on 3 random fields per treatment condition. 1 μM treatment of each retinoid induced a significant increase in the percentage expression of TuJ1 labelled cells, suggesting at this concentration they were inducing differentiation. Values shown represent mean + standard error (SDE), n=3. *p≤0.05, Student's t-test corrected for multiple testing of sample populations using the Bonferroni correction.

To fully characterise the effects of the AH compounds and that of EC23 further, both repeats of the above experiments, followed by further cellular counts for quantification are required. In addition, quantifying the total protein content present would be more accurate, for example, through a Western Blot.

4.4 Discussion

This chapter aimed to evaluate the effects of AH60 and AH61 in stem cell model systems already committed to a neuronal lineage, mainly NSCs and NPCs. These are cell types commonly found in the CNS, and are known to be influenced by a number of small molecules *in vivo*, in particular ATRA.[188, 189] Due to these well established roles *in vivo*, ATRA has subsequently been used as a tool to direct the differentiation of NSCs/NPCs *in vitro* (see Chapter I for full discussion). It was therefore hypothesised that the synthetic compounds, AH60 and AH61, would be able to mimic or improve the profiles exhibited by ATRA.

The first model chosen to be assessed, was a commercially available human embryonic NSC line, ReNcell VM. This cell line, as discussed previously, is derived from the VM of human foetuses, an area known to respond to endogenous ATRA during neurulation in the early embryo.[334] Subsequently, this was demonstrated *in vitro* by the differentiation of ventral mesencephalon progenitors into dopamine neurons. Addition of ATRA to the defined dopamine-inducing differentiation protocol significantly enhanced the number of neurons.[335] More recently, using the ReNcell VM cell line, addition of ATRA was shown to significantly enhance the number of both TuJ1 and NF-200 positive neurons. This displayed that not only did ATRA accelerate neurogenesis, but enhance the maturity of the neuronal derivatives. Furthermore, substituting ATRA for the more stable analogue, EC23, showed significant further improvements.[59] Therefore, it was predicted that AH60 and AH61 should show similar effects.

Experiments were initially carried out to investigate whether AH60 and AH61 would induce similar phenotypes seen to those of ATRA and EC23. Media supplementation at 1 μM led to a neuronal phenotype in both AH60 and AH61 treated cultures. In addition, the total cell number (calculated from DAPI counts) was attenuated in both treatments, similar to that seen for ATRA. This is consistent with MTS data previously collected in our research laboratory.[243] Although for a direct comparison a further MTS assay investigating AH60, AH61 and EC23 would be required. In addition, cell

death has not been investigated, although the morphological data suggests the cells are differentiating, it would be valuable to investigate the toxicity profiles of each of the retinoids. This may also highlight higher, more active, concentrations of tolerated retinoid, which may further enhance differentiation.

Upon immunocytochemical staining, up-regulation of all three chosen markers was visualised. In addition, AH61 was highlighted as being significantly more active than both ATRA and AH60 at 1 μM. Although previously AH61 has been demonstrated as being significantly more active than both ATRA and AH60, this has come at reduced concentrations. The effects seen therefore in this cell model, suggest AH61's increased activity, is not only down to an improved stability and metabolic profile. Upon investigating the dose response of AH60 and AH61, a similar profile as to that seen in the TERA2.cl.SP12 EC cell line was observed for AH61, with AH61 being seen to be 100-fold more active than both, ATRA and AH60. Although, the observed higher activities of AH60, seen in the EC cell model, were not transpired to this NSC model, as both AH60 and ATRA showed similar dose response profiles. This highlights the differences between different stem cell types, and underlines why compounds designed to act on specific stem cell types maybe required.[197]

Finally, a direct comparison of the activity of AH61 to that of EC23 was desired. Comparing published data of EC23 to that seen for AH61 suggested AH61 was significantly more active than its more stable predecessor.[59] Upon repeating the experiments this was proved with all three markers being significantly up-regulated in AH61 treated cultures to EC23. Moreover, the higher levels of expression of the late neuronal markers NF-200 and MAP2ab suggest that AH61 also further enhances the maturation of the differentiating neurons. These findings also suggest that the increased activity of AH61 is not as a result of either reduced metabolism, or enhanced stability, as EC23 is considered to be the more rigid and stable analogue.[228] Therefore one hypothesis is that AH61's enhanced activity over ATRA would be conferred through its increased stability towards isomerisation and reduced metabolism, thus allowing it to remain at an active cellular concentration. In addition, its further increased activity over EC23 is conferred through its greater

structural resemblance to ATRA, and therefore its higher binding affinity for the cognate nuclear receptors. Although, for this to be confirmed RAR binding studies would need to be carried out.

Therefore replacing ATRA or EC23 with AH61 should allow for the production of a greater number of mature neurons from the NSC line, ReNcell VM. This is highly useful, as cell lines derived from this area of the brain have been highlighted as being particularly important for therapeutic transplantation therapies. In particular, in developing therapies associated with Parkinson's disease.[336, 337] Furthermore, the enhance differentiation seen upon utilising AH61 allows for a greater yield of neuronal subtypes, which are required for transplantation, therefore, reducing the number of foetuses that are needed.[338]

The final cell line chosen to analyse the activities of AH60 and AH61 was the adult hippocampal NPC line, AHPC. This cell line was chosen as it had been shown to respond to ATRA and differentiate down a neural lineage.[59] In addition, un-published work within our research group had demonstrated that this cell line also responded to 13cRA, and EC23 induced differentiation.[243] Furthermore, it had been used to identify other neuro-inducing small molecules, such as neuropathiazol, reviewed in Chapter I.[250]

Previous work both within our research group, and that Nakumara, had highlighted the sensitivity of the AHPC cell line to high concentrations of retinoids.[243, 339] This data had shown that upon high doses of retinoids, neuronal survival decreased, with cultures becoming sub-optimal with eventually apoptosis/cell death ensuing. In addition, previous work has also emphasised that cell density was important, with a high cell density required.[243] Taking these considerations into account, the best know conditions were used to assess the activities of AH60 and AH61.

Initially, a broad concentration range was chosen to examine whether the AH series was any less toxic than those that have been previously screened. The data obtained for 10 μM follows the trend that ATRA, and other retinoids, are toxic at this

concentration. At 1 μM all the retinoid treatments promoted neurogenesis, with morphological features apparent throughout the cell cultures. Upon quantifying the total cell number, a significant drop was seen compared to that of the DMSO treated cultures. This, in addition to the morphological data, suggests the cells are committing to differentiation. The apparent lack of any physiological changes in treatment with DMSO also signifies that these changes are from the retinoid treatment and not the solvent. Upon immunocytochemical staining, for both neuronal and glial markers, a significant increase in expression was visualised across all retinoid treatments. There was no significant difference in any of the synthetic compounds, compared to ATRA, suggesting they are equally as active at this concentration. One aspect, which has not been investigated fully, is validating that the reduction in cell number is not down to cell death. This is especially important considering the sensitivity of this cell line.[339] Therefore, to further validate this work a toxicity screen, as carried out on the TERA2.cl.SP12 EC cell line, should be undertaken.

As the concentration was reduced, all the retinoid treatments appeared to lose activity, with the cultures gaining morphologies similar to those of the proliferative controls and DMSO. This was confirmed through quantifying the total cell number in which all treatments did not differ significantly from the control cultures. This was further reinforced through immunocytochemical staining, in which the number of positive neuronal and glia cells dropped. This is preliminary data, and would require repeat experiments to fully validate the results described within this thesis, both through more cellular counts and total protein expression quantification. Although, these preliminary results do suggest, for the first time there appears to be no beneficial effect of AH61 or EC23 over that of ATRA.

A full explanation as to why AH61 is so potent in the ReNcell VM line but not so in the AHPC line could be due to species specificity, as differences have been described in the literature.[331] All the cells lines screened up to the AHPC line have been human, apart from the initial screen in the murine F9 cells. It would be interesting to screen AH61 in an adult human hippocampal cell line to see if the same effects were

observed. Due to current limitations, *i.e.* the availability of adult human brain tissue, as discussed earlier within this Chapter, this is currently not possible. Therefore, alternative models will need to be investigated to further characterise the full biological role of this synthetic retinoid.

Furthermore, to allow for highly specific differentiation of neural progenitor cells, such as the AHPC cell line, alternative small molecules may need to be employed, as stimulation of the retinoid signalling pathway does not induce complete and unambiguous neurogenesis. One possible alternative has been highlighted in the literature as neuropathiazol (reviewed in Chapter I), and this will be further analysed in the next Chapter.[250]

4.5 Conclusions

The first conclusion that can be drawn is that both AH60 and AH61 can induce differentiation of neural progenitor cells. In the human fetal neural progenitor cell line examined, AH61 induces differentiation significantly better then any other compound screened in this model. The exact reasons behind this improved biological profile are unknown, but could be hypothesised to be as a result of improved binding affinity for the receptors/transport proteins involved in the signalling pathway, coupled with increased metabolic and physical stability. Again, identical to previous stem cell systems screened, AH60 has a weaker profile than that of its isomer, AH61. The effects seen in this system are also less apparent than in previous investigations, with AH60 having a near identical biological profile to that of ATRA.

Upon investigating their biological activity in an adult hippocampal NPC system, the same profiles were not observed. For the first time, there was no greater potency of either of the AH series over ATRA. They both appeared to have similar toxicity levels, somewhere between 1 μM and 10 μM, and while they did induce differentiation of the AHPC cells into positive β-III-tubulin and GFAP cells, there was no apparent increase in the activity of the synthetic analogues over ATRA as their concentration was lowered. In addition, the ability of all the compounds screened was not highly specific, inducing high levels of both neuronal and astrocyte differentiation.

Thus to fully realise the potential of AHPCs, and understand their differentiation pathways more accurately the use of alternative small molecules maybe required, which allow for a more specific induction of differentiation as all retinoid treatments appear pleotropic.

Chapter V

Alternative Small Molecules to Probe Stem Cell Biology

5.1 Introduction

Currently the focus of this thesis has resolved around a class of small molecules termed retinoids, and their ability to induce differentiation in both embryonic and neural progenitor cell lines. As the potential of stem cells has become more apparent, ways in which they can be utilised have generated significant amounts of interest. Pluripotent ES cells potentially represent an inexhaustible source of all cell types, if the knowledge to differentiate them reproducibly and efficiently exists.[28] Currently, this is not the case, but one solution to the problem involves using small molecules, and it has generated significant interest over the past decade.[340]

In attempts to harvest the full potential of stem cells, many groups have looked to chemical control as a solution (see Chapter I for full discussion). Although retinoids are classified as small molecules, and there are many published differentiation protocols that utilise them (see Chapters I, III and IV and references within), more recently focus has turned to identifying different classes of compound. Small molecule libraries of compounds have been designed as a simple and cost effective approach to identifying potential targets.[197] This is in an attempt to identify new families of compounds, which would help unlock the full potential of these cells, as molecules are screened for a particular biological activity, in a particular cell type (for a detailed review see Lyssiotis *et al.*).[197]

A number of traditional methods of neural differentiation have shown success, utilising natural signalling components, such as ATRA. For example, one effective protocol developed demonstrated the successful differentiation of mouse ES cells into motor neurons. Briefly, the protocol involved firstly neuralising the cells into neural progenitors through concomitant ATRA treatment, followed by caudalising the cells, also with ATRA. Finally, an agonist of the Hh-mediating signal pathway was employed to ventralise the caudilised neural cells to become motor neurons.[217] However, as ATRA in general is pleiotropic, the identification of other small molecules that allow precise regulation of stem cell differentiation down neuronal lineages was, and still is, desirable. This led to a number of groups screening libraries

of compounds to identify novel compounds to further direct neurogenesis (reviewed in Chapter I).

One such study, carried out by Warashina *et al.* identified a class of compounds that selectively induced differentiation of hippocampal neural progenitors.[250] The class of compounds, 4-aminothiazols, were then subjected to a small SAR study, which identified neuropathiazol, **60**, as being the most potent (Figure 5.1). As discussed in Chapter I, treatment of AHPCs with neuropathiazol, **60**, slowed cell proliferation and differentiated more than 90% into TuJ1 positive cells, with very few GFAP-positive cells visualised. In comparison, treatment with ATRA showed weaker anti-proliferation activity, and large numbers of both TuJ1 and GFAP-positive cells were seen. Furthermore, ATRA showed greater cytotoxicity compared to that of neuropathiazol, **60**. After longer incubation periods AHPCs demonstrated positive staining for mature neuronal markers neurofilament-H and MAP2ab, while RT-PCR analysis demonstrated Sox2 downregulation and NeuroD1 upregulation. Warashina *et al.* also demonstrated that astroglial differentiation, induced by LIF and BMP2, was inhibited by neuropathiazol, **60**, but not demonstrated when ATRA was employed.[250]

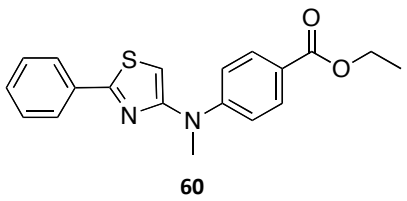

60

Neuropathiazol

Figure 5.1 Structure of neuropathiazol.

Modifications to the retinoid structure, as carried out within this thesis, has had some very positive results, although these were not transpired in adult NPCs using the AHPC cell line. Therefore, carrying on from Chapter IV, in which the potential of the retinoid series of compounds was assessed in an AHPC cell line, a comparison with neuropathiazol was carried out. In addition, the current literature on

neuropathiazol at the time had not identified a mode of action, but suggested from the observations seen that it functioned through a different pathway to ATRA and had a more specific neurogenic inducing activity.[250] Furthermore, the synthetic route to neuropathiazol lacked any characterisation data for all the intermediates, with only limited characterisation data provided for neuropathiazol itself. This suggested that further work was required on this molecule, and other chemical analogues, to assess the full potential of these compounds. Additionally, as a mode of action had not been identified, so potentially neuropathiazol, **60**, could induce neurogenesis in other NPCs lines, NSCs lines and even *pluripotent* stem cell systems, further increased our interest.

5.2 Aims and Objectives

The aim of this Chapter was to further evaluate the small molecule neuropathiazol. Initially, the synthesis and screening of its biological potential, in both the cell line characterised in the literature, and others used within our laboratory was desired. Additionally, the synthesis of further analogues, which were perceived to have a greater biological potential and allow us to hypothesise the potential pathway the molecule acts through were desired.

The objectives, were therefore, to repeat the synthesis of neuropathiazol, completely characterising the product and all intermediates. Demonstrate that the molecule behaved at least as described in the literature, and conduct a more thorough characterisation of its activity in the AHPC cell line. We also assessed the potential for neuropathiazol to differentiate other stem cell lines, including the human embryonic neural stem cell line, ReNcell VM and the embryonal carcinoma stem cell line, TERA2.cl.SP12. In addition, the synthesis of specific neuropathiazol analogues would also be investigated, followed by their complete characterisation.

5.3 Synthesis of Neuropathiazol and Associated Analogues

The literature protocol for the synthesis of neuropathiazol, **60**, began with the cyclisation of 4-(2-chloro-acetylamino)-benzoic acid ethyl ester, **61**, with thiobenzamide, **62**, followed by methylation of the nitrogen (Scheme 5.1).[250]

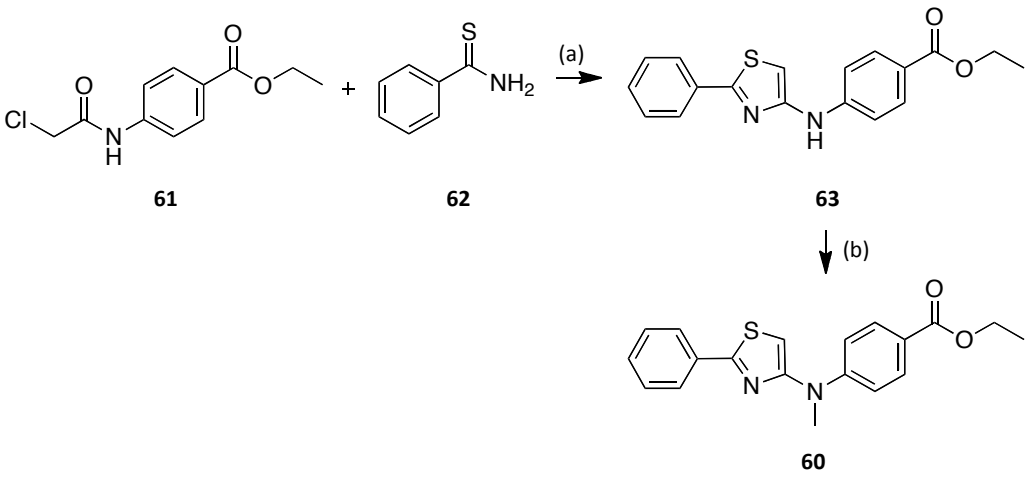

Scheme 5.1 Synthesis of neuropathiazol. Reagents: (a) Dimethylformamide (DMF) or EtOH, 80 ^{o}C, overnight; (b) NaH, MeI, room temperature, 2 hours.[250]

4-(2-Chloro-acetylamino)-benzoic acid ethyl ester, **61**, is not commercially available, thus the synthesis began with a direct amide bond formation, between benzocaine, **64**, and chloroacetic acid, **65** (Equation 5.1). Two different catalysts were investigated and compared with that of 1'1-carbonyldiimidazole (CDI), **67**. The results are presented in Table 5.1, with the structure of the bi-functional catalyst, *N*,*N*-diisopropylamino-benzylboronic acid, **66**, and CDI, **67**, presented in Figure 5.2.

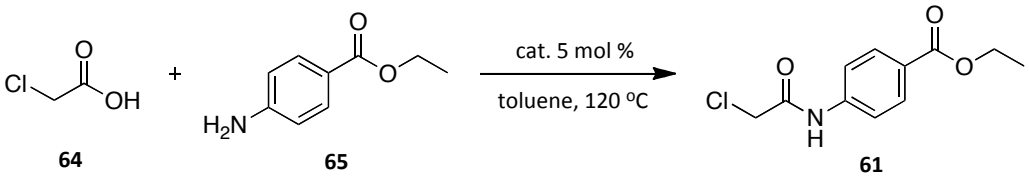

Equation 5.1 Route to 4-(2-chloro-acetylamino)-benzoic acid ethyl ester.

Reaction	Catalyst or Reagent	Time (Hours)	Isolated Yield (%)
1	Boric Acid	48	61
2	Bi-functional Catalyst	48	51
3	CDI	18	49
4	Boric acid	96	67

Table 5.1

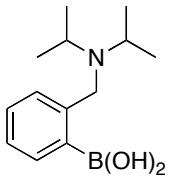

66

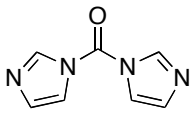

67

Figure 5.2 Structures of *N*,*N*-diisopropylamino-benzyl boronic acid (**66**) and CDI (**67**).

The best result was obtained using boric acid, achieving an acceptable yield of 61% after 48 hours. In an attempt to improve the yield, the reaction time was increased to 96 hours, and although there was an increase in yield to 67%, this was not noteworthy.

With all the reagents required for the synthesis of neuropathiazol, **60**, obtained, the literature method was followed.[250] This initially involved reacting thiobenzamide, **62**, with 4-(2-chloro-acetylamino)-benzoic acid ethyl ester, **61**, in DMF at 80 ^{o}C for 12 hours. The reaction mixture went through a number of colour changes, from yellow through to red before ending as a dark green to black mixture. Analysis of the reaction by TLC clearly demonstrated that a minimum of five compounds were present. After subsequent work-up and removal of the DMF under high vacuum, the resulting crude product was re-crystallised from IPA. Unfortunately, this proved unsuccessful, thus SiO_2 column chromatography was attempted to access the desired product in a pure state. As in all previous attempts, this again proved unsuccessful, with multiple compounds eluting together. The literature also suggested ethanol as an alternative solvent, and thus, this was subsequently attempted. The reaction was initially tried at room temperature, but no reaction was observed. Consequently, the reaction mixture was warmed to 40 ^{o}C and as in the

previous reaction, employing DMF, multiple compounds could be visualised by TLC. Overall, the highest yielding method identified was obtained when the reaction was carried out in DMF at 80 ^{o}C under argon, followed by re-crystallisation from IPA, subsequent SiO_2 column chromatography and finally, repeated re-crystallisation from IPA. This method yielded a dark green solid in 65% yield. While it was unable to fully isolate the compound, it was deemed suitable for the next step in the reaction (Scheme 5.2).

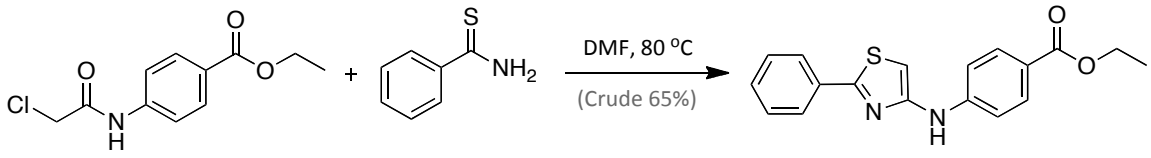

61 **62** **63**

Scheme 5.2

The only literature available on this compound provided no characterisation data, suggesting that it was never directly isolated. This is consistent with the results described above, as this compound appears to have a number of stability issues. Multiple attempts at carrying out the above reaction provided a number of compounds all very different in colour but with near identical proton NMRs of the desired compound. This suggests that the actual compound is most likely colourless/off-white and that the vivid colours obtained are from minor impurities carried through. It was, therefore, accepted that isolation and full characterisation of the intermediate was not feasible, and thus, methylation was carried out on the material obtained from the previous reaction. This was as described in the literature, using sodium hydride and methyl iodide to give, neuropathiazol, **60**, in a good yield of 83% (Scheme 5.3).[250]

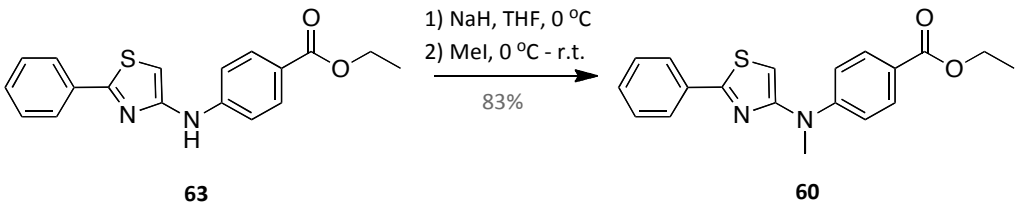

Scheme 5.3

Simultaneously, two related intermediates were synthesised in an attempt to develop more analogues previously not investigated. The first analogue chosen, involved the incorporation of a TMTN group into neuropathiazol, **60**. This would replace the benzyl group present in neuropathiazol, **60**, adding greater bulk, and potentially steering the molecule into acting down the retinoid receptor pathway. To incorporate the TMTN group, the corresponding thioamide was required. This was achieved from initially preparing 6-iodo-1,1,4,4-tetramethyl-1,2,3,4-tetrahydronapthalene, **8**, achieved through identical procedures as previously published and described in Chapter II.[228] This was followed by a Grignard reaction with methyl chloroformate to give the desired methy ester, **68**, in a yield of 88% (Scheme 5.4).

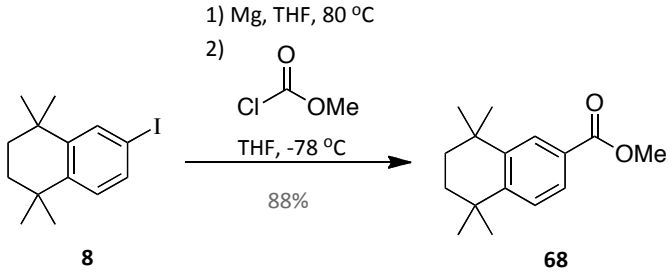

Scheme 5.4

Initially, attempts to generate the amide directly from this compound, including using an excess of 35% ammonia, failed.[341] As direct amide formation proved unsuccessful, saponification to the acid, **69**, followed by formation of the acid chloride was adopted as the more favourable route. Again, $LiOH.H_2O$ was used for

the saponification, in a 1:1 THF and water mixture, which led to the formation of the acid, **69**, as a white solid in a 79% yield (Scheme 5.5).

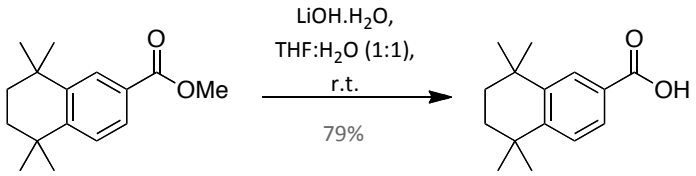

68 **69**

Scheme 5.5

The acid chloride was generated *in situ* through treatment with oxalyl chloride, before reacting directly with an excess of 35% aqueous ammonia solution to yield the amide, **70**. This was identified as a white solid, in a very good yield of 88% (Scheme 5.6).

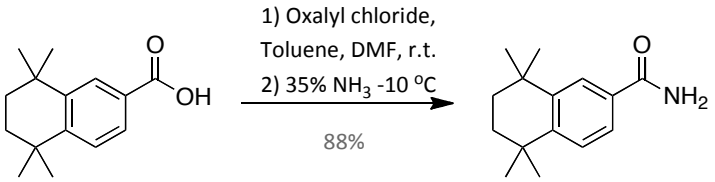

69 **70**

Scheme 5.6

The final step involved the conversion of the amide, **70**, to the thio-amide, **71**, and due to its ease of handling and availability, Lawesson's Reagent was chosen. The initial procedure followed, involved refluxing in benzene, although this was substituted for toluene.[342] The procedure gave two major products by TLC (excluding the spots identified as the bi-products of the Lawesson's reagent). These were subsequently identified as the desired product, 5,5,8,8-tetramethyl-5,6,7,8-tetrahydro-naphthalene-2-carbothioic acid amide, **71**, as the minor product in a 19% yield and the nitrile, 5,5,8,8-tetramethyl-5,6,7,8-tetrahydro-naphthalene-2-carbonitrile, **72**, as the major product in a 52% yield. This result suggested that the

above reaction conditions were too severe, as the desired compound was further reacting to generate the nitrile, **72** (Scheme 5.7).

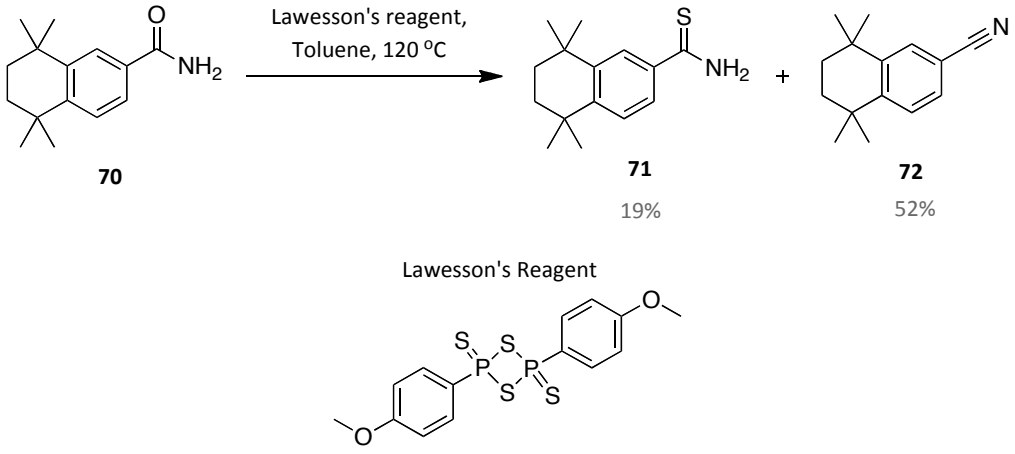

Scheme 5.7

To increase the yield of the desired product, the reaction was re-run in toluene at room temperature. After 18 hours, the desired product was visible by TLC, and as soon as the nitrile, **72**, appeared to be forming, the reaction was stopped and purified. This yielded the thio-amide, **71**, as a yellow solid in an excellent 97% yield. Upon scale up, the same procedure was followed, again running the reaction for 18 hours. This reaction was less successful with the yield dropping to 80%, as the reaction rate appeared to increase, which in turn led to more of the nitrile, **72**, being produced (Scheme 5.8).

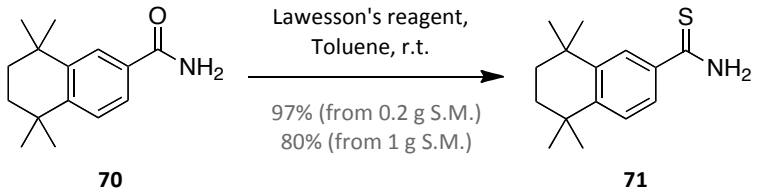

Scheme 5.8

The second analogue desired, was one containing a fluorine atom *ortho* to the carbonyl on the benzene ring. This was thought to be desirable, as recent published work had suggested that binding to RAR receptors was favoured when a fluorine

atom was present at this position.[343] The compound synthesised, AC-261066, **73**, was similar to neuropathiazol in that it was based around a thiazol unit with an aromatic group and a *para* carbonyl functional group, but minus the *N*-linker atom, and a different hydrophobic end (Figure 5.3). Of more interest, was that these compounds had been shown to activate RAR β2 receptors, something which neuropathiazol, **60**, had not, thus possibly steering the analogue towards the RAR receptors.[343]

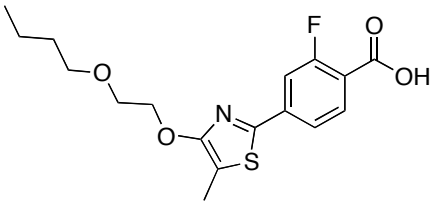

73

Figure 5.3 Structure of AC-261066.

To incorporate the fluorine atom into neuropathiazol, **60**, the synthesis started from 4-amino-2-fluorobenzoic acid, **74**, which was converted directly into the ethyl ester, **75**, using thionyl chloride and ethanol, in a high yield of 93% (Scheme 5.9).[344]

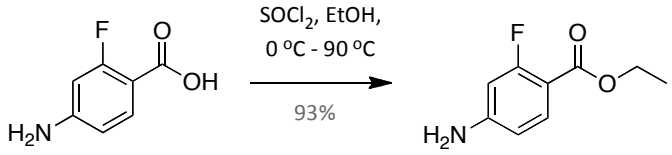

74 **75**

Scheme 5.9

The optimal conditions for the direct amide bond formation, discussed previously within this Chapter, were subsequently employed to generate 4-(2-chloro-acetylamino)-2-fluoro-benzoic acid ethyl ester, **76**, as an off-white solid, in a 64% yield (Scheme 5.10).

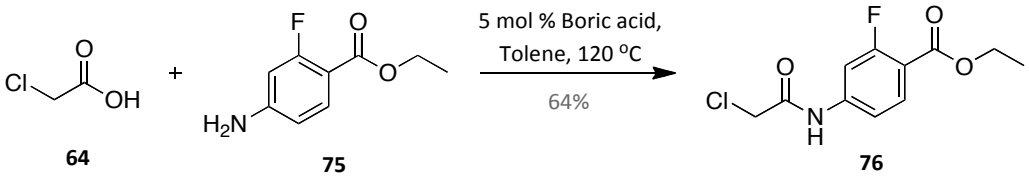

Scheme 5.10

An initial attempt at the formation of 2-fluoro-4-(2-phenyl-thiazol-4-ylamino)-benzoic acid ethyl ester, **77**, was attempted along side earlier thiazole formation reactions, as discussed previously. Initially, this was done under sub-optimal conditions leading to the formation of the highly coloured impurities, which in turn led to purification issues. Consequently, this compound has yet to be identified and characterised fully since a pure sample was never obtained. Following on from the synthesis of neuropathiazol, **60**, the crude compound was carried through, to generate the *N*-methyl derivative, **78**, as it was thought this might aid in purification. Unfortunately, this was not observed, and a single, pure, isolated sample of the fluorinated analogue, **78**, was never isolated. The reactions are summarised in Scheme 5.11.

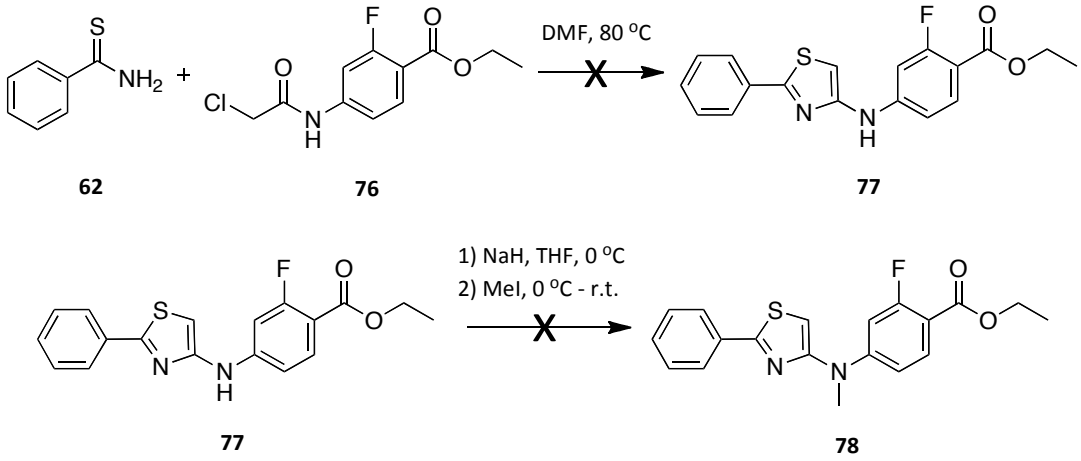

Scheme 5.11

Due to the volume of material available at the time, both reactions were undertaken on a small scale, therefore, would require repeating once more material was available, and once the thiazole formation step had been improved.

In addition to trying to generate the fluorine analogue, **78**, of neuropathiazol, **60**, an identical reaction was investigated using 5,5,8,8-tetramethyl-5,6,7,8-tetrahydro-naphthalene-2-carbothioic amide, **71**, as a substitute for thiobenzamide, **62** (Scheme 5.12). Again, the current best-known conditions were employed, which were identical to those used for synthesising neuropathiazol, **60**. As in all previous reactions attempting to form the thiazole, the reaction degraded into multiple components and products and successful isolation of the product was never achieved. Due to the higher costs and multiple steps involved in synthesising the components required for these two analogues, there was insufficient material available to carry onto the methylation step in an attempt to purify at the end.

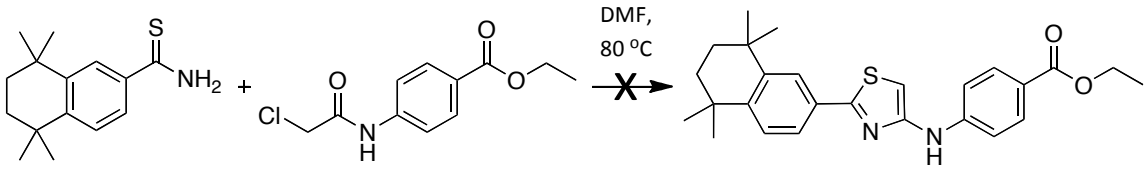

71 **61** **79**

Scheme 5.12

Consequently, since analogues were going to be required, it became apparent that the thiazol formation reaction required modifying, in order to avoid the formation of the highly coloured impurities and large losses of mass associated with this step. The coloured species are most likely *N*-oxide species, formed from the high temperatures of either the reaction, or work-up procedure involved in removing the DMF, although this is unproven. To try and avoid these by-products, the procedure was modified to remove the DMF through aqueous washes, other than under vacuum, while extracting the product into ether. This was followed by reducing the reaction time, which resulted in the reaction being worked-up before turning to a dark green/black colour. The DMF was again removed through aqueous washes, and the

product purified by flash SiO_2 column chromatography. This gave the product as a pale yellow solid, in approximately 25% yield, but as before, not 100% pure by ^1H NMR. The reaction had also not gone to completion, although there were less purification issues than before.

Although the modified work-up had some success, there was still the issue of the high temperatures employed in the reaction itself. At low temperatures, the reaction was not initiated, and at the higher temperatures required for the reaction to complete, highly coloured impurities were generated. In an attempt to increase the reaction rate, molecular sieves were used to remove the water generated, hoping to shift the equilibrium and drive the reaction forward. The temperature had to be kept lower, as once above 60-70 ^oC, the water molecules can move freely in and out of the molecular sieves, thus rendering them inactive. Unfortunately, at 50 ^0C there was no change in the reaction by TLC, while at 60 ^oC there was some product formation. Upon work-up, the DMF was successfully removed through the modified process of aqueous washing, leaving a dark red oil, which once purified by column chromatography, yielded the desired product, as a pale yellow solid, but in a very poor yield (<20%). As the compound was still not 100% pure by ^1H NMR and the yield was significantly lower, this method was abandoned.

The use of a mild base was next attempted, using pyridine (1 equivalent) added to the reaction mixture. Again the reaction was followed at a lower temperature of 50 ^oC, and again no product was observed. The reaction temperature was increased to 70 ^oC, but still reaction turn over by TLC appeared very slow.

As all attempts to form the thiazole in high yield, and in isolation, had proven unsuccessful an alternative approach was investigated. Both the literature, and our own work, had demonstrated the instability of the un-methylated nitrogen associated with all the intermediates, therefore methylation of the nitrogen before cyclisation was explored.[250]

Initially, this was attempted directly on to 4-(2-chloro-acetylamino)-benzoic acid ethyl ester, **61**, since large quantities had been prepared previously through direct amide bond formation. Initially, the reaction conditions employed were those used in the literature preparation of neuropathiazol, **60**.[250] The compound was treated with a large excess of methyl iodide and 5 equivalents of sodium hydride in dry THF at 0 ^{o}C (Scheme 5.13). This reaction was unsuccessful, with multiple compounds identified in the crude that did not separate by SiO_2 column chromatography. The reaction was subsequently repeated with one and two equivalents of sodium hydride, both with one equivalent of methyl iodide, but again, this proved unsuccessful due to too many competing side reactions.

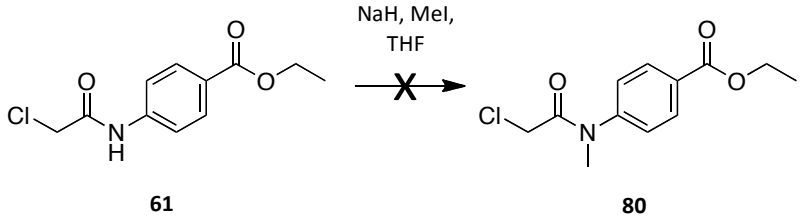

61 **80**

Scheme 5.13

As treatment of 4-(2-chloro-acetylamino)-benzoic acid ethyl ester, **61**, with NaH gave a mixture of compounds, methylation of the original starting material, benzocaine, **65**, was tried. One-pot reductive mono-*N*-alkylation of the aniline using the corresponding aldehyde was attempted. 2-Propanol was added to a flask containing 10 mol% Pd/C followed by the addition of ammonium formate (5 eqivalents) dissolved in water (Scheme 5.14). The mixture was stirred for approximately 1 minute to activate the Pd/C, followed by the addition of para-formaldehyde, and benzocaine, **65**. Regrettably, this again proved unsuccessful, with mostly starting material recovered.

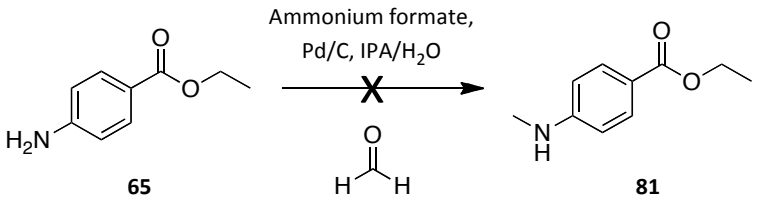

Scheme 5.13

Literature investigations suggested the free carboxylic acid would be more reactive,[345] thus identical conditions were attempted on 4-aminobenzoic acid, **82**. The reaction was left for 1 hour and after purification by column chromatography, the product, **83**, was identified as a white solid in a poor yield of 18%. In an attempt to improve the yield the reaction time was extended from 1 hour to 18 hours, which improved the yield to 30%. Increasing the number of equivalents of the aldehyde was subsequently investigated, but with little improvement seen as 10 equivalents only increased the yield to 33% (Scheme 5.14). As materials for the reaction were cheap and readily available, no further work was attempted to improve this step.

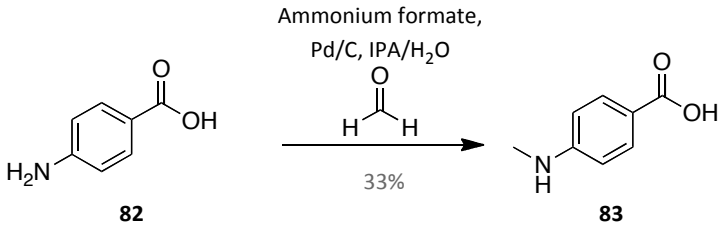

Scheme 5.14

The carboxylic acid, **83**, was then protected as the ethyl ester, using thionyl chloride in ethanol.[344] The product, **81**, was identified as an off-white solid in an excellent 97% yield (Scheme 5.15).

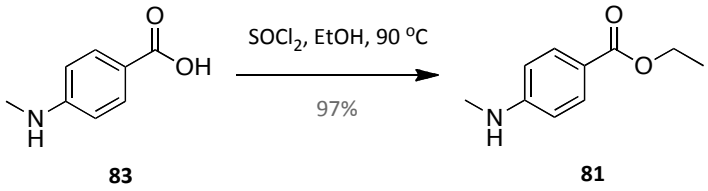

83 **81**

Scheme 5.15

The next step of the synthesis involved forming an amide bond on the nitrogen. Previously, direct amide bond formation had been employed using boric acid as the catalyst, which achieved a yield of 67%. The current synthesis was being carried out on a greatly reduced scale, thus a more efficient coupling was required to maintain a viable amount of material to investigate the important thiazol formation step. Use of the acid chloride was, therefore, chosen, since this was expected to give the highest yield. Although all the starting material was consumed by analysis using TLC, the product, **80**, was isolated in a poorer than expected yield of 55% (Scheme 5.16).

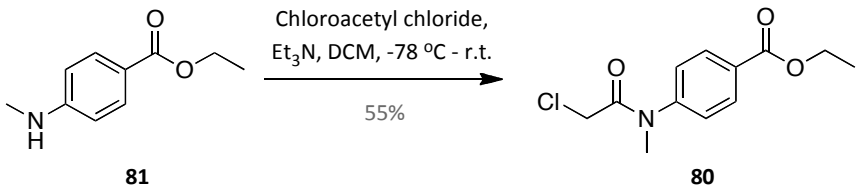

81 **80**

Scheme 5.16

With the *N*-methylated amide species now available, the final step of the new synthetic approach was attempted. Identical conditions for the ring closing thiazol step were employed as described earlier. Briefly, thiobenzamide, **62**, and 4-[2-chloro-acetyl)-methyl-amino]-benzoic acid ethyl ester, **80**, were heated in DMF overnight (Scheme 5.17). As the reaction would go directly to neuropathiazol, **60**, previously identified as a yellow solid, no coloured by-products were expected. Disappointingly, the reaction remained a mixture of mainly starting materials, a small amount of the desired product and one other compound, thought to be the open chain compound, **84**. Further heating for up to one week lead to no visible changes. Lack of material, and poor separation by SiO_2 column chromatography

would mean further work was required in this area to fully characterise this reaction. Early indications are that it also has a very poor turn over, with a very low percentage of the desired product being formed.

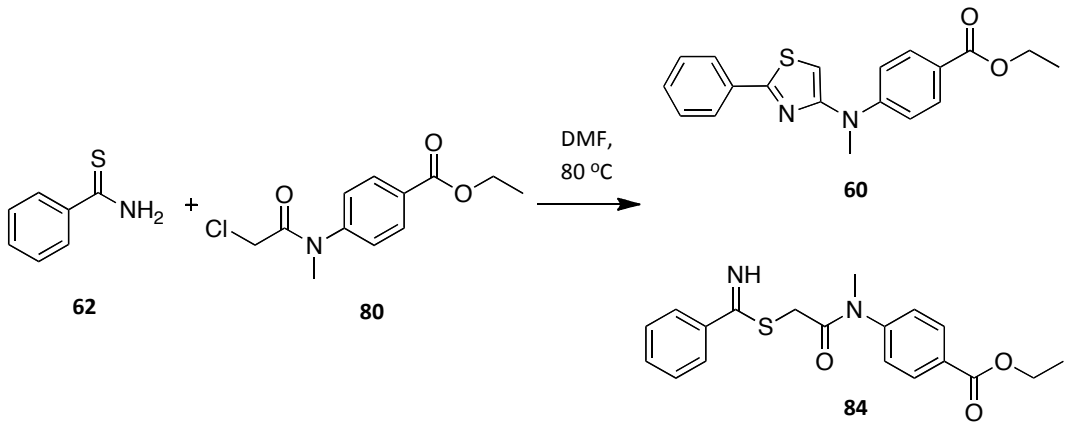

Scheme 5.17

From all the work carried out within this chapter, formation of the thiazole ring proved most challenging, and as of yet, has been relatively unsuccessful with poor yields and impure products obtained. Consequently, the only compound to be assessed biologically was neuropathiazol, **60**, as currently, no other analogues were successfully synthesised.

5.4 Biological Characterisation

5.4.1 Effect on Human EC Stem Cell Differentiation

Initially neuropathiazol was screened in the EC stem cell line, TERA2.cl.SP12 to assess whether it could induce differentiation of *pluripotent* stem cells. This line was chosen as it has been well characterised, and responds well to small molecules, including retinoid treatment (see Chapter I for full discussion). In addition, this would give us an early indication into the molecular pathway associated with neuropathiazol, as if it were to bind to the retinoid receptors and active them, we would see a clear response. This would allow us to confirm, or disprove, the theory stated in the current literature that neuropathiazol acts on a different pathway to ATRA.[250] Furthermore, the current literature on neuropathiazol compared it directly to ATRA, but only in a hippocampal model. We have demonstrated in the previous Chapter that the AHPC cell line is not that responsive to retinoids. Therefore to allow for a more complete comparison of neuropathiazol to ATRA, investigations in known models, which are highly responsive to retinoids, was required.[250]

Initially, protein expression was examined to monitor cell differentiation, performed using flow cytometry. Flow cytometry was chosen, as this would show any changes in the cell type. Cultures of TERA2.cl.SP12 cells were incubated for seven days with both ATRA and neuropathiazol from 10 μM to 0.001 μM. The concentration range chosen was based on prior knowledge gained from screening retinoids in this model. Phase micrograph images were recorded at day 7 prior to the cells being analysed by flow cytometry (Figure 5.4)

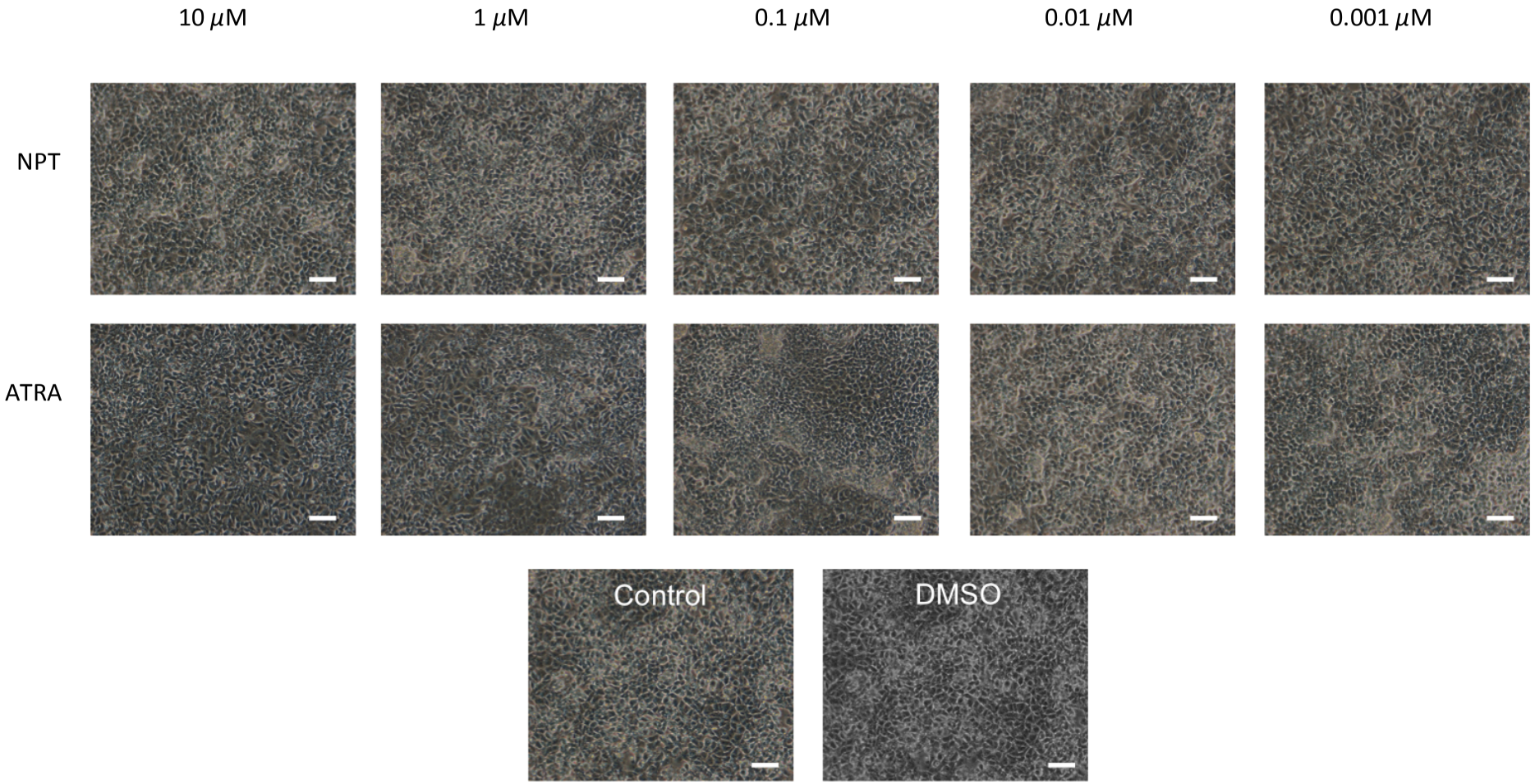

Figure 5.4 Morphologies of TERA2.cl.SP12 cells exposed to ATRA and neuropathiazol (NPT) at 10 μM, 1 μM, 0.1 μM, 0.01 μM and 0.001 μM for 7 days. All treatment of neuropathiazol display a cellular morphology identical to both the untreated control and that of the vehicle, DMSO. Those exposed to ATRA at 10 μM and 1 μM show early characteristic differentiated morphologies. Scale bar: 100 μm.

The phase images indicated that neuropathiazol, over the entire concentration range, had no effect, with the cells retaining a morphology similar to that of the proliferative undifferentiated control. To confirm this observation, flow cytometry was undertaken, investigating the expression levels of two stem cell antigens, SSEA-3 and TRA-1-60, to assess the loss of pluripotency, and A2B5, as a measure of differentiation towards a neural lineage.[206, 292, 293] The data is presented in Figure 5.5.

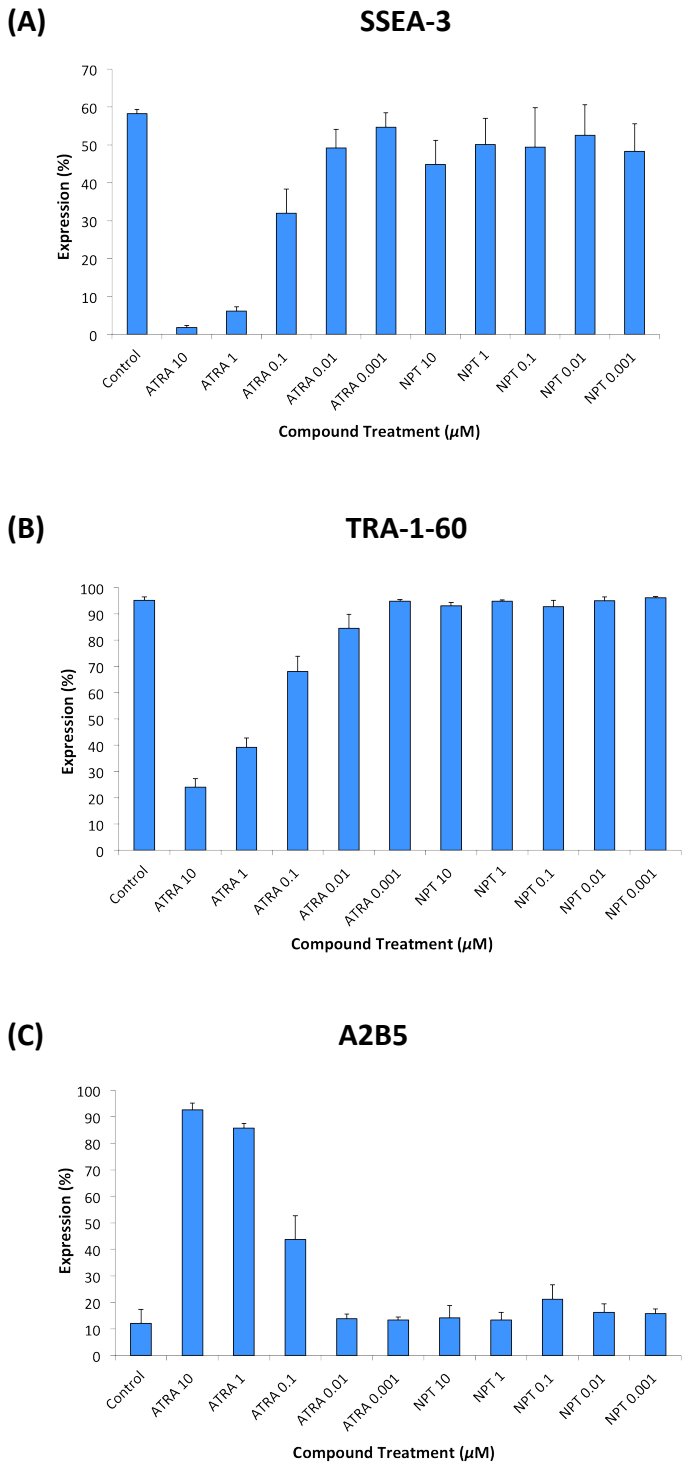

Figure 5.5 Flow cytometric analysis of markers of stem cells SSEA-3 (**A**) and TRA-1-60 (**B**), and a marker of early stage neural cells, A2B5 (**C**). TERA2.cl.SP12 cells were incubated with either ATRA or neuropathiazol (NPT) at 10 μM, 1 μM, 0.1 μM, 0.01 μM or 0.001 μM. Both stem cell markers remained high in all neuropathiazol treatments, while the neural marker remained low. Thus indicating neuropathiazol does not induce differentiation in this specific cell model system. ATRA exhibited its classical profile in this system. Results are presented with ± standard error (SDE), n=3. Per statistical analysis using the Student's t-test corrected for multiple testing of sample populations using the Bonferroni correction there were no significant differences.

The graphs clearly support the conclusion drawn from the phase images. Both stem cell markers, SSEA-3 and TRA-1-60, remain highly expressed in all neuropathiazol treatments. Additionally, A2B5 remains low, identical to the control cells. As expected, the positive control, ATRA, significantly reduced the expression of both stem cell markers, while dramatically up-regulating A2B5 expression at both 10 μM and 1 μM. From this data, it is apparent that neuropathiazol is unable to induce differentiation of pluripotent EC stem cells. Furthermore, it is therefore likely that neuropathiazol does not activate the retinoic acid signalling pathway, and associated retinoid receptors, as this is normally associated with differentiation in this cell line. For conformation of this hypothesis, molecular binding studies on the retinoid receptors would be required.

5.4.2 Effect on Human Embryonic Neural Stem Cells

In a follow on study, and in line with previous work carried out on the synthetic retinoids AH60 and AH61, neuropathiazol was screened for its ability to induce neurogenesis in the human fetal neural stem cell line, ReNcell VM. A concentration series of 1 μM, 0.1 μM, 0.01 μM and 0.001 μM was chosen in accordance with those previously used for screening the retinoids, as it was hypothesised that neuropathiazol would be tolerated over this range. ReNcell VM cell cultures were plated as described in the literature and in the previous Chapter, with neuropathiazol included at the time of growth factor removal.[59] After 7 days the cells were fixed and images of the cells are displayed in Figure 5.6.

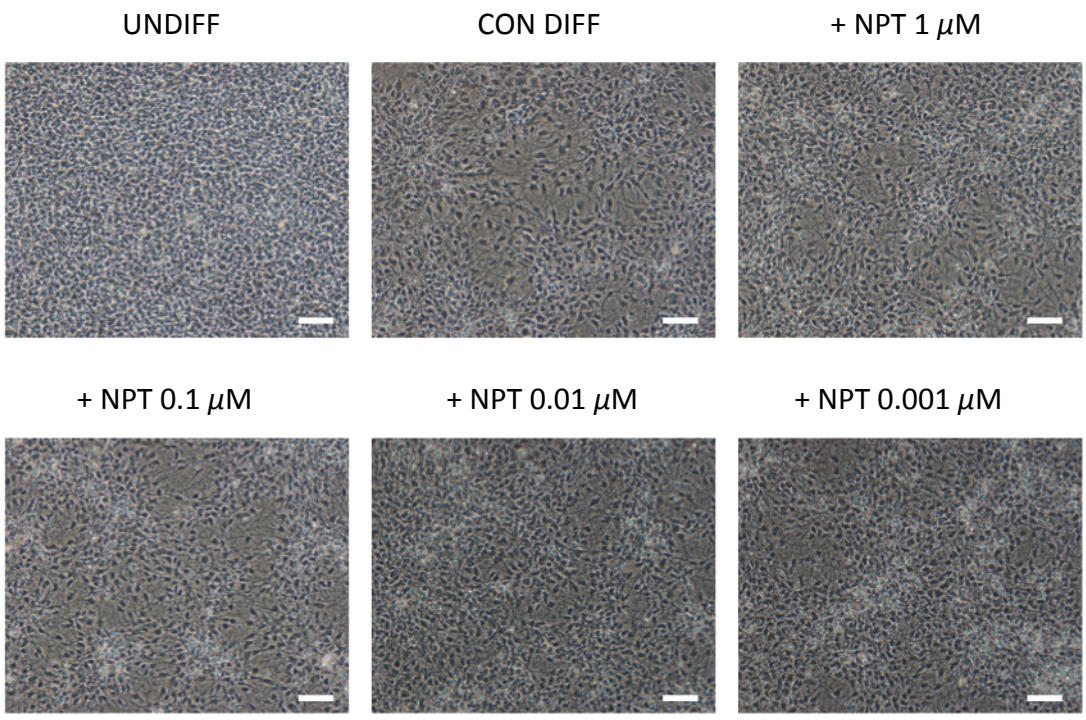

Figure 5.6 Morphologies of ReNcell VM cells after 7 days treatment. Undifferentiated cultures (UNDIFF) retained a homogeneous appearance with cells layering as they become over confluent and sub-optimal. Control differentiated cultures (CON DIFF), in which the growth factors, EGF and FGF were removed, showed areas of proliferative cells surrounded by more sparsely populated areas with numerous neural processes visible. Those treated with neuropathiazol (NPT) also display a highly analogous phenotype, suggesting no enhancement in differentiation. Scale Bars: 100 μm.

In addition, all treatments were stained for the neuronal markers β-III-tubulin, NF-200 and MAP2ab to assess the ability of neuropathiazol to induce neurogenesis. These markers were chosen, as they would allow for a direct comparison to the retinoids screened in Chapter IV. The screening of neuropathiazol in the literature, albeit in a different neural progenitor cell line, had displayed positive up-regulation of these and similar markers. The immunofluorescent micrographs for neuropathiazol, and undifferentiated and control differentiated samples, inlayed with their corresponding nuclear stained DAPI image, are displayed in Figure 5.7. In addition, a positive differentiation control of ATRA was attained (for representative images see Chapter IV).

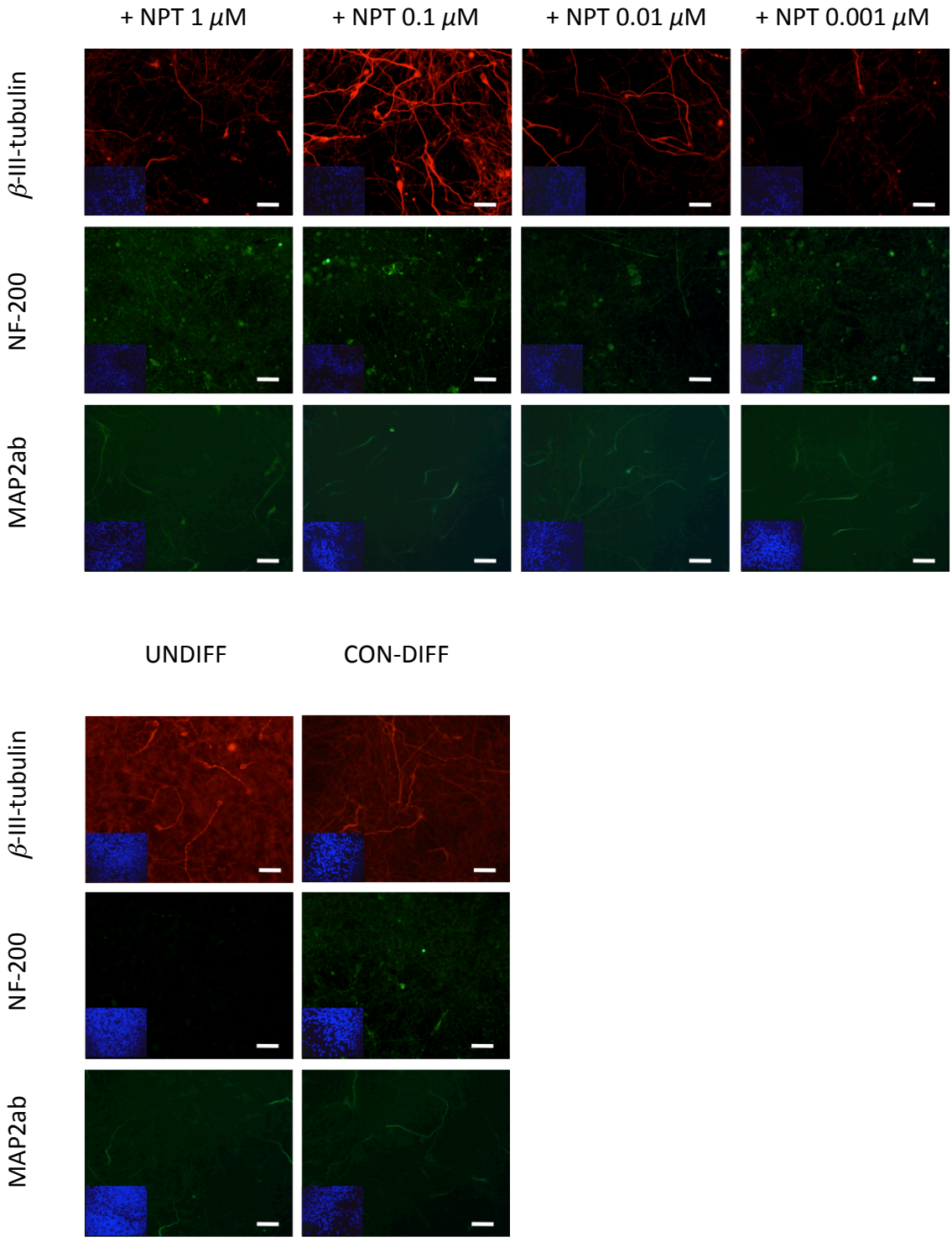

Figure 5.7 Cultures of ReNcell VM cells were induced to differentiate for 7 days under the standard differentiation protocol with the addition of neuropathiazol (NPT) at 1 μM, 0.1 μM, 0.01 μM or 0.001 μM. Immunological evaluation of β-III-tubulin, NF-200 and MAP2ab showed enhanced β-III-tubulin expression in 0.1 μM NPT treated cultures, but little increased expression in all other treatments compared to the undifferentiated (UNDIFF) and control differentiated (CON-DIFF) controls. Scale bar: 50 μm.

From previous data displayed within this thesis it is known that retinoid incorporation (particularly AH61) significantly up-regulates the expression of all three markers (see Chapter IV). Disappointingly, this up-regulation is not seen for neuropathiazol, in which most images display staining profiles characteristic to those of the undifferentiated controls. Upon quantification, again achieved through cell counts, there was clearly no increase in expression of the markers over the chosen concentration range (Figure 5.8). The only exception was that of β-III-tubulin expression at 0.1 μM, although this was not significant when compared to ATRA, it was compared to the control differentiated samples. This, therefore, suggests neuropathiazol does have an effect in this cell line, although it is not as apparent as that seen for some retinoid treatments, most notably AH61. Why this peaks at 0.1 μM and drops off at the higher concentration of 1 μM is unknown. The cells at 1 μM appeared normal under microscopic investigation with no signs of cell death, suggesting that at this concentration, it is inactive and not toxic.

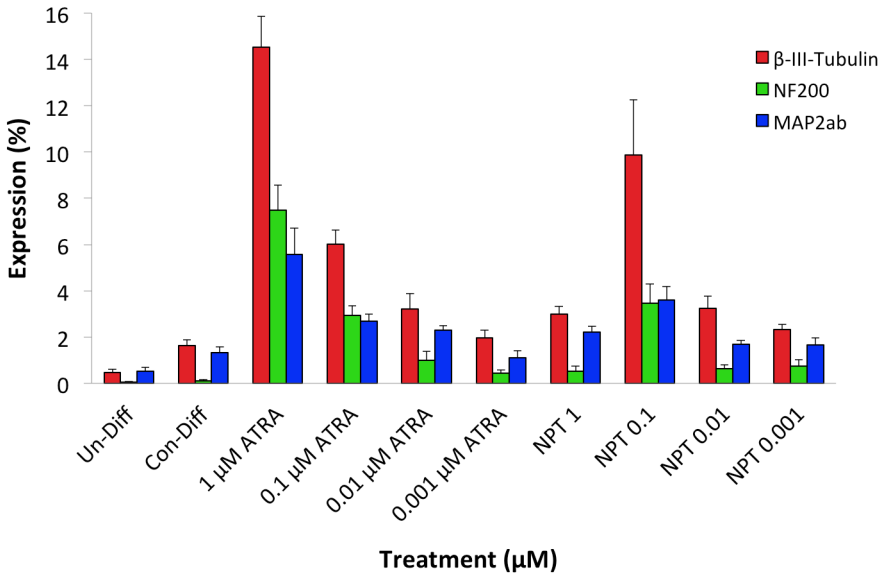

Figure 5.8 A graph displaying the quantification of immunological data as performed by counting positively labelled cells. The increased number of β-III-tubulin, NF-200 and MAP2ab positive cells in neuropathiazol supplemented cultures was not significant compared to control differentiated cultures (Con-Diff), with the exception of β-III-tubulin at 0.1 μM. Triplicate analysis was performed for reproducibility. Values shown represent mean + standard error (SDE), n=9. Per statistical analysis using the Student's t-test corrected for multiple testing of sample populations using the Bonferroni correction there were no significant differences.

From all the data collected, neuropathiazol appears to be inactive, or only slightly active, in the two stem cells models screened. Therefore, to validate that this molecule appears to be specific to a single cell line, its activity in the adult rat hippocampus was investigated.

5.4.3 Effect on Adult Rat Hippocampal Neural Progenitor Cells

Initially, identical experiments were undertaken as described in the literature.[250] Briefly, these involved assessing neuropathiazol's capability to induce selective neurogenesis utilising immunocytochemistry. AHPC cells were exposed to neuropathiazol at 10 μM for 4 days, fixed and stained for the neuronal marker β-III-tubulin and the glial marker GFAP. Both phase and immunological images are presented in Figure 5.9.

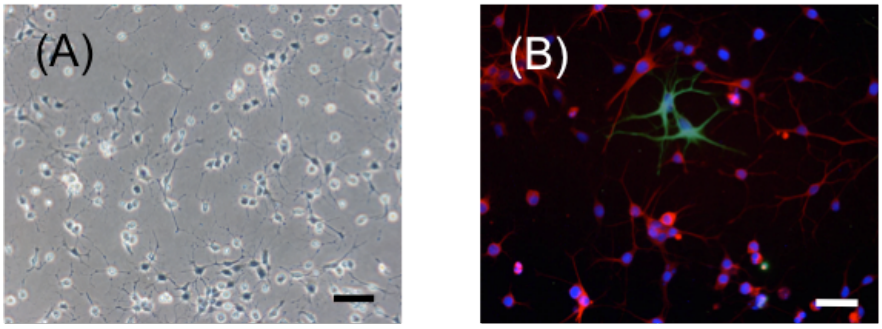

Figure 5.9 AHPC cells exposed for 4 days treatment with neuropathiazol at 10 μM. Phase images (**A**) show rounded cells with multiple outgrowths. Cells stained with markers of neurons (β-III-tubulin, red) and astrocytes (GFAP, green) display neuropathiazol specifically induces neuronal differentiation of AHPC cells (**B**). Scale bar: 100 μm (**A**). Scale bar: 50 μm (**B**).

AHPC cells exposed to neuropathiazol at 10 μM for 4 days exhibited a differentiated morphology, with multiple outgrowths on each cell. When stained for both neuronal and glial markers, consistent with the literature, nearly all the cells stained positive for β-III-tubulin. In comparison, positive staining for GFAP was rarely seen, with many areas not displaying this cell type (image shown above chosen for representation of both cell types).

When the cells were cultured for 7 days, they also stained positive for later stage neurons, including NF-200 (Figure 5.10). From prior investigations, it was known that ATRA is toxic at 10 μM, therefore, cannot be directly compared to neuropathiazol. Therefore, to compare both compounds as accurately as possible, the highest tolerated concentration of ATRA was employed, suggested from the literature as 2 μM. Consistent with data presented in Chapter IV, ATRA displayed a pleotropic profile leading to the expression of both glial and neuronal markers. It was also less effective at inducing the positive expression of later stage neuronal markers, such as NF-200, than neuropathiazol (Figure 5.10).

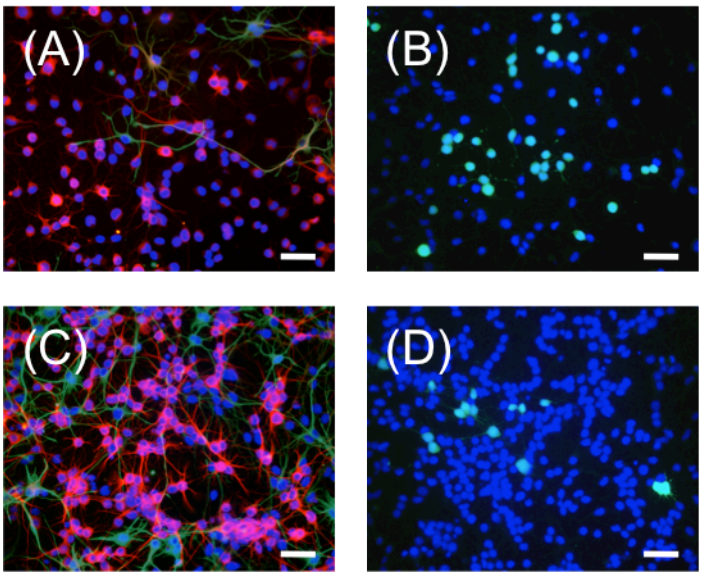

Figure 5.10 AHPC cells exposed for 7 days treatment with neuropathiazol at 10 μM and ATRA at 5 μM. Cells stained with markers of neurons (β-III-tubulin, red) and astrocytes (GFAP, green) display neuropathiazol specifically induces neuronal differentiation of AHPC cells (**A**), whereas ATRA is pleotropic (**C**). Mature neurons were observed with NF-200 (green) (**B**) upon neuropathiazol treatment, but less so with ATRA (**D**). Scale bar: 50 μm.

The data presented above supports that presented in the current literature, confirming the hypothesis that neuropathiazol is a more selective and potent inducer of neurogenesis than ATRA.[250] Preliminary cell counts to quantify TuJ1 expression *versus* GFAP expression further supports the values quoted in the literature, that neuropathiazol differentiates 90% of AHPCs into TuJ1 positive cells (Figure 5.11).

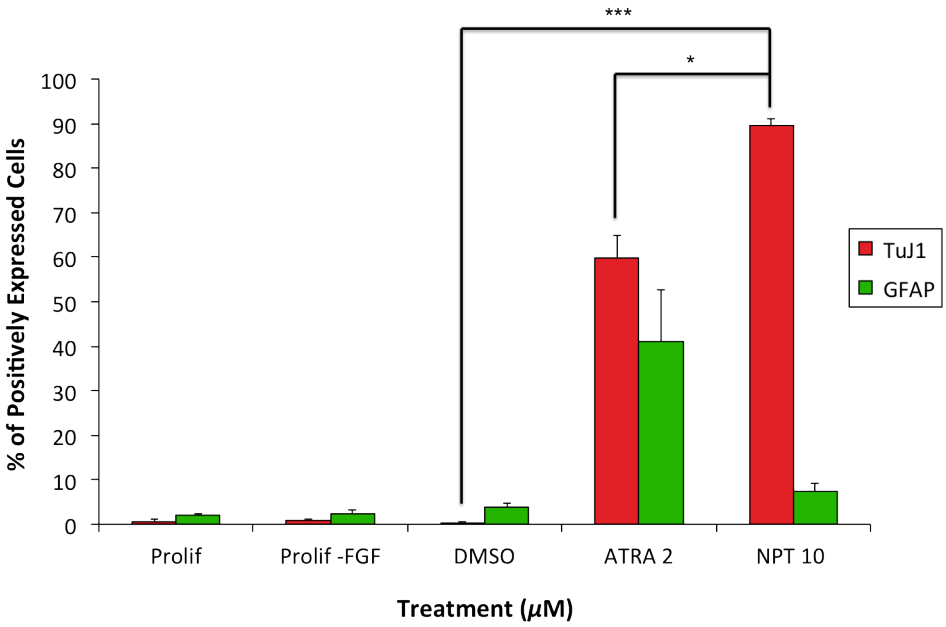

Figure 5.11 Plot displaying the quantification of the percentage expression of TuJ1 and GFAP, as performed by counting labelled cell bodies. Cultures of AHPCs incubated with 10 μM neuropathiazol (NPT) or 2 μM ATRA, for 7 days, subsequently fixed and immunocytochemically stained. Using ImageJ software the number of positive cell bodies were counted on 3 random fields per treatment condition. 10 μM treatment of neuropathiazol induced a significant increase in the percentage expression of TuJ1 labelled cells, over both ATRA and DMSO. Values shown represent mean + standard error (SDE), n=3. *p≤0.05, ***p≤0.0005, Student's t-test corrected for multiple testing of sample populations using the Bonferroni correction.

The literature, however, did not assess whether neuropathiazol retained its potency over a wider concentration range.[250] Thus, in an extension to the literature work, AHPC cells were cultured for 7 days with neuropathiazol at 1 μM, 0.1 μM and 0.01 μM (Figure 5.12).

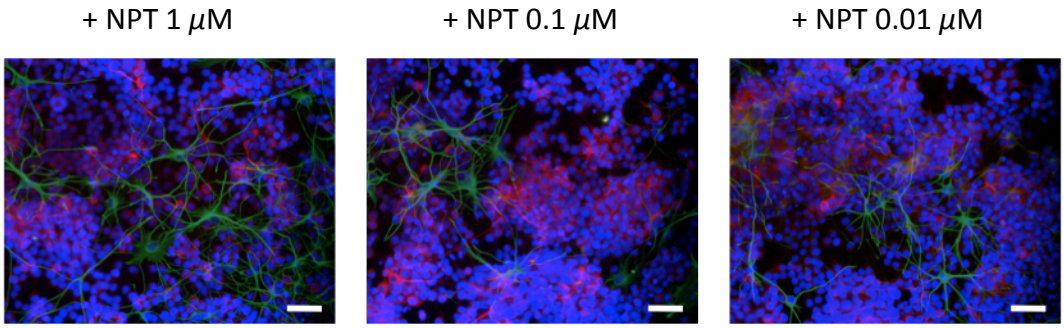

Figure 5.8 AHPC cells exposed for 7 days treatment with neuropathiazol at 1 μM, 0.1 μM and 0.01 μM. Cells stained with markers of neurons (β-III-tubulin, red) and astrocytes (GFAP, green) display neuropathiazol (NPT) is inactive at these concentrations. Scale bar: 50 μm.

When the concentration of neuropathiazol was lowered, inline with that used in the screening of the retinoids, its profile changed significantly. Over the entire concentration range there was no change in morphology from those treated with only the vehicle, DMSO (for comparison see Chapter IV). Neuronal markers were no longer expressed, while the percentage expressing GFAP had increased, consistent with the spontaneous differentiation of neural stem cells upon growth factor withdrawal.[346] These results suggested neuropathiazol was not active below 10 μM, therefore, future screening should take place at 10 μM or higher, once a viability assay has been employed to determine at what concentration neuropathiazol becomes toxic.

5.5 Discussion

In terms of synthesis, there are a number of other potential synthetic routes, which have yet to be completed and fully examined. These have the potential to produce a number of analogues related to neuropathiazol, which would be interesting to screen.

One such solution would be to attempt to synthesise the ring at the start of the synthesis, or start with the thiazol ring and substitute around it. One prospective route would be to start with 4-hydroxy-2-phenyl-1,3-thiazol, **85**, a commercially available compound, and convert this to the corresponding chloride, **86**, through treatment with pyridinium hydrochloride, phosphoric acid and phosphorus oxychloride (Scheme 5.18).[347]

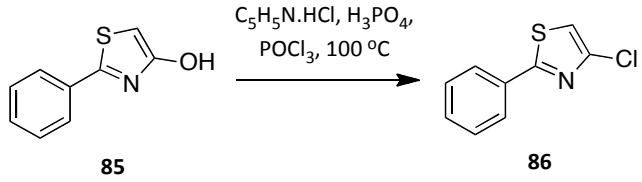

85 **86**

Scheme 5.18

Alternatively, to allow for more variation, there is literature reporting the formation of thiazols from reacting substituted thiobenzamides, **87**, with 1,3-dichloroacetone, **88**, to form chloromethyl thiazoles, **89** (Scheme 5.19).[348] This reaction has the potential to work on other thio-amides such as thiobenzamide or the TMTN thio-amide compound.

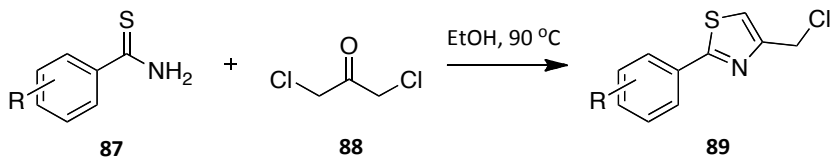

87 **88** **89**

Scheme 5.19

The above series of compounds would be one carbon in size larger, therefore to generate the corresponding TMTN analogue of the 2-phenyl-4-chlorothiazole **86**, substituting 1,3-dichloroacetone, **88**, in the above reaction for chloroacetyl chloride, **90**, may be one solution (Scheme 5.20).

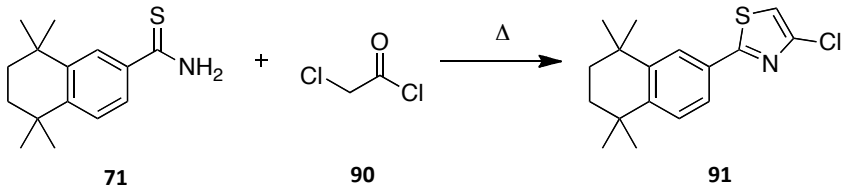

71 **90** **91**

Scheme 5.20

Alternatively, if the direct route described above proved unsuccessful there is literature describing the successful synthesis of 4-*t*-butyldimethylsilyloxy thiazoles, **92** (Scheme 5.21), which potentially could then be deprotected to the alcohol followed by conversion to the chloride.[349] This route has the potential to be transcribed onto the TMTN thioamide substrate, again providing a simple route to 4-chloro-2-[1,1,4,4-tetramethyl-1,2,3,4-tetrahydronaphthalene]-1,3-thiazol, **91**.

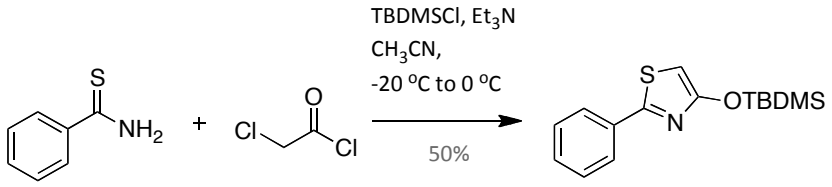

62 **90** **92**

Scheme 5.21

With these compounds in hand, coupling to 4-methylamino-benzoic acid ethyl ester, **81**, would give neuropathiazol, **60**. Alternatively, this could also couple to the TMTN analogue, **91**, shown in scheme 5.20, generating the desired TMTN analogue of neuropathiazol, **93** (Scheme 5.22).

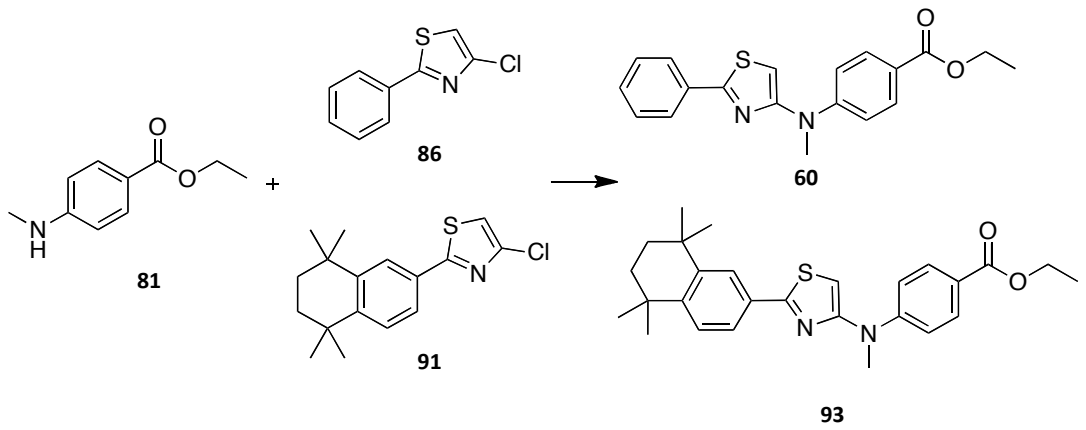

Scheme 5.22

Adaption of the synthesis involving the fluorine atom, by initially methylating on the nitrogen, would then allow for those analogues also to be accessed. Similarly, other linker groups could potentially be investigated, including oxygen, and sulphur as these starting materials are easily accessible and readily available.

Future work on the screening initially needs to fully quantify the data presented on neuropathiazol, which should ideally support that presented in the literature.[250] Currently, only a concentration of 10 μM has been screened (15 μM was presented in the literature[250]), therefore, a viability assay should also be employed to see at what concentration neuropathiazol becomes toxic, and if higher more potent concentrations can be found and exploited. In addition, rescreening neuropathiazol in the ReNcell VM cell line at a higher concentration may be beneficial, as this compound appeared to behave biologically appreciably different to that of the retinoids. Current data suggests it is considerably less toxic than the retinoid compounds, and therefore, would be tolerated at higher and potentially active concentrations.

Since this work has been carried out, the same group to publish the neuropathiazol work have subsequently published further studies.[350] In this report they describe the synthesis of KHS101, **94** (Figure 5.9), afforded from an improved SAR study of neuropathiazol. They have further characterised the molecule stating it has

increased activity and improved pharmacokinetic properties, compared to that of neuropathiazol. It displays increased neuronal differentiation properties of adult rat hippocampal neural progenitor cells, as assessed through RT-PCR for NeuroD, a neurogenic transcription factor, and immunostaining for TuJ1. Similar to neuropathiazol, it appears to be able to inhibit astrocyte-inducing signalling pathways in favour of neuronal differentiation. Additional mechanistic studies showed that KHS101 was linked to cell cycle exit and specific binding to the TACC3 protein, thus suggesting KHS101 mediated interference with TACC3 accelerates neurogenesis through negative regulation of the cell cycle. Currently, a complete understanding of TACC3 and its downstream mechanisms are unknown, yet literature does suggest it plays a crucial role in progenitor cell maintenance.[351-355] Finally, they undertook an *in vivo* study in which they show KHS101 to distribute favourably to the brain, increase neuronal differentiation, while not observing any signs of weight loss, lethargy or other sicknesses.[350]

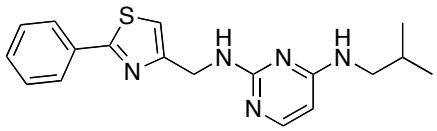

94

Figure 5.9 Structure of KHS101.

In addition to increased biological activities, the synthesis of KHS101 does not involve a thiazole ring forming step, as one of the starting materials ((2-phenyl-1,3-thiazol-4-yl)methyl amine, **96**) already has the ring preformed. Consequently, the two step synthesis of KHS101 (summarised in Scheme 5.23) is high yielding, with an overall yield of 83%. This therefore makes KHS101 a much more promising compound for controlling AHPC differentiation than neuropathiazol, and consequently any future work should concentrate around this new compound.[350]

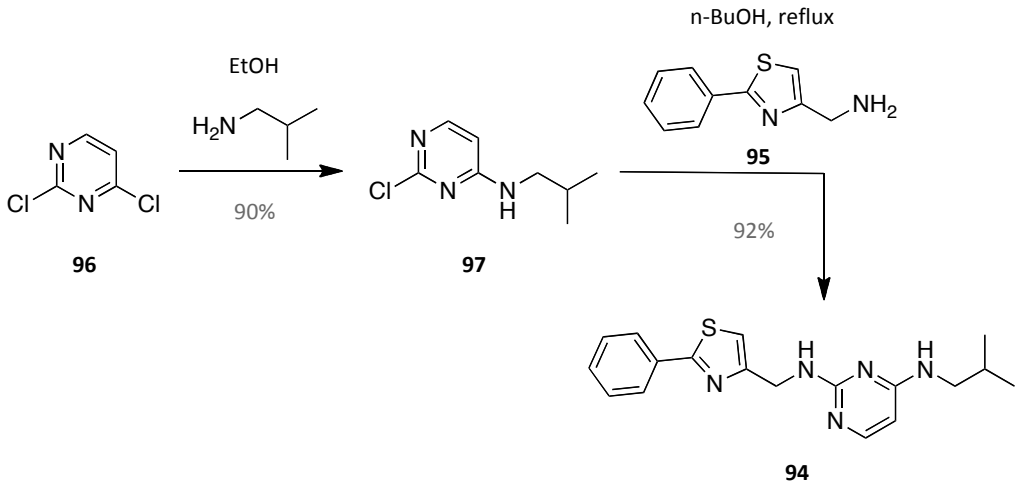

Scheme 5.23 Synthetic Route to KHS101.[350]

Overall this Chapter highlights that small molecules, such as neuropathiazol and KHS101, isolated from chemical library screens, can be powerful tools in modulating NPCs both *in vitro* and *in vivo*. Furthermore, a number of other small molecules have been described in the literature as having the ability to control both the differentiation and self-renewal of stem/progenitor cells.[247, 250, 350, 356-360] These advances are exciting, as the prospects of complete chemical defined control of stems cells, and their derivatives, draws ever closer.

5.6 Conclusions

The first conclusion that can be drawn is that the published synthetic route to neuropathiazol is highly inefficient and challenging. Although we have made considerable advances in optimising this synthetic strategy, it remains unlikely that this approach will be viable, especially in terms of analogue synthesis.

From the preliminary biological characterisation undertaken, neuropathiazol appears to act as described in the literature. This is very interesting, considering no other small molecules have been identified with such specific neural inducing activities. Although, in light of the discovery of KHS101, further work in this field should be invested around this new class of compound, and not that of neuropathiazol. The synthesis of KHS101 also does not involve the problematic thiazole ring-forming step, as it is present in the starting material, similar to some of the proposed new strategies for neuropathiazol in the discussion.

In summary, novel small molecules identified from large library screens, have the potential to be hugely valuable in the stem cell field. Current known pathways, such as the retinoid signalling pathway, are significantly useful for expanding our knowledge, although it is now clear that there are numerous other factors and many undiscovered small molecules which may help unlock the overall picture. Precise control of native adult stem cells opens the potential of orally delivered small molecules as potential regenerative therapies.[361] In addition, there has been literature describing how cancer cells have stem cell-like properties, sharing similar self-renewal mechanisms. A better understanding of stem cell biology may therefore, in turn, help to develop new and improved cancer therapies.[362]

Chapter VI

Conclusions and Future Work

6.1 Concluding Remarks

The work within this thesis has highlighted two new synthetic retinoids, which have the potential to be highly useful to both cell and molecular biologists. Both, AH60 and AH61, have been established as being more resistant to UV induced isomerisation, compared to ATRA. Furthermore, both compounds do not show any signs of degradation upon long term exposure to UV light, with initial metabolic studies also suggesting they are not metabolised *in vitro*. These findings support a common theory seen throughout the literature, that more stable analogues of ATRA are required to further probe the retinoic acid signalling pathway.

Upon biological screening, a clear SAR was highlighted, as none of the 'short' synthetic analogues synthesised (AH36, AH62 and AH66) were biologically active, while the 'extended' analogue (AH98), was only partially active. This suggests that the overall size of the linker region is critical in conferring biological activity, as a small reduction in size leads to a complete loss of biological activity. Conformation at the terminal bond was additionally highlighted as an important factor, as AH60 is approximately 10-fold less potent than AH61, in two of the models screened in this work. This supports previous work carried out in Durham on EC19 and EC23, that small changes in molecular shape have large effects on the biological roles of the compounds.

Additionally, the synthetic retinoids AH60 and AH61 were shown to be active in a number of different model systems, including in particular *pluripotent* EC stem cells and *multipotent* neural stem cells. Although, the increased activity seen for both AH60 and AH61 in the cells lines mentioned above, was not seen in the adult hippocampal neural progenitor cell line. Currently, the exact reasons behind this are unknown, but as stem cell differentiation is regulated by a wide number of signalling pathways, and small molecules, this cannot be unexpected. These findings may indeed highlight differences between embryonic neural stem cells and adult neural

progenitors in their developmental potency, and the role played by the retinoic acid signalling pathway, in lineage development.

Overall, AH61 has been shown to be a highly active synthetic retinoid, compare to that of ATRA. Its increased activity also allows for it to be administered at significantly lower concentrations, thereby avoiding toxic levels associated with ATRA. Furthermore, early indication is that the compound is less toxic than ATRA, and synthetic retinoid EC23, thus potentially making it a viable substitute for therapeutic applications associated with ATRA, but currently limited by ATRA's high toxicity. Future work will undoubtedly expand on the current preliminary biological characterisation of this compound, although early screens highlight AH61 as the current best alternative to ATRA for *in vitro* studies in these systems.

In addition to screening novel retinoids an un-related small molecule, neuropathiazol, was highlighted from the literature as a promising and exciting target. Consequently, the synthesis of neuropathiazol was carried out, in an attempt to improve the current synthetic route, and characterisation. This was followed by a more comprehensive biological screen, in three different cell lines, to further characterise the biological profile of the compound in more detail. This highlighted that neuropathiazol most likely did not act on the retinoic acid signalling pathway, but elicited its activity through another currently an unknown pathway/mechanism. Moreover, the data presented in the literature, that neuropathiazol is a more potent inducer of neurogenesis in AHPCs than ATRA, was confirmed. Although, currently the activity elicited by neuropathiazol, appears to be limited to only this model. As more potent analogues have since been synthesised and highlighted in the literature, further clarification and optimisation of neuropathiazol was abandoned, with any future studies needing to be carried out on KHS101, a more active analogue of neuropathiazol.

6.2 Future Work

- Full quantification of AH60 and AH61 in the TERA2.cl.SP12 cell line needs to be completed. This mainly consists of quantifying the total amount of protein expressed in 21 day induced cell cultures. Preliminary cell counts have been undertaken, but more accurate quantification is required, such as a Western Blot.

- Molecular binding studies also need to be carried out to compare the affinities of AH61 and EC23 to that of ATRA. This would then confirm the hypothesis that AH61's increased potency over EC23 is as a result of higher receptor binding affinities.

- Analysis in ES cells is also required to further confirm the ability of these compounds to induce neuronal differentiation from *pluripotent* stem cell systems.

- Current work being carried out in Durham by D. Tams includes assessing synthetic retinoids, EC23 and AH61, to induce neurogenesis and neuritogenesis from differentiated suspension aggregates of human pluripotent stem cells. This model of neuritogenesis is planned to assess the role of a number of known modulators of axon guidance and to investigate the mechanism by which the use of these retinoids enhances both neural stem cell commitment and neurite outgrowth.

- Finally *in vivo* studies are required to assess the toxicity of the compounds, in addition to probing known roles associated with ATRA. These include neuronal remodelling in the hippocampus, and proliferation and differentiation of keratinocytes, as assessed in mouse (currently being tested by B. Pulman, Durham University). If proven successful futher therapeutic applications should be considered, such as screening for activity against APL.

Chapter VII

Experimental

7.1 Chemical Procedures

7.1.1 General Procedures

All reactions were performed under air unless specified otherwise. All cross-coupling reactions were carried out under argon, using standard Schlenk techniques in oven dried glassware (130 ^{o}C) cooled under a positive pressure of argon. Degassing was carried out by a freeze-pump-thaw procedure (3 cycles).

7.1.2 Reagents

All reagents were purchased from Aldrich, Acros, Alfa Aesar, Lancaster, Fluorochem and Maybridge and used without further purification unless otherwise stated. Dry solvents were dried by the use of a commercial solvent purification system (SPS). Petroleum ether (40:60) refers to the fraction of petroleum ether that boils between 40 and 60 ^{o}C. Where mixtures of solvents have been used for chromatography, the ratios given refer to volumes used.

7.1.3 Chromatography

Thin layer chromatography (TLC) was performed on Polygram SIL G/UV254 plastic backed silica gel plates. Visualisation was achieved using a UV lamp at 254 nm, or staining with basic potassium permanganate. Column chromatography was carried out under medium pressure utilising compressed air on silica gel, 40-60 μ 60 Å obtained from Alfa Aesar.

7.1.4 Analytical Techniques

EI-MS analyses were performed on an Agilent 6890N GC equipped with a 5973N MSD Performance Turbo CI running an EI mode, and an Anatune Focus Autosampler/liquid handler, using UHP helium as the carrier gas. ES-MS analyses were performed on a Thermo-

Electron Corp. Finnigan LTQ-FT mass spectrometer, using the electrospray in positive ion mode (ES+) to generate ions.

Elemental analyses were obtained using an Exeter Analytical CE-440 analyser.

All ^{1}H NMR spectra were analysed in $CDCl_3$, unless otherwise stated, at 400, 500 or 700 MHz on Varian Mercury-400, Varian Inova-500 or Varian VNMRS 700 MHz spectrometers respectively. Spectra are reported as chemical shift δ (ppm) (number of protons, multiplicity, coupling constant *J* (Hz), assignment). All peaks are reported using the residual protic solvent peak of $CHCl_3$ (δ_H = 7.26 ppm), as an internal reference. ^{13}C NMR spectra were analysed in $CDCl_3$ at either 126, or 176 MHz on Varian Inova-500, or Varian VNMRS 700 MHz spectrometers respectively. All peaks reported using the residual protic solvent peak of $CHCl_3$ (δ_C = 77.00 ppm) as an internal reference. ^{11}B NMR spectra were recorded at 128 MHz on a Bruker Avance-400 spectrometer as parts per million downfield shift from external $BF_3.OEt_2$. ^{19}F NMR spectra were recorded at 376 MHz a Bruker Avance-400 spectrometer.

IR spectra were recorded on a Perkin-Elmer Paragon 1000 FT-IR Spectrometer.

Melting points were obtained on a Gallenkamp Variable Heater melting point apparatus.

7.1.5 Typical Procedure for Sonogashira Coupling

To a dried Schlenk flask under a positive pressure of argon was added alkyliodide (1 equivalent), alkyne core (1.1 equivalents) and triethylamine. The mixture was degassed using the freeze-pump-thaw method (×3), followed by addition of palladium(II) acetate (2.5 mol %), triphenylphosphine (5 mol %) and copper(I) iodide (5 mol %). The Schlenk flask was then evaporated and purged with argon (×3) and stirred at room temperature under argon. After 5.5 hours, the mixture was diluted with diethyl ether, passed through Celite™, washed with 5% hydrochloric acid, brine, dried ($MgSO_4$), concentrated and purified by silica gel chromatography (ethyl acetate: petroleum ether, 5:95).

7.1.6 Typical Procedure for Heck-Mizoroki Coupling

To a dried Schlenk tube under a positive pressure of argon was added silver(I) acetate (1.1 equivalents), palladium(II) acetate (5 mol %), tri(*o*-tolyl)phosphine (10 mol %), and dry acetonitrile. The mixture was degassed using the freeze-pump-thaw method (×2), followed by the addition of iodoacrylate (1 equivalent) and vinylboronate (1.15 equivalents). The mixture was degassed using the freeze-pump-thaw method (×2) and heated to 50 °C with vigorous stirring. After 24 hours the mixture was cooled, diluted with diethyl ether and passed through Celite™, washed with 5% hydrochloric acid, water, brine, dried ($MgSO_4$) and purified by silica gel chromatography (ethyl acetate: petroleum ether, 1:9).

7.1.7 Typical Procedure for Saponification of Methyl Esters

The corresponding ester (1 equivalent), was dissolved in a tetrahydrofuran water mixture (3:1, 20 mL) followed by the addition of $LiOH.H_2O$ (4 equivalents). The mixture was stirred at room temperature for 48 hours in the absence of light after which, the reaction was judged to be complete by TLC. The mixture was then acidified to pH 1 by the addition of hydrochloric acid (20%), and extracted with diethyl ether (×2). The sample was concentrated under vacuum to give the crude product, followed by re-crystallisation from acetonitrile.

7.1.8 Specific Experimental Procedures

(*E*)-5-(5,5,8,8-Tetramethyl-5,6,7,8-tetrahydro-naphthalene-2-yl)-penta-2-en-4-ynoic acid **1**

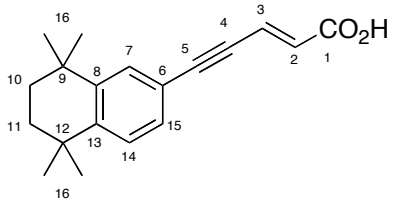

(*E*)-5-(5,5,8,8-Tetramethyl-5,6,7,8-tetrahydro-naphthalen-2-yl)-penta-2-en-4-ynoic acid methyl ester (42 mg, 0.14 mmol) was dissolved in tetrahydrofuran and water (1:1, 2.5 mL), followed by the addition of lithium hydroxide (6 mg, 0.14 mmol) and stirred at room

temperature. After 18 hours the reaction was acidified to pH 1-2 by the addition of 20% hydrochloric acid, and extracted with ether (2 × 20 mL), dried ($MgSO_4$), concentrated and purified by silica gel chromatography (ethyl acetate: petroleum ether, gradient elution). The product was extracted as a pale yellow oil, which slowly solidified and was re-crystallised from petroleum ether to give (*E*)-5-(5,5,8,8-tetramethyl-5,6,7,8-tetrahydro-naphthalene-2-yl)-penta-2-en-4-ynoic acid (34 mg, 85%) as a white crystalline solid; m.p 199.6-200.1 °C; ν_{max}/cm^{-1} 2954 (br OH), 2198 (alkyne), 1682 (C=O), 1615 (C=C), 1418 (Sp^3 C-H), 1297, 1272, 1207, 1107 and 1037; ^{1}H NMR**:** 400 MHz, $CDCl_3$: δ_H 1.29 (6H, s, 2 × Me), 1.30 (6H, s, 2 × Me), 1.70 (4H, s, 2 × CH_2), 6.31 (1H, d, *J* 16.0, H_2), 7.10 (1H, d, *J* 16.0, H_3), 7.2 (1H, dd, *J* 8.0 and 1.5, H_{15}), 7.31 (1H, d, *J* 8.0, H_{14}), 7.46 (1H, d, *J* 1.5 H_7); ^{13}C NMR (176 MHz, $CDCl_3$) δ_C 31.9 (C_{16}), 32.0 (C_{16}), 34.5 ($C_{9/12}$), 34.7 ($C_{9/12}$), 35.0 ($C_{10/11}$), 35.1 ($C_{10/11}$), 85.7 (C_4), 101.3 (C_5), 119.1 (C_6), 127.1 (C_3), 128.3 (C_2), 128.5 (C_{14}), 129.3 (C_{15}), 130.8 (C_7), 145.6 (C_8), 147.4 (C_{13}), 170.8 (C_1); *m/z* (ES) 281.1545 (M^-, $C_{19}H_{22}O_2$, requires 281.1547), 159 and 91; Anal. Calcd. for $C_{19}H_{22}O_2$: C, 80.82; H, 7.85. Found: C, 80.54; H, 7.75.

(*Z*)-5-(5,5,8,8-Tetramethyl-5,6,7,8-tetrahydro-naphthalene-2-yl)-penta-2-en-4-ynoic acid **2**

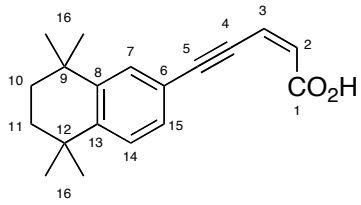

(*Z*)-5-(5,5,8,8-Tetramethyl-5,6,7,8-tetrahydro-naphthalen-2-yl)-penta-2-en-4-ynoic acid methyl ester (115 mg, 0.39 mmol) was dissolved in THF:H_2O (1:1, 5 mL), followed by the addition of lithium hydroxide (16 mg, 0.39 mmol) and stirred at room temperature. After 42 hours the reaction was acidified to pH 1-2 by the addition of 20% hydrochloric acid, and extracted with diethyl ether (2 × 20 mL), dried ($MgSO_4$), concentrated and purified by silica gel chromatography (ethyl acetate: petroleum ether, gradient elution). The product was extracted as a pale yellow oil, which slowly solidified and was re-crystallised from petroleum ether to give (*Z*)-5-(5,5,8,8-tetramethyl-5,6,7,8-tetrahydro-naphthalene-2-yl)-penta-2-en-4-ynoic acid as an off-white solid (93 mg, 85%); m.p. 132.1-133.7 °C; ν_{max}/cm^{-1} 2956 (br OH), 2197 (alkyne), 1692 (C=O), 1587 (C=C), 1490, 1466, 1442, 2152, 1182, and 1106; ^{1}H NMR

(500 MHz, $CDCl_3$) δ_H 1.26 (6H, s, 2 × Me), 1.27 (6H, s, 2 × Me), 1.67 (4H, s, 2 × CH_2), 6.16 (1H, d, *J* 11.5, H_2), 6.49 (1H, d, *J* 11.5, H_3), 7.27 (2H, d, *J* 1.0, $H_{14\ and\ 15}$), 7.46 (1H, s, H_7); ^{13}C NMR (176 MHz, $CDCl_3$) δ_C 29.9 (C_{16}), 31.9 (C_{16}), 31.9 (C_{16}), 34.4 ($C_{9/12}$), 34.7 ($C_{9/12}$), 35.0 ($C_{10/11}$), 35.1 ($C_{10/11}$), 85.5 (C_4), 104.5 (C_5), 119.4 (C_6), 125.4 (C_3), 127.0 (C_2), 127.1 (C_{14}), 129.4 (C_{15}), 130.8 (C_7), 145.5 (C_8), 147.3 (C_{13}), 168.8 (C_1); *m/z* (ES) 281.1545 (M^-, $C_{19}H_{22}O_2$, requires 281.1547), 260, 159 and 91; Anal. Calcd. for $C_{19}H_{22}O_2$: C, 80.82; H, 7.85. Found: C, 80.49; H, 7.84.

6-Iodo-1,1,4,4-tetramethyl-1,2,3,4-tetrahydronaphthalene **8**

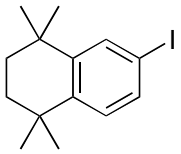

To a mixture of 1,1,4,4-tetramethyl-1,2,3,4-tetrahydronaphthalene (25.00 g, 133 mmol), iodine (13.5 g, 53 mmol) and periodic acid (6.06 g, 27 mmol) was added glacial acetic acid (133 mL), water (27 mL) and concentrated sulphuric acid (98%, 7 mL). The reaction mixture was heated to 70 °C and left overnight. Upon cooling a precipitate formed, which was filtered off, dissolved in hexane, and passed through a short silica gel column (hexane as eluent). The hexane was evaporated and the residue was re-crystallised from ethanol to give the iodide as a white crystalline solid (23.50 g, 66%); m.p. 68.2-70.4 °C (lit.[228] 69.0-70.0 °C). All spectral properties were identical to those reported in the literature.[228]

6-Trimethylsilylethynyl-1,1,4,4-tetramethyl-1,2,3,4-tetrahydronaphthalene **9**

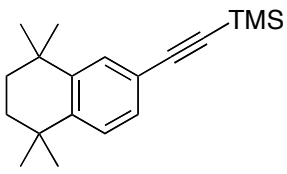

6-Iodo-1,1,4,4-tetramethyl-1,2,3,4-tetrahydronaphthalene, **8**, (3.14 g, 10 mmol), $Pd(PPh_3)_2Cl_2$ (0.07 g, 0.1 mmol) and copper(I) iodide (0.02 g, 0.1 mmol) were added to a 250

mL Schlenk flask, which was evacuated and purged with nitrogen (×3). Triethylamine (150 mL) was added *via* cannula under nitrogen, followed by trimethylsilylacetylene (1.18 g, 12 mmol). After 18 hours at room temperature, triethylamine was evapourated, and the residue re-dissolved in hexane and passed through a short silica gel column to give the crude product as a pale yellow oil after evaporation, which slowly solidified to give an off-white solid. Re-crystallisation from ethanol gave the TMS-acetylene adduct (1.91 g, 67%); m.p. 51.3-53.4 °C (lit.[228] 51.0-52.0 °C). All spectral properties were identical to those reported in the literature.[228]

6-Ethynyl-1,1,4,4-tetramethyl-1,2,3,4-tetrahydronaphthalene **10**

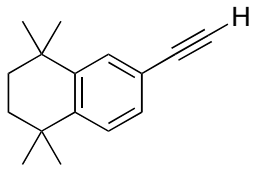

To a solution of 6-trimethylsilylethynyl-1,1,4,4-tetramethyl-1,2,3,4-tetrahydronaphthalene (2.84 g, 10 mmol) in methanol (70 mL) and diethyl ether (70 mL) was added sodium hydroxide (0.26 g, 6.6 mmol) in water (12 mL). After 4 hours at room temperature, the mixture was extracted with diethyl ether, washed with water (×3), dried ($MgSO_4$), and evaporated to give 6-ethynyl-1,1,4,4-tetramethyl-1,2,3,4-tetrahydronaphthalene as a pale yellow oil, that slowly solidified to give a white solid (1.87 g, 97%); m.p. 47.8-49.3 °C (lit.[228] 48.0-49.0 °C). All spectroscopic and analytical properties were identical to those reported in the literature.[228]

Methyl 3-*Z*-iodoacrylate **12**

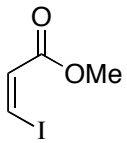

A stirred solution of methyl propiolate (5.3 mL, 59.6 mmol) and sodium iodide (14.4 g, 96 mmol) in acetic acid (22 mL) under argon was heated to 115 ^{o}C. After 1 hour the hot mixture

was poured onto water (100 mL), extracted with ethyl acetate (3 × 100 mL), washed with saturated aqueous sodium hydrogen carbonate (4 × 50 mL), saturated aqueous sodium metabisulphate (50 mL), and brine (50 mL), dried ($MgSO_4$) and evaporated to give the product as a yellow oil (7.28 g, 58%). All spectral properties were identical to those reported in the literature.[363]

Methyl 3-*E*-iodoacrylate **13**

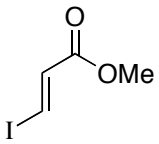

Methyl 3-*Z*-iodoacrylate (1.0 g, 4.7 mmol) was added to a stirred solution of 57% hydroiodic acid (0.1 mL, 0.7 mmol) in benzene (2.5 mL) and the mixture heated to 80 ^{o}C under argon. After 20 hours, the mixture was cooled and partitioned between water (10 mL) and diethyl ether (10 mL). The aqueous phase was extracted with diethyl ether (3 × 10 mL) and the combined organic phase washed with saturated aqueous sodium hydrogen carbonate (15 mL), 5 % aqueous sodium metabisulphite (15 mL) and brine (15 mL). Drying ($MgSO_4$) and evaporation gave methyl 3-*E*-iodoacrylate as a white solid (0.9 g, 85%); m.p. 41.6-43.6 ^{o}C (lit.[261] 41.0-44.0 °C). All spectroscopic and analytical properties were identical to those reported in the literature.[261]

(*Z*)-5-(5,5,8,8-Tetramethyl-5,6,7,8-tetrahydro-naphthalen-2-yl)-penta-2-en-4-ynoic acid methyl ester **14**

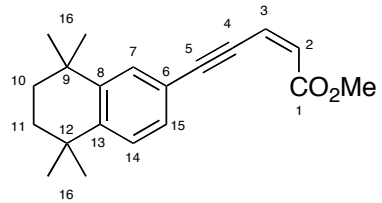

To a dried Schlenk flask under a positive pressure of argon was added methyl 3-(*Z*)-iodoacrylate (180 mg, 0.86 mmol), 6-ethynyl-1,1,4,4-tetramethyl-1,2,3,4-

tetrahydronaphthalene (200 mg, 0.94 mmol) and triethylamine (8 mL). The mixture degassed using the freeze-pump-thaw method (3×), followed by addition of palladium(II) acetate (5 mg, 0.02 mmol), triphenylphosphine (11 mg, 0.04 mmol) and copper(I) iodide (8 mg, 0.04 mmol). The Schlenk flask was then evapourated and purged with argon (3×) and stirred at room temperature under argon. After 5.5 hours, the mixture was diluted with diethyl ether (60 mL), passed through Celite™, washed with 5% hydrochloric acid (2 × 20 mL), brine (20 mL), dried ($MgSO_4$), concentrated and purified by silica gel chromatography (ethyl acetate: petroleum ether, 5:95, as eluent) to give ester as a pale yellow oil which slowly crystallised to an off-white solid (255 mg, 91%); ν_{max}/cm^{-1} 2924, 2200, 1718, 1610, 1492, 1460, 1439, 1392, 1218, and 1172; ^{1}H NMR (700 MHz, $CDCl_3$) δ 1.26 (6H, s, 2 × Me), 1.27 (6H, s, 2 × Me), 1.67 (4H, s, 2 × CH_2), 3.80 (3H, s, OMe), 6.10 (1H, d, *J* 11.0, H_2), 6.36 (1H, d, *J* 11.0, H_3), 7.26 (1H, d, *J* 8.5. H_{14}), 7.28 (1H, dd, *J* 8.5 and 1.5, C_{15}), 7.46 (1H, d, *J* 1.5 C_7); ^{13}C NMR (176 MHz, $CDCl_3$) 29.9 (C_{16}), 31.9 (C_{16}), 32.0 (C_{16}), 34.4 ($C_{9/12}$), 34.7 ($C_{9/12}$), 35.1 ($C_{10/11}$), 35.1 ($C_{10/11}$), 51.7 (O*C*H_3), 85.7 (C_4), 102.6 (C_5), 119.8 (C_6), 123.7 (C_3), 126.9 (C_{14}), 127.3 (C_2), 129.4 (C_{15}), 130.6 (C_7), 145.4 (C_8), 146.9 (C_{13}), 165.6 (C_1); *m/z* (ES) 319.1669 (M+Na, $C_{20}H_{24}O_2$-Na^+ requires 319.1669), 297, 279, 265 and 145; Anal. Calcd. for $C_{20}H_{24}O_2$: C, 81.04; H, 8.16. Found: C, 81.03; H, 8.22.

(*E*)-5-(5,5,8,8-Tetramethyl-5,6,7,8-tetrahydro-naphthalen-2-yl)-penta-2-en-4-ynoic acid methyl ester **15**

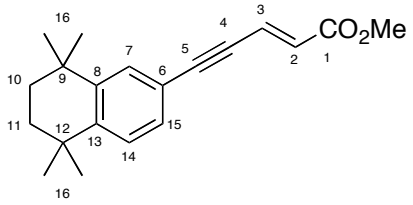

To a dried Schlenk flask under a positive pressure of argon was added methyl 3-(*E*)-iodoacrylate (180 mg, 0.86 mmol), 6-ethynyl-1,1,4,4-tetramethyl-1,2,3,4-tetrahydronaphthalene (200 mg, 0.94 mmol) and triethylamine (8 mL). The mixture degassed using the freeze-pump-thaw method (3×), followed by addition of palladium(II) acetate (10 mg, 0.04 mmol), triphenylphosphine (22 mg, 0.08 mmol) and copper(I) iodide (16 mg, 0.08 mmol). The Schlenk flask was then degassed using the freeze-pump-thaw

method (2×) and stirred at room temperature under argon. After 45 hours, the mixture was diluted with diethyl ether (30 mL), passed through Celite™, washed with 5% hydrochloric acid (2 × 10 mL), brine (10 mL), dried ($MgSO_4$), concentrated and purified by silica gel chromatography (ethyl acetate: petroleum ether, 5:95, as eluent) to give ester as a pale yellow oil, that solidified to an off-white solid (194 mg, 71%); ν_{max}/cm^{-1} 2953, 2918, 2860, 2195, 1719, 1618, 1600; ^1H NMR (700 MHz, $CDCl_3$) δ 1.27 (6H, s, 2 × Me), 1.28 (6H, s, 2 × Me), 1.68 (4H, s, 2 × CH_2), 3.78 (3H, s, OMe), 6.29 (1H, d, *J* 15.0, H_2), 6.99 (1H, d, *J* 15.0, H_3), 7.23 (1H, dd, *J* 8.0 and 1.5, H_{15}), 7.28 (1H, d, *J* 8.0, H_{14}), 7.43 (1H, d, *J* 1.5, H_7); ^{13}C NMR (176 MHz, $CDCl_3$) δ_C 31.8 (C_{16}), 31.9 (C_{16}), 34.4 ($C_{9/12}$), 34.5 ($C_{9/12}$), 35.0 ($C_{10/11}$), 35.1 ($C_{10/11}$), 52.0 (OCH_3), 85.7 (C_4), 99.6 (C_5), 119.3 (C_6), 125.9 (C_3), 127.0 (C_{14}), 129.1 (C_2), 129.2 (C_{15}), 130.6 (C_7), 145.5 (C_8), 147.1 (C_{13}), 166.7 (C_1); *m/z* (ES) 319.16685 (M^+, $C_{20}H_{24}O_2$, requires 319.16685), 297, 279 and 145; Anal. Calcd. for $C_{20}H_{24}O_2$: C, 81.04; H, 8.16. Found: C, 80.81; H, 8.25.

5,5,8,8-Tetramethyl-5,6,7,8-tetrahydronapthalene-2-carbaldehyde **16**

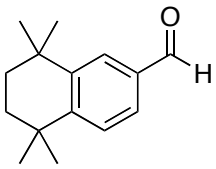

(*Z*)-5-(5,5,8,8-Tetramethyl-5,6,7,8-tetrahydro-naphthalen-2-yl)-penta-2-en-4-ynoic acid methyl ester was dissolved in THF (15 mL) and 20% sodium hydroxide (15 mL) was added drop wise to the solution. The reaction mixture was stirred at reflux (67 ^oC) for 72 hours. The reaction went to multiple spots by TLC and was therefore stopped, cooled to room temperature. The reaction mixture was acidified to pH 1-2 by the addition of 20% hydrochloric acid, and extracted with diethyl ether (2 × 20 mL), dried ($MgSO_4$), concentrated and purified by silica gel chromatography (ethyl acetate: petroleum ether, 5:95). The product was extracted as colourless crystals (15 mg, 8%). All spectral properties were identical to those reported in the literature.[364] ν_{max}/cm^{-1} 2960, 2927, 1696 (C=O), 1602, 1563, 1458, 1364, 1288, 1208 and 1182.

(2*Z*,4*E*)-5-(4,4,6-Trimethyl-[1,3,2-dioxaborinan-2-yl])-penta-2,4-dienoic acid methyl ester **18**

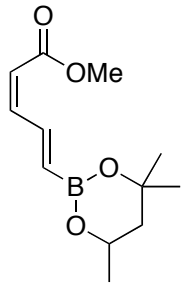

To a dried Schlenk tube under a positive pressure of argon was added silver (I) acetate (434 mg, 2.6 mmol), palladium(II) acetate (27 mg, 0.12 mmol), tri(*o*-tolyl)phosphine (73 mg, 0.24 mmol), and dry acetonitrile (10 mL). The mixture degassed using the freeze-pump-thaw method (2×), followed by the addition of methyl 3-*Z*-iodoacrylate (500 mg, 2.4 mmol) and 4,4,6-trimethyl-2-vinyl-1,3,2-dioxaborane (0.46 mL, 2.8 mmol). The mixture was degassed using the freeze-pump-thaw method (2×) and heated to 50 °C with vigorous stirring. After 23 hours the mixture was cooled, diluted with diethyl ether (70 mL) and passed through Celite™, washed with 5% hydrochloric acid (10 mL), water (20 mL), brine (20 mL), dried ($MgSO_4$) and evaporated to give the crude product as a yellow oil. Purification by silica gel chromatography (ethyl acetate: petroleum ether, 1:9, as eluent) gave (2*Z*,4*E*)-5-(4,4,6-trimethyl-[1,3,2-dioxaborinan-2-yl])-penta-2,4-dienoic acid methyl ester (303 mg, 54 %) as a pale yellow oil. All spectroscopic and analytical properties were identical to those reported in the literature.[261]

(2*E*,4*E*)-5-(4,4,6-Trimethyl-[1,3,2-dioxaborinan-2-yl])-penta-2,4-dienoic acid methyl ester **19**

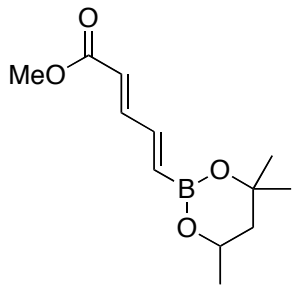

To a dried Schlenk tube under a positive pressure of argon was added silver (I) acetate (430 mg, 2.6 mmol), palladium(II) acetate (27 mg, 0.1 mmol), tri(*o*-tolyl)phosphine (70 mg, 0.2 mmol), and a solution of methyl 3-*E*-iodoacrylate (500 mg, 2.4 mmol) in dry acetonitrile (14.5 mL). The mixture degassed using the freeze-pump-thaw method (2×), followed by the addition of 4,4,6-trimethyl-2-vinyl-1,3,2-dioxaborane (0.46 mL, 2.8 mmol). The mixture was degassed using the freeze-pump-thaw method (2×) and heated to 50 °C with vigorous stirring. After 21 hours the mixture was cooled, diluted with diethyl ether (80 mL) and passed through Celite™, washed with 5% hydrochloric acid (20 mL), water (40 mL), brine (40 mL), dried ($MgSO_4$) and evaporated to give the crude product as a yellow oil. Purification by silica gel chromatography (ethyl acetate: petroleum ether, 1:9, as eluent) gave (2*E*,4*E*)-5-(4,4,6-trimethyl-[1,3,2-dioxaborinan-2-yl])-penta-2,4-dienoic acid methyl ester (499 mg, 90%) as a pale yellow oil. All spectroscopic and analytical properties were identical to those reported in the literature.[261]

(2*Z*,4*Z*)-5-Iodopenta-2,4-dienoic acid methyl ester **29**

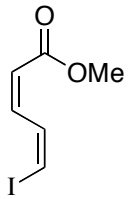

To a solution of (2*Z*,4*E*)-5-(4,4,6-trimethyl-[1,3,2-dioxaborinan-2-yl])-penta-2,4-dienoic acid methyl ester (300 mg, 1.3 mmol) in dry DCM (8 mL) was added to a dry flask under argon

and cooled to -78 °C. Iodine monochloride (1.5 mL of a 1.0 M solution in DCM, 1.5 mmol) was added dropwise, and the mixture stirred for 4 hours. Sodium methoxide (3 mL of a 0.5 M solution in MeOH, 1.5 mmol) was then added dropwise and the mixture allowed to warm to room temperature. After 30 minutes the mixture was diluted with diethyl ether (80 mL), washed with 5% aqueous sodium metabisulphite (40 mL), water (40 mL) and brine (40mL), dried ($MgSO_4$) and evaporated to give the crude product. Purification by silica gel chromatography (ethyl acetate: petroleum ether, 5:95 as eluent, cooled to 0 °C) gave (2*Z*,4*Z*)-5-iodo-penta-2,4-dienoic acid methyl ester as a pale yellow oil (180 mg, 59%). All spectroscopic and analytical properties were identical to those reported in the literature.[261]

(2*E*,4*E*)-5-Iodopenta-2,4-dienoic acid methyl ester **30**

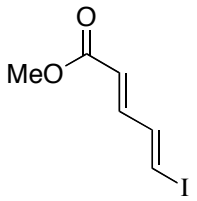

A solution of (2*E*,4*E*)-5-(4,4,6-trimethyl-[1,3,2-dioxaborinan-2-yl])-penta-2,4-dienoic acid methyl ester (230 mg, 1.0 mmol) in dry tetrahydrofuran (5.5 mL) was added to a dry flask under argon and cooled to -78 °C in the absence of light. Sodium methoxide (2.4 mL of a 0.5 M solution in methanol, 1.2 mmol) was added dropwise, and the mixture stirred for 30 minutes. Iodine monochloride (1.5 mL of a 1.0 M solution in DCM, 1.5 mmol) was then added dropwise and the mixture stirred for 1 hour. The mixture was warmed to room temperature, diluted with diethyl ether (65 mL), washed with 5% aqueous sodium metabisulphite (35 mL), water (35 mL) and brine (35 mL), dried ($MgSO_4$) and evaporated to give the crude product. Purification by silica gel chromatography (ethyl acetate: petroleum ether, 5:95 as eluent, cooled to 0 °C) gave (2*E*,4*E*)-5-iodopenta-2,4-dienoic acid methyl ester as a white solid (200 mg, 87 %); m.p. 57.3-60.6 °C (lit.[265] 56.0-61.0 °C). All spectroscopic and analytical properties were identical to those reported in the literature.[265]

(*Z*)-3-Iodobut-2-enoic acid methyl ester **35**

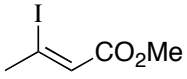

Methyl tetrolate (5.0 g, 50.5 mmol), sodium iodide (11.4 g, 75.8 mmol) and acetic acid (18 mL) were heated to reflux for 1.5 hours. The solution was then cooled to room temperature, and partitioned between 80 mL of water and 80 mL of ether. The aqueous layer was extracted and washed with diethyl ether (2 × 20 mL), after which the organic layers were combined, washed with saturated sodium hydrogen carbonate (2 × 40 mL), 10% sodium thiosulfate (40 mL), and brine (40 mL). Drying ($MgSO_4$) and concentration yielded (*Z*)-3-iodobut-2-enoic acid methyl ester as a pale yellow liquid (10.8 g, 95%). All spectroscopic and analytical properties were identical to those reported in the literature.[268]

(*E*)-3-Iodobut-2-enoic acid methyl ester **36**

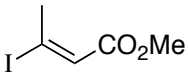

A solution of (*Z*)-3-iodobut-2-enoic acid methyl ester (10.8 g, 47.8 mmol) and HI (0.6 g, 4.8 mmol) in benzene (100 mL) were heated to reflux for 24 hours and then allowed to cool to room temperature. The mixture was partitioned between water (100 mL) and diethyl ether (150 mL), followed by the aqueous phase being extracted with diethyl ether (2 × 25 mL). The combined organic phases were then washed with saturated sodium hydrogen carbonate (50 mL), 5% sodium thiosulfate (50 mL) and brine (50 mL). Drying ($MgSO_4$) and evaporation yielded the crude as a pale yellow oil. Purification by silica gel chromatography (ethyl acetate: petroleum ether, 5:95, as eluent) yielded (*E*)-3-iodobut-2-enoic acid methyl ester as a colourless oil (4.0 g, 37%) and recovered (*Z*)-3-iodobut-2-enoic acid methyl ester (4.3 g, 40%). All spectral and analytical properties were identical to those reported in the literature.[268,365]

(*Z*)-3-Methyl-5-(5,5,8,8-tetramethyl-5,6,7,8-tetrahydro-naphthalen-2-yl)-pent-2-en-4-ynoic acid methyl ester **37**

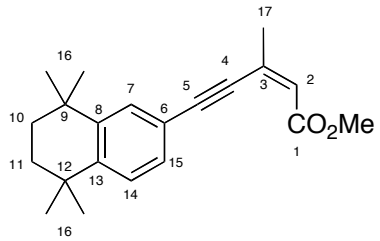

To a dried Schlenk flask flask under a positive pressure of argon was added (*Z*)-3-iodobut-2-enoic acid methyl ester (360 mg, 1.7 mmol), 6-ethynyl-1,1,4,4-tetramethyl-1,2,3,4-tetrahydronaphthalene (400 mg, 1.9 mmol) and triethylamine (10 mL). The mixture was degassed using the freeze-pump-thaw method (3×), followed by the addition of palladium(II) acetate (20 mg, 0.1 mmol), triphenylphosphine (44 mg, 0.2 mmol) and copper(I) iodide (32 mg, 0.2 mmol). The mixture degassed using the freeze-pump-thaw method (2×) and stirred at room temperature under argon. After 24 hours the reaction was diluted with ether (80 mL), passed through Celite™, washed with 5% hydrochloric acid (2 × 20 mL), brine (20 mL), dried ($MgSO_4$) and concentrated under vacuum to give an orange oil. Purification by silica gel column chromatography (ethyl acetate: petroleum ether, 5:95) yielded the product as a pale yellow oil (336 mg, 63%).ν_{max}/cm^{-1} 2955, 2923, 2864, 2190, 1716, 1611, 1440, 1375, 1254, 1194, 1129 and 1041; ^{1}H NMR (700 MHz, $CDCl_3$) δ 1.27 (6H, s, H_{16}), 1.28 (6H, s, H_{16}), 1.68 (4H, s, $H_{10\ and\ 11}$), 2.14 (3H, d, *J* 1.0, H_{17}), 3.77 (3H, s, OMe), 6.01 (1H, d, *J* 1.0, H_2), 7.27 (1H, d, *J* 8.0, H_{14}), 7.29 (1H, dd, *J* 8.0 and 2.0, H_{15}), 7.46 (1H, d, *J* 2.0, H_7); ^{13}C NMR (176 MHz, $CDCl_3$) δ_C 25.6 (C_{17}), 31.9 (C_{16}), 32.0 (C_{16}), 34.4 ($C_{9/12}$), 34.6 ($C_{9/12}$), 35.1 ($C_{10/11}$), 35.2 ($C_{10/11}$), 51.5 (OMe), 87.6 (C_4), 101.5 (C_5), 119.9 (C_6), 123.6 (C_2), 126.9 (C_{14}), 129.4 (C_{15}), 130.5 (C_7), 135.5 (C_3), 145.3 (C_8), 146.7 (C_{13}), 165.8 (C_1); *m/z* (ES) 311.2011 (M+H, $C_{21}H_{27}O_2$, requires 311.2006).

(*E*)-3-Methyl-5-(5,5,8,8-tetramethyl-5,6,7,8-tetrahydro-naphthalen-2-yl)-pent-2-en-4-ynoic acid methyl ester **38**

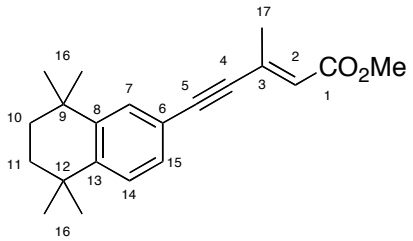

To a dried Schlenk flask flask under a positive pressure of argon was added (*E*)-3-iodobut-2-enoic acid methyl ester (360 mg, 1.7 mmol), 6-ethynyl-1,1,4,4-tetramethyl-1,2,3,4-tetrahydronaphthalene (400 mg, 1.9 mmol) and triethylamine (10 mL). The mixture was degassed using the freeze-pump-thaw method (3×), followed by the addition of palladium(II) acetate (20 mg, 0.1 mmol), triphenylphosphine (44 mg, 0.2 mmol) and copper(I) iodide (32 mg, 0.2 mmol). The mixture degassed using the freeze-pump-thaw method (2×) and stirred at room temperature under argon. After 24 hours the reaction was diluted with ether (80 mL), passed through Celite™, washed with 5% hydrochloric acid (2 × 20 mL), brine (20 mL), dried ($MgSO_4$) and concentrated under vacuum to give an orange oil. Purification by silica gel column chromatography (ethyl acetate: petroleum ether, 5:95) yielded the product as a pale yellow oil (530 mg, 99%).ν_{max}/cm^{-1} 2957, 2195, 1715, 1612, 1433, 1342, 1269, 1198, 1180 and 1135; ^{1}H NMR (700 MHz, $CDCl_3$) δ 1.27 (6H, s, H_{16}), 1.28 (6H, s, H_{16}), 1.68 (4H, s, $H_{10\ and\ 11}$), 2.40 (3H, d, *J* 1.5, H_{17}), 3.73 (3H, s, OMe), 6.15 (1H, q, *J* 1.5, H_2), 7.21 (1H, dd, *J* 8.0 and 1.5, H_{15}), 7.27 (1H, d, *J* 8.0, H_{14}), 7.41 (1H, d, *J* 1.5, H_7); ^{13}C NMR (176 MHz, $CDCl_3$) δ_C 20.3 (C_{17}), 31.9 (C_{16}), 32.0 (C_{16}), 34.5 ($C_{9/12}$), 34.7 ($C_{9/12}$), 35.1 ($C_{10/11}$), 35.1 ($C_{10/11}$), 51.5 (OMe), 90.5 (C_4), 94.9 (C_5), 119.4 (C_6), 123.4 (C_2), 127.0 (C_{14}), 129.2 (C_{15}), 130.5 (C_7), 138.8 (C_3), 145.5 (C_8), 146.8 (C_{13}), 166.9 (C_1); *m/z* (ES) 311.2011 (M+H, $C_{21}H_{27}O_2$, requires 311.2006). 279.

6-Hydroxy-4-methyl-6-(5,5,8,8-tetramethyl-5,6,7,8-tetrahydro-naphthalen-2-yl)-5,6-dihydro-pyran-2-one **39**

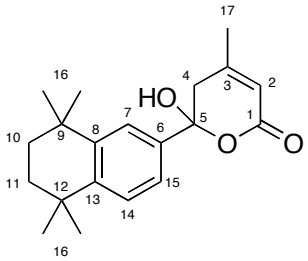

(*Z*)-3-Methyl-5-(5,5,8,8-tetramethyl-5,6,7,8-tetrahydro-naphthalen-2-yl)-pent-2-en-4-ynoic acid methyl ester (336 mg, 1.1 mmol) was added to a stirred solution of lithium hydroxide (135 mg, 3.3 mmol) in a tetrahydrofuran water mixture (3:1, 20 mL) at room temperature. After 72 hours the reaction was judged to be complete and acidified to pH 1/2 by the addition of 20% hydrochloric acid, extracted with diethyl ether (20 mL), dried ($MgSO_4$) and concentrated to the crude as a yellow powder. Purification by silica gel column chromatography (ethyl acetate: petroleum ether, 9:1) yielded 6-hydroxy-4-methyl-6-(5,5,8,8-tetramethyl-5,6,7,8-tetrahydro-naphthalen-2-yl)-5,6-dihydro-pyran-2-one as a bright yellow solid (329 mg, 97%). ν_{max}/cm^{-1} 2962, 2360, 1746, 1456, 1364, 1271 and 1129; ^1H NMR (700 MHz, $CDCl_3$) δ_H 1.25 (6H, s, H_{16}), 1.26 (6H, s, H_{16}), 1.66 (4H, s, $H_{10\ and\ 11}$), 2.10 (3H, d, *J* 2.0 H_{17}), 3.03 (1H, d, *J* 14.0, H_4), 3.21 (1H, d, *J* 14.0, H_4), 5.67 (1H, d, *J* 2.0, H_2), 7.01 (1H, dd, *J* 8.0 and 2.0, H_{15}), 7.16 (1H, d, *J* 2.0, H_7), 7.22 (1H, d, *J* 8.0, H_{14}); ^{13}C NMR (176 MHz, $CDCl_3$) δ_C 13.1 (C_{17}), 32.0 (C_{16}), 32.0 (C_{16}), 32.1 (C_{16}), 32.1 (C_{16}), 34.3 ($C_{9/12}$), 34.4 ($C_{9/12}$), 35.2 ($C_{10/11}$), 35.2 ($C_{10/11}$), 42.6 (C_4), 107.6 (C_5), 119.0 (C_2), 127.1 (C_{14}), 127.8 (C_{15}), 128.7 (C_7), 129.8 (C_6), 144.5 (C_{13}), 145.4 (C_8), 166.9 (C_3), 170.9 (C_1); *m/z* (ES) 337.1774 (M+Na, $C_{20}H_{26}O_3Na$, requires 337.1774), 332, and 315.

(*E*)-3-Methyl-5-(5,5,8,8-tetramethyl-5,6,7,8-tetrahydro-naphthalen-2-yl)-pent-2-en-4-ynoic acid **40**

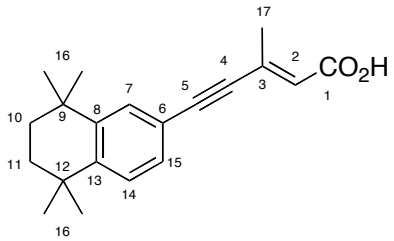

(*E*)-3-Methyl-5-(5,5,8,8-tetramethyl-5,6,7,8-tetrahydro-naphthalen-2-yl)-pent-2-en-4-ynoic acid methyl ester (85 mg, 0.3 mmol) was added to a stirred solution of lithium hydroxide (46 mg, 1.1 mmol) in a tetrahydrofuran water mixture (3:1, 20 mL) at room temperature. After 48 hours the reaction was judged to be complete and acidified to pH 1/2 by the addition of 20% hydrochloric acid, extracted with diethyl ether (20 mL), dried ($MgSO_4$) and concentrated to give an off-white solid. Re-crystallisation from acetonitrile yielded the product as an off-white crystalline solid (25 mg, 31%). ν_{max}/cm^{-1} 2912, 2197, 1688, 1602, 1428, 1296, 1225 and 1145; ^{1}H NMR (700 MHz, $CDCl_3$) δ 1.27 (6H, s, H_{16}), 1.28 (6H, s, H_{16}), 1.68 (4H, s, $H_{10\ and\ 11}$), 2.41 (3H, d, *J* 1.5 H_{17}), 6.18 (1H, d, *J* 1.5, H_2), 7.22 (1H, dd, *J* 8.0 and 1.5, H_{15}), 7.28 (1H, d, *J* 8.0, H_{14}), 7.42 (1H, d, *J* 1.5, H_7); ^{13}C NMR (176 MHz, $CDCl_3$) δ_C 20.6 (C_{17}), 31.9 (C_{16}), 32.0 (C_{16}), 34.5 ($C_{9/12}$), 34.7 ($C_{9/12}$), 35.0 ($C_{10/11}$), 35.1 ($C_{10/11}$), 90.5 (C_4), 96.2 (C_5), 119.3 (C_6), 122.4 (C_2), 127.1 (C_{14}), 129.2 (C_{15}), 130.6 (C_7), 141.3 (C_3), 145.5 (C_8), 147.0 (C_{13}), 169.0 (C_1); *m/z* (ES) 296.1773 (M, $C_{20}H_{24}O_2$, requires 296.1771). 279, 255, 84 and 43.

(2*Z*,4*E*)-3-Methyl-5-(4,4,6-trimethyl-[1,3,2]-dioxaborinan-2-yl)-penta-2,4-dienoic acid methyl ester **47**

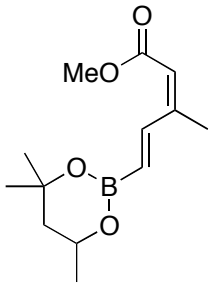

To a dried Schlenk tube under a positive pressure of argon was added (*Z*)-3-iodobut-2-enoic acid methyl ester (500 mg 2.2 mmol), dry acetonitrile (15 mL), palladium(II) acetate (25 mg, 0.1 mmol), tri(*o*-tolyl)phosphine (67 mg, 0.2 mmol), silver(I) acetate (402 mg, 2.4 mmol) and 4,4,6-trimethyl-2-vinyl-1,3,2-dioxaborane (399 mg, 0.4 mL, 2.6 mmol), the mixture degassed using freeze-pump-thaw method (3×) and heated to 50 °C with vigorous stirring. After 22 hours the mixture was cooled, diluted with ether (80 mL), passed through Celite™, washed with 5% hydrochloric acid (20 mL), water (40 mL) and brine (40 mL). Drying ($MgSO_4$) and evaporation gave the crude product as an orange oil. Purification by silica gel chromatography (ethyl acetate: petroleum ether, 1:9, as eluent) gave methyl (2*Z*,4*E*)-3-methyl-5-(4,4,6-trimethyl-1,3,2-dioxaborinan-2-yl) penta-2,4-dienoate (432 mg, 78%) as a clear oil. All spectral and analytical properties were identical to those reported in the literature.[267]

(2*E*,4*E*)-3-Methyl-5-(4,4,6-trimethyl-[1,3,2]-dioxaborinan-2-yl)-penta-2,4-dienoic acid methyl ester **48**

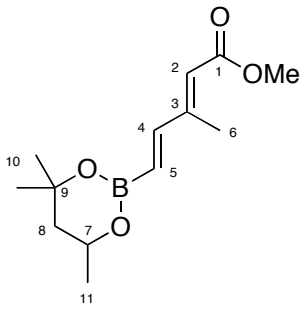

To a dried Schlenk tube under a positive pressure of argon was added (*E*)-3-iodobut-2-enoic acid methyl ester (940 mg 4.2 mmol), dry acetonitrile (15 mL), palladium(II) acetate (47 mg, 0.2 mmol), tri(*o*-tolyl)phosphine (128 mg, 0.4 mmol), silver(I) acetate (758 mg, 4.5 mmol) and 4,4,6-trimethyl-2-vinyl-1,3,2-dioxaborane (752 mg, 0.8 mL, 4.9 mmol), the mixture degassed using freeze-pump-thaw method (3 x) and heated to 50 °C with vigorous stirring. After 22 hours the mixture was cooled, diluted with ether (80 mL), passed through Celite™, washed with 5% hydrochloric acid (20 mL), water (40 mL) and brine (40 mL). Drying ($MgSO_4$) and evaporation gave the crude product as an orange oil. Purification by silica gel chromatography (ethyl acetate: petroleum ether, 1:9 as eluent) gave (2*E*,4*E*)-3-methyl-5-(4,4,6-trimethyl-[1,3,2]-dioxaborinan-2-yl)-penta-2,4-dienoic acid methyl ester (780 mg, 74%) as a clear oil; ν_{max}/cm^{-1} 2976, 2359, 1710, 1596, 1393, 1327, 1290, 1229 and 1153; ^{1}H NMR **(**700 MHz, $CDCl_3$) δ_H 1.28 (3H, d, *J* 6.0, H_{11}), 1.30 (3H, s, H_{10}), 1.31 (3H, s, H_{10}), 1.51 (1H, t, *J* 13.0, H_8), 1.80 (1H, dd, *J* 13.0 and 2.5, H_8), 2.25 (3H, d, *J* 1.0, H_6), 3.70 (3H, s, O*Me*), 4.21-4.27 (1H, m, H_7), 5.87 (1H, s, H_2), 5.93 (1H, d, *J* 18.0, H_5) and 6.92 (1H, d, *J* 18.0, H_4); ^{13}C NMR(176 MHz, $CDCl_3$) δ_C 13.5 (C_6), 23.3 (C_{10}), 28.3 (C_{11}), 31.4 (C_{12}), 46.1 (C_8), 51.3 (OMe), 65.2 (C_7), 71.3 (C_9), 121.0 (C_2), 129-130 (C_5) 149.2 (C_4), 153.2 (C_3) and 167.8 (C_1); δ_B (128 MHz, $CDCl_3$) 26 (brs); *m/z* (ES) 252.1643 (M, $C_{13}H_{21}BO_4$, requires 252.1642). 237, 221, 196, 152, 137, 124 and 83.

(2*Z*,4*E*)-5-Iodo-3-methyl-penta-2,4-dienoic acid methyl ester **49**

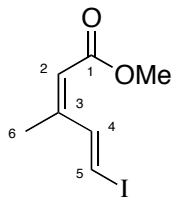

To a dried Schlenk tube under a positive pressure of argon was added a solution of (2*Z*,4*E*)-3-methyl-5-(4,4,6-trimethyl-[1,3,2]-dioxaborinan-2-yl)-penta-2,4-dienoic acid methyl ester (150 mg, 0.6 mmol), in dry tetrahydrofuran (3 mL), and the tube cooled to -78 °C in the absence of light. Sodium methoxide (1.5 mL of a 0.5 M solution in MeOH, 0.7 mmol) was added dropwise and the mixture stirred for 30 minutes, followed by the addition of iodine monochloride (1 mL of a 1.0 M solution in DCM, 1.0 mmol) dropwise. The mixture was stirred for 1 hour, warmed to room temperature, diluted with diethyl ether (40 mL), washed with 5% sodium metabisulphite (20 mL), water (20 mL) and brine (20 mL). Drying ($MgSO_4$) and evaporation gave the crude product as an orange oil. Purification by silica gel chromatography (ethyl acetate: petroleum ether, 1:9, as eluent), gave the product as an oil, which slowly crystallised to an off-white solid (147 mg, 98%); ν_{max}/cm^{-1} 3068 (C-H stretch), 2982 (Sp^3 C-H), 2946 (Sp^3 C-H), 1710 (C=O), 1612 (C=C), 1553, 1432 (Sp^3 C-H), 1382, 1241, 1192 and 1150; ^{1}H NMR **(**500 MHz, $CDCl_3$) δ_H 1.98 (3H, d, *J* 1.2, H_6), 3.72 (3H, s, O*Me*), 5.66 (1H, s, H_2), 6.94 (1H, d, *J* 15.0, H_5), 8.61 (1H, d, *J* 15.0, H_4); ^{13}C NMR (126 MHz, $CDCl_3$) δ_C 20.5 (C_6), 51.5 (OCH_3), 87.2 (C_5), 117.4 (C_2), 142.7 (C_4), 149.6 (C_3), 166.4 (C_1); *m/z* (EI) 252 (M^+), 221, 193, and 126; Anal. Calcd for $C_7H_9IO_2$: C, 33.36; H, 3.60. Found: C, 33.44; H, 3.60.

Methyl (2*E*,4*E*)-5-iodo-3-methylpenta-2,4-dienoate **50**

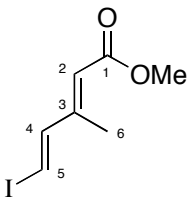

To a dried Schlenk tube under a positive pressure of argon was added a solution of (2*E*,4*E*)-3-methyl-5-(4,4,6-trimethyl-[1,3,2]-dioxaborinan-2-yl)-penta-2,4-dienoic acid methyl ester (700 mg, 2.8 mmol), in dry THF (10 mL), and the tube cooled to -78 ^{o}C in the absence of light. Sodium methoxide (6.9 mL of a 0.5 M solution in MeOH, 3.5 mmol) was added dropwise and the mixture stirred for 30 minutes, followed by the addition of iodine monochloride (4.7 mL of a 1.0 M solution in DCM, 4.7 mmol) dropwise. The mixture was stirred for 1 hour, warmed to room temperature, diluted with diethyl ether (80 mL), washed with 5% sodium metabisulphite (30 mL), water (30 mL) and brine (30 mL). Drying ($MgSO_4$) and evaporation gave the crude product as an orange oil. Purification by silica gel chromatography (ethyl acetate: petroleum ether, 1:9, a eluent), gave the product as a clear oil (602 mg, 86%); All spectral and analytical properties were identical to those reported in the literature.[366] ν_{max}/cm^{-1} 3070 (C-H stretch), 3013 (Sp^3 C-H), 2943 (Sp^3 C-H), 1708 (C=O), 1612 (C=C), 1433 (Sp^3 C-H), 1386, 1359, 1234, 1190 and 1153; ^{1}H NMR **(**400 MHz, $CDCl_3$) δ_H 2.24 (3H, d, *J* 1.2, H_6), 3.71 (3H, s, O*Me*), 5.74 (1H, q, *J* 0.8, H_2), 6.89 (1H, d, *J* 15.0, H_5), 7.10 (1H, d, *J* 15.0, H_4); ^{13}C NMR δ_C (126 MHz, $CDCl_3$) δ_C 13.6 (C_6), 51.5 (OMe), 84.8 (C_5), 120.0 (C_2), 148.5 (C_4), 151.4 (C_3), 167.2 (C_1); *m/z* (EI) 252 (M^+), 221, 193, 126 and 125.

(2*Z*,4*E*)-2-Methyl-7-(5,5,8,8-tetramethyl-5,6,7,8-tetrahydro-naphthalen-2-yl)-hepta-2,4-dien-6-ynoic acid methyl ester **51**

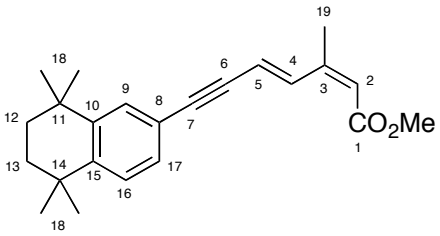

(2*Z*,4*E*)-5-Iodo-3-methyl-penta-2,4-dienoic acid methyl ester (325 mg, 1.3 mmol), 6-ethynyl-1,1,4,4-tetramethyl-1,2,3,4-tetrahydronaphthalene (331 mg, 1.6 mmol) and triethylamine (6 mL) were added to a dried Schlenk tube and the mixture degassed using the freeze-pump-thaw method (3×). Palladium(II) acetate (14 mg, 0.1 mmol), triphenylphosphine (32 mg, 0.1 mmol) and copper(I) iodide (23 mg, 0.1 mmol), were then added and the mixture degassed by freeze-pump-thaw (3×). The mixture was stirred at room temperature for 5 hours, diluted with ethyl acetate (80 mL), passed through Celite™, washed with 5% hydrochloric acid (20 mL, 2×), brine (20 mL), dried ($MgSO_4$) and concentrated. Purification by silica gel chromatography (Petroleum ether: ethyl acetate, 95:5, as eluent) yielded the product as an off-white solid (380 mg, 88%); ν_{max}/cm^{-1} 2956 (Sp^3 C-H), 2192 (alkyne), 1713 (C=O), 1610 (C=C), 1453, 1432 (Sp^3 C-H), 1228 and 1155; ^{1}H NMR **(**400 MHz, $CDCl_3$) δ_H 1.28 (6H, s, H_{18}), 1.29 (6H, s, H_{18}), 1.68 (4H, s, $H_{12\ and\ 13}$), 2.04 (3H, d, *J* 1.2, H_{19}), 3.74 (3H, s, OC*H*$_3$), 5.73 (1H, s, H_2), 6.23 (1H, d, *J* 16.0, H_5), 7.22 (1H, dd, *J* 1.5 and 8.0, H_{17}), 7.27 (1H, d, *J* 8.0, H_{16}), 7.44 (1H, d, *J* 1.5, H_9), 8.17 (1H, d, *J* 16.0, H_4); ^{13}C NMR (126 MHz, $CDCl_3$) δ_C 20.6 (C_{19}), 31.9 (C_{18}), 32.0 (C_{18}), 34.5 ($C_{11/14}$), 34.6 ($C_{11/14}$), 35.1 ($C_{12/13}$), 35.2 ($C_{12/13}$), 51.5 (OMe), 88.2 (C_6), 96.3 (C_7), 115.9 (C_5), 118.3 (C_2), 120.2 (C_8), 126.9 (C_{16}), 129.0 (C_{17}), 130.4 (C_9), 137.7 (C_4), 145.4 (C_{10}), 146.2 (C_{15}), 149.8 (C_3), 166.6 (C_1); *m/z* (ES) 354.2424 ($M^+NH_4^+$, $C_{23}H_{32}O_2N_1$, requires 354.2428), 337, 299, 279 and 237; Anal. Calcd for $C_{23}H_{28}O_2$: C, 82.10; H, 8.39. Found: C, 81.40 H, 8.49.

(2*E*,4*E*)-2-Methyl-7-(5,5,8,8-tetramethyl-5,6,7,8-tetrahydro-naphthalen-2-yl)-hepta-2,4-dien-6-ynoic acid methyl ester **52**

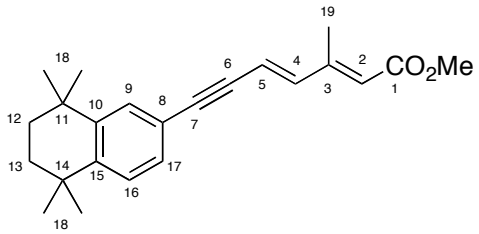

Methyl (2*E,*4*E*)-5-iodo-3-methylpenta-2,4-dienoate (500 mg, 1.98 mmol), 6-ethynyl-1,1,4,4-tetramethyl-1,2,3,4-tetrahydronaphthalene (509 mg, 2.4 mmol) and triethylamine (10 mL) were added to a dried Schlenk tube and the mixture degassed using the freeze-pump-thaw method (3x). Palladium(II) acetate (22 mg, 0.1 mmol), triphenylphosphine (52 mg, 0.2 mmol) and copper(I) iodide (38 mg, 0.2 mmol), were then added and the mixture degassed by freeze-pump-thaw (3×). The mixture was stirred at room temperature for 5 hours, diluted with ethyl acetate (80 mL), passed through Celite™, washed with 5% hydrochloric acid (2 × 20 mL), brine (20 mL), dried ($MgSO_4$) and concentrated. Purification by silica gel chromatography (Petroleum ether: ethyl acetate, 95:5, as eluent) yielded the product as a yellow oil (510 mg, 76%); ν_{max}/cm^{-1} 2956 (Sp^3 C-H), 2192 (alkyne), 1715 (C=O), 1608 (C=C), 1490, 1434 (Sp^3 C-H), 1358, 1232 and 1154; ^{1}H NMR 500 MHz, $CDCl_3$: δ_H 1.27 (6H, s, H_{18}), 1.28 (6H, s, H_{18}), 1.68 (4H, s, $H_{12\ and\ 13}$), 2.31 (3H, d, *J* 1.2, H_{19}), 3.73 (3H, s, OC*H*$_3$), 5.84 (1H, s, H_2), 6.24 (1H, d, *J* 16.0, H_5), 6.70 (1H, d, *J* 16.0, H_4), 7.21 (1H, dd, *J* 1.5 and 8.0, H_{17}), 7.26 (1H, d, *J* 8.0, H_{16}), 7.41 (1H, d, *J* 1.5, H_9); ^{13}C NMR (126 MHz, $CDCl_3$) δ_C 13.4 (C_{19}), 31.9 (C_{18}), 32.0 (C_{18}), 34.5 ($C_{11/14}$), 34.6 ($C_{11/14}$), 35.1 ($C_{12/13}$), 35.1 ($C_{12/13}$), 51.5 (OMe), 87.6 (C_6), 96.0 (C_7), 114.7 (C_5), 120.1 (C_2), 120.4 (C_8), 127.0 (C_{16}), 128.9 (C_{17}), 130.3 (C_9), 143.7 (C_4), 145.4 (C_{10}), 146.3 (C_{15}), 151.4 (C_3), 167.4 (C_1); *m/z* (ES) 337.2164 (M^+H^+, $C_{23}H_{29}O_2$, requires 337.2162), 337, 305 and 215.

(2*Z*,4*E*)-2-Methyl-7-(5,5,8,8-tetramethyl-5,6,7,8-tetrahydro-naphthalen-2-yl)-hepta-2,4-dien-6-ynoic acid **53**

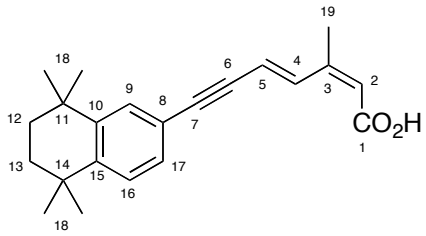

(2*Z*,4*E*)-2-Methyl-7-(5,5,8,8-tetramethyl-5,6,7,8-tetrahydro-naphthalen-2-yl)-hepta-2,4-dien-6-ynoic acid methyl ester (200 mg, 0.6 mmol), was dissolved in a THF water mixture (3:1, 10 mL) followed by the addition of lithium hydroxide (200 mg, 2.4 mmol). The mixture was stirred at room temperature for 48 hours in the absence of light after which, the reaction was judged to be complete by TLC. The mixture was then acidified to pH 1 by the addition of 20% hydrochloric acid, and extracted with diethyl ether (2 × 20 mL). Purification by silica gel chromatography (ethyl acetate: petroleum ether, 1:9, followed by gradient elution) yielded the product as a yellow powder, which was re-crystallised from acetonitrile to give a bright yellow solid (148 mg, 77%); m.p. 226.9-227.8 °C; ν_{max}/cm^{-1} 2500-3500 (br OH), 2190 (alkyne), 1676 (C=O), 1609 (C=C), 1487, 1454, 1364, 1279, 1258, 1249, and 1188; ^{1}H NMR: (500 MHz, $CDCl_3$) δ_H 1.27 (6H, s, H_{18}), 1.28 (6H, s, H_{18}), 1.67 (4H, s, $H_{12\ and\ 13}$), 2.08 (3H, d, *J* 1.0, H_{19}), 5.76 (1H, s, H_2), 6.28 (1H, d, *J* 16.0, H_5), 7.23 (1H, dd, *J* 1.5 and 8.0, H_{17}), 7.26 (1H, d, *J* 8.0, H_{16}), 7.44 (1H, d, *J* 1.5, H_9), 8.10 (1H, d, *J* 16.0, H_4); ^{13}C NMR: (126 MHz, $CDCl_3$) δ_C 20.9 (C_{19}), 31.9 (C_{18}), 32.0 (C_{18}), 34.5 ($C_{11/14}$), 34.6 ($C_{11/14}$), 35.1 ($C_{12/13}$), 35.2 ($C_{12/13}$), 88.1 (C_6), 97.1 (C_7), 116.8 (C_5), 117.6 (C_2), 120.1 (C_8), 126.9 (C_{16}), 129.1 (C_{17}), 130.5 (C_9), 137.2 (C_4), 145.4 (C_{10}), 146.3 (C_{15}), 152.1 (C_3), 170.5 (C_1); *m/z* (ES) 321.1860 (M^-, $C_{22}H_{26}O_2$, requires 321.1860), 260, 186, 159 and 91; Anal. Calcd for $C_{22}H_{26}O_2$: C, 81.95; H, 8.13. Found: C, 80.95; H, 8.13.

(2*E*,4*E*)-2-Methyl-7-(5,5,8,8-tetramethyl-5,6,7,8-tetrahydro-naphthalen-2-yl)-hepta-2,4-dien-6-ynoic acid **54**

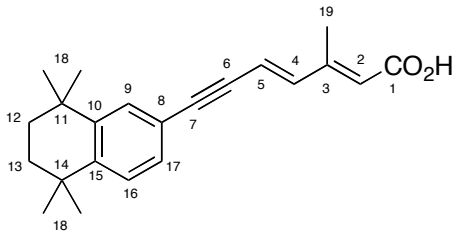

(2*E*,4*E*)-2-Methyl-7-(5,5,8,8-tetramethyl-5,6,7,8-tetrahydro-naphthalen-2-yl)-hepta-2,4-dien-6-ynoic acid methyl ester (510 mg, 1.5 mmol), was dissolved in a THF water mixture (3:1, 20 mL) followed by the addition of lithium hydroxide (250 mg, 5.9 mmol). The mixture was stirred at room temperature for 48 hours in the absence of light after which, the reaction was judged to be complete by TLC. The mixture was then acidified to pH 1 by the addition of 20% hydrochloric acid, and extracted with diethyl ether (2 × 20 mL). The sample was concentrated under vacuum to give the crude as a yellow powder. This was re-crystallised from acetonitrile to yielded the product as a bright yellow crystalline solid (394 mg, 82%); m.p. 205.1-206.7 °C; ν_{max}/cm^{-1} 2500-3500 (br OH), 2194 (alkyne), 1679 (C=O), 1604 (C=C), 1488, 1459, 1255 and 1185; ^{1}H NMR: **(**700 MHz, $CDCl_3$) δ_H 1.27 (6H, s, H_{18}), 1.28 (6H, s, H_{18}), 1.68 (4H, s, $H_{12\ and\ 13}$), 2.32 (3H, d, *J* 1.0, H_{19}), 5.87 (1H, s, H_2), 6.29 (1H, d, *J* 16.0, H_5), 6.73 (1H, d, *J* 16.0, H_4), 7.21 (1H, dd, *J* 1.5 and 8.0, H_{17}), 7.27 (1H, d, *J* 8.0, H_{16}), 7.41 (1H, d, *J* 1.5, H_9); ^{13}C NMR**:** (126 MHz, $CDCl_3$) δ_C 13.6 (C_{19}), 31.9 (C_{18}), 32.0 (C_{18}), 34.4 ($C_{11/14}$), 34.6 ($C_{11/14}$), 35.1 ($C_{12/13}$), 35.1 ($C_{12/13}$), 87.5 (C_6), 96.6 (C_7), 115.6 (C_5), 119.9 (C_2), 120.0 (C_8), 127.0 (C_{16}), 129.0 (C_{17}), 130.3 (C_9), 143.5 (C_4), 145.4 (C_{10}), 146.4 (C_{15}), 153.7 (C_3), 172.0 (C_1). *m/z* (ES) 321.1858 (M^-, $C_{22}H_{26}O_2$, requires 321.1860), 260, 186, 159 and 91; Anal. Calcd for $C_{22}H_{26}O_2$: C, 81.95; H, 8.13. Found: C, 81.87; H, 8.10.

(2*E*,4*E*,6*E*)-3-Methyl-7-(4,4,6-trimethyl-[1,2,3]-dioxaborinan-2-yl)-hepta-2,4,6-trienoic acid methyl ester **55**

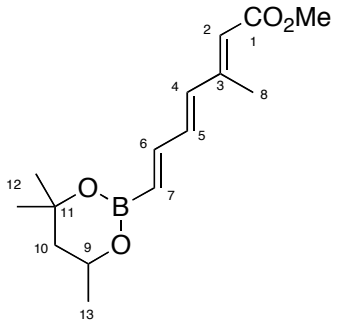

To a dried Schlenk tube under a positive pressure of argon was added palladium(II) acetate (16.5 mg, 0.1 mmol), silver(I) acetate (296 mg, 1.6 mmol), tri(*o*-tolyl)phosphine (45 mg, 0.1 mmol), methyl (2*E*,4*E*)-5-iodo-3-methylpenta-2,4-dienoate (0.37 g, 1.5 mmol) and acetonitrile (10 mL). The mixture was degassed using the freeze-pump-thaw method (2×) followed by the addition of 4,4,6-trimethyl-2-vinyl-1,3,2-dioxaborane (265 mg, 1.7 mmol). Finally the mixture was degassed by freeze-pump-thaw (2×) before being heated to 50 °C with vigorous stirring. After 22 hours the reaction was cooled to room temperature, diluted with ether (60 mL), passed through Celite™, washed with 5% hydrochloric acid (20 mL), water (40 mL) and brine (20 mL), dried ($MgSO_4$) and concentrated under vacuum. The product was purified by silica gel column chromatography (ethyl acetate: petroleum ether, 1:9) to give the product as a pale yellow oil (274 mg, 67%). ν_{max}/cm^{-1} 2973, 1711, 1614, 1391, 1303, 1237, and 1150; ^{1}H NMR (700 MHz, $CDCl_3$) δ_H 1.28 (3H, d, *J* 6.0, H_{13}), 1.31 (3H, s, H_{12}), 1.31 (3H, s, H_{12}), 1.51 (1H, t, *J* 14.0, H_{10}), 1.80 (1H, dd, *J* 14.0 and 3.0, H_{10}), 2.30 (3H, s, H_8), 3.71 (3H, s, O*Me*), 4.21-4.27 (1H, m, H_9), 5.68 (1H, d, *J* 17.0, H_4), 5.81 (1H, s, H_2), 6.36 (1H, d, *J* 17.0, H_7), 6.63 (1H, dd, *J* 17.0 and 11.0, H_6) and 6.99 (1H, dd, *J* 17.0 and 11.0, H_5); ^{13}C NMR (176 MHz, $CDCl_3$) δ_C 13.9 (C_8), 23.3 (C_{13}), 28.3 (C_{12}), 31.4 (C_{12}), 46.1 (C_{10}), 51.2 (OMe), 65.1 (C_9), 71.1 (C_{11}), 119.9 (C_2), 130.0-132.0 (C_7), 136.6 (C_6), 137.9 (C_4), 146.0 (C_5), 152.6 (C_3) and 167.5 (C_1); *m/z* (ES) 278.1802 (M, $C_{15}H_{24}BO_4$, requires 278.1798). 190, 174, 162, 144, 136, 58, 52 and 44.

(2*E*,4*E*,6*E*)-7-Iodo-3-methyl-hpta-2,4,6-trienoic acid methyl ester **56**

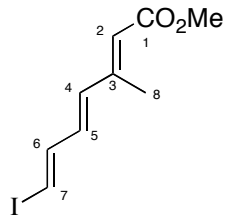

To a dried Schlenk tube under a positive pressure of argon was added (2*E*,4*E*,6*E*)-3-methyl-7-(4,4,6-trimethyl-[1,2,3]-dioxaborinan-2-yl)-hepta-2,4,6-trienoic acid methyl ester (0.2 g, 0.7 mmol) in dry tetrahydrofuran (5 mL) The mixture was cooled to -78 ^{o}C in the absence of light, followed by the addition of sodium methoxide (1.8 mL of a 0.5 M solution in methanol, 0.9 mmol). After 30 minutes iodine monochloride (1.2 mL of a 0.5 M solution in DCM, 1.2 mmol) was added and stirred for 1 hour. The reaction was warmed to room temperature, diluted with diethyl ether (30 mL), washed with sodium metabisulphite (30 mL), water (30 mL), and brine (30 mL), dried ($MgSO_4$) and concentrated to give an orange oil. Purification by silica gel chromatography (ethyl acetate: petroleum ether, 1:9, cooled to 0 °C) yielded the product as a pale yellow oil (131 mg, 65%). ν_{max}/cm^{-1} 2946 (Sp^3 C-H), 1710 (C=O), 1609 (C=C), 1557, 1433 (Sp^3 C-H), 1390, 1357, 1238, 1189 and 1152; ^{1}H NMR **(**500 MHz, $CDCl_3$) δ_H 2.31 (3H, d, *J* 1.0, C_8), 3.73 (3H, s, O*Me*), 5.87 (1H, s, H_2), 6.28 (1H, d, *J* 15.0, H_4), 6.51 (1H, dd, *J* 15.0 and 11.0, H_5), 6.62 (1H, d, *J* 15.0, H_7), and 7.16 (1H, dd, *J* 15.0 and 11.0, H_6); ^{13}C NMR (126 MHz, $CDCl_3$) δ_C 13.8 (C_8), 51.4 (OMe), 83.4 (C_7), 120.7 (C_2), 133.8 (C_5), 136.3 (C_4), 145.0 (C_6), 151.8 (C_3), 167.5 (C_1); *m/z* (ES) 277.9799 (M, $C_9H_{11}IO_2$, requires 277.9798). 247, 219, 127, 91, 65 and 50.

(2*E*,4*E*,6*E*)-3-Methyl-9-(5,5,8,8-tetramethyl-5,6,7,8-tetrahydro-naphthalen-2-yl)-nona-2,4,6-trien-8-ynoic acid methyl ester **57**

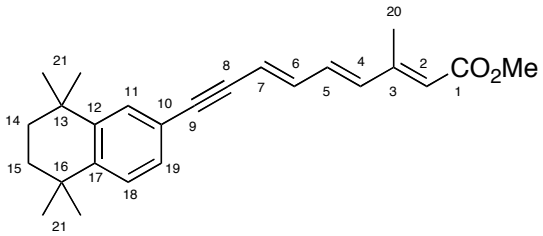

(2*E*,4*E*,6*E*)-7-Iodo-3-methyl-hpta-2,4,6-trienoic acid methyl ester (130 mg, 0.467 mmol), 6-ethynyl-1,1,4,4-tetramethyl-1,2,3,4-tetrahydronaphthalene (120 mg, 0.565 mmol) and triethylamine (5 mL) were added to a dried Schlenk tube and the mixture degassed using the freeze-pump-thaw method (3×). Palladium(II) acetate (4.5 mg, 0.02 mmol), triphenyl phosphine (10.5 mg, 0.04 mmol) and copper(I) iodide (7.6 mg, 0.04 mmol) were then added and the mixture degassed by freeze-pump-thaw (3×) and stirred at room temperature for 5 hours. The reaction was diluted with ether (60 mL), passed through Celite™, washed with 5% hydrochloric acid (2 × 20 mL), brine (20 mL), dried ($MgSO_4$) and concentrated under vacuum to give an orange oil. Purification by silica gel column chromatography (ethyl acetate: petroleum ether, 5:95) yielded the product as a pale yellow oil (122 mg, 72%).ν_{max}/cm^{-1} 2955, 2181, 1709, 1604, 1435, 1358, 1240, and 1153; ^{1}H NMR **(**700 MHz, $CDCl_3$) δ_H 1.27 (6H, s, H_{21}), 1.28 (6H, s, H_{21}), 1.67 (4H, s, $H_{14\ and\ 15}$), 2.31 (3H, s, H_{20}), 3.71 (3H, s, OMe), 5.82 (1H, s, H_2), 5.99 (1H, d, *J* 15.0, H_7), 6.34 (1H, d, *J* 15.0, H_4), 6.67 (1H, dd, *J* 15.0 and 11.0, H_5), 6.74 (1H, dd, *J* 15.0 and 11.0, H_6), 7.19 (1H, dd, *J* 8.0 and 1.5, H_{19}), 7.27 (1H, d, *J* 8.0, H_{18}), 7.39 (1H, d, *J* 1.5, H_{11}); ^{13}C NMR (176 MHz, $CDCl_3$) δ_C 13.9 (C_{20}), 31.9 (C_{21}), 31.9 (C_{21}), 34.6 ($C_{13/16}$), 34.6 ($C_{13/16}$), 35.1 ($C_{14/15}$), 35.1 ($C_{14/15}$), 51.3 (OMe), 88.2 (C_8), 95.5 (C_9), 98.8 (C_3), 115.0 (C_7), 120.2 (C_2), 120.4 (C_{10}), 127.0 (C_{18}), 128.8 (C_{19}), 130.1 (C_{11}), 134.0 (C_5), 137.5 (C_4), 140.6 (C_6), 145.3 (C_{12}), 146.1 (C_{17}), 167.5 (C_1); *m/z* (ES) 363.2322 (M+H, $C_{25}H_{31}O_2$, requires 363.2319). 331, 289 and 215.

(2*E*,4*E*,6*E*)-3-Methyl-9-(5,5,8,8-tetramethyl-5,6,7,8-tetrahydro-naphthalen-2-yl)-nona-2,4,6-trien-8-ynoic acid **58**

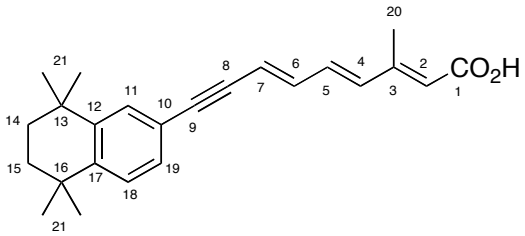

(2*E*,4*E*,6*E*)-3-Methyl-9-(5,5,8,8-tetramethyl-5,6,7,8-tetrahydro-naphthalen-2-yl)-nona-2,4,6-trien-8-ynoic acid methyl ester (120 mg, 0.331 mmol) was added to a stirred solution of lithium hydroxide (42 mg, 0.993 mmol) in a tetrahydrofuran water mixture (3:1, 10 mL) at 4 °C. After the reaction was judged to be complete by TLC the reaction mixture was acidified to pH 1/2 by the addition of 20% hydrochloric acid, extracted with diethyl ether (20 mL), dried ($MgSO_4$) and concentrated to give an orange oil. Purification by silica gel chromatography (petroleum ether: ethyl acetate, 9:1) yielded the product as a yellow solid (100 mg, 87%) in a ratio of two isomers (1:0.4). ^{1}H NMR **(**700 MHz, $CDCl_3$) δ_H 1.26 (6H, s, H_{21}), 1.27 (6H, s, H_{21}), 1.67 (4H, s, $H_{14\ and\ 15}$), 2.32 (3H, s, H_{20}), 5.85 (1H, s, H_2), 6.01 (1H, d, *J* 14.0, H_7), 6.36 (1H, d, *J* 14.0, H_4), 6.68-6.77 (2H, m, $H_{5\ and\ 6}$), 7.19 (1H, dd, *J* 8.0 and 1.5, H_{19}), 7.28 (1H, d, *J* 8.0, H_{18}), 7.39 (1H, d, *J* 1.5, H_{11}). ^{13}C NMR (176 MHz, $CDCl_3$) δ_C 14.1 (C_{20}), 31.9 (C_{21}), 31.9 (C_{21}), 32.0 (C_{21}), 34.4 ($C_{13/16}$), 34.6 ($C_{13/16}$), 35.1 ($C_{14/15}$), 35.1 ($C_{14/15}$), 88.1 (C_8), 95.8 (C_9), 99.0 (C_3), 115.6 (C_7), 119.4 (C_2), 120.2 (C_{10}), 126.9 (C_{18}), 128.8 (C_{19}), 130.2 (C_{11}), 134.8 (C_5), 137.2 (C_4), 140.5 (C_6), 145.4 (C_{12}), 146.1 (C_{17}), 154.4 (C_1); *m/z* (ES) 347.2016 (M-H, $C_{24}H_{27}O_2$, requires 347.2017).

4-[Methyl-(2-phenyl-thiazol-4-yl)-amino]-benzoic acid ethyl ester **60**

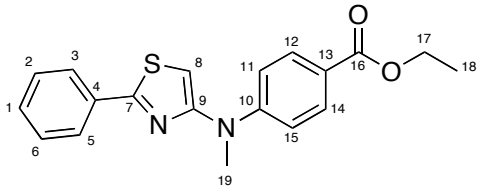

4-(2-Phenyl-thiazol-4-ylamino)-benzoic acid ethyl ester (0.10 g, 0.3 mmol) was added to a suspension of NaH (20 mg, 0.5 mmol) in dry THF (5 mL) at 0 ^{o}C and stirred for 10 minutes. Methyl iodide (0.71 g, 5.0 mmol) was then added and stirred for 20 minutes. The reaction mixture was diluted with ethyl acetate (40 mL), washed with brine (40 mL), dried ($MgSO_4$), filtered and concentrated under vacuum. Purification by flash column chromatography (ethyl acetate: hexanes, 1:7), gave an off-white solid. Re-crystallisation from toluene gave the product as a bright yellow solid (0.86 g, 83%). All spectral and analytical properties were identical to those reported in the literature.[250] ν_{max}/cm^{-1} 3102, 1693, 1604, 1509, 1277, 1184 and 1103; ^{1}H NMR (500 MHz, $CDCl_3$) δ 1.38 (3H, t, *J* 7.0, CH_3), 3.52 (3H, s, CH_3), 4.34 (2H, q, *J* 7.0, CH_2), 6.67 (1H, s, H_8), 7.12 (2H, dd, *J* 9.0, H_{11} H_{15}), 7.43 (3H, m, H_1 H_2 H_6), 7.95 (4H, m, H_3 H_5 H_{12} H_{14}); ^{13}C NMR (126 MHz, $CDCl_3$) 14.7 (C_{18}), 39.3 (C_{19}), 60.7 (C_{17}), 102.9 (C_8), 116.3 (C_{11} C_{15}), 121.8 (C_{13}), 126.4 (C_3 C_5), 129.2 (C_2 C_6), 130.4 (C_1), 131.0 (C_{12} C_{14}), 133.7 (C_4), 151.5 (C_{10}), 157.2 (C_9), 166.2 (C_7), 166.9 (C_{16}); *m/z* (ES) 339.1162 (M+H, $C_{19}H_{19}O_2N_2S_1$, requires 339.1162).

4-(2-Chloro-acetylamino)-benzoic acid ethyl ester **61**

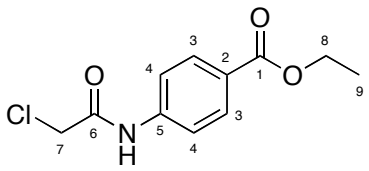

Chloroacetic acid (2.00 g, 21.0 mmol), benzocaine (3.3 g, 20.0 mmol) and boric acid (63 mg, 1.0 mmol) were dissolved in toluene (100 mL) and heated to reflux using Dean-Stark apparatus. After 96 hours, the reaction was cooled to room temperature, concentrated under vacuum, dissolved in diethyl ether (150 mL), washed with 5% hydrochloric acid (150

mL), saturated sodium hydrogen carbonate (150 mL), and brine (100 mL), dried ($MgSO_4$), and concentrated to give a white solid. Re-crystallisation from toluene yielded the product as a white fluffy solid (3.24 g, 67%); m.p. 121.1-122.4 °C; ν_{max}/cm^{-1} 3343, 2985, 2904, 1683, 1598, 1534, 1404 and 1272; ^1H NMR (700 MHz, $CDCl_3$) δ 1.40 (3H, t, *J* 7.0, CH_3), 4.21 (2H, s, CH_2), 4.37 (2H, q, *J* 7.0, CH_2), 7.65 (2H, d, *J* 9.0, H_4), 8.05 (2H, d, *J* 9.0, H_3), 8.36 (1H, brs, NH); ^{13}C NMR (176 MHz, $CDCl_3$) 14.5 (C_9), 43.1 (C_7), 61.2 (C_8), 119.3 (C_4), 127.2 (C_2), 131.1 (C_3), 140.8 (C_5), 164.1 (C_6), 166.1 (C_1); *m/z* (ES) 242 (M^+) and 228; Anal. Calcd. for $C_{11}H_{12}ClNO_3$: C, 54.67; H, 5.00; N, 5.86. Found: C, 54.75; H, 4.93; N, 5.56.

4-(2-Phenyl-thiazol-4-ylamino)-benzoic acid ethyl ester **63**

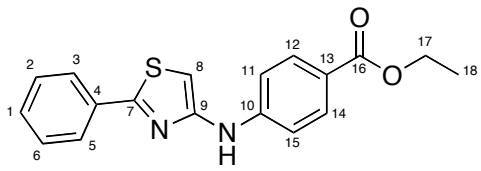

To a solution of thiobenzamide (0.60 g, 4.4 mmol) in DMF (5 mL) was added ethyl 4-(2-chloroacetoamido)benzoate (1.03 g, 4.3 mmol). The reaction was stirred at 80 ^oC for 12 hours under argon and the DMF was removed under vacuum, to yield a brown solid. Re-crystallisation from IPA, followed by silica gel column chromatography (ethyl acetate: hexanes, 1:1), and subsequent re-crystallisation from IPA yielded the product as a green solid (0.85 g, 65%); ^1H NMR (500 MHz, $CDCl_3$) δ 1.40 (3H, t, *J* 7.0, CH_3), 4.37 (2H, q, *J* 7.0, CH_2), 6.63 (1H, s, H_8), 6.95 (1H, broad singlet, NH), 7.17 (2H, d, *J* 8.8, H_{11} H_{15}), 7.46 (3H, m, H_1 H_2 H_6), 7.94 (2H, m, H_3 H_5), 8.01 (2H, d, *J* 8.8, H_{12} H_{14}); ^{13}C NMR (126 MHz, $CDCl_3$) 14.7 (C_{18}), 60.8 (C_{17}), 95.5 (C_8), 115.0 (C_{11} C_{15}), 122.3 (C_{13}), 126.4 (C_3 C_5), 129.3 (C_2 C_6), 130.5 (C_1), 131.7 (C_{12} C_{14}), 133.4 (C_4), 146.5 (C_{10}), 151.8 (C_9), 166.3 (C_7), 166.7 (C_{16}).

5,5,8,8-Tetramethyl-5,6,7,8-tetrahydronaphthalene-2-carboxylic acid methyl ester **68**

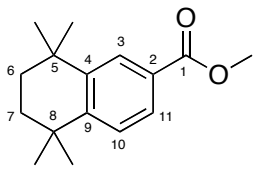

Magnesium turnings (110 mg, 4.6 mmol) were heated under argon followed by the dropwise addition of 6-iodo-1,1,4,4-tetramethyl-1,2,3,4-tetrahydronaphthalen (1.00 g, 3.2 mmol) in tetrahydrofuran (20 mL), and heated to reflux followed by the addition of 1,2-dibromoethane (0.20 g, 1.1 mmol). After initiation the remaining iodide was added dropwise over a further 30 minutes. Upon complete addition the reaction was kept at reflux for 30 minutes, cooled to room temperature followed by dropwise addition to a stirred solution of methyl chloroformate (0.42 g, 4.8 mmol) at -78 ^{o}C under argon. After 30 minutes the reaction mixture was warmed to room temperature, washed with 5% hydrochloric acid (40 mL), brine (40 mL), dried ($MgSO_4$), and concentrated under vacuum. Purification by silica gel column chromatography (ethyl acetate: petroleum ether, 15:85) yielded the product as a clear oil. All spectral and analytical properties were identical to those reported in the literature.[367]; ν_{max}/cm^{-1} 2957, 2930, 2864, 1719, 1254, 1191 and 1116; ^{1}H NMR (700 MHz, $CDCl_3$) δ 1.29 (6H, s, 2xCH_3), 1.32 (6H, s, 2xCH_3), 1.70 (4H, s, 2xCH_2), 3.89 (3H, s, OCH_3), 7.36 (1H, d, *J* 8.0, H_{10}), 7.78 (1H, dd, *J* 8.0 & 1.5, H_{11}), 8.03 (1H, d, *J* 1.5, H_3); ^{13}C NMR (176 MHz, $CDCl_3$) 31.9 (2xCH_3), 32.0 (2xCH_3), 34.6 (CH_2), 34.8 (CH_2), 52.0 (OCH_3), 126.8 (C_{11}), 126.9 (C_{10}), 127.7 (C_2), 128.3 (C_3), 145.3 (C_4), 150.5 (C_9), 167.5 (C_1); *m/z* (ES+) 247.1694 (M^+, $C_{16}H_{23}O_2$, requires 247.1693) and 195.

5,5,8,8-Tetramethyl-5,6,7,8-tetrahydronaphthalene-2-carboxylic acid **69**

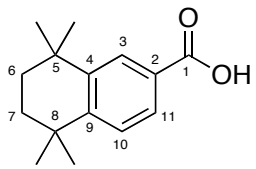

5,5,8,8-Tetramethyl-5,6,7,8-tetrahydronaphthalene-2-carboxylic acid methyl ester (5.00 g, 20.3 mmol) was dissolved in a 1:1 mixture of tetrahydrofuran and water (100 mL), followed by the addition of lithium hydroxide (5.10 g, 121.8 mmol). The reaction was stirred at room temperature for 72 hours. Diluted with 10% sodium hydroxide (150 mL), extracted with diethyl ether (2 × 150 mL), the aqueous layer acidified to pH 1/2 with 20% hydrochloric acid, extracted with diethyl ether (2 × 150 mL), dried ($MgSO_4$) and concentrated under vacuum to yield a white solid (3.7 g, 79%); m.p. 209.4-210.9 °C; ν_{max}/cm^{-1} 2500-3500 (br) 1682, 1608, 1455, 1423, 1361, 1311, 1292 and 1266; ^{1}H NMR (500 MHz, $CDCl_3$) δ 1.31 (6H, s, 2xCH_3), 1.32 (6H, s, 2xCH_3), 1.71 (4H, s, 2xCH_2), 7.40 (1H, d, *J* 8.3, H_{10}), 7.84 (1H, dd, *J* 8.3 & 1.8, H_{11}), 8.08 (1H, d, *J* 1.8, H_3); ^{13}C NMR (126 MHz, $CDCl_3$) 31.9 (2xCH_3), 32.0 (2xCH_3), 34.6 ($C_{5/8}$), 35.0 ($C_{5/8}$), 35.0 ($C_{6/7}$), 35.1 ($C_{6/7}$), 126.7 (C_2), 127.1 (C_{10}), 127.4 (C_{11}), 129.1 (C_3), 145.6 (C_4), 151.7 (C_9), 172.4 (C_1); *m/z* (ES) 255.1358 (M+Na, $C_{15}H_{20}O_2Na_1$, requires 255.1356), 218, 176.

5,5,8,8-Tetramethyl-5,6,7,8-tetrahydronaphthalene-2-carboxylic acid amide **70**

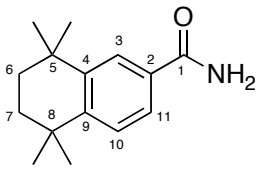

5,5,8,8-Tetramethyl-5,6,7,8-tetrahydronaphthalene-2-carboxylic acid (2.00 g, 8.6 mmol) was dissolved in toluene (150 mL) followed by the addition of a catalytic amount of dimethyl formamide (0.2 mL) and oxalyl chloride (1.30 g, 10.4 mmol). The reaction mixture was stirred at room temperature for 10 minutes, before being concentrated under vacuum, to yield off white oil. Addition of a large excess of 35% aqueous ammonia solution (50 mL) at –10 ^{o}C lead to the formation of a white precipitate. The reaction mixture was warmed to

room temperature, diluted with brine (50 mL), extracted with diethyl ether (2 × 50 mL), dried ($MgSO_4$) and concentrated under vacuum to yield a white solid (1.80 g, 88%); m.p. 148.2-149.4 °C; ν_{max}/cm^{-1} 3437, 3170, 2954, 2922, 2863, 1641, 1613, 1553, 1395, 1277 and 1141; ^1H NMR (700 MHz, $CDCl_3$) δ 1.27 (6H, s, 2xCH_3), 1.29 (6H, s, 2xCH_3), 1.69 (4H, s, 2xCH_2), 6.00 (1H, bs, NH), 6.13 (1H, bs, NH), 7.35 (1H, d, *J* 8.2, H_{10}), 7.49 (1H, dd, *J* 8.2 & 2.0, H_{11}), 7.81 (1H, d, *J* 2.0, H_3); ^{13}C NMR (176 MHz, $CDCl_3$) 31.7 (2xCH_3), 31.7 (2xCH_3), 34.4 (C_5), 34.5 (C_8), 34.8 ($C_{6/7}$), 34.9 ($C_{6/7}$), 124.1 (C_{11}), 126.1 (C_3), 126.8 (C_{10}), 130.5 (C_2), 145.5 (C_4), 149.4 (C_9), 169.8 (C_1); *m/z* (ES+) 232.1696 (M+H, $C_{15}H_{22}ON$, requires 232.1696).

5,5,8,8-Tetramethyl-5,6,7,8-tetrahydro-naphthalene-2-carbothioic acid amide **71**

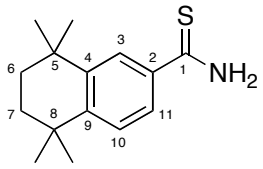

5,5,8,8-Tetramethyl-5,6,7,8-tetrahydronaphthalene-2-carboxylic acid amide (200 mg, 0.9 mmol), and Lawessons Reagent (199 mg, 0.5 mmol) were stirred at room temperature in dry toluene under argon for 24 hours. The reaction mixture was concentrated under vacuum, followed by purification by flash silica gel column chromatography (dichloromethane, 100%) to yield the titled compound as a yellow solid (200 mg, 97%); m.p. 174.9-176.3 °C; ν_{max}/cm^{-1} 3380, 3276, 3150, 2956, 2918, 2855, 2368, 2012, 1638, 1615,1458, 1406, 1321, 1280, 1263 and 1155; ^1H NMR (500 MHz, $CDCl_3$) δ 1.28 (6H, s, 2xCH_3), 1.31 (6H, s, 2xCH_3), 1.69 (4H, s, 2xCH_2), 7.23 (1H, bs, NH), 7.33 (1H, d, *J* 8.3 H_{10}), 7.59 (1H, dd, *J* 8.3 & 2.1, H_{11}), 7.82 (1H, bs, NH), 7.84 (1H, d, *J* 2.1, H_3); ^{13}C NMR (126 MHz, $CDCl_3$) 31.9 (2xCH_3), 32.0 (2xCH_3), 34.7 (C_5), 34.8 (C_8), 35.0 ($C_{6/7}$), 35.1 ($C_{6/7}$), 124.1 (C_{11}), 125.9 (C_3), 127.1 (C_{10}), 136.7 (C_2), 145.5 (C_4), 150.0 (C_9), 203.3 (C_1); *m/z* (ES+) 248.1468 (M^+, $C_{15}H_{22}N_1S_1$, requires 248.1467).

5,5,8,8-Tetramethyl-5,6,7,8-tetrahydro-naphthalene-2-carbonitrile **72**

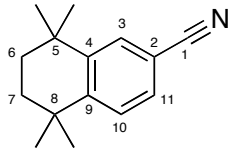

5,5,8,8-Tetramethyl-5,6,7,8-tetrahydronaphthalene-2-carboxylic acid amide (200 mg, 0.9 mmol), and Lawessons Reagent (199 mg, 0.5 mmol) were stirred at reflux in dry toluene under argon for 2 hours. The reaction mixture was cooled to room temperature, concentrated under vacuum, followed by purification by silica gel flash column chromatography (hexane: dichloromethane, 2:3) to yield the product as a white crystalline solid (121 mg, 57%); m.p. 68.3-68.9 °C; ν_{max}/cm^{-1} 2964, 2919, 2855, 2226, 1604, 1489, 1455, 1397, 1361, 1276 and 1183; ^{1}H NMR (700 MHz, $CDCl_3$) δ 1.27 (12H, s, 4xCH_3), 1.68 (4H, s, 2xCH_2), 7.37 (2H, d, *J* 0.7 H_{10} & H_{11}), 7.58 (1H, s, H_3); ^{13}C NMR (176 MHz, $CDCl_3$) 31.5 (2xCH_3), 31.6 (2xCH_3), 34.3 (C_5), 34.5 (C_8), 34.7 (C_6 & C_7), 109.3 (C_2), 119.5 (C_1), 127.5 (C_{10}), 128.8 (C_{11}), 130.8 (C_3), 146.3 (C_4), 150.6 (C_9); *m/z* (EI+) 213.1512 (M+, $C_{15}H_{19}N$, requires 213.1512).

4-Amino-2-fluorobenzoic acid ethyl ester **75**

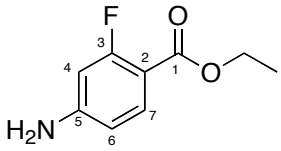

To a stirred solution of 4-amino-2-fluorobenzoic acid (0.50 g, 3.2 mmol) in ethanol (25 mL), cooled to 0 ^{o}C, was added thionyl chloride (0.58 g, 4.8 mmol) dropwise over 10 minutes. The reaction was heated to reflux for 18 hours, cooled to room temperature, and the ethanol removed under vacuum. The solid was re-dissolved in ethyl acetate (100 mL), washed with sodium hydrogen carbonate (100 mL), dried ($MgSO_4$), and concentrated under vacuum to give the desired compound as a white solid (550 mg, 93%). All spectral and analytical properties were identical to those reported in the literature.[368] m.p. 123.8-125.2 °C; ν_{max}/cm^{-1} 3421, 3337, 2984, 1689, 1630, 1609, 1569, 1366, 1346, 1266, 1248, 1146 and 1077; ^{1}H NMR (500 MHz, $CDCl_3$) δ 1.36 (3H, t, *J* 7.0, CH_3), 4.19 (2H, brs, NH_2), 4.32 (2H, q, *J* 7.0,

CH_2), 6.33 (1H, dd, *J* 13.0 & 2.5, H_4), 6.40 (1H, dd, *J* 8.5 & 2.5, H_6), 7.75 (1H, t, *J* 8.5, H_7); ^{13}C NMR (126 MHz, $CDCl_3$) δ 14.6 (CH_3), 60.8 (CH_2), 102.0 (d, *J* 26.0, C_4), 108.3 (d, *J* 10.0, C_2), 110.2 (C_6), 134.0 (d, *J* 2.5, C_7), 152.7 (d, *J* 12.0, C_5), 164.2 (d, *J* 258.0, C_3), 164.8 (d, *J* 4.0, C_1); ^{19}F NMR (376 MHz, $CDCl_3$) δ -108.1 (dd, *J* 13.5 & 8.5); *m/z* (ES+) 184.0766 (M^+, $C_9H_{11}O_2N_1F_1$, requires 184.0768) and 153; Anal. Calcd. for $C_9H_{10}FNO_2$: C, 59.01; H, 5.50; N, 7.65. Found: C, 59.00; H, 5.50; N, 7.57.

4-(2-Chloro-acetylamino)-2-fluoro-benzoic acid ethyl ester **76**

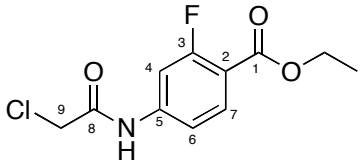

Chloroacetic acid (53 mg, 0.6 mmol), 4-amino-2-fluorobenzoic acid ethyl ester (98 mg, 0.5 mmol) and boric acid (2 mg, 0.1 mmol), were dissolved in toluene (20 mL) and heated to reflux using a Dean-Stark apparatus. After 56 hours the reaction was cooled to room temperature, concentrated under vacuum, dissolved in ether (40 mL), washed with 5% hydrochloric acid (40 mL), saturated sodium hydrogen carbonate (40 mL), and brine (40 mL), dried ($MgSO_4$), and concentrated to give an off-white solid. Re-crystallisation from toluene yielded the product as a white fluffy solid (90 mg, 64%); m.p. 111.9-113.9 °C; ν_{max}/cm^{-1} 3348, 2982, 2910, 1692, 1621, 1597, 1533, 1509, 1478, 1401, 1335, 1261, 1195, 1141 and 1087; ^1H NMR (500 MHz, $CDCl_3$) δ 1.38 (3H, t, *J* 7.0, CH_3), 4.20 (2H, s, CH_2), 4.37 (2H, q, *J* 7.0, CH_2), 7.25 (1H, d, *J* 8.0, H_6), 7.65 (1H, d, *J* 12.5, H_4), 7.93 (1H, t, *J* 8.0, H_7), 8.46 (1H, brs, NH); ^{13}C NMR (126 MHz, $CDCl_3$) δ 14.5 (CH_3), 43.1 (CH_2Cl), 61.6 (CH_2), 108.2 (d, *J* 28.0, C_4), 114.8 (d, *J* 4.0, C_6), 115.3 (d, *J* 10.0, C_2), 133.2 (d, *J* 2.0, C_7), 142.2 (d, *J* 12.0, C_5), 162.8 (d, *J* 260.0, C_3), 164.1 (d, *J* 4.0, C_1), 164.4 (C_8); ^{19}F NMR (376 MHz, $CDCl_3$) δ -106.0 (dd, *J* 12.5 & 8.0); *m/z* (ES-) 258 (M^-); Anal. Calcd. for $C_{11}H_{11}ClFNO_3$: C, 50.88; H, 4.27; N, 5.39. Found: C, 51.17; H, 4.29; N, 5.33.

4-[(2-Chloro-acetyl)-methyl-amino]-benzoic acid ethyl ester **80**

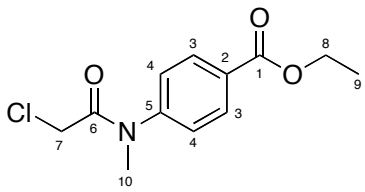

To a dry two-neck flask under argon was added 4-methylamino-benzoic acid ethyl ester (0.08 g, 0.4 mmol), in dry DCM (5 mL). The reaction mixture was cooled to − 78 ^{o}C, triethylamine (0.07 mL, 0.5 mmol) was added, followed by chloroacetyl chloride (0.04 mL, 0.5 mmol), dropwise. After 10 minutes the reaction was warmed to room temperature and stirred for 18 hours. The reaction mixture was evaporated, and purified by silica gel column chromatography (chloroform: ethyl acetate; 4:1) to yield the product as a white solid (0.06 g, 55 %); ^{1}H NMR (700 MHz, $CDCl_3$) δ 1.39 (3H, t, *J* 7.2, CH_3), 3.33 (3H, s, NCH_3), 3.85 (2H, s, CH_2), 4.39 (2H, q, *J* 7.2, CH_2), 7.32 (2H, d, *J* 8.5, H_4), 8.11 (2H, d, *J* 8.5, H_3); ^{13}C NMR (176 MHz, $CDCl_3$) 14.5 (C_9), 38.1 (C_{10}), 41.5 (C_7), 61.6 (C_8), 127.1/127.6 (C_4), 130.8 (C_2), 131.6/131.8 (C_3), 146.8 (C_5), 165.6 (C_1), 166.3 (C_6); *m/z* (EI) 257 (M+H), 206, 179, 150, 134 and 90.

4-Methylamino-benzoic acid ethyl ester **81**

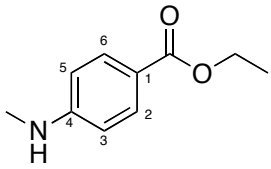

To a stirred solution of 4-methyl aminobenzoic acid (0.07 g, 0.5 mmol) in ethanol (5 mL), cooled to 0 ^{o}C, was added thionyl chloride (0.05 mL, 0.7 mmol) dropwise. The reaction was warmed to room temperature, followed by heating at reflux for 18 hours. Upon completion, the reaction was cooled to room temperature, and evaporated. The reaction mixture was re-dissolved in ethyl acetate (100 mL), washed with $NaHCO_3$ (50 mL), dried ($MgSO_4$), and concentrated under vacuum to yield the product as a white solid (0.08 g, 97 %); m.p. 65.5-66.5 ^{o}C (lit.[370] 66-67 ^{o}C); ^{1}H NMR (400 MHz, $CDCl_3$) δ 1.36 (3H, t *J* 7.1, CH_3), 2.87 (3H, s, NCH_3), 4.23 (1H, bs, NH), 4.31 (2H, q, *J* 7.1, CH_2), 6.54 (2H, d, *J* 9.0 Ar 3.0 & 5.0), 7.88 (2H, d, *J*

9.0, Ar 2.0 & 6.0); ^{13}C NMR (100 MHz, $CDCl_3$) 14.5 (CH_3), 30.2 (NCH_3), 60.1 (CH_2), 111.1 (C_3 C_5), 118.6 (C_1), 131.5 (C_2 C_6), 152.8 (C_4), 166.9 (C=O); *m/z* (ES) 180.1018 (M+H), $C_{10}H_{14}O_2N_1$, requires 180.1019) and 152.

4-Methylamino-benzoic acid **83**

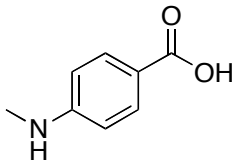

To a suspension of Pd/C (0.29 g, 0.3 mmol) in 2-propanol (20 mL) was added ammonium formate (0.87 g, 13.8 mmol) dissolved in water (2 mL). The reaction mixture was stirred for 1 minute to activate the Pd/C. 4-Aminobenzoic acid (0.38 g, 2.8 mmol) and para-formaldehyde (0.83 g, 27.5 mmol) were then added, and the reaction mixture stirred at room temperature for 18 hours. The reaction mixture was filtered through Celite™, concentrated under vacuum, re-dissolved in ethyl acetate, washed with brine, dried ($MgSO_4$), and concentrated under vacuum. Purification by silica gel column chromatography (chloroform: ethyl acetate; 2:1) yielded the product as a white solid (0.137 g, 33 %); m.p. 152-153 ^{o}C (lit.[369] 151.5-152.5 ^{o}C). All spectral properties were identical to those reported in the literature.[369] ^{1}H NMR (500 MHz, $CDCl_3$) δ 2.91 (3H, s, CH_3), 6.57 (2H, d, *J* 8.8 Ar), 7.94 (2H, d, *J* 8.8, Ar).

7.2 Biological Procedures

7.2.1 General Cell Culture

Cells were cultured in a humidified atmosphere of 5% CO_2 in air at 37 °C, in a CO_2 incubator (Sanyo). Cultures were handled in using aseptic techniques in a class (II) bio-safety flow hood (ESCO Airstream or BSC-EN). Cultures incubated with retinoid compounds were handled in reduced light conditions to account for the instability of ATRA. All plastic-wear was purchased from Nunc or Becton Dickinson unless otherwise stated. Phase contrast images of growing cultures were obtained using a light microscope (Nikon Diaphot 300) and photomicrographs captured using digital photography (Nikon). H_2O refers to high purity water unless otherwise stated. Precise media recipes and culture techniques are described here on in under specific cell line procedures.

7.2.2 Test Compound Stocks

In preparation for use in cell culture experiments, stock solutions of synthetic compounds, ATRA (Sigma) and 13cRA (Sigma) were prepared in DMSO (Sigma) to concentrations of 10 mM. Aliquotted stock solutions were stored at – 80 ^{o}C in the dark.

7.2.3 F9 Cell Procedures

The cells used were a kind gift from Prof. Colin A. B. Jahoda, Durham University.

7.2.3.1 Tissue culture

F9 cells were cultured in Dulbecco's Modified Eagle's Medium (DMEM) (Sigma) supplemented with 50 mL of 10% fetal calf serum (FCS) (Gibco), 5 mL of 2 mM L-Glutamine, 1.1 mL of Penicillin/Streptomycin solution (200 active units) (Gibco) and 0.5 μg/ml Kanamycin. Cultures were passaged using 0.25% trypsin EDTA solution (Cambrex).

7.2.3.2 Lac Z Staining Protocol

Cells were grown in 24-well culture plates seeded at 400,000 cells/well in 0.8 mL of standard growth media. After 6 hours the media is changed with the addition of any test compounds being added to the media. After 18 hours incubation the cultures were fixed in ice-cold 4% paraformaldehyde (Sigma) in phosphate-buffered saline (PBS) for 1 hour at 4 ^{o}C, followed by three washes in rinse buffer (prepared from 2.36 g of Sodium Phosphate (Sigma), 0.038 g of Magnesium Chloride (Sigma), 20 mg of Sodium Deoxycholate (Sigma), 40 μL NP40S Tergitol Solution (Sigma), in PBS solution to a total volume of 200 mL at a pH of 7.3) for a minimum of 5 minutes. Cultures were immediately stained using freshly prepared staining solution (prepared from 25 μL of Potassium Ferricyanide from a 0.2 M stock, 25 μL of Potassium Ferrocyanide from a 0.2 M stock and 25 μL X-Gal from 40 mg/mL stock made up to 1 mL in Rinse Buffer) (250 μL per well) for 18 hours at room temperature in the absence of light.

7.2.4 TERA2.cl.SP12 Cell Procedures

7.2.4.1 Tissue Culture

Human pluripotent TERA2.cl.SP12 embryonal carcinoma stem cells were maintained under standard laboratory conditions as described by Przyborski.[209,211] In brief, cells were cultured in DMEM (Sigma) supplemented with 10% FCS (Gibco), 2mM L-glutamine and 100 active units each of penicillin and streptomycin (Gibco). Cultures were passaged using acid-washed glass beads (VWR) unless a single-cell suspension was required for counting, in which case a 0.25% trypsin EDTA (Cambrex) solution was used. Cultures intended for flow cytometric and RT-PCR analysis were set up in T25 flasks (Becton Dickinson) while 12-well plates (Nunc) were used for immunocytochemical studies and cell viability/apoptopic analysis.

7.2.4.2 MTS Cell Viability Assay

Cells were cultured on 24-well plates (Nunc). 50,000 cells per well were seeded and either cultured in proliferation media (control), or differentiation media containing compounds under investigation. Cells were cultured for up to 14 days, with samples analysed at 3, 7 and 14 day time points. For the assay 200 μl of MTS reagent, CellTiter 96 AQ_{ueous} One Solution Cell Proliferation Assay (Promega) was added to 1 mL of media per well. A control well containing no cells was also set up in an identical manner. The solutions were titurated then

incubated for 4 hours at 37 ^{o}C. The resulting colorimetric change was recorded as an absorbance, read at 490 nm on a Nanodrop Spectrophotometer ND-100™. All conditions were carried out in triplicate and were standardised against the no-cell control to remove any background absorbance.

7.2.4.3 Flow Cytometry

Flow cytometry analysis was carried out on live cells using antibodies recognising cell surface markers. The expression of markers indicative of the stem cell (SSEA-3 (University of Iowa Hybridoma Bank) and TRA-1-60 (generous gift from Prof. P. Andrews, University of Sheffield)) or neural cell (A2B5, R&D Systems) phenotype was determined to indicate the status of cellular differentiation by TERA2.cl.SP12 cells. Suspensions of single EC cells of their differentiated derivatives were formed by the addition of 1 mL 0.25% trypsin/EDTA solution. The cell suspension was divided accordingly for flow cytometry and RT-PCR (see later) analysis accordingly. Cells were added to a 96-well plate (0.2 x 10^6 cells per well) as a suspension in wash buffer (0.1% bovine serum albumin (BSA) in PBS) for incubation with primary (1:20 SSEA-3 and TRA-1-60, or 1:10 A2B5) and fluorescein isothiocyanate (FITC)-conjugated secondary antibody (Sigma, 1:100) as previously described. Labelled cells were analysed in a Guave EasyCyte™ Plus System (Millipore) flow cytometer. Thresholds determining the numbers of positively expressing cells were set against the negative control antibody P3X (used neat, generous gift from Prof. P. Andrews, University of Sheffield).

7.2.4.4 Real Time quantitative PCR (RT-PCR)

RT-PCR was carried out on cells immediately lysed after treatment with 0.25% trypsin/EDTA. Commercial RNA extraction kits and procedures (Qiagen) and reverse transcription procedures (Applied Biosystems) were followed. In brief, cells were lysed, homogenised using a 20-gauge needle, and passed through an RNeasy spin column. DNase digestion was carried out, before the RNA was extracted from the column as a suspension in RNase free water. Amounts of RNA extracted were determined using a Nanodrop Spectrophotometer ND-100™, followed by analysis on a 1% Agrose gel. Reverse transcription was then carried out using a high-capacity cDNA reverse transcription kit and a thermal cycler. cDNA was stored at – 20 ^{o}C before analysis by RT-PCR. The expression of specific genes indicative of pluripotency, Nanog (Hs02387400_g1, Applied Biosystems) and Oct-4 (Hs03005111_g1,

Applied Biosystems) and neural and ventral phenotype, Pax6 (Hs00240871_m1, Applied Biosystems) were investigated and quantified against GAPDH (4333764F, Applied Biosystems). RT-PCR analysis was done on an Applied Biosystems RT-PCR system.

7.2.4.5 Immunocytochemistry

Cells were grown in 12-well culture plates for immunocytochemical analysis. Confluent cultures of stem cells and their differentiated derivatives were fixed in ice-cold 4% paraformaldehyde (Sigma) in PBS for 30 minutes at room temperature, followed by three washes in PBS. Cell membranes were permeabilised by treatment with 1% Triton-X-100 (Sigma) in PBS for 10 minutes at room temperature. Non-specific binding of antibodies was blocked using a solution of 1% goat serum (Sigma) in PBS containing 0.2% Tween-20 (Sigma). Fixed cells were incubated with blocking solution on a bench-top shaker for 30 minutes at room temperature. Primary antibodies: β-III-Tubulin (Covance, 1:600); NF-200 (Sigma, 1:200) were diluted in blocking solution and incubated with the cells for 1 hour at room temperature. After washing (three times for a minimum of 15 minutes at room temperature in PBS) cells were incubated in FITC-conjugated secondary antibody (Alexafluor 488 (Molecular Probes, 1:600) and Cy3 (Jackson Labs, 1:600)) for 1 hour. After two washes in PBS for 15 minutes the cells were incubated with PBS containing Hoechst 33342 nuclear staining dye (Molecular Probes, 1:1000) for 15 minutes before the cells were stored in PBS. Imaging was performed on a fluorescent microscope under restricted light conditions (Nikon Diaphot 300). Fluorescence photomicrographs, including Hoecsht 33342, were acquired using the appropriate filter sets and customised digital camera (Nikon).

7.2.5 ReNcell VM Procedures

7.2.5.1 Cell culture

All plastic-ware was purchased from Nunc unless otherwise stated. Before use, plastic-wear was coated with laminin solution (Sigma) diluted in DMEM:F12 to 20 μg/ml. For coating of T75 flasks, 5 mL of diluted laminin solution was added per flask and incubated at 37 °C for at least 6 hours. Flasks were washed twice with media prior to use. ReNcell 197VM progenitor cells (Millipore) were cultured in serum free conditions using methods previously described by Donato *et al*.[57] Briefly, DMEM:F12 (1:1, Gibco) was supplemented with B27 (Invitrogen),

2 mM L-Glutamine (Sigma), 0.5 mL Gentamycin (Gibco), and 1 mL 50 mg/ml Heparin solution (Sigma). For proliferation, 20 ng/mL FGF and 20 ng/mL EGF were added to the media immediately prior to use. Cultures were passaged using 0.25% trypsin EDTA solution and trypsin action was inhibited with soy-bean trypsin inhibitor solution (Sigma).

7.2.5.2 Differentiation Protocol

Cultures were incubated with trypsin to obtain a single cell suspension as outlined above, and 100,000 cells/well were seeded into laminin-treated 12 well plates. Cultures were allowed to reach 75% confluency whereupon media was replaced with standard differentiation media, without (differentiation control) or with retinoid supplementation, as previously described by Christie *et al*.[59] Briefly, standard differentiation media was made up as described above, but without FGF of EGF. Initial experiments used retinoids at a single concentration of 1 μM. Subsequent concentration effects were investigated at 1 μM, 0.1 μM, 0.01 μM and 0.001 μM concentrations. Cultures were incubated for 7 days before being processed for further analysis.

7.2.5.3 Phase Contrast Microscopy

Phase contrast images of growing cultures were obtained using a light microscope (Nikon Diaphot 300) and photomicrographs captured using digital photography (Nikon).

7.2.5.4 Immunocytochemistry

Cell fixing was performed by incubation with ice-cold 4% PFA in PBS (Sigma) for 30 minutes at RT, followed by 3 washes with PBS. Cell membranes were permeablised by treatment with 1% Triton-X-100 (Sigma) in PBS for 10 minutes at room temperature. Non-specific binding of antibodies was blocked using a solution of 1% goat serum (Sigma) in PBS containing 0.2% Tween-20 (Sigma). Dilution of primary antibodies was carried out in blocking solution, and incubated with the cells for 1 hour at room temperature (β-III-Tubulin antibody (Covance) was diluted 1:600. NF-200 antibody (AbCam) was diluted 1:200. MAP2ab antibody (Sigma) was diluted 1:400). Cells were washed 3 times for 15 minutes in PBS followed by one hour incubation in the dark at RT with appropriately diluted FITC-conjugated (Alexafluor 488, diluted 1:600) or Cy3-conjugated (JacksonLabs, diluted 1:600) secondary antibody. A further 2 washes of PBS were carried out in the dark, followed by

incubation with 1 µg/mL Hoechst 33342 nuclear staining dye (Molecular Probes, diluted in PBS). Cultures were washed twice more in PBS, and left in the final wash for immediate imaging. Fixed and immunostained cultures were examined using a fluorescent microscope under restricted light conditions (Nikon Diaphot 300). Hoechst 33342 images and the corresponding fluorescent photomicrographs were collated and stored using the appropriate filter sets and an adapted digital camera (Nikon). Triplicate experiments were carried out for reproducibility.

7.2.6 Adult Hippocampal Progenitor Cells (AHPC)

7.2.6.1 Cell Culture

All plastic-ware was purchased from Nunc. Before use, plastic-ware was coated with poly-L-ornithine (Sigma) diluted in H_2O to 10 μg/mL for 12-24 hours at room temperature in a tissue culture hood. The culture-ware was then washed 2 times with sterile H_2O, followed by coating in laminin in sterile PBS at 5 μg/mL for 24 hours at 37 ^{o}C in an incubator. Excess laminin was then removed through aspiration, the flasks sealed and wrapped in cling film and stored at -20 ^{o}C for up to 6-8 months.

Before use the flasks were warmed to room temperature, and washed in PBS. Cells were cultured under serum free conditions at all times as outlined in protocols from the Salk Institute.[58,218] To expand the cell cultures proliferative media was used, consisting of DMEM/F12 (high glucose) (Gibco), supplemented with 1 x N2 supplement (Gibco), 2 mM L-glutamine (Sigma), 20 ng/mL bFGF (Sigma, just added before use) and 100 active units of penicillin/streptomycin (Gibco). To maintain optimum cultures, media was changed every 3 days, and cultures were passaged at ~90 % confluence. To passage cells, the media was aspirated, 1 mL trypsin-versene solution (Cambrex) added and rocked gently over the cells, with any excess immediately removed. Cells were dislodged from the plastic-ware by gentle tapping, and re-suspended in 10 mL DMEM/F12. The suspension was pelleted by centrifugation at 12000 rpm for 3 minutes. The supernatant was removed and the pellet re-suspended in 1 mL proliferation media and triturated to gain a single cell suspension. Cells then went a 1:5 to 1:10 split depending on cell number and were transferred to new poly-L-ornithine/laminin coated plastic-ware.

7.2.6.2 Differentiation Protocol

AHPC cell cultures were induced to differentiate with the introduction of 1 µM ATRA (Sigma) diluted in DMSO, or test compounds diluted in DMSO, into the media, alongside the reduction of bFGF concentration down to 1 ng/mL. In preparation for each experiment, cultures which had reached ~90 % confluence were treated with trypsin-versene solution to obtain a single cell suspension as outline previously. Cell number was subsequently determined using a haemocytometer under a light microscope. Unless otherwise stated, cells were seeded at 100,000 cells per well in a 4-well plate (Nunc). Cultures were maintained for up to 14 days, with the media refreshed every 3 days.

7.2.6.3 Immunocytochemistry

Cell fixing was performed by incubation with ice-cold 4% PFA in PBS (Sigma) for 30 minutes at RT, followed by 3 washes with PBS. Cell membranes were permeablised by treatment with 1% Triton-X-100 (Sigma) in PBS for 10 minutes at room temperature. Non-specific binding of antibodies was blocked using a solution of 1% goat serum (Sigma) in PBS containing 0.2% Tween-20 (Sigma). Dilution of primary antibodies was carried out in blocking solution, and incubated with the cells for 1 hour at room temperature (β-III-Tubulin antibody (Covance) was diluted 1:600. NF-200 antibody (AbCam) was diluted 1:200). Cells were washed 3 times for 15 minutes in PBS followed by one hour incubation in the dark at RT with appropriately diluted FITC-conjugated (Alexafluor 488, diluted 1:600) or Cy3-conjugated (JacksonLabs, diluted 1:600) secondary antibody. A further 2 washes of PBS were carried out in the dark, followed by incubation with 1 µg/mL Hoechst 33342 nuclear staining dye (Molecular Probes, diluted in PBS). Cultures were washed twice more in PBS, and left in the final wash for immediate imaging. Fixed and immunostained cultures were examined using a fluorescent microscope under restricted light conditions (Nikon Diaphot 300). Hoechst 33342 images and the corresponding fluorescent photomicrographs were collated and stored using the appropriate filter sets and an adapted digital camera (Nikon).

Chapter VIII

References

8.1 References

1) R. Jaenisch and R. Young, *Cell*, 2008, **132**, 567-582.

2) G. R. Martin, *Proc. Natl. Acad. Sci. USA*, 1981, **78**, 7634-7638.

3) M. J. Evans and M. Kaufman, *Nature*, 1981, **292**, 154-156.

4) J. Rossant, *Cell*, 2008, **132**, 527-531.

5) S. H. Orkin and L. I Zon, *Cell*, 2008, **132**, 631-644.

6) S. H. Orkin, *Nat. Rev. Genet*., 2000, **1**, 57-64.

7) R. M. Cinalli, P. Rangan and R. Lehmann, *Cell*, 2008, **132**, 559-562.

8) S. Yamanaka, *Cell Stem Cell*, 2007, **1**, 39-49.

9) R. Briggs and T. J. King, *Proc. Natl. Acad. Sci. USA*, 1952, **38**, 455-463.

10) I. Wilmut, A. E. Schnieke, J. McWhir, A. J. Kind and K. H. Cambell, *Nature*, 1997, **385**, 810-813.

11) J. B. Gurdon and J. A. Byrne, *Proc. Natl. Acad. Sci. USA*, 2003, **100**, 8048-8052.

12) X. Yang, S. L. Smith, X. C. Tian, H. A. Lewin, J. P. Renard and T. Wakayama, *Nat. Genet*., 2007, **39**, 295-302.

13) T. Wakayama, V. Tabar, I. Rodriguez, A. C. F. Perry, L. Studer and P. Mombaerts, *Science*, 2001, **292**, 740-743.

14) S. Wakayama, M. L. Jakt, M. Suzuki, R. Araki, T, Hikichi, S. Kishigami, H. Ohta, N. V. Thuan, E. Mizutani, Y. Sakaide, S. Senda, S. Tanaka, M. Okada, M. Miyake, M. Abe, S. Nishikawa, K. Shiota and T. Wakayama, *Stem Cells*, 2006, **24**, 2013-2033.

15) R. A. Miller and F. H. Ruddle, *Cell*, 1976, **9**, 45-55.

16) M. Tada, Y. Takahama, K. Abe, N. Nakatsuji and T. Tada, *Curr. Biol*., 2001, **11**, 1553-1558.

17) C. A. Cowan, J. Atienza, D. A. Melton and K. Eggan, *Science*, 2005, **309**, 1369-1373.

18) J. Yu, M. A. Vodyanik, P. He, I. I. Slukvin and J. A. Thomson, *Stem Cells*, 2006, **24**, 168-176.

19) K. Takahashi and S. Yamanaka, *Cell*, 2006, **126**, 663-676.

20) N. Maherali, R. Sridharan, W. Xie, J. Utikal, S. Eminli, K. Arnold, M. Stadtfeld, Y. Tachechko, J. Tchieu, R. Jaenisch, K. Plath and K. Hochedlinger, *Cell Stem Cell*, 2007, **1**, 55-70.

21) K. Okita, T. Ichisaka and S. Yamanaka, *Nature*, 2007, **448**, 313-317.

22) M. Wernig, A. Meissner, R. Foreman, T. Brambrink, M. Ku, K. Hochedlinger, B. E. Bernstein and R. Jaenisch, *Nature*, 2007, **448**, 318-324.

23) K. Takahashi, K. Tanabe, M. Ohnuki, M. Narita, T. Ichisaka, K. Tomoda and S. Yamanaka, *Cell*, 2007, **131**, 861-872.

24) I. H. Park, R. Zhao, J. A. West, A. Yabuuchi, H. Huo, T. A. Ince, P. H. Lerou, M. W. Lensch and G. Q. Daley, *Nature*, 2008, **451**, 141-146.

25) J. Yu, M. A. Vodyanik, K. Smuga-Otto, J. Antosiewicz-Bourget, J. L. Frane, S. Tian, J. Nie, G. A. Jonsdottir, V. Ruotti, R. Stewart, I. I. Slukvin and J. A. Thomson, *Science*, 2007, **318**, 1917-1920.

26) M. Nakagawa, M. Koyanagi, K. Tanabe, K. Takahashi, T. Ichisaka, T. Aoi, K. Okita, Y. Mochiduki, N. Takizawa and S. Yamanaka, *Nat. Biotechnol*., 2008, **26**, 101-106.

27) M. Wernig, A. Meissner, J. Cassady and R. Jaenisch, *Cell Stem Cell*, 2008, **2**, 10-12.

28) C. E. Murry and G. Keller, *Cell*, 2008, **132**, 661-680.

29) J. K. Ichida, J. Blanchard, K. Lam, E. Y. Son, J. E. Chung, D. Egli, K. M. Loh, A. C. Carter, F. P. Di Giorgio, K. Koszka, D. Huangfu, H. Akutsu, D. R. Liu, L. L. Rubin and K. Eggan, *Cell Stem Cell*, 2009, **5**, 491-503.

30) Y. Matsui, K. Zsebo and B. L. Hogan, *Cell*, 1992, **70**, 841-847.

31) Y. Jiang, B. N. Jahagirdar, R. L. Reinhardt, R. E. Schwartz, C. D. Keenek, X. R. Ortiz-Gonzalezk, M. Reyes, T. Lenvik, T. Lund, M. Blackstad, J. Du, S. Aldrich, A. Lisberg, W. C. Lowk, D. A. Largaespada and C. M. Verfaillie, *Nature*, 2002, **418**, 41-49.

32) M. Kanatsu-Shinohara, K. Inoue, J. Lee, M. Yoshimoto, N. Ogonuki, H. Miki, S. Baba, T. Kato, Y. Kazuki, S. Toyokuni, M. Toyoshima, O. Niwa, M. Oshimura, T. Heike, T. Nakahata, F. Ishino, A. Ogura and T. Shinohara, *Cell*, 2004, **119**, 1001-1012.

33) K. Guan, K. Nayernia, L. S. Maier, S. Wagner, R. Dressel, J. H. Lee, J. Nolte, F. Wolf, M. Li, W. Engel and G. Hasenfuss, *Nature,* 2006, **440**, 1199-1203.

34) N. Haraguchi, H. Ishii, K. Mimori, F. Tanaka, M. Ohkuma, H. M. Kim, H. Akita, D. Takiuchi, H. Hatano, H. Nagano, G. F. Barnard, Y. Doki and M. Mori, *J. Clin. Invest*., 2010, **120**, 3326-3339.

35) J. E. Visvader and G. J. Lindeman, *Nat. Rev. Cancer*, 2008, **8**, 755-768.

36) T. Lapidot, C. Sirard, J. Vormoor, B. Murdoch, T. Hoang, J. Caceres-Cortes, M. Minden, B. Paterson, M. A. Caligiuri and J. E. Dick, *Nature*, 1994, **367**, 645-648.

37) S. Meng, D. Tripathy, E. P. Frenkel, S. Shete, E. Z. Naftalis, J. F. Huth, P. D. Beitsch, M. Leitch, S. Hoover, D. Euhus, B. Haley, L. Morrison, T. P. Fleming, D. Herlyn, L. W. M. M. Terstappen, T. Fehm, T. F. Tucker, N. Lane, J. Wang and J. W. Uhr, *Clin. Cancer Res*., 2004, **10**, 8152-8162.

38) L. J. Kleinsmith and G. B. Pierce, *Cancer Res.* 1964, **24**, 1544-1551.

39) A. I. Caplan, *J. Orthopaedic Res*., 1991, **9**, 641-650.

40) J. J. Minguell, A. Erices and P. Conget, *Exp. Biol. Med.,* 2001, **226**, 507-520.

41) B. Short, N. Brouard, T. Occhiodoro-Scott, A. Ramakrishnan and P. J. Simmons, *Arch. Med. Res.,* 2003, **34**, 565-571.

42) T. Schroeder, *Cell Stem Cell,* 2010, **6**, 203-207.

43) C. Blanpain, V. Horsley and E. Fuchs, *Cell*, 2007, **128**, 445-458.

44) C. Blanpain and E. Fuchs, *Nature Rev. Mol. Cell Biol*., 2009, **10**, 207–217.

45) H. J. Snippert, A. Haegebarth, M. Kasper, V. Jaks, J. H. van Es, N. Barker, M. van de Wetering, M. van den Born, H. Begthel, R. G. Vries, D. E. Stange, R. Toftgård, H. Clevers, *Science*, 2010, **327**, 1385–1389.

46) C. Blanpain, *Nature*, 2010, **464**, 686-687.

47) N. L. Kennea and H. Mehmet, *J. Pathol.,* 2002, **197**, 536-550.

48) Y. N. Jan and L. Y. Jan, *Nature*, 1998, **392**, 775–778.

49) P. Taupin and F. H. Gage, *J. Neurosci. Res.,* 2002, **69**, 745-749.

50) M. B. Luskin, *Neuron*, 1993, **11**, 173–189.

51) H. A. Cameron, C. S. Wolley, B. S. McEwen and E. Gould, *Neurosci.*, 1993, **56**, 337–344

52) P. S. Eriksson, E. Perfilieva, T. Bjork-Eriksson, A. M. Alborn, C. Nordborg, D. A. Peterson and F. H. Gage, *Nat. Med*., 1998, **4**, 1313–1307.

53) F. H. Gage, *Science*, 2000, **287**, 1433–1438.

54) A. Bjorklund and O. Lindvall, *Nat. Neurosci*., 2000, **3**, 537-544.

55) S. E. Lazic and R. A. Barker, *J. Hematother. Stem Cell Res*., 2003, **12**, 635-642.

56) F. Rossi and E. Cattaneo, *Nat. Rev. Neurosci*., 2002, **3**, 401-409.

57) R. Donato, E. A. Miljan, S. J. Hines, S. Aouabdi, K. Pollock, S. Patel, F. A Edwards and J. D. Sinden, *BMC Neurosci*., 2007, **8**, 36-47.

58) F. H. Gage, P. W. Coates, T. D. Palmer, H. Georg Kuhn, L. J. Fisher, J. O. Suhonen, D. A. Peterson, S. T. Suhr and J. Ray, *Proc. Natl. Acad. Sci. USA*, 1995, **92**, 11879-11883.

59) V. B. Christie, D. J. Maltman, A. P. Henderson, A. Whiting, T. B. Marder, L. Lako and S. A. Przyborski, *J. Neurosci. Methods*, 2010, **193**, 239-245.

60) J. Takahashi, T. D. Palmer and F. H. Gage, *J. Neurobiol*., 1999, **38**, 65-81.

61) T. Reya and H. Clevers, *Nature*, 2005, **434**, 843-850.

62) F. Rijsewijk, M. Schuermann, E. Wagenaar, P. Parren, D. Weigel and R. Nusse, *Cell*, 1987, **50**, 649-657.

63) Q. Eastman and R. Grosschedl, *Curr. Opin. Cell Biol*., 1999, **11**, 233-240.

64) B. W. Doble and J. R. Woodgett, *J. Cell Sci*., 2003, **116**, 1175-1186.

65) Y. Li, Q. Zhang, X. Yin, W. Yang, Y. Du, P. Hou, J. Ge, C. Liu, W. Zhang, X. Zhang, Y. Wu, H. Li, K. Liu, C. Wu, Z. Song, Y. Zhao, Y. Shi and H. Deng, *Cell Res*., 2011, **21**, 196-204.

66) W. Li, H. Zhou, R. Abujarour, S. Zhu, J. Y. Joo, T. Lin, E. Hao, H. R. Schöler, A. Hayek and S. Ding, *Stem Cells*, 2009, **27**, 2992-3000.

67) M. Lepourcelet, Y. P. Chen, D. S. France, H. Wang, P. Crews, F. Petersen, C. Bruseo, A. W. Wood and R. A. Shivdasani, *Cancer Cell*, 2004, **5**, 91-102.

68) B. Chen, M. E. Dodge, W. Tang, J. Lu, Z. Ma, C. Fan, S. Wei, W. Hao, J. Kilgore, N. S. Williams, M. G. Roth, J. F. Amatruda, C. Chen and L. Lum, *Nat. Chem. Biol*., 2009, **5**, 100-107.

69) S. A. Huang, Y. M. Mishina, S. Liu, A. Cheung, F. Stegmeier, G. A. Michaud, O. Charlat, E. Wiellette, Y. Zhang, S. Wiessner, M. Hild, X. Shi, C. J. Wilson, C.

Mickanin, V. Myer, A. Fazal, R. Tomlinson, F. Serluca, W. Shao, H. Cheng, M. Shultz, C. Rau, M. Schirle, J. Schlegl, S. Ghidelli, S. Fawell, C. Lu, D. Curtis, M. W. Kirschner, C. Lengauer, P. M. Finan, J. A. Tallarico, T. Bouwmeester, J. A. Porter, A. Bauer and F. Cong, *Nature*, 2009, **461**, 614-620.

70) C. Nusslein-Volhard and E. Wieschaus, *Nature*, 1980, **287**, 795-801.

71) D. Huangfu D and K. V. Anderson, *Development*, 2006, **133**, 3-14.

72) A. P. McMahon, P. W. Ingham and C. J. Tabin, *Curr. Top. Dev. Biol*., 2003, **53**, 1-114.

73) M. Pasca di Magliano and M. Hebrok, *Nat. Rev. Cancer*, 2003, **3**, 903-911.

74) T. Østerlund and P. Kogerman, *Trends in Cell. Biol*., 2006, **16**, 176-180.

75) J. E. Hooper and M. P. Scott, *Nat. Rev. Mol. Cell Biol*., 2005, **6**, 306-317.

76) P. W. Ingham and A. P. McMahon, *Genes Dev*., 2001, **15**, 3059-3087.

77) M. K. Cooper, J. A. Porter, K. E. Young and P. A Beachy, *Science*, 1998, **280**, 1603-1607.

78) J. P. Incardona, W. Gaffield, R. P. Kapur and H. Roelink, *Development*, 1998, **125**, 3553-3562.

79) J. K. Chen, J. Taipale, K. E. Young, T. Maita and P. E. Beachy, *Proc. Natl. Acad. Sci. USA*, 2002, **99**, 14071-14076.

80) S. Sinha and J. K. Chen, *Nat. Chem. Biol*., 2006, **2**, 29-30.

81) X. Wu, S. Ding, Q. Ding, N. S. Gray and P. G. Schultz, *J. Am. Chem. Soc*., 2002, **124**, 14520-14521.

82) M. Lauth, Å. Bergström, T. Shimokawa and R. Toftgård, *Proc. Natl. Acad. Sci. USA*, 2007, **104**, 8455-8460.

83) J. Lee, X. Wu, M. Pasca di Magliano, E. C. Peters, Y. Wang, J. Hong, M. Hebrok, S. Ding, C. Y. Cho and P. G. Schultz, *ChemBioChem*, 2007, **8**, 1916-1919.

84) M. Y. Wu and C. S. Hill, *Dev. Cell*, 2009, **16**, 329-343.

85) J. P. Annes, J. S. Munger and D. B. Rifkin *J. Cell Sci*., 2003, **116**, 217-224.

86) X. H. Feng and R. Derynck, *Annu. Rev. Cell Dev. Biol*., 2005, **21**, 659-693.

87) J. Massagué, *Nature Rev. Mol. Cell Biol*., 2000, **1**, 169–178.

88) S. Itoh, F. Itoh, M. J. Goumans and P. Ten Dijke, *Eur. J. Biochem*., 2000, **267**, 6954–6967.

89) A. Moustakas, S. Souchelnytskyi and C. H. Heldin, *J. Cell Sci*., 2001, **114**, 4359–4369.

90) R. Derynck and Y. E. Zhang, *Nature*, 2003, **425**, 577-584.

91) T. Watabe, A. Nishihara, K. Mishima, J. Yamashita, K. Shimizu, K. Miyazawa, S. Nishikawa and K. Miyazono, *J. Cell Biol*., 2003, **163**, 1303-1311.

92) J. Hao, M. A. Daleo, C. K. Murphy, P. B. Yu, J. N. Ho, J. Hu, J. Hu, R. T. Peterson, A. K. Hatzopoulos, and C. C. Hong, *PLoS One*, 2008, **3**, e2904.

93) M. Borowiak, R. Maehr, S. Chen, A. E. Chen, W. Tang, J. L. Fox, S. L. Schreiber and D. A. Melton, *Cell Stem Cell*, 2009, **4**, 348-358.

94) E. C. Lai, *Development*, 2004, **131**, 965-973.

95) G. Weinmaster and R. Kopan, *Development*, 2006, **133**, 3277-3282.

96) T. H. Morgan, *Am. Nat*., 1917, **51**, 513-544.

97) J. Kanungo, Y. Zheng, N. D. Amin and H. C. Pant, *J. Neurochem*., 2008, **106**, 2236-2248.

98) K. Cullion, K. M. Draheim, N. Hermance, J. Tammam, V. M. Sharma, C. Ware, G. Nikov, V. Krishnamoorthy, P. K. Majumder and M. A. Kelliher, *Blood*, 2009, **113**, 6172-6181.

99) D. M. Ornitz and N. Itoh, *Genome. Biol*., 2001, **2**, reviews3005.1-3005.12.

100) B. Reuss, O. von Bohlen and O. Halbach, *Cell Tissue Res*., 2003, **313**, 139-157.

101) N. Gotoh, *Curr. Stem Cell Res. Ther*., 2009, **4**, 9-15.

102) C. J. Powers, S. W. McLeskey and A Wellstein, *Endocr. Relat. Cancer*, 2000, **7**, 165-197.

103) W. H. Burgess, C. A. Dionne, J. Kaplow, R. Mudd, R. Friesel, A. Zilberstein, J. Schlessinger and M. Jaye, *Mol. Cell Biol*., 1990, **10**, 4770-4777.

104) J. K. Wang, H. Xu, H. C. Li and M. Goldfarb, *Oncogene*, 1996, **13**, 721-729.

105) H. Kouhara, Y. R. Hadari, T. Spivak-Kroizman, J. Schilling, D. Bar-Sagi, I. Lax and J. Schlessinger, *Cell*, 1997, **89**, 693-702.

106) R. Bansal, S. Magge and S. Winkler, *J. Neurosci. Res*., 2003, **74**, 486-493.

107) S. D. Barrett, A. J. Bridges, D. T. Dudley, A. R. Saltiel, J. H. Fergus, C. M. Flamme, A. M. Delaney, M. Kaufman, S. LePage, W. R. Leopold, S. A. Przybranowski, J. Sebolt-Leopold, K. Van Becelaere, A. M. Doherty, R. M.

Kennedy, D. Marston, W. A. Howard Jr., Y. Smith, J. S. Warmus and H. Tecle, *Bioorg. Med. Chem. Lett*., 2008, **18**, 6501-6504.

108) J. Rinehart, A. A. Adjei, P. M. LoRusso, D. Waterhouse, J. Randolph Hecht, R. B. Natale, O. Hamid, M. Varterasian, P. Asbury, E. P. Kaldjian, S. Gulyas, D. Y. Mitchell, R. Herrera, J. S. Sebolt-Leopold and M. B. Meyer, *J. Clin. Oncol*., 2004, **22**, 4456-4462.

109) R. D. Semba, *J. Nutr*., 1999, **129**, 783-791.

110) M. B. Sporn, N. M. Dunlop, D. L. Newton and J. M. Smith, *Fed. Proc*., 1976, **35**, 1332-1338.

111) IUPAC-IUB Joint Commission on Biochemical Nomenclature, *Eur. J. Biochem*., 1982, **129**, 1-5.

112) M. B. Sporn and A. B. Roberts, *Ciba Foundation Symposia*, 1985, **113**, 1-5.

113) R. Blomhoff and H. K. Blomhoff, *J. Neurobiol*., 2006, **66**, 606-630.

114) C. Liebecq, *J. Mol. Biol*., 1998, **275**, 527-537.

115) T. Moore, *Biochem J.*, 1930, **24**, 692-702.

116) J. A. Olson and O. Hayaishi, *Proc. Natl. Acad. Sci. U.S.A.*, 1965, **54**, 1364-1370.

117) D. S. Goodman and H. S. Huang, *Science*, 1965, **149**, 879-880.

118) X. Wang, R. M. Russell, C. Liu, F. Stickel, D. E. Smith and N. I. Krinsky, *J. Biol. Chem.*, 1996, **271**, 26490-26498.

119) C. Kiefer, S. Hassel, J. M. Lampert, K. Vogt, M. O. Lederer, D. E. Breihaupt and J. von Lintig, *J. Biol. Chem.*, 2001, **276**, 14110-14116.

120) F. M. Herr and D. E. Ong, *Biochemistry*, 1992, **31**, 6748-6755.

121) N. Noy, *Biochem. J*., 2000, **348**, 481-495.

122) D. S. Goodman, H. S. Huang and T. Shirator, *J. Lipid Res*., 1965, **6**, 390-396.

123) R. Blomhoff, M. H. Green, T. Berg and K. R. Norum, *Science*, 1990, **250**, 399-404.

124) E. H. Harrison, *Annu. Rev. Nutr.*, 2005, **25**, 87-103.

125) E. H. Harrison and M. Z. Gad, *J. Biol. Chem*., 1989, **264**, 17142-17147.

126) D. E. Ong, *Arch. Dermatol*., 1987, **123**, 1693-1695.

127) R. Blomhoff, M. Rasmussen, A. Nilsson, K. R. Norum, T. Berg, W. S. Blaner, M. Kato, J. R. Mertz, D. S. Goodman, U. Eriksson and P. A. Peterson, *J. Biol. Chem*., 1985, **260**, 3560-3565.

128) L. Quadro, W. S. Blaner, D. J. Salchow, S. Vogel, R. Piantedosi, P. Gouras, S. Freeman, M. P. Cosma, V. Colantuoni and M. E. Gottesman, *EMBO J.*, 1999, **18**, 4633-4644.

129) M. Kanai, A. Raz and D. S. Goodman, *J. Clin. Invest.*, 1968, **47**, 2025-2044.

130) G. Zanotti and R. Berni, *Vitam. Horm.*, 2004, **69**, 271-295.

131) J. O. Alvsaker, F. B. Haugli and S. G. Laland, *Biochem. J.,* 1967, **102**, 362-366.

132) D. E. Ong and F. Chytil, *Nature*, 1975, **255**, 74-75.

133) C. C. Chen and J. Heller, *J. Biol. Chem*., 1977, **252**, 5216-5221.

134) M. Sundaram, A. Sivaprasadarao, M. M. DeSousa and J. B. C. Findlay, *J. Biol. Chem*., 1998, **273**, 3336-3342.

135) R. Kawaguchi, J. M. Yu, J. Honda, J. Hu, J. Whitelegge, P. Ping, P. Wiita, D. Bok and H. Sun, *Science*, 2007, **315**, 820-825.

136) M. T. P. Ho, J. B. Massey, H. J. Pownall, R. E. Anderson and J. G. Hollyfield, *J. Biol. Chem*., 1989, **264**, 928-935.

137) N. Noy and Z. J. Xu, *Biochemistry*, 1990, **29**, 3878-3883.

138) A. R. Moise, N. Noy, K. Palczewski and W. S. Blaner, *Biochemistry*, 2007, **46**, 4449-4458.

139) G. Siegenthaler and J. H. Saurat, *Biochem. Biophys. Res. Commun*., 1987, **143**, 418-423.

140) C. Folli, V. Calderone, I. Ramazzina, G. Zanotti and R. Berni, *J. Biol. Chem.*, 2002, **277**, 41970-41977.

141) M. Lidén and U. Eriksson, *J. Biol. Chem.*, 2006, **281**, 13001-13004.

142) K. Niederreither, V. Fraulob, J. M. Garnier, P. Chambon and P. Dolle, *Mech. Dev.*, 2002, **110**, 165-171.

143) P. N. MacDonald and D. E. Ong, *J. Biol. Chem*., 1987, **262**, 10550-10556.

144) J. L. Napoli, *Clin. Immunol. Immunopathol.,* 1996, **80**, S52-S62.

145) D. Dong, S. E. Ruuska, D. J. Levinthal and N. Noy, *J. Biol. Chem.*, 1999, **274**, 23695-23698.

146) A. Budhu, R. Gillilan and N. Noy, *J. Mol. Biol.*, 2001, **305**, 939-949.

147) M. E. Newcomer, R. S. Pappas and D. E. Ong, *Proc. Natl. Acad. Sci. USA*, 1993, **90**, 9223-9227.

148) P. Germain, P. Chambon, G. Eichele, R. M. Evans, M. A. Lazar, M. Leid, A. R. De Lera, R. Lotan, D. J. Mangelsdorf and H. Gronemeyer, *Pharm. Rev.*, 2006, **58**, 712-725.

149) P. Germain, P. Chambon, G. Eichele, R. M. Evans, M. A. Lazar, M. Leid, A. R. De Lera, R. Lotan, D. J. Mangelsdorf and H. Gronemeyer, *Pharm. Rev.*, 2006, **58**, 760-772.

150) R. M. Evans, *Science*, 1988, **240**, 889-895.

151) A. Chawla, J. J. Repa, R. M. Evans and D. J. Mangelsdorf, *Science*, 2001, **294**, 1866-1870.

152) A. R. de Lera, W. Bourguet, L. Altucci and H. Gronemeyer, *Nat. Rev. Drug Disc*., 2007, **6**, 811-820.

153) S. Nagpal, S. Friant, H. Nakshatri and P. Chambon, *EMBO J.,* 1993, **12**, 2349-2360.

154) P. Kastner, M. Mark, N. Ghyselinck, W. Krezel, V. Dupé, J. M. Grondona and P. Chambon, *Development*, 1997, **124**, 313-326.

155) C. K. Glass and M. G. Rosenfeld, *Genes Dev.*, 2000, **14**, 121-141.

156) N. J. McKenna and B. W. O'Malley, *Cell*, 2002, **108**, 465-474.

157) V. Perissi and M. G. Rosenfeld, *Nat. Rev. Mol. Cell Biol.*, 2005, **6**, 542-554.

158) P. Germain, J. Iyer, C. Zechel and H. Gronemeyer, *Nature*, 2002, **415**, 187-192.

159) D. J. Mangelsdorf and R. M. Evans, *Cell*, 1995, **83**, 841-850.

160) F. Rastinejad, *Curr. Opin. Struct. Biol.*, 2001, **11**, 33-38.

161) R. Kurokawa, M. Soderstorm, A. Horlein, S. Halachmi, M. Brown, M. G. Rosenfield and C. K. Glass, *Nature*, 1995, **377**, 451-454.

162) L. Altucci and H. Gronemeyer, *Nat. Rev. Cancer*, 2001, **1**, 181-193.

163) M. Petkovich, N. J. Brand, A. Krust and P. Chambon, *Nature*, 1987, **330**, 444-450.

164) V. Giguere, E. S. Ong, P. Segui and R. M. Evans, *Nature*, 1987, **330**, 624-629.

165) N. Brand, M. Petkovich, A. Krust, P. Chambon, H. Dethe, A. Marchio, P. Tiollais and A. Dejean, *Nature*, 1988, **332**, 850-853.

166) D. Benbrook, E. Lernhardt and M. Pfahl, *Nature*, 1988, **333**, 669-672.

167) A. Zelent, A. Krust, M. Petkovich, P. Kastner and P. Chambon, *Nature*, 1989, **339**, 714-717.

168) A. Krust, P. Kastner, M. Petkovich, A. Zelent and P. Chambon, *Proc. Natl. Acad. Sci. USA*, 1989, **86**, 5310-5314.

169) P. Dolle, E. Ruberte, P. Leroy, G. Morrisskay and P. Chembon, *Development*, 1990, **110**, 1133-1151.

170) G. Allenby, M. T. Bocquel, M. Saunders, S. Kazmer, J. Speck, M. Rosenberger, A. Lovey, P. Kastner, J. F. Grippo and P. Chambon, *Proc. Natl. Acad. Sci. USA.*, 1993, **90**, 30-34.

171) D. J Mangelsdorf, E. S. Ong, J. A. Dyck and R. M. Evans, *Nature*, 1990, **345**, 224-229.

172) M. Mark, N. B. Ghyselinck and P. Chambon, *Annu. Rev. Pharmacol. Toxicol.*, 2006, **46**, 451-480.

173) A. A. Levin, L. J. Sturzenbecker, S. Kazmer, T. Bosakowski, C. Huselton, G. Allenby, J. Speck, C. Kratzeisen, M. Rosenberger, A. Lovey and J. F. Grippo, *Nature,* 1992, **355**, 359-361.

174) S. A. Kliewer, K. Umesono, D. J. Mangelsdorf and R. M. Evans, *Nature*, 1992, **355**, 446-449.

175) R. Lotan, X. C. Xu, S. M. Lippman, J. Y. Ro, J. S. Lee, J. J. Lee and W. K. Hong, *N. Engl. J. Med.*, 1995, **332**, 1405-1410.

176) H. Kagechika and K. Shudo, *Med. Chem.*, 2005, **48**, 5875-5883.

177) B. Blumberg, *Seminars in Cell Dev. Biol.*, 1997, **8**, 417-428.

178) G. Wald, *Nature*, 1968, **219**, 800-807.

179) A. C. Ross, *Proc. Soc. Exp. Biol. Med.*, 1992, **200**, 303-320.

180) J. N. Thompson and G. A. J. Pitt, *Proceedings of the Royal Society of London, Series B, Biological Sciences*, 1964, **159**, 510-535.

181) M. Maden, *Proc. Nutr. Soc.*, 2000, **59**, 65-73.

182) J. Mey and P. McCaffery, *Neuroscientist*, 2004, **10**, 409-421.

183) K. W. Ng, H. Zhou, S. Manji and T. J. Martin, *Crit. Rev. Eukaryot Gene Expr.*, 1995, **5**, 219-253.

184) L. J. Gudas and J. A. Wagner, *J. Cell. Physiol.*, 2011, **226**, 322-330.

185) P. Kastner, P. Mark and P. Chambon, *Cell*, 1995, **83**, 859-869.

186) R. M. Niles, *J. Nutr.*, 2003, **133**, 282S-286S.

187) D. C. Diez and K. G. Storey, *Bioessays*, 2004, **26**, 857-869.

188) M. Maden, *Nat. Rev. Neurosci.*, 2002, **3**, 843-853.

189) M. N. Vergara, Y. Arsenijevic and K. Rio-Tsonis, *J. Neurobiol.*, 2005, **64**, 491-507.

190) M. Clagett-Dame and H. F. DeLuca, *Annu. Rev. Nutr.*, 2002, **22**, 347-381.

191) P. McCaffery, J. Zhang and J. E. Crandall, *J. Neurobiol.*, 2006, **66**, 780-791.

192) R. H. Zetterstrom, E. Lindqvist, A. Mata de Urquiza, A. Tomac, U. Eriksson, T. Perlmann and L. Olson, *Eur. J. Neurosci.*, 1999, **11**, 407-416.

193) S. Jacobs, D. C. Lie, K. L. DeCicco, Y. Shi, L. M. DeLuca, F. H. Gage and R. M. Evans, *Proc. Natl. Acad. Sci. USA.*, 2006, **103**, 3902-3907.

194) S. Cocco, G. Diaz, R. Stancampiano, A. Diana, M. Carta, R. Curreli, L. Sarais and F. Fadda, *Neuroscience*, 2002, **115**, 475-482.

195) V. B. Christie, T. B. Marder, A. Whiting and S. A. Przyborski, *Mini Rev. Med. Chem.*, 2008, **8**, 601-608.

196) Y. Xu, Y. Shi and S. Ding, *Nature*, 2008, **453**, 338-344.

197) C. A. Lyssiotis, L. L. Lairson, A. E. Boitano, H. Wurdak, S. Zhu and P. G. Schultz, *Angew. Chem. Int. Ed*., 2011, **50**, 200-242.

198) E. L. Wilson and E. Reich, *Cell*, 1978, **15**, 385-392.

199) S. Strickland and V. Mahdavi, *Cell*, 1978, **15**, 393-403.

200) D. R. Soprano, B. W. Teets and K. J. Soprano, *Vitamins and Hormones,* 2007, **75**, 69-95.

201) E. M. V. Jones-Villeneuve, M. W. McBurney, K. A. Rogers and V. I. Kalnins, *J. Cell Biol.*, 1982, **94**, 253-262.

202) L. Wei, W. S. Blaner, D. S. Goodman and M. C. Nguyen-Huu, *Mol. Endocrinol.*, 1989, **3**, 454-463.

203) S. Roach, S. Cooper, W. Bennett and M. F. Pera, *Eur. Urol.*, 1993, **23**, 82-88.

204) I. Damjanov, B. Horvat and Z. Gibas, *Lab. Invest.*, 1993, **68**, 220-232.

205) P. W. Andrews, *Dev. Biol.*, 1984, **103**, 285-293.

206) P. W. Andrews, E. Nudelman, S. Hakomori and B. A. Fenderson, *Differentiation*, 1990, **43**, 131-138.

207) S. A. Przyborski, I. E. Morton, A. Wood and P. W. Andrews, *Eur. J. Neurosci.*, 2000, **12**, 3521-3528.

208) S. A. Przyborski, S. Smith and A. Wood, *Stem Cells*, 2003, **21**, 459-471.

209) S.A. Przyborski, *Stem Cells*, 2001, **19**, 500-504.

210) R. Stewart, V. B. Christie and S. A. Przyborski, *Stem Cells*, 2003, **21**, 248-256.

211) S. A. Przyborski, V. B. Christie, M. W. Hayman, R. Stewart and G. M. Horrocks, *Stem Cells Dev*., 2004, **13**, 400-408.

212) R. Stewart, L. Coyne, M. Lako, R. F. Halliwell and S. A. Przyborski, *Stem Cells Dev.*, 2004, **13**, 646-657.

213) L. Coyne, M. Shan, S. A. Przyborski, R. Hirakawa and R. F. Halliwell, *Neurochem. Int*., 2011, doi.org/10.1016/j.neuint.2011.01.022.

214) A. C. Chen and L. J. Gudas, *J. Biol. Chem.*, 1996, **271**, 14971-14980.

215) A. P. Tighe and L. J. Gudas, *J. Cell. Physiol.,* 2004, **198**, 223-229.

216) S. Erceg, S. Lainez, M. Ronaghi, P. Stojkovic, M. A. Perez-Arago, V. Moreno-Manzano, R. Moreno-Palanques, R. Planells-Cases and M. Stojkovic, *PLoS ONE*, 2008, **3**, e2122.

217) H. Wichterle, I. Lieberam, J. A. Porter and T. M. Jessell, *Cell*, 2002, **110**, 385-397.

218) T. D. Palmer, J. Ray and F. H. Gage, *Mol. Cell Neurosci*., 1995, **6**, 474-486.

219) D. R. Piper, T. Mujtaba, M. S. Rao and M. T. Lucero, *J. Neurophysiol*, 2000, **84**, 534-548.

220) P. Wu, Y. I. Tarasenko, Y. Gu, L. Y. Huang, R. E. Coggeshall and Y. Yu, *Nat. Neurosci*., 2002, **5**, 1271-1278.

221) Y. Chen, B. Stevens, J. Chang, J. Milbrandt, B. A. Barres and J. W. Hell, *J. Neurosci. Methods,* 2009, **171**, 239-247.

222) W. K. Hong and L. M. Itri, in *The Retinoids: Biology, Chemistry, and Medicine,* Raven Press Ltd., New York, 1994, 597–630.

223) E. J. Lammer, D. T. Chen, R. M. Hoar, N. D. Agnish, P. J. Benke, J. T. Braun, C. J. Curry, P. M. Fernhoff, A. W. Grix, I. T. Lott, J. M., Richard and S. C. Sun, *N. Engl. J. Med.*, 1985, **313**, 837–841.

224) K. K. Sulik, C. S. Cook and W. S. Webster, *Development,* 1988*,* **103,** 213–232.

225) R. B. Armstrong, K. O. Ashenfelter, C. Eckhoff, A. A. Levin and S. S. Shapiro, in *The Retinoids: Biology, Chemistry, and Medicine,* Raven Press Ltd., New York, 1994, 545–572.

226) R. P. Warrell, Jr., H. de Thé, Z. –Y. Wang and L. Degos, *N. Engl. J. Med.*, 1993, **329,** 177–189.

227) T. Suzuki, S. R. Kunchala, M. Matsui and A. Murayama, *J. Nutr. Sci. Vitaminol (Tokyo)*, 1998, **44**, 729-736.

228) V. B. Christie, J. H. Barnard, A. S. Batsanov, C. E. Bridgens, E. B. Cartmell, J. C. Collings, D. J. Maltman, C. P. F. Redfern, T. B. Marder, S. A. Przyborski and A. Whiting, *Org. Biomol. Chem*., 2008, **6**, 3497-3507.

229) A. Murayama A, T. Suzuki and M. Matsui, *J. Nutrit. Sci. Vita.*, 1997, **43**, 167-176.

230) W. Bollag and E. E. Holdener, *Ann. Oncol*., 1992, **3**, 513-526.

231) J. H. Barnard, J. C. Collings, A. Whiting, S. A. Przyborski and T. B. Marder, *Chem. Eur. J*. 2009, **15**, 11430-11442.

232) M. B. Sporn, N. M. Dunlop, D. L. Newton and W. R. Henderson, *Nature*, 1976, **263**, 110-113.

233) L. Altucci, M. D. Leibowitz, K. M. Ogilvie, A. R. De Lera and H. Gronemeyer, *Nat. Rev. Drug Discovery*, 2007, **6**, 793-810.

234) H. Kagechika and K. Shudo, *J. Med. Chem*., 2005, **48**, 5875-5883.

235) H. Kagechika, *Curr. Med. Chem*., 2002, **9**, 591-608.

236) M. I. Dawson, *Curr. Med. Chem.:Anti-Cancer Agents*, 2004, **4**, 199-230.

237) H. Greschik and D. Moras, Curr. *Top. Med. Chem*., 2003, **3**, 1573-1599.

238) L. J. Schiff, W. H. Okamura, M. I. Dawson and P. D. Hobbs, Structure-Biological Activity Relationships of New Synthetic Retinoids on Epithelial Differentiation of Cultured Hamster Trachea, in *Chemistry and Biology of Synthetic Retinoids*, CRC Press: Boca Raton, FL, 1990, 307-393.

239) A. M. McCormick, J. L. Napoli, H. K. Schnoes and H. F. DeLuca, *Biochemistry,* 1978, **17**, 4085-4090.

240) A. B. Roberts, M. D. Nichols, D. L. Newton and M. B. Sporn, *J. Biol. Chem*., 1979, **254**, 6296-6302.

241) C. A. Frolik, Metabolism of Retinoids, *in The Retinoids*, Vol. 2 (Eds: M. B. Sporn and D. S. Goodman), Academic Press: New York, 1984, 177-208.

242) J. Marill, N. Idres, C. C. Capron, E. Nguyen and G. G. Chabot, *Curr. Drug Meta*., 2003, **4**, 1-10.

243) V. B. Christie, *P.h.D Thesis*, Durham University, 2008.

244) M. Frank-Kamenetsky, X. M. Zhang, S. Bottega, O. Guicherit, H. Wichterle, H. Dudek, D. Bumcrot, F. Y. Wang, S. Jones, J. Shulok, L. L. Rubin and J. A. Porter, *J. Biol.,* 2002, **1**, 10.

245) T. D. Palmer, J. Takahashi and F. H. Gage, *Mol. Cell Neurosci.,* 1997, **8**, 389-404.

246) L. Santerelli, M. Saxe, C. Gross, A. Surget, F. Battaglia, S. Dulawa, N. Weisstaub, J. Lee, R. Duman, O. Arancio, C. Belzung and R. Hen, *Science,* 2003, **301**, 805-809.

247) J. Hsieh, K. Nakashima, T. Kuwabara, E. Mejia and F. H. Gage, *Proc. Natl. Acad. Sci. USA*, 2004, **101**, 16659-16664.

248) S. Ding, T. Y. H. Wu, A. Brinker, E. C. Peters, W. Hur, N. S. Gray and P. G. Schultz, *Proc. Natl. Acad. Sci. USA*, 2003, **100**, 7632-7637.

249) J. P. Saxe, H. Wu, T. K. Kelly, M. E. Phelps, Y. E. Sun, H. I. Kornblum and J. H. Huang, *Chem. Biol.,* 2007, **14**, 1019-1030.

250) M. Warashina, K. H. Min, T. Kuwabara, A. Huynh, F. H. Gage, P. G. Schultz and S. Ding, *Angew., Chem. Int. Ed*., 2006, **45**, 591-593.

251) J. F. Arens and D. A. Van Dorp, *Nature*, 1946, **157**, 190-191.

252) O. Isler, W. Huber, A. Ronco, and M. Kofler, *Helv. Chim, Acta*, 1947, **30**, 1911-1927.

253) S. A. Ross, P. J. McCaffery, U. C. Drager, and L. M. De Luca, *Physiol. Rev*., 2000, **80**, 1021-1054.

254) A. L. Fields, D. R. Soprano and K. J. Soprano, *J. Cell. Biochem*., 2007, **102**, 886-898.

255) H. Suzuki, *Org. Synth*., 1971, **51**, 94-96.

256) K. Sonogashira, Y. Tohda and N. Hagihara, *Tetrahedron Lett*., 1975, **16**, 4467-4470.

257) K. Sonogashira, *J. Organomet. Chem*., 2002, **653**, 46-49.

258) J. D. White, J. C. Amedio, Jr. S. Gut, S. Ohira and L. R. Jayasinghe, *J. Org. Chem*., 1992, **57**, 2270-2284.

259) H. Zhai, Q. Chen, J. Zhao, S. Luo and X. Jia, *Tetrahedron Lett*., 2003, **44**, 2893-2894.

260) S. K. Stewart and A Whiting, *Tetrahedron Lett*., 1995, **36**, 3925-3928.

261) A. S. Batsanov, J. P. Knowles and A Whiting, *J. Org. Chem*., 2007, **72**, 2525-2532.

262) N. Hénaff and A. Whiting, *Org. Lett*., 1999, **1**, 1137-1139.

263) N. Hénaff and A. Whiting, *Tetrahedron*, 2000, **56**, 5193-5204.

264) A. P. Lightfoot, S. J. R. Twiddle and A. Whiting, *Org. Biomol. Chem*., 2005, **3**, 3167-3172.

265) A. S. Batsanov, J. A. K. Howard, A. P. Lightfoot, S. J. R. Twiddle and A. Whiting, *Eur. J. Org. Chem.*, 2005, 1876-1883.

266) A. S. Batsanov, J. P. Knowles, B. Samsam and A. Whiting, *Adv. Synth. Catal*., 2008, **350**, 227-233.

267) J. P. Knowles, *P.h.D Thesis*, Durham University, 2008.

268) G. B. Dudley, K. S. Takaki, D. D. Cha and R. L. Danheiser, *Org. Lett*., 2000, **2**, 3407-3410.

269) J. A. Thomson, J. Itskovitz-Eldor, S. S. Shapiro, M. A. Waknitz, J. J. Swiergiel, V. S. Marshall and J. M. Jones, *Science*, 1998, **282**, 1145-1147.

270) A. Bradley, M. Evans, M. Kaufman and E. Robertson, *Nature*, 1984, **309**, 255-256.

271) G. Keller, *Genes Dev*., 2005, **19**, 1129-1155.

272) M. Serra, S. B. Leite, C. Brito, J. Costa, M. J. T. Carrondo and P. M. Alves, *J. Neurosci. Res*., 2007, **85**, 3557-3566.

273) Y. R. Ahuja, V. Vijayalakshmi and K. Polasa, *Toxicology*, 2007, **231**, 1-10.

274) S. Adler, C. Pellizzer, L. Hareng, T. Hartung and S. Bremer, *Toxicol. In Vitro*, 2008, **22**, 200-211.

275) J. McNeish, *Nat. Rev. Drug Discov*., 2004, **3**, 70-80.

276) C. M. Zhao, W. Deng and F. H. Gage, *Cell*, 2008, **132**, 645-660.

277) H. LingLing and H. Tao, *Sci. China Ser. C-Life Sci*., 2008, **51**, 287-294.

278) J. Kim, J. M. Auerbach, J. A. Rodríguez-Gómez, I. Velasco, D. Gavin, N. Lumelsky, S. Lee, J. Nguyen, R. Sánchez-Pernaute, K. Bankiewicz and R. McKay, *Nature*, 2002, **418**, 50-56.

279) J. W. Langston, *J. Clin. Invest*., 2005, **115**, 23-25.

280) I. Ginis, Y. Q. Luo, T. Miura, S. Thies, R. Brandenberger, S. Gerecht-Nir, M. Amit, A. Hoke, M. K. Carpenter, J. Itskovitz-Eldor and M. S. Rao, *Dev. Biol*., 2004, **269**, 360-380.

281) P. W. Andrews, S. A. Przyborski and J. A. Thomnson, in *Stem Cell Biology*, ed. D. R. Marshak, D. G. Gardner and D. Gottlieb, Cold Spring Harbor Laboratory Press, New York, 2001, 231-266.

282) P. W. Andrews, *R. Soc*., 2002, **357**, 405-417.

283) J. S. Draper, H. D. Moore, L. N. Ruban, P. J. Gokhale and P. W. Andrews, *Stem Cells Dev*., 2004, **13**, 325-336.

284) R. Josephson, C. J. Ording, Y. Liu, S. Shin, U. Lakshmipathy, A. Toumadje, B. Love, J. D. Chesnut, P. W. Andrews, M. S. Rao and J. M. Auerbach, *Stem Cells*, 2007, **25**, 437-446.

285) E. G. Bernstine, M. L. Hooper, S. Grandchamp and B. Ephrussi, *Proc. Natl. Acad. Sci. USA.*, 1973, **70**, 3899-3903.

286) E. Lehtonen, A. Laasonen and J. Tienari, *Int. J. Dev. Biol*., 1989, **33**, 105-116.

287) M. Wagner, B. Han and T. M. Jessell, *Development*, 1992, **116**, 55-66.

288) H. de Thé, M. M. Vivanco-Ruiz, P. Tiollais, H. Stunnenberg and A. Dejean, *Nature*, 1990, **343**, 177-180.

289) H. M. Sucov, K. K. Murakami and R. M. Evans, *Proc. Natl. Acad. Sci. USA.*, 1990, **87**, 5392-5396.

290) J. Føgh and G. Trempe, in *Human Tumour Cells in Vitro*, Plenum Press, New York, 1975.

291) P. W. Andrews, I. Damjanov, D. Simon, G. S. Banting, C, Carlin, N. C. Dracopoli and J. Føgh, *Lab. Invest*., 1984, **50**, 147-162.

292) P. W. Andrews, P. N. Goodfellow, L. H. Shevinsky, D. L. Bronson and B. B. Knowles, *Int. J. Cancer*, 1982, **29**, 523-531.

293) P. W. Andrews, G. Banting, I. Damjanov, D. Arnaud and P. Avner, *Hybridoma*, 1984, **3**, 347-361.

294) J. Nichols, B. Zevnik, K. Anastassiadis, H. Niwa, D. Klewe-Nebenius, I. Chambers, H. Schöler and A. Smith, *Cell*, 1998, **95**, 379-391.

295) I. Chambers, D. Colby, M. Robertson, J. Nichols, S. Lee, S. Tweedie and A. Smith, *Cell*, 2003, **113**, 643-655.

296) I. Chambers and A. Smith, *Oncogene*, 2004, **23**, 7150-7160.

297) I. Chambers, J. Silva, D. Colby, J. Nichols, B. Nijmeijer, M. Robertson, J. Vrana, K. Jones, L. Grotewold and A. Smith, *Nature*, 2007, **450**, 1230-1234.

298) T. Glaser, L. Jepeal, J. G. Edwards, S. R. Young, J. Favor and R. L. Maas, *Nat. Genet*., 1994, **7**, 463–471.

299) L. St-Onge, B. Sosa-Pineda, K. Chowdhury, A. Mansouri and P. Gruss, *Nature*, 1997, **387**, 406–409.

300) T. I. Simpson and D. J. Price, *Bioessays*, 2002, **24**, 1041–1051.

301) S. N. Sansom, D. S. Griffiths, A. Faedo, D. –J. Kleinjan, Y. Ruan, J. Smith, V. V. Heyningen, J. L. Rubenstein and F. J. Livesey, *PLoS Genet.,* 2009, **5**, e1000511.

302) V. C. Njar, *Mini Rev. Med. Chem*., 2002, **2**, 261-269.

303) V. C. Njar, L. Gediya, P. Purushottamachar, P. Chopra, T. S. Vasaitis, A. Khandelwal, J. Mehta, C. K. Huynh, A. Belosay and J. Patel, *Bioorg. Med. Chem*., 2006, **14**, 4323-4340.

304) J. B. Patel, C. K. Huynh, V. D. Handratta, L. K. Gediya, A. M. Brodie, O. G. Goloubeva, O. O. Clement, I. P. Nanne, D. R. Soprano and V. C. Njar, *J. Med. Chem*., 2004, **47**, 6716-6729.

305) V. A. Miller, J. R. Rigas, J. R. F. Muindi, W. P. Tong, E. Venkatraman, M. G. Kris and R. P. Warrell Jr., *Cancer Chemother. Pharmacol*., 1994, **34**, 522-526.

306) J. R. F. Muindi, S. R. Frankel, W. H. Miller Jr., A. Jakubowski, D. A., Scheinberg, C. W. Young, E. Dmitrosky and R. P. Warrell Jr., *Blood*, 1992, **79**, 299-303.

307) J. R. F. Muindi, S. R. Frankel, C. Huselton, F. DeGrazia, W. A Garland, C. W. Young and R. P. Warrell Jr., *Cancer Res*., 1992, **52**, 2138-2142.

308) G. M. Horrocks, L. Lauder, R. Stewart and S. A. Przyborski, *Biochem. Biophys. Res. Commun.,* 2003, **304**, 411-416.

309) J. M. Wu, A. M. Di Pietrantonio and T. C. Hsieh, *Apoptosis*, 2001, **6**, 377-388.

310) J. A. Barltrop, T. C. Owen, A. H. Cory and J. G. Cory, *Bioorg. Med. Chem. Lett*., 1991, **1**, 611-614.

311) A. H. Cory, T. C. Owen, J. A. Barltrop and J. G. Cory, *Cancer Commun.,* 1991, **3**, 207-212.

312) T. M. Buttke, J. A. McCubrey and T. C. Owen, *J. Immunol. Methods,* 1993, **157**, 233-240.

313) N. J. Marshall, C. J. Goodwin and S. J. Holt, *Gtowth Regul.,* 1995, **5**, 69-84.

314) Y. B. Liu, D. A. Peterson, H. Kimura and D. Schubert, *J. Neurochem.,* 1997, **69**, 581-593.

315) I. D. Trayner, A. P. Rayner, G. E. Freeman and F. Farzaneh, *J. Immunol. Methods*, 1995, **186**, 275-284.

316) M. W. McBurney, E. M. V. Jones-Villeneuve, M. K. S. Edwards and P. J. Anderson, *Nature,* 1982, **299**, 165-167.

317) T. H. El-Metwally and T. E. Adrian, *Biochem. Biophys. Res. Commun.,* 1999, **257**, 596-603.

318) S. Adler, C. Pellizzer, M. Paparella, T. Hartung and S. Bremer, *Toxicol. In Vitro,* 2006, **20**, 265-271.

319) C. E. Bridgens, *P.h.D Thesis*, Durham University, 2009.

320) P. W. Andrews, E. Gonczol, S. A. Plotkin, M. Dignazio and J. W. Oosterhuis, *Differentiation*, 1986, **31**, 119-126.

321) H. Baharvand, N. Z. Mehrjardi, M. Hatami, S. Kiani, M. Rao and M. M. Haghighi, *Int. J. Dev. Biol.,* 2007, **51**, 371-378.

322) Y. Elkabetz, G. Panagiotakos, G. Al Shamy, N. D. Socci, V. Tabar and L. Studer, *Genes Dev.,* 2008, **22**, 152-165.

323) S. C. Zhang, X. J. Li, M. A. Johnson and M. T. Pankratz, *Philos. Trans. R. Soc. Lond. Ser. B.,* 2008, **363**, 87-99.

324) M. E. Huang, Y. C. Ye, S. R. Chen, J. R. Chai, J. X. Lu, L. Zhoa, L. J. Gu and Z. Y. Wang, *Blood*, 1988, **72**, 567–572.

325) S. Castaigne, C. Chomienne, M. T. Daniel, P. Ballerini, R. Berger, P. Fenaux and L. Degoset, *Blood*, 1990, **76**, 1704–1709.

326) R. P. Warrell Jr., S. R. Frankel, W. H. Miller Jr., D. A. Scheinberg, L. M. Itri, W. N. Hittelman, R. Vyas, M. Andreeff, A. Tafuri, A. Jakubowski, J. Gabrilove, M. S. Gordon and E. Dmitrovsky, *N. Engl. J. Med*., 1991, **324**, 1385-1393.

327) L. S. Wright, K. R. Prowse, K. Wallace, M. H. Linskens and C. N. Svendsen, *Exp. Cell Res*., 2006, **312**, 2107-2120.

328) C. V. Dang, L. M. Rasar, E. Emison, S. Kim, Q. Li, J. E. Prescott, D. Wonsey and K. Zeller, *Exp. Cell Res*., 1999, **253**, 63-77.

329) S. U. Kim, *Neuropathology*, 2004, **24**, 159-171.

330) M. A. Mena, M. J. Casarejos, C. Estrada and J. G. de Yebenes, *J. Neural Transm. Park. Dis. Dement. Sect*., 1994, **8**, 85-97.

331) J. Ray and F. H. Gage, *Mol. Cell Neurosci*., 2006, **31**, 560-573.

332) N. S. Roy, S. Wang, L. Jiang, J. Kang, A. Benraiss, C. Harrison-Restelli, R. A. R. Fraser, W. T. Couldwell, A. Kawaguchi, H. Okano, M. Nedergaard and S. A. Goldman, *Nature Med*., 2000, **6**, 271-277.

333) T. D. Palmer, P. H. Schwartz, P. Taupin, B. Kaspar, S. A. Stein and F. H. Gage, *Nature*, 2001, **411**, 42-43.

334) R. J. Haselbeck and G. Duester, *Alcohol Clin. Exp. Res.,* 1998, **22**, 1607-1613.

335) S. S. Riaz, S. Theofilopoulos, E. Jauniaux, G. M. Stern and H. F. Bradford, *Dev. Brain Res.,* 2004, **153**, 39-51.

336) A. Martinez-Serrano and A. Bjorklund, *Trends Neurosci.,* 1997, **20**, 530-538.

337) E. M. Torres, E. Dowd and S. B. Dunnett, *Neuroscience,* 2008, **154**, 631-640.

338) C. W. Olanow, J. H. Kordower and T. B. Freeman, *Trends Neurosci.,* 1996, **19**, 102-109.

339) Y. Liu, H. Kagechika, J. Ishikawa, H. Hirano, S. Matsukuma, K. Tanaka and S. Nakamura, *J. Neurochem.,* 2008, **106**, 1104-1116.

340) S. Ding and P. G. Schultz, *Nat. Biotechnol*., 2004, **22**, 833-840.

341) J. I. Levin, E. Turos and S. M. Weinreb, *Syn. Comm.,* 1982, **12**, 989-993.

342) B. G. Shearer, E. Y. Chao, D. E. Uehling, D. N. Deaton, C. Cowan, B. W. Sherman, T. Milliken, W. Faison, K. Brown, K. K. Adkison and F. Lee, *Bioorg. Med. Chem. Lett*., 2007, **17**, 4670-4677.

343) B. W. Lund, A. E. Knapp, F. Piu, N. K. Gauthier, M. Begtrup, U. Hacksell and R. Olsson, *J. Med. Chem*., 2009, **52**, 1540-1545.

344) B. D. Hosangadi and R. H. Dave, *Tetrahedron Lett.,* 1996, **37**, 6375-6378.

345) E. Byun, B. Hong, K. A. De Castro, M. Lim and H. Rhee, *J. Org. Chem.*, 2007, **72**, 9815-9817.

346) R. Ambasudhan and S. Ding, *Chemistry and Biology*, 2007, **14**, 974-975.

347) M. Begtrup and L. B. L. Hansen, *Acta Chemica Scandinavica*, 1992, **46**, 372-383.

348) N. A. Colabufo, F. Berardi, M. G. Perrone, M. Cantore, M. Contino, C. Inglese, M. Niso and R. Perrone, *ChemMedChem*., 2009, **4**, 188-195.

349) I. E. Kopka, *Tetrahedron Lett*., 1988, **29**, 3765-3768.

350) H. Wurdak, S. Zhu, K. H. Min, L. Aimone, L. L. Lairson, J. Watson, G. Chopiuk, J. Demas, B. Charette, R. Halder, E. Weerapana, B. F. Cravatt, H. T. Cline, E. C. Peters, J. Zhang, J. R. Walker, C. Wu, J. Chang, T. Tuntland, C. Y. Cho and P. G. Schultz, *Proc. Natl. Acad. Sci. USA*, 2010, **107**, 16542-16547.

351) M. Aitola, C. M. Sadek, J. A. Gustafsson and M. Pelto-Huikko, *J. Histochem. Cytochem*., 2003, **51**, 455-469.

352) M. Garriga-Canut and S. H. Orkin, *J. Biol. Chem*., 2004, **279**, 23597-23605.

353) R. P. Piekorz, A. Hoffmeyer, C. D. Duntsch, C. McKay, H. Nakajima, V. Sexl, L. Snyder, J. Rehg and J. N. Ihle, *EMBO J*., 2002, **21**, 653-644.

354) C. M. Sadek, M. Pelto-Huikko, M. Tujague, K. R. Steffensen, M. Wennerholm and J. A. Gustafsson, *Gene Expr. Patterns*, 2003, **3**, 203-211.

355) Z. Xie, L. Y. Moy, K. Sanada, Y. Zhou, J. J. Buchman and L. H. Tasi, *Neuron*, 2007, **56**, 79-93.

356) S. Chen, J. T. Do, Q. Zhang, S. Yao, F. Yan, E. C. Peters, H. R. Scholer, P. G. Schultz and S. Ding, *Proc. Natl. Acad. Sci. USA*, 2006, **103**, 17266-17271.

357) A. Kochegarov, *Expert Opin. Ther. Pat.,* 2009, **19**, 275-281.

358) J. W. Schneider, Z. Gao, S. Li, M. Farooqi, T. Tang, I. Bezprozvanny, D. E Frantz and J. Hsieh, *Nat. Chem. Biol.,* 2008, **4**, 408-410.

359) X. Wu and P. G. Schultz, *J. Am. Chem. Soc.,* 2009, **131**, 12497-12515.

360) S. Zhu, H. Wurdak, J. Wang, C. A. Lyssiotis, E. C. Peters, C. Y. Cho, X. Wu and P. G. Schultz, *Cell Stem Cell,* 2009, **4**, 416-426.

361) G. M. Rishton, *Recent Pat. CNS Drug Discov*., 2008, **3**, 200-208.

362) S. Chen, S. Hilcove and S. Ding, *Mol. BioSyst*., 2006, **2**, 18-24.

363) E. Piers, T. Wong, P. D. Coish and C. Rogers, *Can. J. Chem*., 1994, **72**, 1816-1819.

364) M. I. Dawson, P. D. Hobbs, K. A. Derdzinski, W. Chao, G. Frenking, G. H. Loew, A. M. Jetten, J. L. Napoli, J. B. Williams, B. P. Sani, J. J. Willie and L. J. Schiff, *J. Med. Chem*., 1989, **32**, 1504-1517.

365) S. H. Chen, R. F. Horvath, J. Joglar, M. J. Fisher and S. J. Danishefsky, *J. Org. Chem*., 1991, **56**, 5834-5845.

366) B. Dominguez, B Iglesias and A. R. De Lera, *Tetrahedron*, 1999, **55**, 15071-15098.

367) P. C. Myhre and W. M. Schubert, *J. Org. Chem.,* 1960, **25**, 708-711.

368) M. Teng, T. T. Duong, E. S. Klein, M. E. Pino and R. A. S. Chandraratna, *J. Med. Chem*., 1996, **39**, 3035-3038.

369) M. Selva, P. Tundo and A. Perosa, *J. Org. Chem.*, 2003, **68**, 7374-7378.

370) S. J. Benkovic, T. H. Barrows and P. R. Farina, *J. Am. Chem. Soc*., 1973, **95**, 8414–8420.

Appendix 1: Selected Crystallographic Data for AH61 (for full data see accompanying CD)

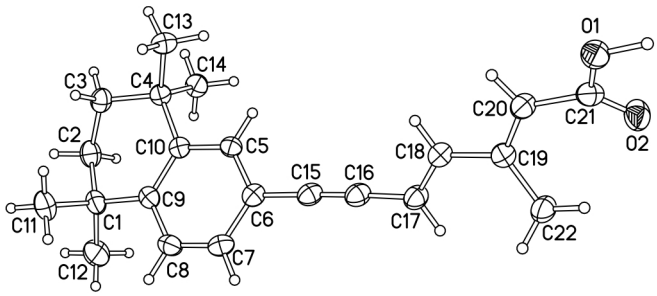

Empirical formula	C22H26O2
Formula weight	322.43
Temperature/K	393(2)
Crystal system	monoclinic
Space group	$P2_1/n$
a/Å	8.5727(3)
b/Å	19.6233(9)
c/Å	11.7421(6)
α/°	90.00
β/°	109.958(9)
γ/°	90.00
Volume/$Å^3$	1856.68(14)
Z	4
$\rho_{calc}mg/mm^3$	1.153
m/mm^{-1}	0.072
F(000)	696
Crystal size/mm^3	0.42 × 0.20 × 0.12
2Θ range for data collection	4.16 to 55°
Index ranges	-11 ≤ h ≤ 10, -25 ≤ k ≤ 23, -15 ≤ l ≤ 15
Reflections collected	15914
Independent reflections	4264[R(int) = 0.0299]
Data/restraints/parameters	4264/0/231

Goodness-of-fit on F^2	1.040
Final R indexes [I>=2σ (I)]	R_1 = 0.0422, wR_2 = 0.1067
Final R indexes [all data]	R_1 = 0.0592, wR_2 = 0.1171
Largest diff. peak/hole / e $Å^{-3}$	0.243/-0.163

Bond Lengths.

Atom	Atom	Length/Å	Atom	Atom	Length/Å
O1	C21	1.3229(16)	C6	C7	1.3974(19)
O2	C21	1.2249(17)	C6	C15	1.4361(18)
C1	C2	1.532(2)	C7	C8	1.3747(19)
C1	C9	1.5282(18)	C8	C9	1.4021(18)
C1	C11	1.5385(19)	C9	C10	1.4064(17)
C1	C12	1.536(2)	C15	C16	1.2015(19)
C2	C3	1.512(2)	C16	C17	1.4201(18)
C3	C4	1.5331(18)	C17	C18	1.3404(18)
C4	C10	1.5327(17)	C18	C19	1.4536(18)
C4	C13	1.5333(18)	C19	C20	1.3449(18)
C4	C14	1.5405(17)	C19	C22	1.5028(18)
C5	C6	1.3951(17)	C20	C21	1.4681(18)
C5	C10	1.3976(17)			

Bond Angles.

Atom	Atom	Atom	Angle/˚	Atom	Atom	Atom	Angle/˚
C2	C1	C11	110.24(12)	C7	C8	C9	122.65(12)
C2	C1	C12	107.96(12)	C8	C9	C1	118.90(11)
C9	C1	C2	110.19(10)	C8	C9	C10	118.03(12)
C9	C1	C11	108.78(11)	C10	C9	C1	123.07(11)
C9	C1	C12	111.06(11)	C5	C10	C4	118.20(11)
C12	C1	C11	108.59(12)	C5	C10	C9	118.92(11)
C3	C2	C1	111.96(11)	C9	C10	C4	122.85(11)
C2	C3	C4	112.64(11)	C16	C15	C6	178.07(14)
C3	C4	C13	107.51(11)	C15	C16	C17	178.25(15)
C3	C4	C14	110.11(10)	C18	C17	C16	124.08(12)
C10	C4	C3	110.33(10)	C17	C18	C19	125.37(12)
C10	C4	C13	111.30(10)	C18	C19	C22	117.95(11)
C10	C4	C14	108.94(10)	C20	C19	C18	117.77(12)
C13	C4	C14	108.63(11)	C20	C19	C22	124.28(12)
C6	C5	C10	122.21(11)	C19	C20	C21	126.08(12)
C5	C6	C7	118.45(12)	O1	C21	C20	113.08(12)
C5	C6	C15	121.20(12)	O2	C21	O1	122.86(12)
C7	C6	C15	120.35(12)	O2	C21	C20	124.01(12)
C8	C7	C6	119.62(12)				